REPORT TO DECC

LONG-TERM ATMOSPHERIC MEASUREMENT AND INTERPRETATION

(OF RADIATIVELY ACTIVE TRACE GASES)

DECC contract number: GA0201

Annual Report (May 2013 - April 2014)

Date: 1st May 2014

University of Bristol: Simon O'Doherty, Aoife Grant, Anita Ganesan, Dan Say, Ann Stavert

Met Office: Alistair J. Manning

rdscientific: Richard G. Derwent

INSCON: Peter Simmonds

Terra Modus: Dickon Young

UEA: Stephen Humphrey, David Oram, Bill Sturges

Contents

1 Executive Summary

1.1 Project Summary

Monitoring the atmospheric concentrations of gases is important in assessing the impact of international policies related to the atmospheric environment. The effects of control measures on chlorofluorocarbons (CFCs), halons and HCFCs (hydrochlorofluorocarbons) introduced under the 'Montreal Protocol of Substances that Deplete the Ozone Layer' are now being observed. Continued monitoring is required to assess the overall success of the Protocol and the implication for atmospheric levels of replacement compounds such as hydrofluorocarbons (HFCs). Similar analysis of gases regulated by the Kyoto Protocol on greenhouse gases will likewise assist policy makers.

Since 1987, high frequency, real time measurements of the principal halocarbons and radiatively active trace gases have been made as part of the Global Atmospheric Gases Experiment (GAGE) and Advanced Global Atmospheric Gases Experiment (AGAGE) at Mace Head, County Galway, Ireland. For much of the time, the measurement station, which is situated on the Atlantic coast, monitors clean westerly air that has travelled across the North Atlantic Ocean. However, when the winds are easterly, Mace Head receives substantial regional scale pollution in air that has travelled from the industrial regions of Europe. The site is therefore uniquely situated to record trace gas concentrations associated with both the Northern Hemisphere background levels and with the more polluted air arising from Europe.

An observation network for the UK (UK DECC network) has been created, along with Mace Head, it consists of three tall tower stations: Angus Tower near Dundee; Tacolneston near Norwich; and Ridge Hill near Hereford. Ridge Hill became operational in February 2012, Tacolneston in July 2012 and Angus Tower began operating for the network in May 2013. The expanded network makes it possible to resolve emissions on a higher resolution across the UK, to Devolved Administration (DA) level.

This project has two principle aims:

- **Estimate the background atmospheric concentrations of the principle greenhouse and ozone-depleting gases from DECC network observations.**

- **Estimate the UK (down to Devolved Administration level) and North-West European emissions of the principle greenhouse and ozone-depleting gases using the DECC network observations and compare these to the compiled inventory.**

The atmospheric measurements and emission estimates of greenhouse gases provide an important independent cross-check for the national greenhouse gas inventories (GHGI) of emissions submitted annually to the United Nations Framework Convention on Climate Change (UNFCCC). The GHGI are estimated through in-country submissions of Activity Data and Emission Factors that are, in some cases, very uncertain. Independent emissions verification is considered good practice by the Intergovernmental Panel on Climate Change (IPCC).

1.2 Background atmospheric trends

The Met Office particle transport model, NAME (Numerical Atmospheric dispersion Modelling Environment), is run in backward-running mode to estimate the dilution of emissions from recent (within 30-days) surface releases to a concentration at the observing station, Mace Head on the west coast of Ireland. These, so called air history maps, have been produced for each 2-hour period from 1989 until present day. NAME is 3-dimensional therefore it is not just surface transport that is modelled, an air parcel can travel from the surface to a high altitude and then back to the surface but only those times when the air parcel is within the lowest 100 m above the ground will it be recorded in the surface air history maps. The impact of air from higher altitudes arriving at the surface at Mace Head is also separately recorded. The model domain covers North America to Russia and North Africa to the Arctic Circle and extends to more than 10 km vertically. No chemical

or deposition processes were modelled; this is realistic given the long atmospheric lifetimes of the gases considered.

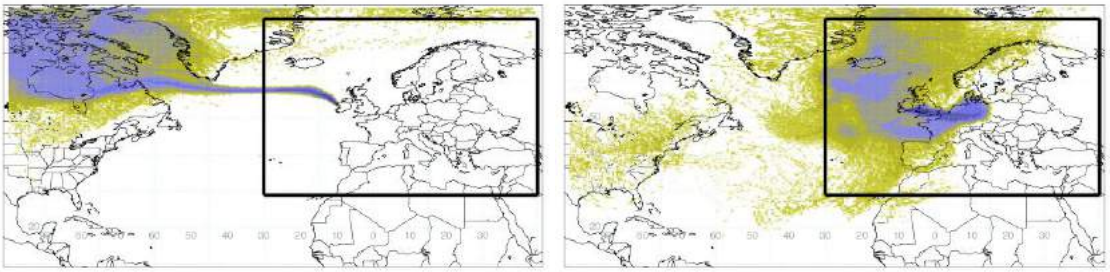

(a) (b)

Figure 1: Examples of 2-hour air history surface maps derived from NAME (a) baseline period (b) regionally polluted period. The maps describe which surface areas (defined as within 100 m of the surface) in the previous 30-days impact the observation point at a particular time.

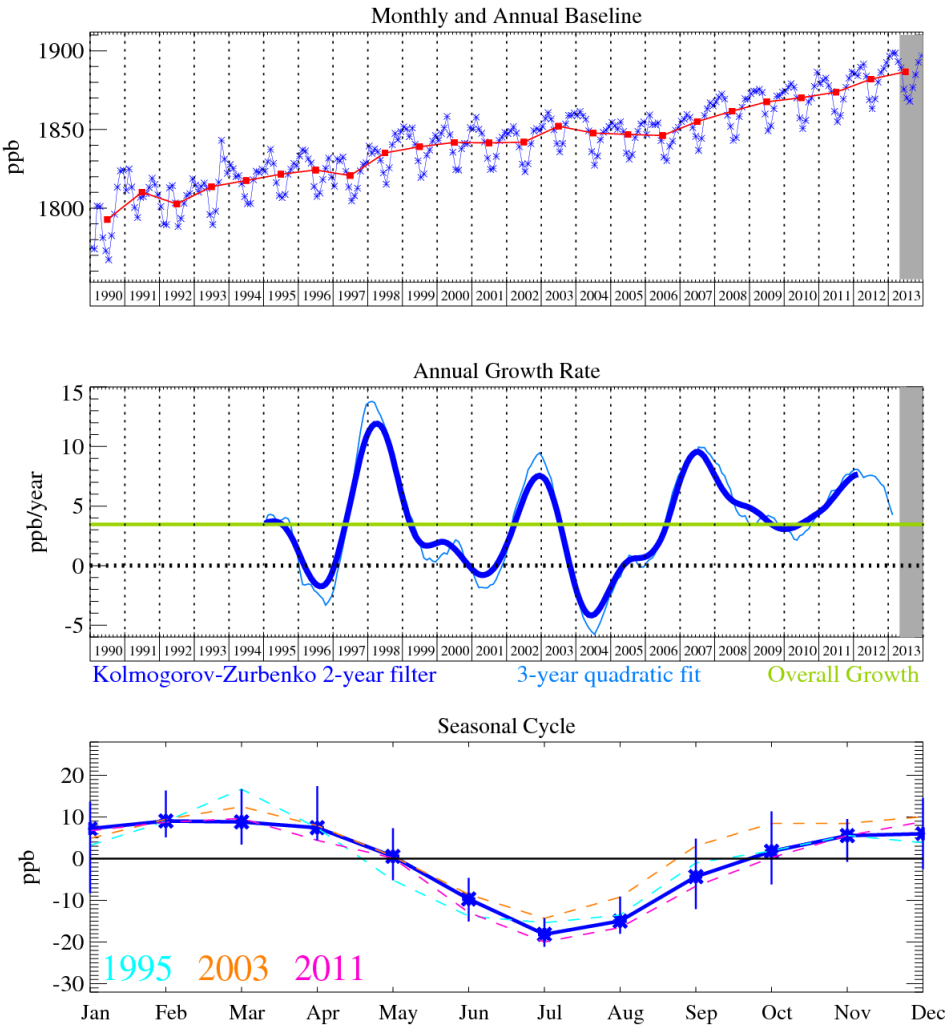

Figure 2: Methane: Monthly (blue) and annual (red) baseline mole fractions (top plot); Annual (blue) and overall average growth rate (green) (middle plot); Seasonal cycle (de-trended) with year-to-year variability (lower plot). Grey area covers un-ratified and therefore provisional data.

The first step is to estimate the Northern Hemisphere atmospheric background concentration (referred to as the baseline) of each gas measured at Mace Head; their long-term baseline trends and growth rates and their seasonal cycle. Baseline concentration times are defined here as those times when the air mass arriving at Mace Head has not been influenced by significant emissions within the previous few weeks (varying depending on how quickly the winds move the air from the edge of the defined model domain to Mace Head, i.e. those times when the air is well mixed and is

representative of the Northern Hemisphere background concentration. Figure 1 shows two example air history maps, the one on the left shows a 2-hour period when the air mass will be considered baseline, the one on the right, when the air mass is not considered baseline because of the recent influence of Europe, a source region. Times when the air has rapidly descended to Mace Head from the upper troposphere (defined here as above 9 km) are also not considered baseline because many gases have a strong vertical gradient, usually decreasing concentration with height.

Fitting a time-varying line through just those Mace Head observations recorded within the 2-hour time periods when the air masses are representative of the Northern Hemisphere baseline it is possible to extract from the observational data an estimate of the hourly baseline across the entire measurement record. The hourly baseline can then be further interrogated to estimate monthly and annual values, reveal whether the Northern Hemisphere atmospheric concentration is growing or declining and the strength of the baseline seasonal cycle. Figure 2 shows the results for methane.

1.3 Estimates of regional emissions

By removing the time-varying baseline concentrations from the raw measurement data, a time-series of excursions from the baseline, averaged over each 2-hour period, for each observed gas has been generated. The perturbations above baselines, observed across the UK DECC network, are driven by emissions on regional scales that have yet to be fully mixed on the hemisphere scale and are the principle tool used to estimate surface emissions across north-west Europe. A method for estimating emissions from observations, referred to as 'Inversion Technique for Emission Modelling' (InTEM), has been developed over many years and is used here to estimate Devolved Administration (DA), UK and North-West European (NWEU = UK + Ireland + France + Germany + Denmark + the Netherlands + Belgium + Luxembourg) emissions using the observations from the UK DECC network.

InTEM links the observation time-series with the NAME air history estimates of how surface emissions dilution as they travel to the observation stations. An estimated emission distribution when combined with the NAME output can be transformed into a modelled time-series at each of the measurement stations. The modelled and the observed time-series can be compared using a single or a range of statistics (referred to as a cost function) to produce a skill score for that particular emission distribution. InTEM uses a well known best-fit technique, simulated annealing, to search for the emission distribution that produces a modelled times-series that has the best statistical match to the observations. InTEM can either start from a random emission distribution or from an inventory-defined distribution.

In order for InTEM to provide robust solutions for every area within the modelled domain, each region needs to significantly contribute to the air concentrations at the UK DECC network on a reasonable number of time periods. If the signal from an area is only rarely or poorly seen by the network, then its impact on the cost function is minimal and the inversion method will have little skill at determining its true emission. The contributions that different grid boxes make to the observed air concentration varies from grid to grid. Grid boxes that are distant from the observation site contribute little to the observation, whereas those that are close have a large impact. In order to balance the contribution from different grid boxes, those that are more distant are grouped together into increasingly larger regions. The grouping cannot extend beyond country (or DA) boundaries. The country boundaries extend into the surrounding seas to reflect both emissions from shipping, off-shore installations and river runoff but also because the inversion has geographical uncertainty.

There is significant uncertainty in the emissions that are estimated. Uncertainty arises from many factors: errors in the baseline estimate; emissions that vary over time-scales shorter than the inversion time-period e.g. diurnal, seasonal or intermittent; heterogeneous emissions i.e. emissions that vary within the regions solved for; errors in the transport model (NAME) or the underpinning 3-dimensional meteorology; errors in the observations themselves. The potential magnitudes of these uncertainties have been estimated and are incorporated within InTEM to inform the uncertainty of the modelled results.

1.4 Summary of the main findings

- The Northern Hemisphere atmospheric concentrations of all Kyoto gases are increasing. Monthly (blue) and annual (red) mole fractions are shown for three gases (Figure 3), CH_4 is shown in Figure 2.

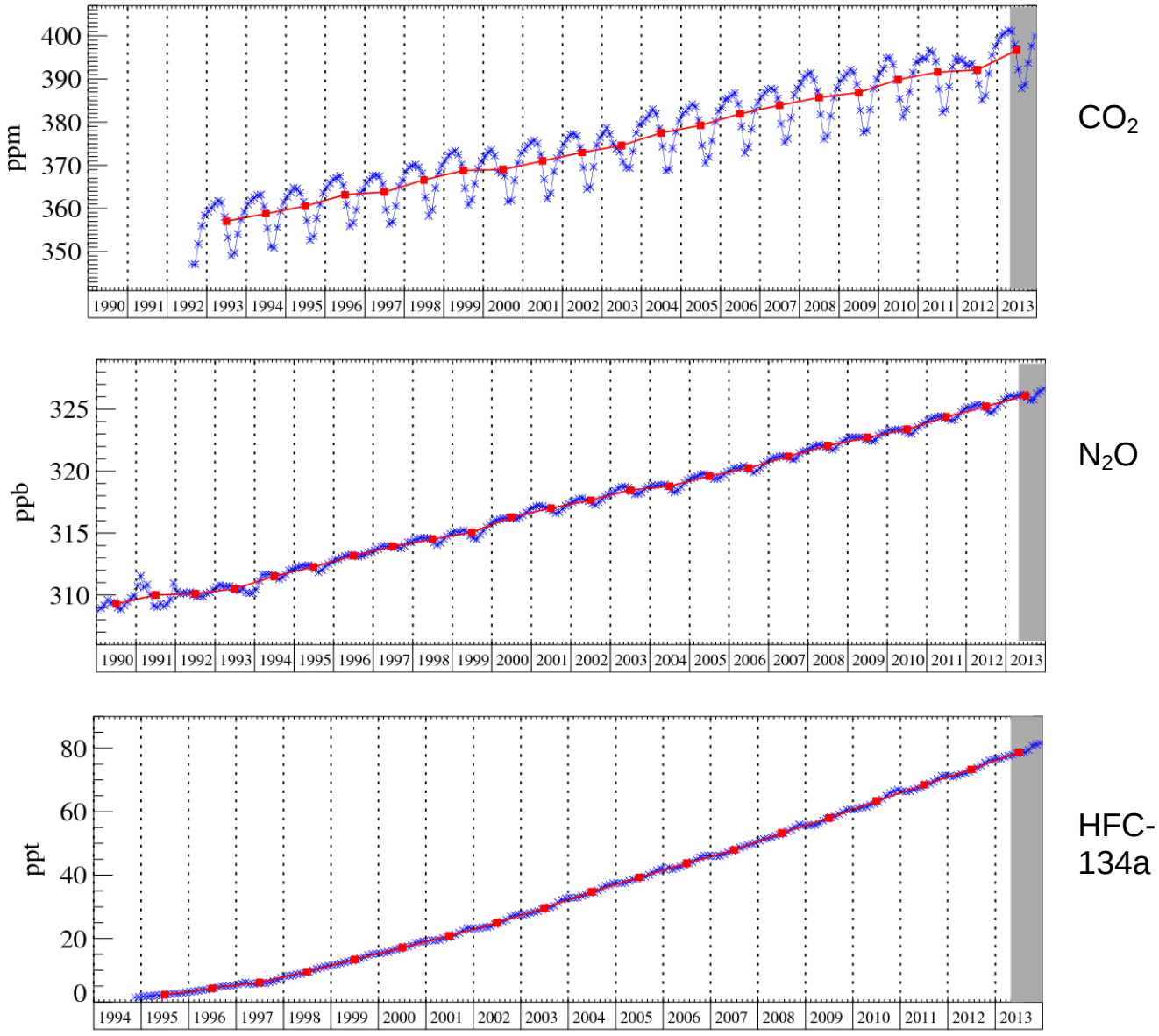

Figure 3: Northern Hemisphere monthly (blue) and annual (red) baseline mole fractions for CO_2, N_2O and HFC-134a.

- Carbon dioxide (CO_2): The anthropogenic component of CO_2 is very difficult to assess because of the very significant, temporally and spatially varying biogenic sink/source terms. In this report the correlation between anthropogenic CO_2 and carbon monoxide (CO) has been exploited to estimate the UK anthropogenic component. The agreement between the GHGI and InTEM estimates is fair but the uncertainty in the InTEM estimates are considerably larger than those reported for the GHGI. Other gases such as ethane and propane could be used together with the CO as surrogates for CO_2 anthropogenic emissions. Isotopes could also play a significant role in disentangling the CO_2 observations into their anthropogenic and biogenic components.

- Methane (CH_4): The UK InTEM estimates are lower than the Greenhouse Gas Inventory (GHGI) estimates (as reported to the UNFCCC in 2014) in the 1990s but there is good agreement from 2003 onwards. The inclusion of the extended DECC network observations allows the InTEM time frame to be reduced from 3-year to 1-year, good agreement is maintained.

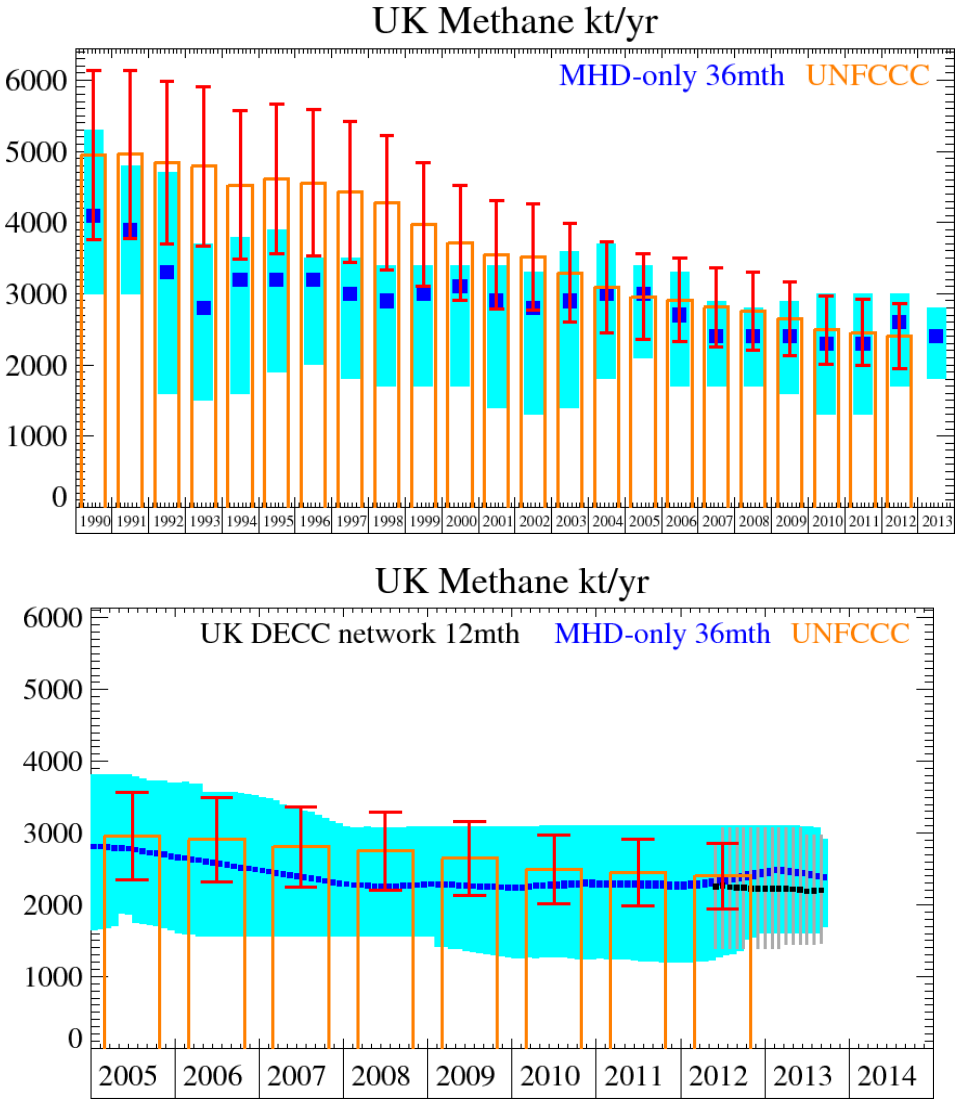

Figure 4: Emission (kt/y) estimates for UK (MHD-only and DECC network) comparing InTEM (blue) and the GHGI submitted to the UNFCCC (orange). The InTEM uncertainty bars represent the 5th and 95th percentiles (light blue) and red bars uncertainty in the GHGI.

- Nitrous oxide (N_2O): The UK GHGI and InTEM estimates are broadly in agreement. The uncertainty of the GHGI is very significant compared to the uncertainty estimated for the InTEM results. Both the 3-year Mace Head (MHD)-only and the extended DECC network 1-year InTEM estimates are showing a positive trend in the latter period. The difference between the MHD-only and the DECC network results show the value of moving to a higher temporal resolution. It will be important to see whether this positive InTEM trend continues and whether the GHGI shows an upturn in 2013.

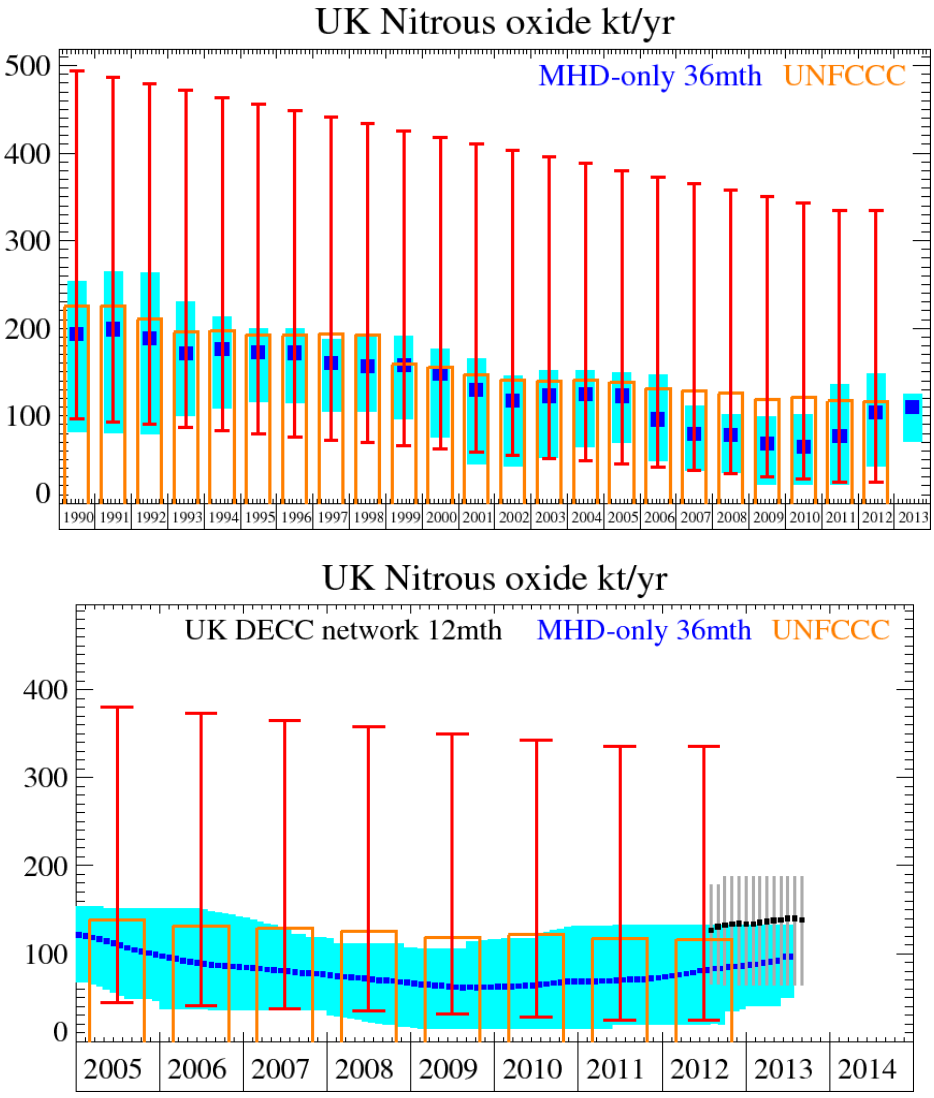

Figure 5: Emission (kt/y) estimates for UK (upper: MHD-only and lower: DECC network) comparing InTEM (blue) and the GHGI submitted to the UNFCCC (orange). The InTEM uncertainty bars represent the 5th and 95th percentiles (light blue) and red bars uncertainty in the GHGI.

- HFC-134a: The UK GHGI is approximately double that estimated by InTEM and well outside the uncertainties of the two methods. The emission factors used for each country across NWEU for the UNFCCC inventory have significant variation and maybe the cause of this significant difference.

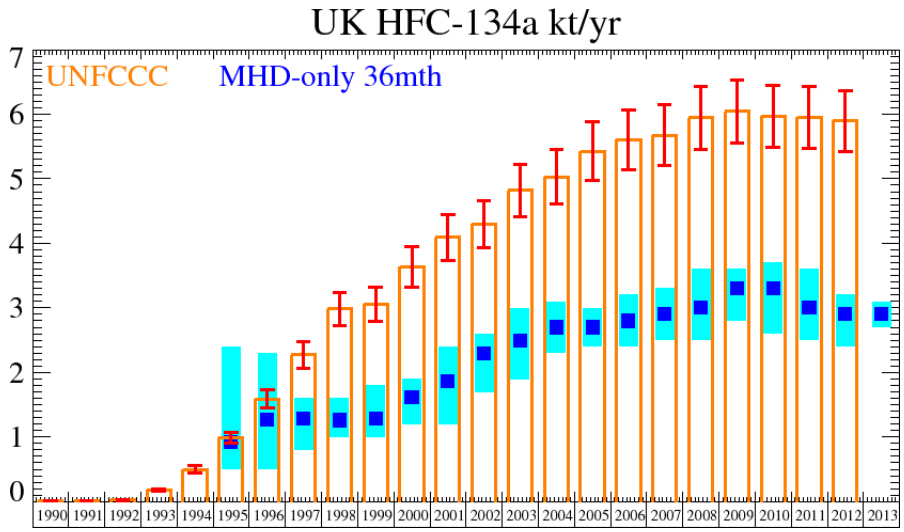

Figure 6: Emission (kt/y) estimates for UK comparing InTEM (blue) and the GHGI submitted to the UNFCCC (orange). The InTEM uncertainty bars represent the 5th and 95th percentiles (light blue) and red bars uncertainty in the GHGI.

- HFC-125 and HFC-32: The UK GHGI estimates for these gases (used in refrigerant blends) are increasing. UK InTEM estimates agree with the GHGI up until 2009 after which time InTEM emission estimates level off. For NWEU, both the InTEM and GHGI estimates are increasing. It is possible the balance between UK and non-UK NWEU usage of these gases is changing over time.

- For HFC-143a: UK InTEM is ~20% higher than GHGI, UK InTEM now falling whereas GHGI growing.

- HFC-152a, HFC-23, HFC-227ea, HFC-43-10mee, PFC-14, PFC-116, PFC-218: These gases are reported in the main document.

- Sulphur hexafluoride (SF_6): The UK InTEM estimates are consistently elevated compared to the GHGI, however the InTEM uncertainty ranges do encompass the inventory estimates. The NWEU InTEM estimates are higher than the inventory until 2010 after which the agreement is good.

- Nitrogen trifluoride (NF_3) has been added to the list of compounds being measured by the Medusa GC-MS at Mace Head and is amongst the first *in situ* measurements made of this potent greenhouse gas.

- Mace Head, Ridge Hill, Tacolneston and Angus (DECC network) instruments have generally operated well and with minimal data loss over the measurement period. Inter-comparison exercises have been completed at Angus with the European InGOS project to assess data comparability and consistency.

1.5 Summary of headline progress

1. **All the UK DECC Network sites are operational**. The compounds measured at each site are shown in Table 1. This is the first network of its kind in the UK (and Europe) and has been a major achievement of this contract.
2. **Mace Head** continues to be a baseline station at the forefront of global atmospheric research. This is evident through the high volume of peer-reviewed publications related to work using the Mace Head observational record. The publications related to this contract are detailed in the publication section of this report. In addition, the inclusion of Mace Head in many new EU funded atmospheric research programmes, such as ICOS, InGOS, ACTRIS, and continued support from other global programmes such as AGAGE and NOAA-ESRL indicates its international significance.
3. **New funding** (external to this contract) has been secured by the University of Bristol to ensure that measurements of the key GHGs (CO_2, CH_4, N_2O and CO) continue at Tall Tower Angus (TTA) using state-of-the-art cavity ringdown spectrometers (CRDS).
4. **Uncertainty within InTEM has been further investigated.** The components that make up the uncertainty in the inversion modelling have been isolated so as to allow more precise quantification. The uncertainty has been split into components from: repeatability of the observations (measurement error); variability of the observation within the InTEM time period (2-hour); uncertainty in modelling the dispersion of the gases within the atmosphere; the influence of sub-gridscale local emissions.
5. **Estimating UK CO_2 emissions.** The method for estimating UK CO_2 emissions has been further revised. Due to the strong biogenic CO_2 signal in the observations the current inversion method is not directly applicable to CO_2. Further use has been made of the CO inversion estimates and the reported CO:CO_2 emission ratio to estimate UK emissions of CO_2.
6. **NF_3**. Mole fractions of this gas are being acquired at Mace Head and will be reported by the end of 2014.
7. **Mid-latitude Northern Hemisphere baseline trends updated on website**. The trends are also presented in this report and have been extended up to and including March 2014.
8. **UK emission estimates**. Inversion emission estimates for the UK and North West Europe are reported up to and including 2013 and have been compared to the 2014 reported GHGI UK inventory (the 2014 GHGI submission covers emissions up to and including 2012).
9. **UNFCCC verification appendix chapter** for the UK National Inventory Report (NIR) submission was delivered (March 2014).

1.6 Focus of current research

Incorporating the extended DECC network observations into InTEM has been achieved but some simplifications have been made. In the work presented here the Mace Head derived baseline is applied across the network (albeit with larger uncertainty) however this implies that the air reaching the other stations has a similar history as that arriving at Mace Head. It is envisaged that this simplification will be considered in more detail and other options investigated.

2 Introduction

2.1 Objectives

This project has two principle aims:

- **Estimate the background atmospheric concentrations of the principle greenhouse and ozone-depleting gases from the DECC network observations.**

- **Estimate the UK (down to Devolved Administration level) and North-West European emissions of the principle greenhouse and ozone-depleting gases using the DECC network observations and compare these to the compiled inventory.**

2.1.1 For the measurement section of the project the objectives are:

1. To either lease, purchase or otherwise provide, and maintain instrumentation to obtain measurements of the gases listed in Annex 1 and to run the atmospheric observation site at Mace Head, Ireland.

2. To continue high quality real-time measurements of the gases listed in Annex 1 at Mace Head, Ireland, including routine in situ GC-MS measurements of hydrofluorocarbons (HFCs), perfluorocarbons (PFCs), hydrochlorofluorocarbons (HCFCs), methyl bromide, halons and other halogenated gases relevant to stratospheric ozone depletion and climate change.

3. To either lease, purchase or otherwise provide, and maintain instrumentation to obtain measurements of the major Kyoto gases (CO_2, CH_4, and N_2O) and to run atmospheric observation sites at any proposed additional site/s across the UK.

4. To make high-quality real time measurements of the major Kyoto gases at any additional observation site(s), consistent with the requirements set out above.

5. To continue international collaboration and data exchange within the global Advanced Global Atmospheric Gases Experiment (AGAGE) project. This will include, inter alia, the determination of global magnitude and latitudinal distribution of the surface sources of greenhouse gases

6. To provide data to help study the atmospheric behaviour of trace gases, to estimate source gas strengths in the UK and NW Europe and to study the concentrations and trends in the total chlorine/bromine content of the atmosphere and the oxidising capacity of the atmosphere

7. To maintain an up-to-date calibrated database of any of the trace gases measured under contract to DECC at Mace Head and any additional site/s, and to maintain a secondary database of any measurements made as part of the AGAGE global network.

8. To continue technical development of measurement methodologies to improve reliability and accuracy wherever possible.

2.1.2 For the interpretation part of the project the objectives are:

9. To quantify anthropogenic emissions (by source gas) of halocarbons, and anthropogenic emissions (by source gas, also source gas removal by sinks) of greenhouse gases, at the North West European, UK and Devolved Administrations (DA) levels and to use these for inventory verification.

10. To identify new substances with ozone depleting or radiative forcing properties, and quantify these where necessary.

11. To assess trends in emissions and concentrations of greenhouse gases and halocarbons and identify departure from expected trends, and the causes of any noted departure.

12. To identify additional sources of data for assessing compliance and verification of emissions inventories, particularly work initiated under the auspices of Working Group 1 of the EU Monitoring Mechanism and other EU programmes currently underway and report on these to DECC, with forewarning of upcoming meetings and their objectives.

2.2 Detail on Specific Work Programme Items

1. Assess and report concentrations of direct and indirect greenhouse gases measured at Mace Head and any additional site/s.

Mole fraction data from Mace Head are submitted to the Carbon Dioxide Information Analysis Center (CDIAC, http://cdiac.ornl.gov) every six months. CDIAC is the primary climate-change data and information analysis centre of the U.S. Department of Energy. The CDIAC data are automatically reformatted and sent to the World Data Centre (WDC) for Greenhouse Gases (WDCGG, http://ds.data.jma.go.jp/gmd/wdcgg/) which is one of the WDCs under the WMO (World Meteorological Organisation) GAW (Global Atmospheric Watch) programme that serve to gather, archive and provide data on greenhouse gases and other related gases in the atmosphere and ocean. As part of the European InGOS project, the Mace Head data submitted to CDIAC data is also submitted to the EBAS database (http://ebas.nilu.no/). The observations from the UK DECC network are submitted directly to EBAS every six months.

The reported baseline concentrations (mole fractions), annual growth rates and seasonal cycles along with instrumentation and calibration details are presented in the "UK DECC Network" website (http://www.metoffice.gov.uk/atmospheric-trends/).

2. Analyse and update annually global baseline atmospheric concentration trends and European emissions of the gases in Annex 1. Comparisons should be made with inventory data, and if relevant production and consumption figures provided by industry to the EU.

For each gas, baseline atmospheric concentration trends for the mid-latitude northern hemisphere have been reported quarterly through the website and are reported in Sections 5 and 6.

For each gas measured by the UK DECC network, an estimate of the UK and North West European (NWEU) (comprising of Ireland, UK, France, Belgium, The Netherlands, Luxembourg, Germany, Denmark) annual emissions have been made using the InTEM system (see Sections 5 and 6). The UK estimates for SF_6, N_2O and CH_4 have been sub-divided to DA level. Where available the InTEM results have been compared against GHG inventory and other emission data.

3. Identify departure from expected trends in concentration and emissions of gases listed in Annex 1 and identify causes of these variations. Identify and assess the reasons for any departure from expected trends in concentration.

The trends in the mid-latitude northern hemisphere baseline concentrations of each gas are discussed in Sections 5 and 6. The UK emission trends of each gas are discussed and any departures from the expected have been highlighted.

4. Identify any additional sources of data for monitoring gases listed in Annex 1.

The additional UK DECC network stations, Ridge Hill, Tacolneston and Angus are discussed in Section 3 (for more detail see the Appendix, and the website www.metoffice.gov.uk/atmospheric-trends)

Relevant observations from the wider ICOS network will be included within the InTEM analysis. This work will be facilitated through collaborations within the EU InGOS programme and the NERC GAUGE programme.

5. Make and update annually estimates of European and UK emissions of direct and indirect GHG and provide comparisons with the UKGHGI, EMEP and the EEA emissions inventories. Any discrepancies with emissions inventories should be highlighted and discussed.

InTEM has been applied to the direct and indirect greenhouse gases measured by the UK DECC network. Annual UK (and subdivided to DA level for SF_6, N_2O and CH_4) and NW European emission estimates using Mace Head (MHD) observations are reported in Sections 5 and 6 The observations from Ridge Hill (RGL), Tacolneston (TAC) and Angus (TTA), along with those from Mace Head, have been used within InTEM to estimate UK and DA emissions of N_2O, CH_4 and SF_6, from 2012 onwards.

Where data are available these estimates have been compared to those reported elsewhere, most notably those reported through the UNFCCC programme, and the discrepancies are discussed. Due to the significant biogenic emissions and sinks of CO_2, estimating the anthropogenic emissions of CO_2 has been treated separately.

6. Identify new ozone depleting or global warming substances of potential policy interest, and provide details to DECC. Investigate the potential and feasibility for further expanding the policy relevance of Mace Head or any other sites' data, by considering other classes of atmospheric trace gases such as hydrocarbons, oxygenated species, perfluorocarbons, very long lived molecules, and oxygen concentrations.

It is a primary aim of the AGAGE program and UK DECC Network to identify new ozone depleting or global warming substances and where possible add these compounds to the ever increasing number of substances measured using the Medusa GC-MS at Mace Head, and more recently at Tacolneston. However, with this type of activity there will always be a compromise between the number of substances measured and the precision of the measurement that can be achieved. For this reason, it normally takes a reasonable amount of time between identification of a new compound, assessment of the implication of adding the compound to the analysis list (i.e. degradation of measurement performance for existing compounds) and agreeing that the importance of the scientific questions that can be answered from the addition of the compound, warrant its inclusion. This process has taken place for two sets of compounds over the last few years: nitrogen trifluoride (NF_3); and the higher molecular weight perfluorocarbons (PFCs). A discussion of potential new compounds is given in Section 8 (see Objective 10).

7. Identify any gaps in existing data from Mace Head and any additional site/s that could potentially be of policy relevance.

Isotope measurements of CO_2, CH_4 and N_2O have the potential to add further constraints to the inversion system, for example by providing additional information on the emissions from different source sector categories. The scope and challenges of isotope observations are significant but will be investigated in collaboration with the NERC GAUGE programme that will be undertaking a measurement campaign of some of the principle isotopes of CO_2, CH_4 and N_2O.

8. Liaise with Hadley Centre over 3D atmospheric chemistry modelling being carried out at the Hadley Centre and provide data for model validation purposes, if required.

The monthly time-series of baseline concentrations and average seasonal cycles of all of the gases measured at Mace Head and the other AGAGE stations considered are provided to the Hadley Centre (part of the Met Office). Currently the data provided, although of direct relevance, is not widely used. To facilitate raising awareness of this useful source of data, the Met Office staff directly involved in this contract have been moved into the Hadley Centre, into the 'Earth System and Mitigation Science' group.

9. Investigate the use that could be made of new or additional sources of data such as isotope measurements or flux data, in conjunction with data from Mace Head and the additional site/s, or from any other sites that could potentially be of policy relevance, for verifying GHG emissions.

Through the new NERC funded GAUGE programme, new sources of data will become available. These include, inter-calibrated information from ground-based, airborne, ferry-borne, balloon-borne, and space-borne sensors, including new sensor technology and isotope measurements. (http://www.greenhouse-gases.org.uk/). The contractors are also partners in this new programme and will feed through the results from the use of these new data sources in a timely manner. As discussed above, use will also be made of relevant and available non-UK ICOS observations e.g. through the EU InGOS programme. (link to Objective 9). There are some isotope measurements made at Mace Head ($\Delta^{14}CO_2$ by University of Heidelberg and $\delta^{13}CO_2$ by NOAA) although, in isolation, these measurements do not provide a great deal of useful information about UK anthropogenic/biogenic emissions. As part of the NERC GAUGE programme we propose to use the existing "baseline" measurements at Mace Head, extend them and make new UK "pollution" measurements at one of the other UK DECC network sites and from the FAAM aircraft, to provide information that will be more policy relevant for verifying GHG emissions. The revised GAUGE proposed isotope work is detailed in Section 3 and has recently been agreed by NERC (links to Objective 9).

10. Provide advice, as requested by DECC, on the relative roles of radiatively active trace gases in forcing climate change and, where possible, compute global warming potentials (GWPs) for any new substances identified.

This has taken place for the higher molecular weight perfluorocarbons (PFCs) and also in consideration of new gases of potential policy interest, see Section 8.

11. Report on developments in the understanding of anthropogenic and natural sources and sinks of carbon dioxide, methane and nitrous oxide, using seasonal trends in emissions and analysis of annual trends

Annual UK and North West European emission estimates, through the use of inversion modelling, of carbon dioxide (CO_2), methane (CH_4) and nitrous oxide (N_2O) are reported in Section 5. The agreement between the anthropogenic inventory and the InTEM results for N_2O is good. The uncertainty ranges in the InTEM N_2O results are considerably smaller than those reported in the inventory. For CH_4 the UK InTEM results are consistently lower than the inventory pre-2000 estimates but agree, within the uncertainty, post-2002. The magnitude of the uncertainties in the InTEM CH_4 estimates are comparable to those reported for the inventory. For N_2O and CH_4 it has been assumed that on the NWEU scale the biogenic emissions are small compared to the anthropogenic contribution. For CO_2 the same assumption is not plausible and so an alternative route through the ratio to anthropogenic carbon monoxide has been used to estimate UK anthropogenic CO_2 emissions. The InTEM CO_2 estimates calculated through this method have very significant uncertainties compared to the reported inventory uncertainties.

Isotopic measurements may also aid our understanding of this split, but the paucity of observations will make this very challenging. The scope and challenges of isotope observations is discussed above.

12. Compare data from Mace Head and any additional site/s with data from other national and international studies, where appropriate.

The consortium is part of the AGAGE community and regularly compares analyses where appropriate. CSIRO (Australia) conducts comprehensive comparisons between all of the data measured by AGAGE (including Mace Head) and other global sites around the world. A selection of recent comparisons that have taken place at Mace Head are detailed in the Appendix (refer to Objective 9).

13. Provide assistance and as requested by DECC, on validation of European and national-level trace gas emission inventories, and on monitoring compliance with international protocols and agreements or other research conducted for the contract.

Each year a verification annex has been prepared under this contract and has been included in the UK National Inventory Report submission to the UNFCCC.

14. Ensure information-exchange and coordination with complementary European Union projects on verification of greenhouse gas emissions, for example CarboEurope, NitroEurope, IPCC reports, guidelines or studies, and attend inverse-modelling workshops arranged under the auspices of the EU Monitoring Mechanism.

The contractors are active members and share information with the AGAGE, ICOS, InGOS and GAUGE programmes and are available to contribute to IPCC reports, guidelines and studies, SPARC assessments, and attend appropriate workshops as required.

15. Advise on developments in remote sensing techniques in general as applied to measurement of atmospheric trace gases and inventory verification.

Through the NERC GAUGE programme this area will be given great focus. Within GAUGE, specific use will be made of the methane GOSAT satellite data. The contractors will liaise with Dr. Hartmut Bosch of the University of Leicester who is leading this GAUGE work package. Satellite information will be used within the global inversion studies, the success of these efforts will be reported to DECC as they come to fruition.

16. Make provision for up to 5 days' ad-hoc policy support per year to DECC's Climate and Energy: Science team.

Apart from providing advice for the production of a government POSTnote, no work has been conducted under this item although the team involved in this project are available should the DECC Science team require it.

17. Provide quarterly project updates, annual project reports, and an end of contract project report.

Quarterly and annual contract reports have been produced as specified in the milestone plan. These reports, in addition to being delivered to DECC, have also been made available (when released by DECC) through the contract website (http://www.metoffice.gov.uk/atmospheric-trends).

18. Host a website containing information about Mace Head and any other observation sites. The website should contain up to date project reports, the interpreted and ratified observations data, and be updated at least once every three months.

A website (http://www.metoffice.gov.uk/atmospheric-trends) containing all relevant information relating to this work has been further developed. Each observation site is described in detail, including geographical location, photographs and the gases measured. The record of monthly and annual baseline mass mixing ratios, the growth rates and the seasonal cycles for each gas (see Figure 70), together with relevant information about each gas, are displayed and updated quarterly. All contract reports, containing information on baseline trends and emission estimates, are available through the website. The comparison of the UK InTEM emission estimates with the GHGI (GreenHouse Gas Inventory) have been added to the website and will be updated annually.

2.3 Publications

Arnold, T., D. J. Ivy, C. M. Harth, M. K. Vollmer, J. Mühle, P. K. Salameh, L. P. Steele, P. B. Krummel, R. H. J. Wang, D. **Young**, C. R. Lunder, O. Hermansen, T. S. Rhee, J. Kim, S. Reimann, S. **O'Doherty**, P. J. Fraser, P. G. **Simmonds**, R. G. Prinn, and R. F. Weiss, HFC-43-10mee atmospheric abundances and global emission estimates, *Geophysical Research Letters*, doi:10.1002/2013GL059143, 2014.

Rigby, M., R. G. Prinn, S. **O'Doherty**, B. R. Miller, D. Ivy, J. Mühle, C. M. Harth, P. K. Salameh, T. Arnold, R. F. Weiss, P. B. Krummel, L. P. Steele, P. J. Fraser, D. **Young**, and P. G. **Simmonds**, Recent and future trends in synthetic greenhouse gas radiative forcing, *Geophysical Research Letters*, doi:10.1002/2013GL059099, 2014.

Thompson, R. L., F. Chevallier, A. M. Crotwell, G. Dutton, R. L. Langenfelds, R. G. Prinn, R. F. Weiss, Y. Tohjima, T. Nakazawa, P. B. Krummel, L. P. Steele, P. Fraser, S. **O'Doherty**, K. Ishijima, and S. Aoki, Nitrous oxide emissions 1999 to 2009 from a global atmospheric inversio**n**, *Atmospheric Chemistry & Physics*, *14*(4), 1801–1817, doi:10.5194/acp-14-1801-2014, 2014.

Fraser, P. J., B. L. Dunse, A. J. **Manning**, S. Walsh, R. H. J. Wang, P. B. Krummel, L. P. Steele, L. W. Porter, C. Allison, S. **O'Doherty**, P. G. **Simmonds**, J. Mühle, R. F. Weiss, and R. G. Prinn, Australian carbon tetrachloride emissions in a global context, *Environmental Chemistry*, *11*(1), 77, doi:10.1071/EN13171, 2014.

Simmonds, P. G., A. J. **Manning**, M. Athanassiadou, A. A. Scaife, R. G. **Derwent**, S. **O'Doherty**, C. M. Harth, R. F. Weiss, G. S. Dutton, B. D. Hall, C. Sweeney, and J. W. Elkins, Interannual fluctuations in the seasonal cycle of nitrous oxide and chlorofluorocarbons due to the Brewer-Dobson circulation, *Journal of Geophysical Research: Atmospheres*, *118*(19), 10,694–10,706, doi:10.1002/jgrd.50832, 2013.

Ganesan, A. L., A. Chatterjee, R. G. Prinn, C. M. Harth, P. K. Salameh, A. J. **Manning**, B. D. Hall, J. Mühle, L. K. Meredith, R. F. Weiss, S. **O'Doherty**, and D. **Young**, The variability of methane, nitrous oxide and sulfur hexafluoride in Northeast India, *Atmospheric Chemistry & Physics*, *13*(21), 10633–10644, doi:10.5194/acp-13-10633-2013, 2013.

Kirschke, S., P. Bousquet, P. Ciais, M. Saunois, J. G. Canadell, E. J. Dlugokencky, P. Bergamaschi, D. Bergmann, D. R. Blake, L. Bruhwiler, P. Cameron-Smith, S. Castaldi, F. Chevallier, L. Feng, A. Fraser, M. Heimann, E. L. Hodson, S. Houweling, B. Josse, P. J. Fraser, P. B. Krummel, J.-F. Lamarque, R. L. Langenfelds, C. Le Quéré, V. Naik, S. **O'Doherty**, P. I. Palmer, I. Pison, D. Plummer, B. Poulter, R. G. Prinn, M. Rigby, B. Ringeval, M. Santini, M. Schmidt, D. T. Shindell, I. J. Simpson, R. Spahni, L. P. Steele, S. A. Strode, K. Sudo, S. Szopa, G. R. van der Werf, A. Voulgarakis, M. van Weele, R. F. Weiss, J. E. Williams, and G. Zeng, Three decades of global methane sources and sinks, *Nature Geoscience*, *6*(10), 813–823, doi:10.1038/ngeo1955, 2013.

Fraser, A., P. I. Palmer, L. Feng, H. Boesch, A. Cogan, R. Parker, E. J. Dlugokencky, P. J. Fraser, P. B. Krummel, R. L. Langenfelds, S. **O'Doherty**, R. G. Prinn, L. P. Steele, M. van der Schoot, and R. F. Weiss, Estimating regional methane surface fluxes: the relative importance of surface and GOSAT mole fraction measurements, *Atmospheric Chemistry & Physics*, *13*(11), 5697–5713, doi:10.5194/acp-13-5697-2013, 2013.

Pieterse, G., M. C. Krol, A. M. Batenburg, C. A. M. Brenninkmeijer, M. E. Popa, S. **O'Doherty**, A. **Grant**, L. P. Steele, P. B. Krummel, R. L. Langenfelds, H. J. Wang, A. T. Vermeulen, M. Schmidt, C. Yver, A. Jordan, A. Engel, R. E. Fisher, D. Lowry, E. G. Nisbet, S. Reimann, M. K. Vollmer, M. Steinbacher, S. Hammer, G. Forster, W. T. Sturges, and T. Röckmann, Reassessing the variability in atmospheric H_2 using the two-way nested TM5 model, *Journal of Geophysical Research: Atmospheres*, *118*(9), 3764–3780, doi:10.1002/jgrd.50204, 2013.

Rigby, M., R. G. Prinn, S. O'Doherty, S. A. Montzka, A. McCulloch, C. M. Harth, J. Mühle, P. K. Salameh, R. F. Weiss, D. **Young**, P. G. **Simmonds**, B. D. Hall, G. S. Dutton, D. Nance, D. J. Mondeel, J. W. Elkins, P. B. Krummel, L. P. Steele, and P. J. Fraser, Re-evaluation of the lifetimes of the major CFCs and CH_3CCl_3 using atmospheric trends, *Atmospheric Chemistry & Physics*, *13*(5), 2691–2702, doi:10.5194/acp-13-2691-2013, 2013.

Arnold, T., C.M. Harth, J. Mühle, A.J. **Manning**, P.K. Salameh, J. Kim, D.J. Ivy, L.P. Steele, V.V. Petrenko, J.P. Severinghaus, D. Baggenstos, and R.F. Weiss, Nitrogen trifluoride global emissions estimated from updated atmospheric measurements, PNAS 2013 110 (6) 2029-2034, 2013, d oi:10.1073/pnas.1212346110.

Logan, J.A., Staehelin, J., Megretskaia, I.A., Cammas, J.-P, Thouret, V., Claude, H., De Backer, H., Steinbacher, M., Scheel, H.-E., Stubi, R.,Frohlich, M., and **Derwent,** R. Changes in ozone over Europe: Analysis of ozone measurements from sondes, regular aircraft (MOZAIC) and alpine surface sites. Journal of Geophys.Res., 117,D09301,doi:10.1029/2011JD016952.

Parrish, D.D., Law, K.S., Staehelin, J., **Derwent**, R., Cooper, O.R.,Tanimotot, H., Volz-Thomas, A., Gilge, S., Scheel, H.-E., Steinbacher, M., and Chan, E. Long-term changes in lower tropospheric baseline ozone concentrations at northern mid-latitudes. Atmos. Chem. Phys., 12, 11485-11504, 2012.

Parrish, D.D., Law, K.S., Staehelin, J., **Derwent**, R., Cooper, O.R.,Tanimotot, H., Volz-Thomas, A., Gilge, S., Scheel, H.-E., Steinbacher, M.,and Chan, E. Lower tropospheric ozone at northern mid-latitudes: Changing seasonal cycle. Geophys. Res. Letters, 40, 1-6, 2013, DOI: 10.1002/grl.50303, 2013.

Rigby, M., R. G. Prinn, S. **O'Doherty**, S. A. Montzka, A. McCulloch, C. M. Harth, J. Mühle, P. K. Salameh, R. F. Weiss, D. **Young**, P. G. **Simmonds**, B. D. Hall, G. S. Dutton, D. Nance, D. J. Mondeel, J. W. Elkins, P. B. Krummel, L. P. Steele, and P. J. Fraser, Re-evaluation of the lifetimes of the major CFCs and CH3CCl3 using atmospheric trends, Atmos. Chem. Phys., 13(5), 2691–2702, doi:10.5194/acp-13-2691-2013, 2013.

2.4 Meetings

- AGAGE meeting (Jeju, S. Korea, 11th -17th May 2013)
- Mace Head site visit (Ireland,16th- 23rd June 2013)
- DECC4 meeting (Bristol, 25th June 2013) – New sites meeting
- GAUGE coordination meeting (University of Edinburgh, 28th July 2013)
- DECC project meeting (Bristol 1st October 2013)
- Tacolneston site visit (Norfolk, 2nd – 3rd October 2013)
- AGAGE meeting Boston, USA, 14th -18th October 2013)
- Ridge Hill site visit (Herefordshire, 30th October 2013)
- Ridge Hill site visit (Herefordshire, 1st November 2013)
- DECC5 meeting (London, 28th November 2013) – New sites meeting
- InGOS Project review meeting (Brussels, 2nd December 2013)
- GAUGE meeting (University of Bristol, 6th – 8th January 2014)
- InGOS workpackage meeting (Zurich, 13th – 15th January 2014)
- Bilsdale site installation (Yorkshire, 27th – 31st January 2014)
- Ridge Hill site visit (Herefordshire, 20th February 2014)
- GAUGE stakeholder meeting (London, 12th March 2014)
- DECC meeting (London, 13th March 2014)
- FAAM meeting (Cranfield University, 18th March 2014)
- Bilsdale site visit (Yorkshire 20th – 21st March 2014)
- AGAGE meeting (Ascona, Switzerland, 26th April – 3rd May 2014)

2.5 Related information

Project website: www.metoffice.gov.uk/atmospheric-trends

3 Instrumentation

Sites -> Species	Mace Head MHD	Tacolneston TAC	Ridge Hill RGL	Angus TTA
CO_2	Picarro 2301*(1)*	Picarro 2301*(1)*	Picarro 2301*(1)*	Picarro 2301*(1)*
CH_4	Picarro 2301(1), GC-FID*(40)*	Picarro 2301*(1)*	Picarro 2301*(1)*	Picarro 2301(1)
N_2O	GC-ECD*(40)*	GC-ECD*(20)*	GC-ECD*(20)*	-
SF_6	Medusa*(120)*	GC-ECD*(20),* Medusa*(120)*	GC-ECD*(20)*	-
H_2	GC-RGA*(40)*	GC-RGA*(20)*	-	-
CO	GC-RGA*(40)*	GC-RGA*(20)*	-	-
CF_4	Medusa*(120)*	Medusa*(120)*	-	-
C_2F_6	Medusa*(120)*	Medusa*(120)*	-	-
C_3F_8	Medusa*(120)*	Medusa*(120)*	-	-
c-C_4F_8	Medusa*(120)*	Medusa(120*)*	-	-
HFC-23	Medusa*(120)*	Medusa*(120)*	-	-
HFC-32	Medusa*(120)*	Medusa*(120)*	-	-
HFC-134a	Medusa*(120)*	Medusa*(120)*	-	-
HFC-152a	Medusa*(120)*	Medusa*(120)*	-	-
HFC-125	Medusa*(120)*	Medusa*(120)*	-	-
HFC-143a	Medusa*(120)*	Medusa*(120)*	-	-
HFC-227ea	Medusa*(120)*	Medusa*(120)*	-	-
HFC-236fa	Medusa*(120)*	Medusa*(120)*	-	-
HFC-43-10mee	Medusa*(120)*	Medusa(120)	-	-
HFC-365mfc	Medusa*(120)*	Medusa*(120)*	-	-
HFC-245fa	Medusa*(120)*	Medusa*(120)*	-	-
HCFC-22	Medusa*(120)*	Medusa*(120)*	-	-
HCFC-141b	Medusa*(120)*	Medusa*(120)*	-	-
HCFC-142b	Medusa*(120)*	Medusa*(120)*	-	-
HCFC-124	Medusa*(120)*	Medusa*(120)*	-	-
CFC-11	Medusa*(120)*	Medusa*(120)*	-	-
CFC-12	Medusa*(120)*	Medusa*(120)*	-	-
CFC-13	Medusa*(120)*	Medusa*(120)*	-	-
CFC-113	Medusa*(120)*	Medusa*(120)*	-	-
CFC-114	Medusa*(120*	Medusa*(120)*	-	-
CFC-115	Medusa*(120)*	Medusa*(120)*	-	-
H-1211	Medusa*(120)*	Medusa*(120)*	-	-
H-1301	Medusa*(120)*	Medusa*(120)*	-	-
H-2402	Medusa*(120)*	Medusa*(120)*	-	-
CH_3Cl	Medusa*(120)*	Medusa*(120)*	-	-
CH_3Br	Medusa*(120)*	Medusa*(120)*	-	-
CH_3I	Medusa*(120)*	Medusa*(120)*	-	-
CH_2Cl_2	Medusa*(120)*	Medusa*(120)*	-	-
CH_2Br_2	Medusa*(120)*	Medusa*(120)*	-	-
$CHCl_3$	Medusa*(120)*	Medusa*(120)*	-	-
$CHBr_3$	Medusa*(120)*	Medusa*(120)*	-	-
CCl_4	Medusa*(120)*	Medusa*(120)*	-	-
CH_3CCl_3	Medusa*(120)*	Medusa*(120)*	-	-
$CHCl=CCl_2$	Medusa*(120)*	Medusa*(120)*	-	-
$CCl_2=CCl_2$	Medusa*(120)*	Medusa*(120)*	-	-

Table 1: Operational sites, instrumentation and observed species. Number in brackets indicates frequency of calibrated air measurement in minutes.

3.1 Sites

A brief summary of site operations is presented below; a more detailed account of operations over the past year is presented in the Appendices. A more detailed description of the instrumentation is detailed on the website.

3.1.1 Mace Head (MHD)

- Medusa GC-MS: Overall, the Medusa experienced a number of trap related problems over the reporting period. These problems have caused periods of downtime, but mainly have only impacted the most volatile compounds – PFC-14, PFC-116, SF_6, HFC-23. A solution has been found, after an extended period of troubleshooting.
- NF_3 was added to the list of measured compounds in June 2013.
- GC-MD: The MD proved yet again to be a most reliable system and performed well for the reporting period. Most of the data loss resulted from ancillary equipment failure or late gas delivery.

3.1.2 Ridge Hill (RGL)

- Ridge Hill began operation in February 2012 and has collected 26 months of data from two sample inlets at 45 m and 90 m.
- GC-ECD: The ECD instrument has undergone a trouble free year.
- CRDS: The CRDS has been running well over the last 12 months.

3.1.3 Tacolneston (TAC)

- Tacolneston began operation in July 2012 and has collected 21 months of data
- Medusa GC-MS: The Medusa has generally performed well since it was installed. CF_4 data was lost during January 2013 due to coolant problems. A significant improvement in precision was achieved for many species after the introduction of the rolling SIM windows.
- GC-MD: The MD has operated well since it was installed.
- CRDS: The CRDS sampling from 54 m and 100 m inlets has operated without problems during the period. In January 2013, additional measurements from the 185 m inlet were initiated.

3.1.4 Angus (TTA)

- The University of Bristol (UoB) took over routine operation of Angus in January 2013 and has collected 16 months of data since this transition. Sampling from an inlet at 222 m continues using a Picarro G2301 CRDS instrument, which measures CH_4 and CO_2. This equipment was purchased from a NERC grant.
- The site has operated well during the past 12 months, and is visited by a local site operator on a monthly basis to carry out routine maintenance and repairs.
- The sample inlet does not currently have a sample cup or shield, which can allow liquid water to enter the sample line. If the manual water drain at the foot of the tower is not emptied on a regular basis, there is the possibility of water entering the Picarro CRDS. Owing to the very wet conditions over winter 2013-2014, there had been several water contamination episodes, resulting in some data loss over this period.
- An inter-comparison exercise with the European InGOS project was conducted in February 2014.

4 Description of data analysis methods

4.1 Introduction

This chapter discusses the methods used to analyse the observations from the UK DECC network. The following chapter presents the results for the key gases that are reported through the UNFCCC process and then, following that, the analysis of the remaining gases observed by the UK DECC Network.

The first section describes the method for estimating the long-term Northern Hemisphere atmospheric baseline trend, the growth rate and the seasonal cycle of each gas measured at Mace Head given knowledge of the recent history of the air as it travels to the station.

The subsequent section presents the InTEM (Inversion Technique for Emission Modelling) inversion system. This is the tool that is used to estimate the UK and North West European (NWEU) (UK + Ireland + France + Germany + Belgium + The Netherlands + Luxembourg + Denmark) emissions of each gas for each year from 1990 or from when the observations started.

4.2 Northern Hemisphere Atmospheric Baseline Trend Analysis

4.2.1 Summary

The Met Office particle transport model, NAME (Numerical Atmospheric dispersion Modelling Environment), is run in backward-running mode to estimate the dilution of emissions from recent (within 30-days) surface releases to a concentration at the observing station, Mace Head on the west coast of Ireland. These, so called air history maps, have been produced for each two hour period from 1989 until present day. NAME is 3-dimensional therefore it is not just surface transport that is modelled, an air parcel can travel from the surface to a high altitude and then back to the surface but only those times when the air parcel is within the lowest 100 m above the ground will it be recorded in the surface air history maps. The impact of air from higher altitudes arriving at the surface at Mace Head is also separately recorded. The model domain covers North America to Russia and North Africa to the Arctic Circle and extends to more than 10 km vertically. No chemical or deposition processes were modelled; this is realistic given the long atmospheric lifetimes of the gases considered.

The first step is to estimate the Northern Hemisphere atmospheric background concentration (referred to as the baseline) of each gas measured at Mace Head; their long-term baseline trends and growth rates and their seasonal cycle. Baseline concentration times are defined here as those times when the air mass arriving at Mace Head has not been influenced by significant emissions within the previous few weeks (varying depending on how quickly the winds move the air from the edge of the defined model domain to Mace Head, i.e. those times when the air is well mixed and is representative of the Northern Hemisphere background concentration. Figure 7 shows two example air history maps, the one on the left shows a 2-hour period when the air mass will be considered baseline, the one on the right, when the air mass is not considered baseline because of the recent influence of Europe, a source region. Times when the air has rapidly descended to Mace Head from the upper troposphere (defined here as above 9 km) are also not considered baseline because many gases have a strong vertical gradient, usually decreasing concentration with height.

Fitting a time-varying line through just those Mace Head observations recorded within the 2-hour time periods when the air masses are representative of the Northern Hemisphere baseline it is possible to extract from the observational data an estimate of the hourly baseline across the entire measurement record. The hourly baseline can then be further interrogated to estimate monthly and annual values, reveal whether the Northern Hemisphere atmospheric concentration is growing or declining and the strength of the baseline seasonal cycle. Figure 22 shows the results for methane.

4.2.2 Introduction

This section describes the method behind the analysis of the baseline concentrations of the Mace Head observations from Feb 1989 - Mar 2014 inclusive. Baseline concentration times are defined here as those times when the air mass arriving at Mace Head has not been influenced by significant emissions within the previous few weeks (varies depending on how quickly the winds move the air from the edge of the defined computational domain to Mace Head – see below), i.e. those times when the air is well mixed and is representative of the mid-latitude Northern Hemisphere background concentration.

The observations at Mace Head from 1989 to March 2014 have been analysed for each gas measured. The principle tool used to estimate the baseline concentrations is the NAME dispersion model. The methodology used is presented first, followed by the analysis of each individual gas. The analysis considers the long-term trend of the monthly and annual baseline concentrations, their rate of growth and their seasonal cycle.

4.2.3 Methodology

This section describes in detail how the monthly baseline concentrations for each gas observed at Mace Head were derived. There are several specific stages to the process and the section is broken down into these segments with examples were possible.

The NAME model is run in backwards mode to estimate the recent history (30 days) of the air on route to Mace Head. Air history maps, such as those shown in Figure 7, have been calculated for each 2-hour period from 2003 until Mar 2014 using UM meteorology and from 1989-2002 using ERA-Interim meteorology, amounting to more than 100,000 maps. The model output estimates the 30-day time-integrated air concentration (dosage) at each grid box (40 km horizontal resolution and 0-100 m above ground level) from a release of 1 g/s at Mace Head (the receptor). The model is 3-dimensional therefore it is not just surface transport that is modelled, an air parcel can travel from the surface to a high altitude and then back to the surface but only those times when the air parcel is within the lowest 100 m above the ground will it be recorded in the surface maps. The impact of air from higher altitudes arriving at the surface at Mace Head is also, separately, recorded. The computational domain covers 100^{o}W to 45.125^{o}E longitude (North America to Russia) and 10^{o}N to 80.125^{o}N (North Africa to Arctic Circle) latitude and extends to more than 10 km vertically (actual height varies depending on version of meteorology used). For each 2-hour period, 40,000 inert model particles were used to describe the dispersion. No chemical or deposition processes were modelled; this is realistic given the long atmospheric lifetimes of the vast majority of gases considered.

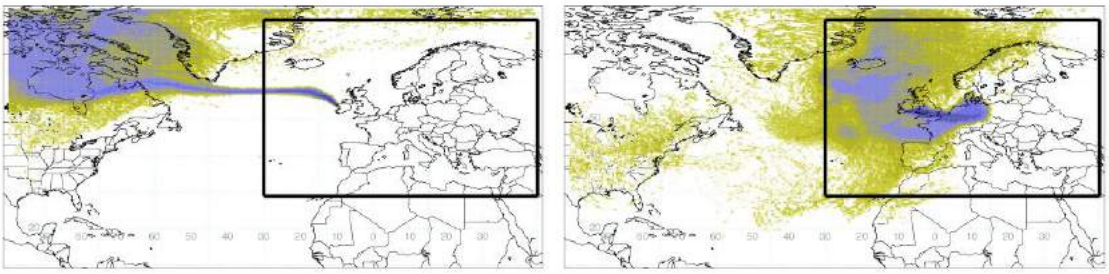

(a) (b)

Figure 7: Examples of 2-hour air history surface maps derived from NAME (a) baseline period (b) regionally polluted period. The air-history surface maps describe which surface areas (defined as within 100 m of the surface) in the previous 30-days impact the observation point at a particular time.

By dividing the dosage (g s/m^3) by the total mass emitted (3600 s/hr x 2hr x 1 g/s) and multiplying by the geographical area of each grid box (m^2), the model output is converted into a dilution matrix (s/m). Each element of this matrix *D* dilutes a continuous emission (*e*) of 1 g/m^{2}s from a given grid box over the previous 30 days to an air concentration (g/m^3) at the receptor (*o*) during a 2-hour period.

$$D\,\underline{e} = \underline{o} \qquad \text{…Equation 1}$$

Baseline concentrations are defined here as those that have not been influenced by significant emissions within the previous 30-days of travel on route to Mace Head, i.e. those that are well mixed and are representative of the mid-latitude Northern Hemisphere background concentrations.

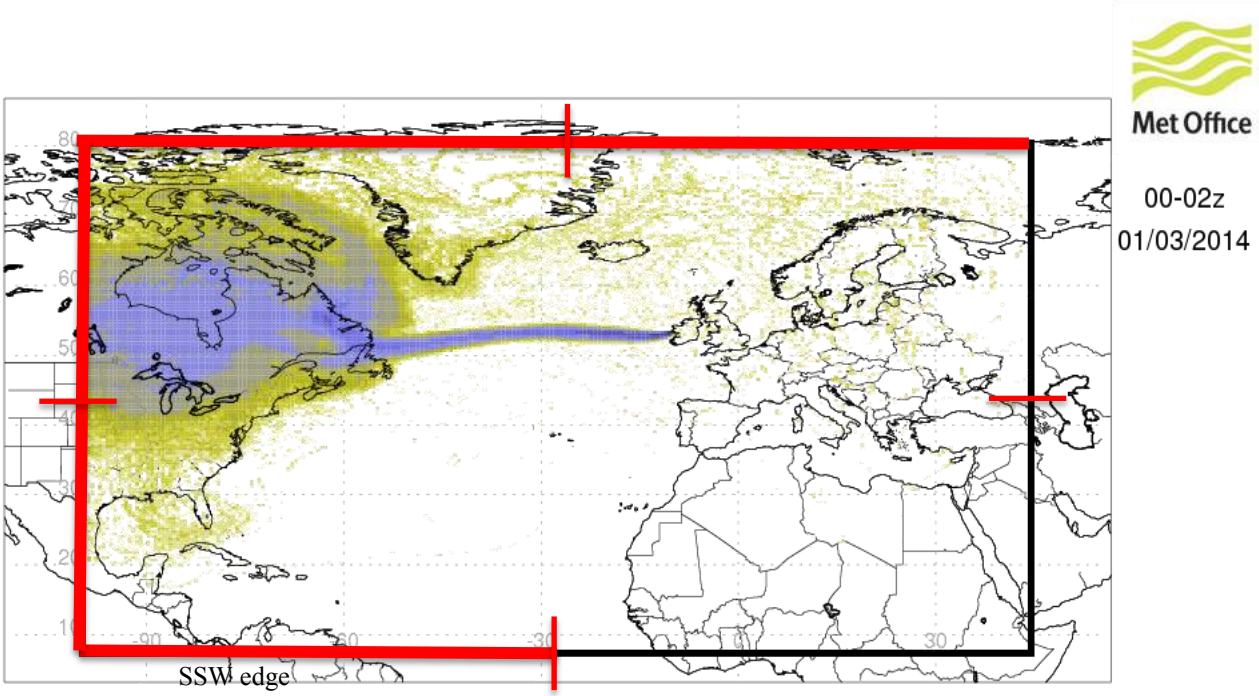

Figure 8: Dominant baseline edges are shown in red.

A 2-hour period is classed as 'baseline' if it meets the following criteria:

- **The total air concentration from the nine grid boxes centred on and surrounding Mace Head is less than ten times the *dilution sensitivity limit* i.e. local emissions do not significantly contribute.**
- **The total air concentration contribution from a population map is less than an arbitrary limit. The limit is set so that it is clear that populated regions have not significantly contributed.**
- **The dominant edge where the particles enter the domain is from the south-west, west or north (see Figure 8).**
- **The percentage of air entering directly from the south-south-west edge does not overly dominate (more than 1.5 times west or north edges)**
- **Less than 20% of the air entering the domain has come from higher than 9km, i.e. from the upper troposphere.**

In order to define a *dilution sensitivity limit* it is necessary to arbitrarily decide on a level of emission that would produce an agreed response at the observation point. In this study we chose an emission of 100 kt CH_4 /yr/grid to produce a 10 ppb impact. As shown later, 10 ppb is approximately the noise found in the baseline signal for methane and an emission of 100 kt/year is about 4% of the estimated UK release of methane in 2006. 10 ppb CH_4 is equivalent to ~7 ug/m^3. Assuming a horizontal grid resolution of 40 km at a latitude of 50^o N, 100 kt CH_4 /yr/grid is approximately ~2 ug/m^2/s, thus the *dilution sensitivity limit* is calculated, using equation 1, to be 3.4 s/m (~2.2e-9 s/m^3 at Mace Head).

The *dilution sensitivity limit* is attempting to define a threshold above which an emission source would generate a concentration at Mace Head that would be discernible above the baseline noise. The same limit value is used for all of the gases analysed. The chosen limit is arbitrary but the impact of doubling it is small.

Figure 9 shows a three-month extract of the methane observations measured at Mace Head. The observations have been colour coded to indicate whether, using the above classification, the air mass they were sampled from was considered baseline. For the baseline analysis all non-baseline observations are removed.

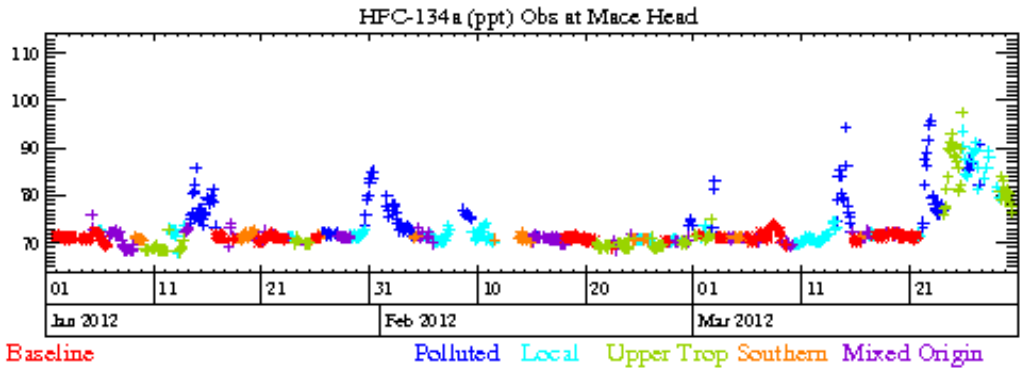

Figure 9: 3-month time-series of Mace Head HFC-134a observations showing the impact of the baseline and non-baseline classification. The baseline observations are shown in red.

The points defined as baseline using the above methodology still have a certain level of noise. The principle reasons for this are; unexpected short-lived emissions e.g. forest fires in Canada or from shipping, local emissions that are not identified using the above criteria above, incorrectly modelled meteorology or transport, i.e. European or southerly or upper troposphere air defined as baseline by error.

Irrespective of the methodology used to identify these events some will inevitably be classed as baseline when it is inappropriate to do so. To capture such events the baseline data are statistically filtered to isolate and remove these non-baseline observations. For each baseline point in turn, the baseline points in a 40-day window surrounding this central value are considered and, provided that there are sufficient points (>11 with at least 4 in each third of the window or more than 18 in two thirds), a quadratic is fitted to these values. The standard deviation of the actual points and the fitted curve is calculated (*std*) and if the current baseline value is more than *x std* away from the fitted value it is marked for exclusion from the baseline observations. After all baseline points have been considered, those to be excluded are removed. The process is repeated nine times, each time the value for *x* is gradually reduced from 6 to 2, thus ensuring that those points statistically far from the fitted baseline do not unduly affect the points to be excluded by skewing the fitted curve. If there are insufficient baseline points in a 40-day window the values are only included if the spread in the points is small and there are at least 5

For each hour in the time-series the baseline points in a running 40-day window are fitted using a quadratic function and the value extracted for the current hour in question. The process is then advanced by an hour and repeated. If there are insufficient baseline points well spaced within the window (at least 3 in each quarter) it is gradually extended up to 150-days.

For each hour within the observation time record a smoothed baseline concentration is estimated by taking the median of all fitted baseline values within a 20-day time window. If there are fewer than 72 baseline values in the time window then the window is steadily increased up to a maximum of 40 days. If there are still insufficient points then no smoothed baseline concentration is estimated for that hour.

The noise or potential error in the smoothed baseline concentration is estimated to be the standard deviation of the difference between the observations classed as baseline and the smoothed baseline concentrations at the corresponding times. Figure 10 shows, on a much-expanded y-axis compared to Figure 9, the typical spread of baseline observations about the smoothed continuous baseline estimate.

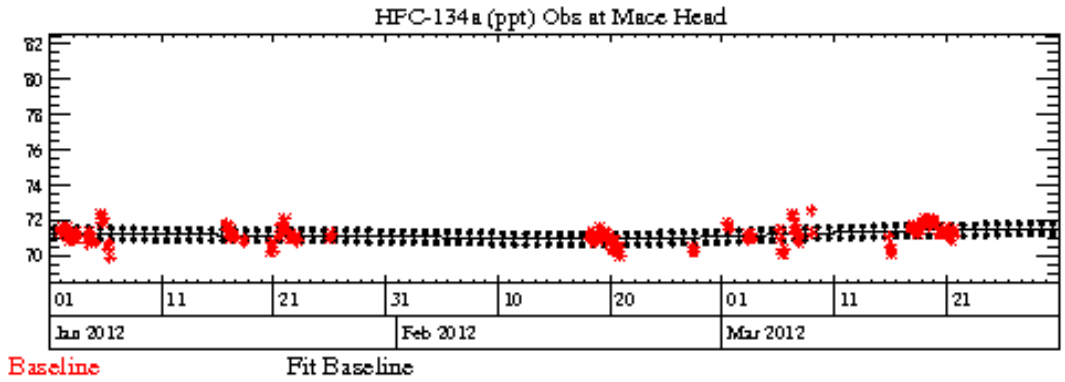

Figure 10: Observations of HFC-134a at Mace Head within a 3-month period classed as baseline (red) with the estimated daily baseline mole fractions with uncertainty for the same period (black). Note: the y-axis has been expanded compared to Figure 9.

The hourly baseline concentrations are split into two components, a long-term trend and a residual component (seasonal cycle). Two methods have been used:

- **Kolmogorov–Zurbenko method**

A Kolmogorov–Zurbenko (KZ) filter involves *k* time iterations of a moving average of a given time duration and is ideally suited to this type of problem. For this application, the length of the moving average window was set to one year and the number of iterations was set to four. With these parameters a 12-month moving average was applied to the data four times, thereby approximately removing wavelengths smaller than 2-years. At each hour in the time-series the 12-month average of the baseline mass mixing ratios centred on this hour is calculated. This is the long-term trend component, subtracting this from the actual hourly baseline estimate at this time gives the residual.

- **3-year quadratic method**

At each hour calculate the 12-month average centred on this hour (y_a). For the three-year period centred on this hour calculate the quadratic line using standard value decomposition that best-fits (minimises) the difference between the computed time-series and y_a. This is the long-term trend component, subtracting this from the actual hourly baseline estimate at this time gives the residual.

Monthly and annual baseline concentrations are estimated by averaging all of the long-term trend daily baseline values within the appropriate time window. A monthly value is estimated if there are at least 21 daily values within the month, this ensures a good representation of the whole month. An annual value is estimated if there are at least 330 daily values within the calendar year, ensuring a good representation of the whole year.

The annual growth rate on a particular day is defined as the local slope of the long-term trend on that day. The local slope is estimated by linearly fitting a best-fit line through the trend concentration values for the day before, current day and day after. Monthly averages of these growth rates are shown for each gas.

The daily residual concentration values are averaged for each month over the data period studied to produce a seasonal cycle. The mean seasonal cycles for each gas are shown for each gas. The range of values for each month is also shown, along with the first, middle and last individual year seasonal cycles.

Gas	1990	1991	1992	1993	1994	1995	1996	1997	1998	1999
CFC-11 (GCMD)	264	267	268	269	268	267	266	264	263	261
CFC-12 (GCMD)	496	506	516	522	529	533	537	540	542	544
CFC-13										
CFC-113 (GCMD)	75.5	81.1	84.2	85.0	84.6	84.6	84.3	83.8	83.2	82.7
CFC-113										
CFC-115										8
HCFC-124										1.3
HCFC-141b						5.1	7.2		11.3	13.3
HCFC-142b						8.0	9.3	10.6	11.4	12.4
HCFC-22										145
HFC-125										1.3
HFC-134a						2.3	4.3	6.2	9.6	13.4
HFC-143a										
HFC-152a						1.2	1.2	1.4	1.9	2.2
HFC-23										
HFC-32										
HFC-227ea										
HFC-236fa										
HFC-245fa										
HFC-365mfc										
HFC-4310mee										
PFC-14										
PFC-116										
PFC-218										
PFC-318										
SF6										
SO2F2										
CH3Cl										533
CH2Cl2							35.9	35.9	34.8	31.7
CHCl3 (GCMD)						12.1	12.5	11.9	12.0	11.4
CHCl3							12.3	11.9	12.5	12.7
CH3CCl3 (GCMD)	151	151	150	139	125	111	95	79	66	55
CH3CCl3										
CCl4 (GCMD)			105	104	103	102	101	100	99	98
CHClCCl2										
CCl2CCl2										
CH3Br										11
Halon-1211						3.5	3.6		4.0	4.2
Halon-1301										2.8
Halon-2402										
CH2Br2										
CHBr3										
CH3I										
CH4 (ppb)	1793	1810	1803	1814	1818	1822	1824	1821	1835	1839
C2H6										
CO (ppb)						118	128	116	146	123
CO2 (ppm)				357	359	361	363	364	367	369
N2O (ppb)	309	310	310	310	312	312	313	314	315	315
O3 (ppb)	35.3	36.2	34.8	35.3	37.1	35.2	37.1	37.9	40.2	41.7
H2 (ppb)						509	514	507	519	520

Table 2: Annual Northern hemisphere baseline mass mixing ratios for all gases measured at Mace Head 1990-1999 (ppt unless stated).

Gas	2000	2001	2002	2003	2004	2005	2006	2007	2008	2009
CFC-11 (GCMD)	260	259	256	255	253	250	248	246	244	243
CFC-12 (GCMD)	546	546	546	546	545	544	543	541	539	536
CFC-13					2.8	2.8			2.9	2.9
CFC-113 (GCMD)	82.2	81.5	80.7	79.9	79.3	78.7	77.8	77.1	76.6	75.9
CFC-113						78.8	77.9		76.6	76.0
CFC-115	8.1	8.2	8.1	8.2	8.4	8.4	8.4	8.4	8.4	8.4
HCFC-124	1.4	1.6	1.6	1.6	1.6	1.6	1.6	1.6	1.6	1.6
HCFC-141b	15.1	16.3	17.6	18.6	19.1	19.1	19.5	20.2	20.9	21.2
HCFC-142b	13.6	14.6	15.0	15.5	16.3	16.9	18.0	19.2	20.5	21.4
HCFC-22	151	158	164	169	175	180	187	195	204	211
HFC-125	1.6	2.1	2.4	3.0	3.7	4.2	5.0	5.8	6.9	7.9
HFC-134a	17.1	20.9	25.0	29.6	34.7	39.3	43.7	47.9	53.3	58.0
HFC-143a					5.5	6.4	7.4	8.4	9.5	10.7
HFC-152a	2.5	2.9	3.4	4.1	4.8	5.6	6.8	7.8	8.8	8.9
HFC-23									22.5	23.1
HFC-32					1.1	1.6	2.1	2.7	3.4	4.1
HFC-227ea								0.4	0.5	0.6
HFC-236fa								0.1	0.1	0.1
HFC-245fa								0.9	1.1	1.2
HFC-365mfc						0.3	0.4	0.5	0.5	0.6
HFC-4310mee										
PFC-14					74.9	75.5	76.2	76.9	77.6	78.1
PFC-116					3.6	3.7	3.8	3.9	4.0	4.1
PFC-218					0.4	0.5	0.5	0.5	0.5	0.5
PFC-318										
SF6					5.6	5.8	6.1	6.3	6.6	6.9
SO2F2						1.5	1.5	1.6	1.6	1.7
CH3Cl	516	510	512	520	521	524	520	526	533	528
CH2Cl2	30.4	29.3	29.4	31.1	31.2	30.7	32.5	34.4	36.0	36.6
CHCl3 (GCMD)	11.0	11.7	10.9	11.2	11.4	11.1	11.1	11.0	11.4	10.9
CHCl3	11.7	10.5	10.2	11.0	11.0	10.9	11.2	10.5	10.3	10.0
CH3CCl3 (GCMD)	47	39	32	27	23	19	16	13	11	9
CH3CCl3		39	31	27	23	19	16	13	11	9
CCl4 (GCMD)	97	96	95	94	93	92	91	90	89	88
CHClCCl2				1.3		1	1	1.1	0.8	0.7
CCl2CCl2		5.0	4.8	4.8	4.8	3.9	3.8	3.5	3.4	3.0
CH3Br	10.4	9.8	9.1	8.8	9.0	9.9	9.5	9.1	9.1	8.6
Halon-1211	4.3	4.4	4.4	4.4	4.5	4.5	4.5	4.4	4.4	4.3
Halon-1301	2.9	3.0	3.0	3.1	3.1	3.2	3.2	3.2	3.3	3.3
Halon-2402						0.5	0.5	0.5	0.5	0.5
CH2Br2							1.6	1.6	1.6	1.6
CHBr3						5.3	5.7	4.7	4.7	4.7
CH3I		1.4	1.6	1.7	1.8	1.9	1.4	1.6	1.3	1.0
CH4 (ppb)	1842	1841	1842	1852	1848	1847	1846	1855	1862	1868
C2H6						1280	1300	1320	1360	1080
CO (ppb)	119	116	126	136	123	123	122	120	119	115
CO2 (ppm)	369	371	373	375	378	379	382	384	386	387
N2O (ppb)	316	317	318	318	319	320	320	321	322	323
O3 (ppb)	40.8	40.2	40.7	40.7	40.2	40.4	41.2	40.2	41.8	40.9
H2 (ppb)	511	507	511	512	509	512	516	511	514	510

Table 3: Annual Northern hemisphere baseline mass mixing ratios for all gases measured at Mace Head 2000-2009 (ppt unless stated).

Gas	2010	2011	2012	2013	AvGrow	AvGr12
CFC-11 (GCMD)	241	238	236	235	-1.2	-1.7
CFC-12 (GCMD)	533	531	528	526	1.5	-2.7
CFC-13	2.9	3	3	3	0.02	0.02
CFC-113 (GCMD)	75.3	74.9	74.3	73.6	0.0	-0.8
CFC-113	75.2	74.5	74	73.4	-0.7	-0.6
CFC-115	8.4	8.4	8.4	8.4	0.03	-0.01
HCFC-124	1.5	1.4	1.4	1.3	0.01	-0.06
HCFC-141b	22	23	24.1	24.9	0.9	0.9
HCFC-142b	21.9	22.7	23	23.3	0.9	0.2
HCFC-22	219	226	230	236	6.6	5.4
HFC-125	9.2	10.8	12.4	14.3	0.9	1.8
HFC-134a	63.4	68.4	73.3	78.7	4.3	5.3
HFC-143a	11.9	13.2	14.5	15.9	1.2	1.4
HFC-152a	9.4	9.9	10.1	10.1	0.5	0.02
HFC-23	23.7	24.6	25.5	26.6	0.8	1.0
HFC-32	5.2	6.5	7.7	9.4	0.9	1.5
HFC-227ea	0.6	0.7	0.8	0.9	0.08	0.11
HFC-236fa	0.1	0.1	0.1	0.1	0.01	0.01
HFC-245fa	1.3	1.5	1.7	1.9	0.16	0.19
HFC-365mfc	0.6	0.7	0.8	0.8	0.07	0.07
HFC-4310mee		0.2	0.2	0.2	0.01	0.01
PFC-14	78.7	79.5	80.3	80.9	0.7	0.7
PFC-116	4.1	4.2	4.3	4.4	0.08	0.07
PFC-218	0.6	0.6	0.6	0.6	0.02	0.01
PFC-318		1.3	1.4	1.4	0.04	0.04
SF6	7.2	7.5	7.8	8.1	0.3	0.3
SO2F2	1.7	1.8	1.9	2.1	0.08	0.15
CH3Cl	530	518	526	530	-1	10
CH2Cl2	40.0	39.5	41.8	51.0	0.7	7.4
CHCl3 (GCMD)	11.5	11.6	11.6	12.1	-0.03	0.22
CHCl3	10.9	10.9	10.8	11.7	-0.05	0.45
CH3CCl3 (GCMD)	8	7	5	5	-6.3	-1.0
CH3CCl3	7.8	6.5	5.4	4.5	2.8	-1.0
CCl4 (GCMD)	87	86	85	84	-1	-1
CHClCCl2	0.6	0.4	0.3	0.4	-0.1	0.1
CCl2CCl2	3	2.7	2.5	2.4	-0.2	-0.1
CH3Br	8.3	8.3	8.3	7.8	-0.2	-0.3
Halon-1211	4.2	4.2	4.1	4.0	0	-0.1
Halon-1301	3.3	3.3	3.3	3.4	0.04	0.02
Halon-2402	0.5	0.5	0.5	0.4	-0.01	-0.01
CH2Br2	1.7	1.6	1.6	1.7	0.01	0.08
CHBr3	5.3	4.4	4.1	5.2	-0.1	0.5
CH3I	0.9	1.0	0.9	0.7	-0.06	-0.07
CH4 (ppb)	1870	1874	1882	1887	4.3	6.8
C2H6	1400	1390	1530	1540	40	130
CO (ppb)	120	116	125	119	0.4	3.3
CO2 (ppm)	390	392	394		1.93	2.09
N2O (ppb)	323	324	325	326	0.7	0.8
O3 (ppb)	40.3	39.7	40.5	40.7	0.3	1.0
H2 (ppb)	510	517	517	519	0.6	1.5

Table 4: Annual Northern hemisphere baseline mole fractions for all gases measured at Mace Head 2010-2013 (ppt unless stated) and Northern hemisphere baseline growth rates (ppt/yr unless stated): over all years (fifth) and most recent (last column).

4.2.4 Baseline Mole Fractions

For each gas observed at Mace Head a baseline analysis has been performed. ECMWF meteorology is used from 1989 – 2002 inclusive and Met Office meteorology from 2003-2014 inclusive. The figures that follow show, for each gas, the monthly and annual baselines, the changing baseline growth rates and the average seasonal cycle seen within the observations. The gases are grouped into two families; Kyoto and non-Kyoto gases. Table 1 summarises the annual baseline mole fractions within the observation period for each of the gases considered.

4.3 Regional emission estimation

4.3.1 Summary

By removing the time-varying baseline concentrations from the raw measurement data, a time-series of excursions from the baseline, averaged over each 2-hour period, for each observed gas has been generated. The perturbations above baselines, observed across the UK DECC network, are driven by emissions on regional scales that have yet to be fully mixed on the hemisphere scale and are the principle tool used to estimate surface emissions across north-west Europe. A method for estimating emissions from observations, referred to as 'Inversion Technique for Emission Modelling' (InTEM), has been developed over many years and is used here to estimate Devolved Administration (DA), UK and North-West European (NWEU) emissions using the observations from the UK DECC network.

InTEM links the observation time-series with the NAME air history estimates of how surface emissions dilution as they travel to the observation stations. An estimated emission distribution when combined with the NAME output can be transformed into a modelled time-series at each of the measurement stations. The modelled and the observed time-series can be compared using a single or a range of statistics (referred to as a cost function) to produce a skill score for that particular emission distribution. InTEM uses a well known best-fit technique, simulated annealing, to search for the emission distribution that produces a modelled times-series that has the best statistical match to the observations. InTEM can either start from a random emission distribution or from an inventory-defined distribution.

In order for InTEM to provide robust solutions for every area within the modelled domain, each region needs to significantly contribute to the air concentrations at the UK DECC network on a reasonable number of time periods. If the signal from an area is only rarely or poorly seen by the network, then its impact on the cost function is minimal and the inversion method will have little skill at determining its true emission. The contributions that different grid boxes make to the observed air concentration varies from grid to grid. Grid boxes that are distant from the observation site contribute little to the observation, whereas those that are close have a large impact. In order to balance the contribution from different grid boxes, those that are more distant are grouped together into increasingly larger regions. The grouping cannot extend beyond country (or DA) boundaries. The country boundaries extend into the surrounding seas to reflect both emissions from shipping, off-shore installations and river runoff but also because the inversion has geographical uncertainty.

There is significant uncertainty in the emissions that are estimated. Uncertainty arises from many factors: errors in the baseline estimate; emissions that vary over time-scales shorter than the inversion time-period e.g. diurnal, seasonal or intermittent; heterogeneous emissions i.e. emissions that vary within the regions solved for; errors in the transport model (NAME) or the underpinning 3-dimensional meteorology; errors in the observations themselves. The potential magnitudes of these uncertainties have been estimated and are incorporated within InTEM to inform the uncertainty of the modelled results.

4.3.2 InTEM (Inversion Technique for Emission Modelling)

The observation time-series, together with the NAME model output predicting the recent history of the air, was used to estimate the emission distribution of each gas over North West Europe. The iterative best-fit technique, simulated annealing [Press *et al* 1992], was used to optimise these regional emission estimates using a statistical skill score (cost function) comparing the observed and modelled time-series at the observational network. The technique, referred to as InTEM, starts

from a set of random emission maps, it then searches for the emission map that produces a modelled time series at the observational network that most accurately mimics the observations.

The aim of InTEM is to estimate the spatial distribution of emissions across a defined geographical area (Figure 11). In the equation to solve (Equation 1) the set of observations (*o*) and the dilution matrix (*D*) estimated using NAME, are known. The observations are in volume mixing ratios. The dilution matrix has units (s/m) and is calculated from the time-integrated air concentrations produced by the NAME model. The dilution matrix has *t* rows equal to the number of 2-hour periods considered and has *n* columns equal to the number of grid points in the defined geographical domain. This matrix dilutes a continuous emission of 1 g/m^2s over a given grid to an air concentration (g/m^3) at the receptor during a 2-hour period. The observations are converted from volume mixing ratio [ppb] to air concentration (g/m^3) using the modelled temperature and pressure at the observation point.

The inversion domain is chosen to be a smaller subset of the full domain used for the air history maps. It covers 14.30^o W – 30.76^o E longitude and 36.35^o N – 66.30^o N latitude and is shown as the black box in Figure 7. The smaller domain covers all of Europe and extends into the Atlantic and has an intrinsic horizontal resolution of 0.352^o longitude by 0.234^o latitude. The inversion domain needs to be smaller to ensure re-circulating air masses are fully represented but also because emission sources very distant from the UK DECC network have little discernible impact on the concentration at the stations, i.e. the signal would be too weak to be seen. The inversion method assumes baseline concentration air enters the inversion domain regardless of direction and altitude. For the eastern, southern and upper edges in particular this will be incorrect. Emissions in Russia and around the Black Sea would be expected to elevate the atmospheric concentrations along the eastern edge, and due to the latitudinal and vertical gradient it would be reasonable to assume below mid-latitudinal baseline concentration air enters from the south and above. Those times when significant air enters from the south or from the upper edge (9km) are excluded from the inversion process as they cannot be accurately modelled. This issue is overcome in the inversion by solving for, but not analysing, the estimated emissions in any grid on the edge of the inversion domain. It is assumed that the error of above or below baseline concentration air entering the domain will be absorbed into the solutions in these edge grids.

In order for the best-fit algorithm to provide robust solutions for every area within the domain, each region needs to significantly contribute to the air concentration at the UK DECC network on a reasonable number of time periods. If the signal from an area is only rarely or poorly seen by the network, then its impact on the cost function is minimal and the inversion method has little skill at determining its true emission.

The contribution that different grid boxes make to the observed air concentration varies from grid to grid. Grid boxes that are distant from the observation site contribute little to the observation, whereas those that are close have a large impact. In order to balance the contribution from different grid boxes, those that are more distant are grouped together into increasingly larger blocks. The grouping varies for each time period considered and between the different gases due to varying meteorology and the impact of missing observations respectively. The underlying horizontal grid resolution is approximately 25 km (0.352^o longitude by 0.234^o latitude) and is equal to the resolution of the NAME output. The base grid used is shown in Figure 11(a) and conforms to country (and DA) boundaries. The country boundaries extend into the surrounding seas to reflect both emissions from shipping, off-shore installations and river runoff but also because the inversion has geographical uncertainty. Each area from the base grid is then considered in turn. If the contribution (impact) from an area at the network is above a defined threshold then the area is sub-divided into two areas. This splitting process is continued until each area just falls below the threshold or the fine (25km) grid resolution is reached. An example grid used in the inversion process when only Mace Head (MHD) observations are available is shown in Figure 11(b). The threshold used for the splitting process has been arbitrarily defined as 600 (50 days x 12 [number of 2-hour periods per day] = 600) times and the *dilution sensitivity limit* threshold is 3.4 s/m, as derived in the baseline analysis. The sensitivity of the emission results to this arbitrary choice of threshold is, through investigation, considered to be below the baseline sensitivity that is included in the inversions. However this uncertainty will be

considered in more detail in the final year of the project and will be reported on in the final contract report.

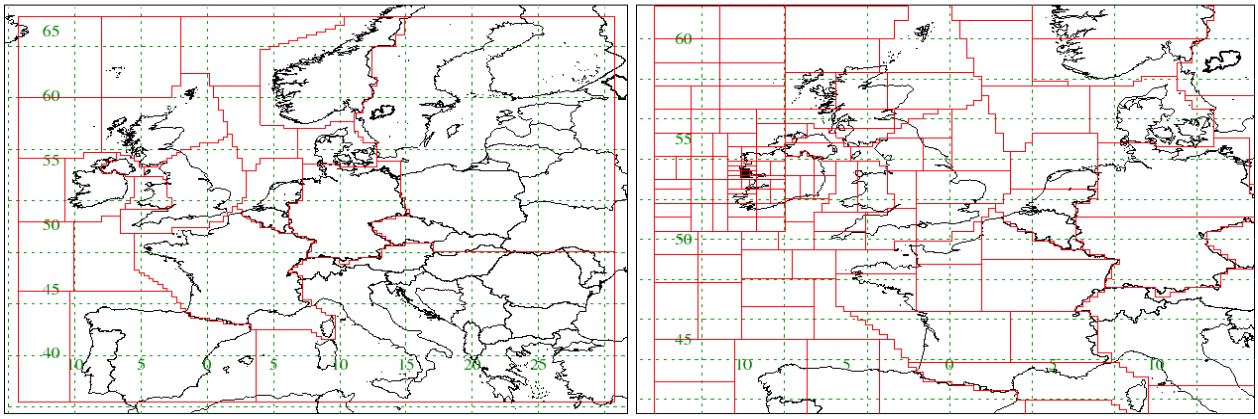

(a) (b)

Figure 11: (a) Base regions conforming to country (and Devolved Administration) boundaries (b) Example of the distribution of the different sized regions used by InTEM to estimate regional emissions (finest scale of the grid is ~25 km) when only MHD observations are available.

The modelled time-series at each measurement station is calculated by applying the current emission map to the dilution matrix for that station (Equation 1).

The inversion process works by iteratively choosing different emissions, varying the emission magnitudes and distributions, with the aim of minimising the mismatch between the observations and the modelled concentrations. No *a priori* conditions are set. The relative skill of a derived emission map is tested by comparing the modelled and observed time-series by using a cost function.

The cost function described here uses the baseline uncertainty as discussed and described in the previous section. This uncertainty varies from gas to gas depending on how well a smooth baseline can be constructed through the 'clean' observations.

An upper (lower) time-series of observations is constructed by adding (subtracting) the baseline uncertainty to the actual observations. These two time-series enclose a range of values that are entirely plausible within the uncertainty of the baseline definition. Given a modelled emission distribution (emission map), a modelled time-series is constructed. The sum of the absolute magnitudes of the modelled minus observed values normalised by the uncertainty at each time is calculated and used as a measure of the skill of the current modelled emission map. The uncertainty at each 2-hour period is comprised of different elements:

a) Observational uncertainty: The repeatability of the observation and the variability of the observations within the 2-hour window.
b) Baseline uncertainty: As discussed above.
c) Uncertainty of modelling local emissions: Local (sub-grid scale) emissions cannot be effectively modelled, therefore the degree of influence of the local area at each time is used to increase the uncertainty at that time.

The iteration process is repeated until the future potential improvement in skill in the emission map is estimated to be negligible.

To simulate uncertainties in the meteorology, dispersion and observations the inversion process is applied to three observation time-series; (a) the actual observations (b) observations minus the baseline noise and (c) observations plus the baseline noise.

Any periods that were classed as baseline but were removed by the statistical filtering are removed from the analysis as these are considered to be unrepresentative of air from that sector. Times

when the surface air is classed as being significantly influenced by upper troposphere or southerly air masses are likewise removed from the analysis.

The 'local' contribution is estimated by summing the surface contributions from the 9 grids surrounding the observation station. Times with significant local influence are typically characterised by low wind speeds and low boundary layer heights and thus poor dispersion conditions. During such times the meteorological models used, with horizontal resolutions of between 25 and 80 km, are poor at correctly resolving the local flows as they are dominated by sub-grid scale processes, e.g. land-sea breezes.

For inversions when only MHD observations are available solutions are calculated for three-year periods. When observations from other stations are available the time period is reduced to one-year. After solutions have been estimated for a particular time period, the time period is moved on by one month and the process repeated, e.g. Jan'95 – Dec'97, Feb'95 – Jan'98, etc.

A monthly/annual estimate of emission is calculated by averaging all of the solutions that contain a complete month/calendar year within the solved-for time period. The range for each month/year for each geographical region is calculated from the same sample of solutions and is taken as the 5th and 95th percentile solutions.

Figure 12 is an example of the observed and modelled time series of air concentration for CH_4 for 2010 at Mace Head. The magnitudes and patterns are similar and demonstrate that the inversion process is able to derive an emission map that produces a good match to the observations.

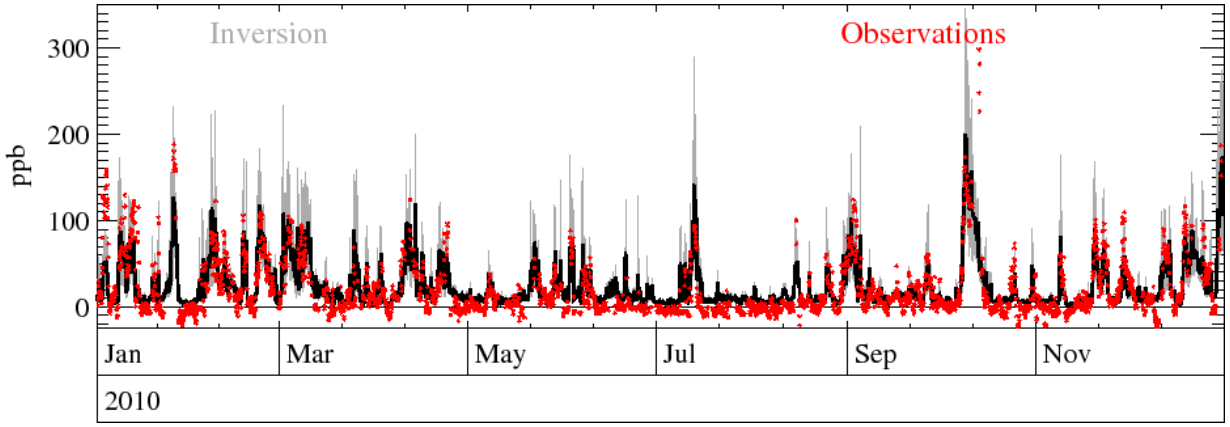

Figure 12: Time series of observed and best-fit modelled CH_4 mole fractions (deviation from baseline) at Mace Head for the first three months of 2010 (solid black line = Inversion, grey = uncertainty in inversion, red crosses = observations).

Emission totals from specific geographical areas are calculated by summing the emissions from each 25 km grid box in that region (Figure 13). The emissions are also presented after they have been re-distributed by the population distribution in the inversion grid that has been used. The population distribution map used is shown in Figure 14. This final step does not in anyway alter the emissions per country, it is purely to demonstrate the likely distribution of the emissions. For some gases, such as HFC-134a, this re-distribution is entirely justified as all emissions are anthropogenic and are related to mobile air conditioning (e.g. cars) and therefore will have a strong correlation with population. For other gases, e.g. CH_4, or PFC-14 the correlation with population is less strong as there is a significant contribution from other sectors e.g. the agricultural sector for CH_4 and aluminium production for PFC-14.

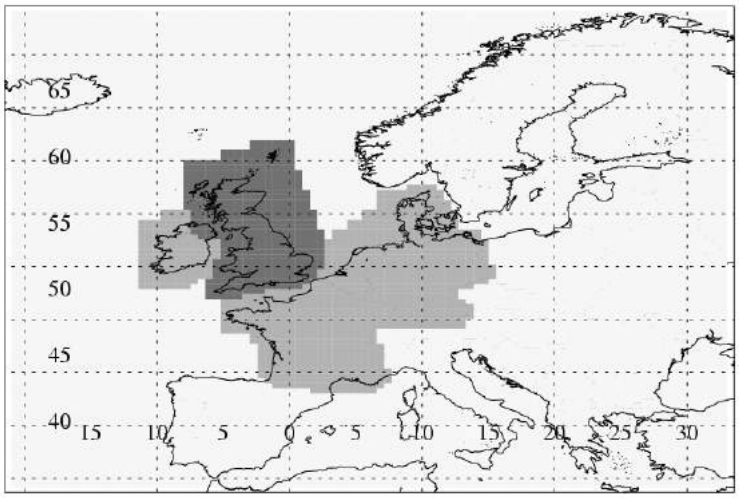

Figure 13: Geographical areas used to define UK and North West European (NWEU) regional totals

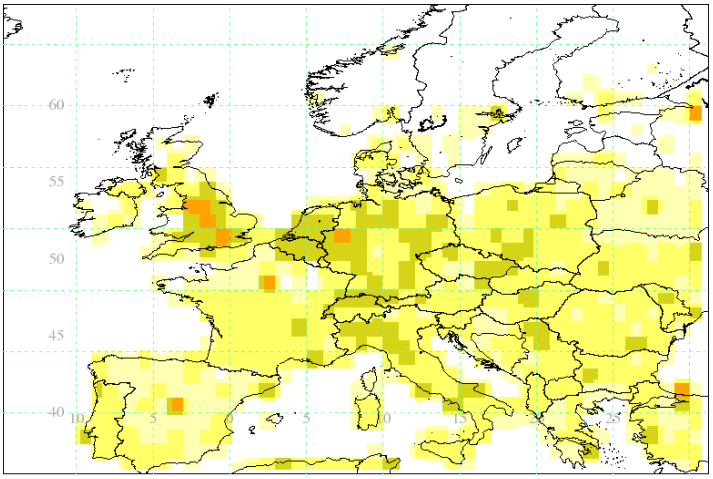

Figure 14: Population distribution used to re-distribute emissions within inversion grid.

All of the emissions are assumed constant in time and are geographically static within each inversion study period. This is clearly a significant simplification. A sudden, but subsequently maintained, change in emission, will be picked up by solving multiple 3-year periods covering slightly different time periods, i.e. solving for a 3-year period and then advancing by one month. Enhanced emissions in any particular season, e.g. increased N_2O emissions in spring following fertilizer application, will not be resolved when the time period is 3-years.

All areas of the domain are assumed to impact reasonably equally on the measurement network. The grouping of grid cells together, so that each area contributes approximately equally to the observations, attempts to ensure this but clearly there will be some variability. Also large grid cells could have significant variability actually within the grid itself especially if there are significant orographic features within the grid, e.g. the Alps. This may lead to errors if certain parts of the grid are more frequently sampled than others. However because of the large travel distances and therefore time elapsed between emission in these large grids and measurement the impact of this will be small. Also by only reporting emissions within NWEU this issue is assumed small.

The inversion method makes no distinction between anthropogenic and natural sources and thus its estimates are for the combined total, making direct comparisons with the UNFCCC inventory difficult. For most of the gases analysed here the natural emissions are estimated to be small in comparison to the anthropogenic emissions. For example, for CH_4 the natural emissions in NWEU are estimated to be 240 kt/yr [Bergamaschi *et al.* 2005].

It is also important to recognise that the release of certain gases to the atmosphere, e.g. N_2O released from agricultural practices, may occur many miles from its actual source and therefore

adds to the uncertainty of using the maps to attribute emissions to particular regions. The area considered to be the UK includes the waters directly surrounding the UK (Figure 13), so the impact of this is considered to be small for the UK. This would be problematic if the individual contributions of Belgium or The Netherlands for example were presented and is the reason why only the NWEU total is considered. The most significant region in relation to this issue is the border between Northern Ireland and Ireland, however due to the proximity to Mace Head and the corresponding high resolution of the output there the impact is assumed small.

The transport modelling and thus the inversion algorithm also assume that the loss processes associated with each gas are negligible within the regional domain. Given the atmospheric lifetimes of the vast majority of the gases studied here this is considered to be a robust assumption. The clear exception is $CHClCCl_2$, which has a lifetime of around a week depending on the season of the year.

4.4 Improvements to InTEM (April 2011 – April 2014)

This section describes the technical improvements to the InTEM modelling system during the contract period. There have been improvements to how the baseline is estimated and how uncertainty in the inversion process is represented and split into its constituent components.

4.4.1 Improve baseline classification

Use where the air enters the computational model domain to better define baseline times. This involves splitting the model edge into 8 sectors e.g. west-north-west, west-south-west, south-south-west etc., and also recording when significant air that has recently been in the upper troposphere (above 9 km) arrives at the observation station.

4.4.2 Baseline algorithm amended

The baseline algorithm was amended to incorporate where the air enters the model domain. For the air to be classed as baseline the vast majority of the air has to enter the domain from the SSW, west or northern edges. Also excluded are times when significant air has descended from the upper troposphere.

4.4.3 Below baseline observations not fixed to zero

Previously any observation that was below baseline, leading to a negative perturbation above baseline, was assigned a value of zero. This was because only the perturbation was available within the cost function routine. This has been altered so that the baseline is now also available. This means that the 2-hourly averaged observations can now be directly compared to the modelled deviations + estimated baseline, thereby removing the need for this zeroing step. The size of these negative deviations therefore now impact on the skill score assigned to each modelled emission map.

4.4.4 Each observation has an individual uncertainty

The uncertainty (+/- about the mean baseline) associated with each modelled observation is now available. This means that the uncertainty can change over the measurement period. This uncertainty is made up of different elements:

- Uncertainty in the baseline within a time window (6-months) centred on the current time.
- Observational repeatability
- Observational variability within each 2-hour period.
- Uncertainty due to the degree of impact of any local emissions.
- Baseline uncertainty of the measurement stations in the network, with the exception of Mace Head where the baseline is defined, is doubled.

4.4.5 Alternate cost function has been developed

The distance of model time-series from the observations, relative to the baseline uncertainty, is a good measure of the quality of the current emission map and fully takes into account the allowable uncertainty at each observation time. The contribution to the score of an emission map is increased

as the difference between the modelled value and the observed value increases. The maximum cost any one observation is limited by tending to the logarithm of the difference.

Cost function:

$D_t = ABS(M_t – O_t)/U_t$

If $D_t < 2$ then $C_t = D_t * D_t$ (Range = 0 – 4)
If $2 <= D_t < 8$ then $C_t = 2 + D_t$ (Range = 4 – 10)
If $D_t >= 8$ then $C_t = 10 + \log(D_t – 8 + 1)$ (Range = 10+)

M_t = Modelled value at time *t*
O_t = Observed value to time *t*
U_t = Overall uncertainty at time *t*
C_t = Cost of the mis-match at time *t*

4.4.6 Solve with High and Low baseline possibilities

The baseline has an uncertainty. The inversion system is now solved three times, once with the mean baseline, once using the lower limit of the baseline possibility and once with the upper limit. Any systematic bias in the estimated baseline is thus considered within the uncertainty of the emission estimates.

4.4.7 Baseline trends / Cycles

The estimation of the long-term trend, growth rate and seasonal cycle of each gas has been improved. The hourly baseline concentrations are split into two components, a long-term trend and a residual component (seasonal cycle). Two methods are now used (to illustrate the uncertainty in this estimation process), see sections 4.2 for more details:

- **Kolmogorov–Zurbenko method**

- **3-year quadratic method**

4.4.8 New inversion grid that conforms to country outlines

Within the inversion system, InTEM, the basic core grid resolution of the maps is approximately 25 km. In order to balance the contributions from different regions these core grid boxes need to be grouped together as the distance from the observation point increases. In previous studies the grids have been grouped into 2x2, 4x4, 8x8, 16x16 and 32x32 larger grids. However this grouping takes no account of country borders therefore different countries will appear under the same large grid box, see Figure 15. This grouping has been improved so that the grouping ultimately conforms to the country borders. The borders of countries of interest now serve to limit the largest size that each region can become. Figure 16 shows the extent of each of these large regions with each region independently coloured (the actual colour is irrelevant). These large regions are sub-divided into smaller domains depending on the amount of information each region contributes to the observation point. Figure 17 shows the outcome of the new gridding process. Note that the country borders are extended into the surrounding seas and oceans to ensure a country's emissions are fully captured.

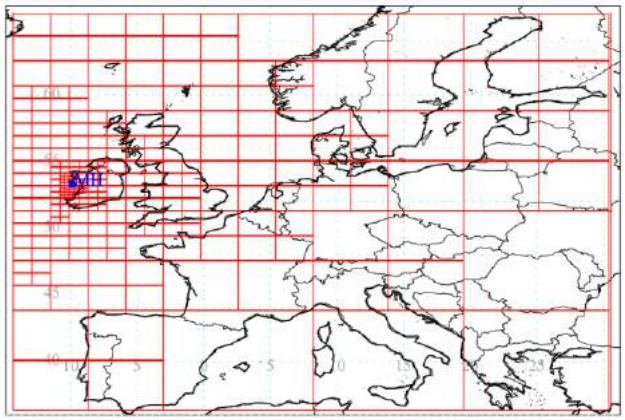

Figure 15: Grid resolution from old system for a 3-year inversion period with Mace Head observations.

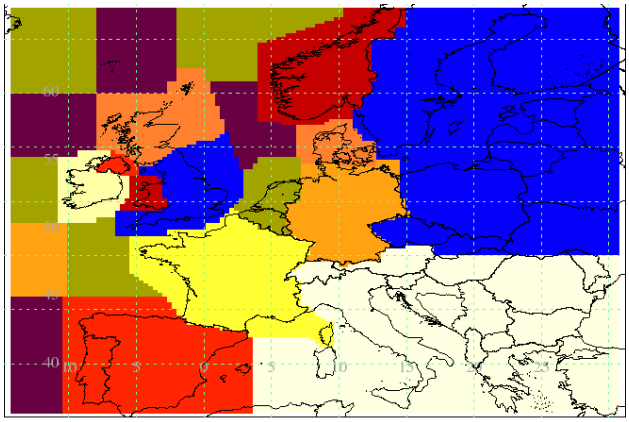

Figure 16: Extent of the large regions used to define the new inversion grid

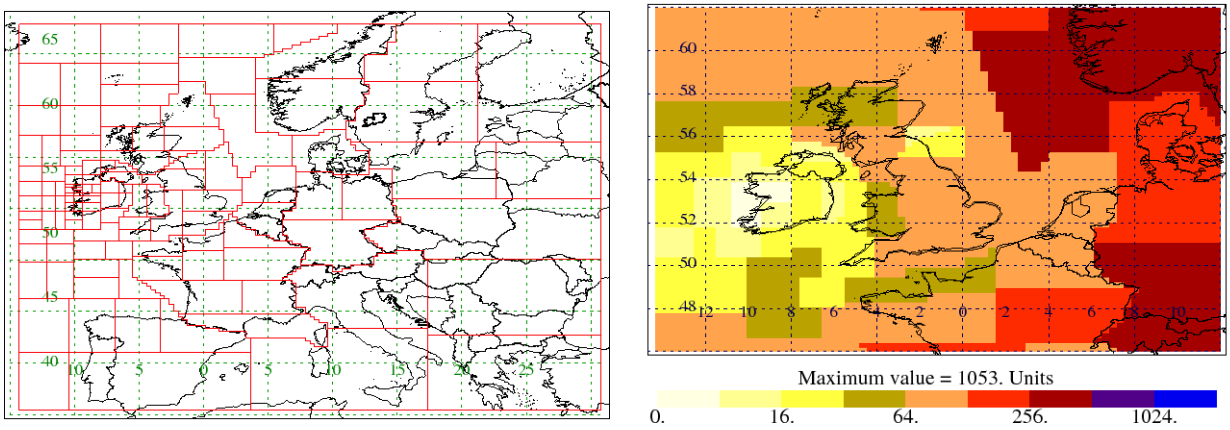

Figure 17: New inversion grid (regions) that conforms to country boundaries (Left); Example of the number of core basic grids in each of the inversion regions (Right).

The new gridding system within InTEM allows a cleaner distinction between different countries and this is important when emissions are estimated from the Devolved Administrations (DAs).

4.5 Incorporating new UK DECC network observations

The observations from Ridge Hill (Mar 2012), Tacolneston (Jul 2012) and Angus (May 2013) have been incorporated into the inversion system. The Ridge Hill N_2O and SF_6 observations prior to July 2012 have significantly more noise due to the temperature instability in the housing unit at the station. Previously these were discarded but now are included as the increased noise is included in the observational uncertainty. The baseline estimated from the Mace Head observations was

assumed to be appropriate for the new sites and have been used throughout this analysis (see Figures 18 and 19). The close proximity of Mace Head to the new sites relative to the inversion domain justifies this approach but is an area where future improvements can be made.

Angus CH_4 data have only been used from May 2013. Earlier data have required significant re-analysis to ensure sufficient quality and were not ready in time for this analysis. In future work these earlier measurements will be included.

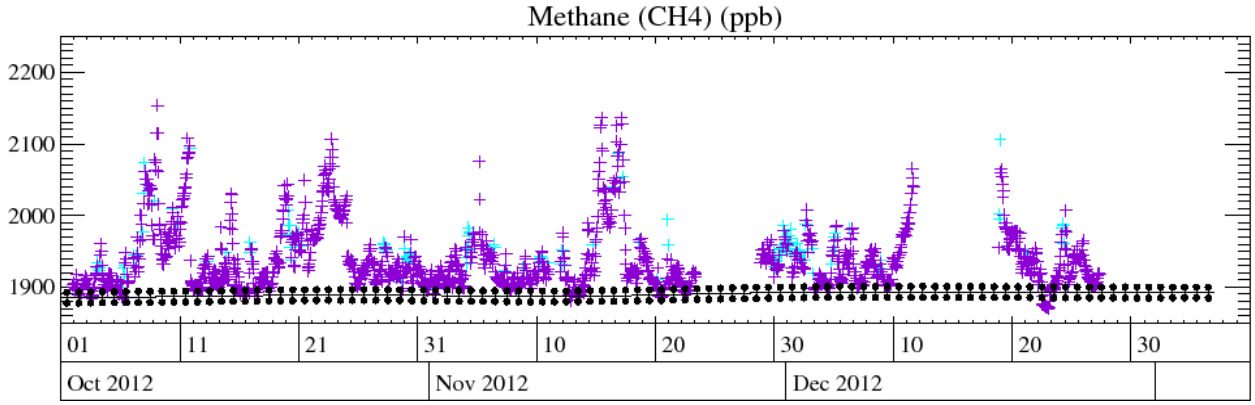

Figure 18: Portion of Ridge Hill CH_4 observations over-plotted with Mace Head baseline. Light blue points classed as local but are used in the inversion, albeit with larger uncertainty.

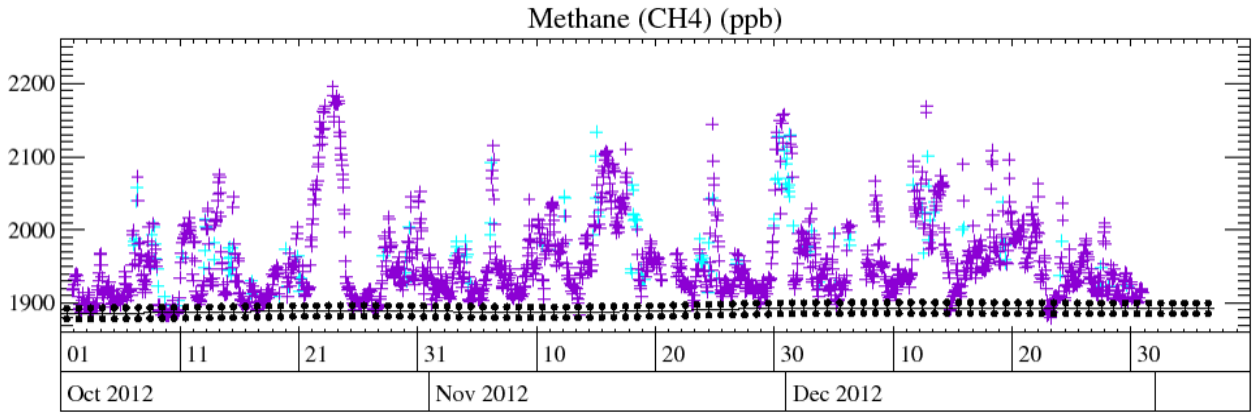

Figure 19: Portion of Tacolneston CH_4 observations over-plotted with Mace Head baseline. Light blue points classed as local but are used in the inversion, albeit with larger uncertainty.

CH_4 observations are recorded at two heights at Ridge Hill and three at Tacolneston. The observations from both heights at Ridge Hill (45 m and 90 m) are included. Currently only the lower two observations at Tacolneston (54 m and 100 m) are used. In future work the upper (185 m) observational record will be included. Any significant vertical gradient in the observations that will not be well modelled will simply lead to an increase in the observational uncertainty at that time.

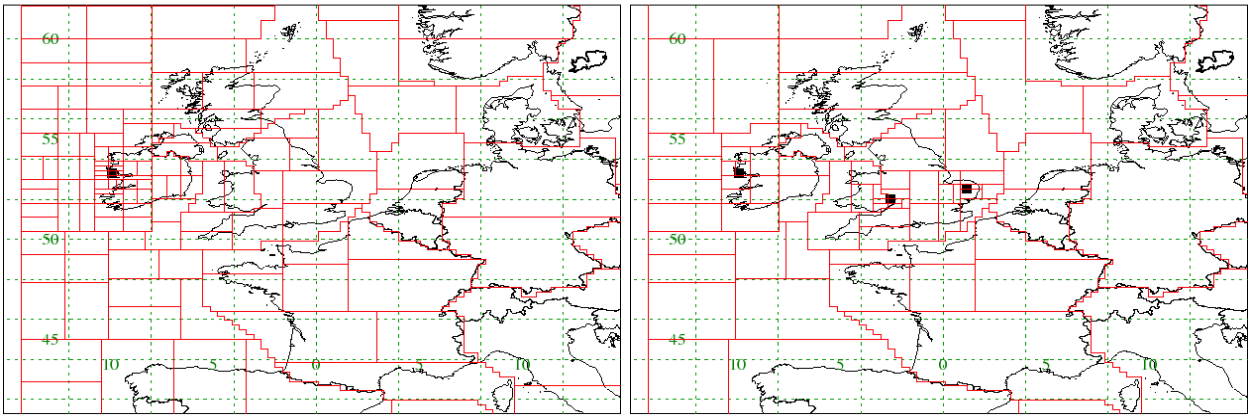

(a) (b)

Figure 20: (a) InTEM grid used for SF_6 for the period Jan 2010 – Dec 2012 MHD-only (b) InTEM grid used for SF_6 for the period Jul 2012 – Dec 2012 3-sites.

The inversion results using the whole UK DECC network (1-year time periods) are presented for each gas in the Kyoto basket and compared to the (3-year time period) Mace Head-only inversions.

4.6 Devolved Administration emission estimates

This section describes how the UK emission totals per year per gas have been sub-divided into four devolved administration (DA) areas; Scotland, Northern Ireland, Wales and England. Figure 21 shows the four regions that have been defined to make up the UK emission region. As previously noted the UK (and DA) region extends into the sea areas to reflect the fact that: (a) some of the anthropogenic emissions may occur out to sea for example oil/gas extraction or river run-off where material is transported out to sea before it is released to the atmosphere, and (b) the inversion system will have a degree of spatial error and so allowing some extension beyond the land-country areas is appropriate.

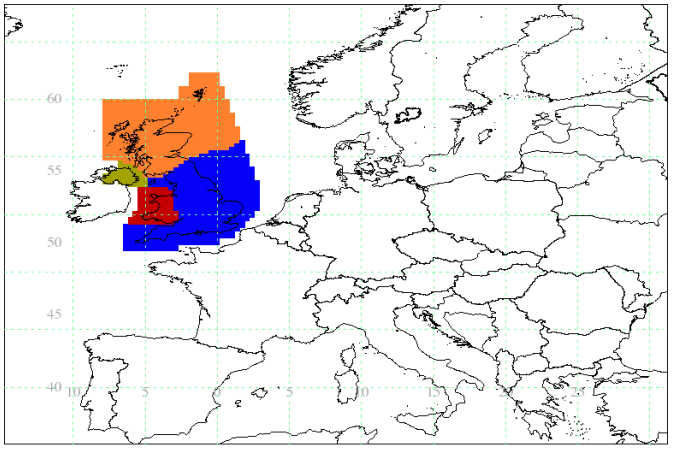

Figure 21: The UK region as defined in the inversion system. The separate colours indicate the four devolved administration areas.

The emissions per gas per year per DA for SF_6, N_2O and CH_4 from a preliminary analysis are presented in the relevant sections for these gases. Only 2012 -2014 observations have been used in this analysis to date because the extended UK DECC network only started in March 2012. The UK emissions are usually dominated by the emissions from England. The relative uncertainties in the DA regions with smaller geographical areas are larger.

5 Results and analysis of gases reported to the UNFCCC

5.1 Introduction

This section discusses the atmospheric trends and regional emissions of the gases that are measured at the UK DECC network and that are reported to the UNFCCC (United Nations Framework Convention on Climate Change). Table 5 describes the principle uses of each of the gases, their radiative efficiency, atmospheric lifetime and global warming potential in a 100-year framework (GWP_{100}).

Gas	Chemical Formula	Main Use	Radiative Efficiency (W $m^{-2}ppb^{-1}$)	Atmos. lifetime (years)	GWP_{100}
HFC-125	CHF_2CF_3	Refrigeration blend, fire suppression	0.23	30.5	3,420
HFC-134a	CH_2FCF_3	Mobile air conditioner	0.16	13.5	1,370
HFC-143a	CH_3CF_3	Refrigeration blend	0.13	51.4	4,470
HFC-152a	CH_3CHF_2	Aerosol propellant, foam-blowing agent	0.09	1.6	133
HFC-23	CHF_3	Bi-product of manufacture of HCFC-22	0.19	228	14,200
HFC-32	CH_2F_2	Refrigeration blend	0.11	5.4	716
HFC-227ea	CF_3CHFCF_3	Fire suppression, inhalers, foam blowing	0.26	35.8	3,580
PFC-14	CF_4	Bi-product alum. production, electronics	0.08	>50,000	5,820
PFC-116	C_2F_6	Electronics, bi-product alum. production	0.26	>10,000	12,010
PFC-218	C_3F_8	Electronics, bi-product alum. production	0.26	2,600	8,690
PFC-318	C_4F_8	Semiconductor and electronics industries	0.32	3,200	10,300
SF_6	SF_6	Circuit breaker in high voltage switchgear	0.52	3,200	22,800
CH_4	CH_4	Landfill, farming, energy, wetlands	0.00037	9.8	25
CO_2	CO_2	Combustion	0.0000138	indefinite	1
N_2O	N_2O	Nylon manufacture, farming	0.00303	114	298

Table 5: The principle use, radiative efficiency, atmospheric lifetime and 100-year global warming potential of the gases measured by the UK DECC network and that are reported to the UNFCCC.

In this chapter InTEM results are presented for each of these gases.

For the majority of the gases, those considered to be significantly anthropogenic in origin, the InTEM emission estimates are also presented after a further post-processing step. This additional step redistributes the emissions within each solved-for region according to the population distribution within each region. The total emissions per region and country are unaffected by this post-processing step. It is considered that these population-weighted distributions give a good indication of the actual spread of the emissions at horizontal resolutions that cannot be achieved through the use of just the UK DECC network observations. The statistical match between the observations and the modelled time-series at the network are negligibly affected by this post-processing step because it only affects emissions within each solved-for grid cell.

5.2 Methane (CH_4)

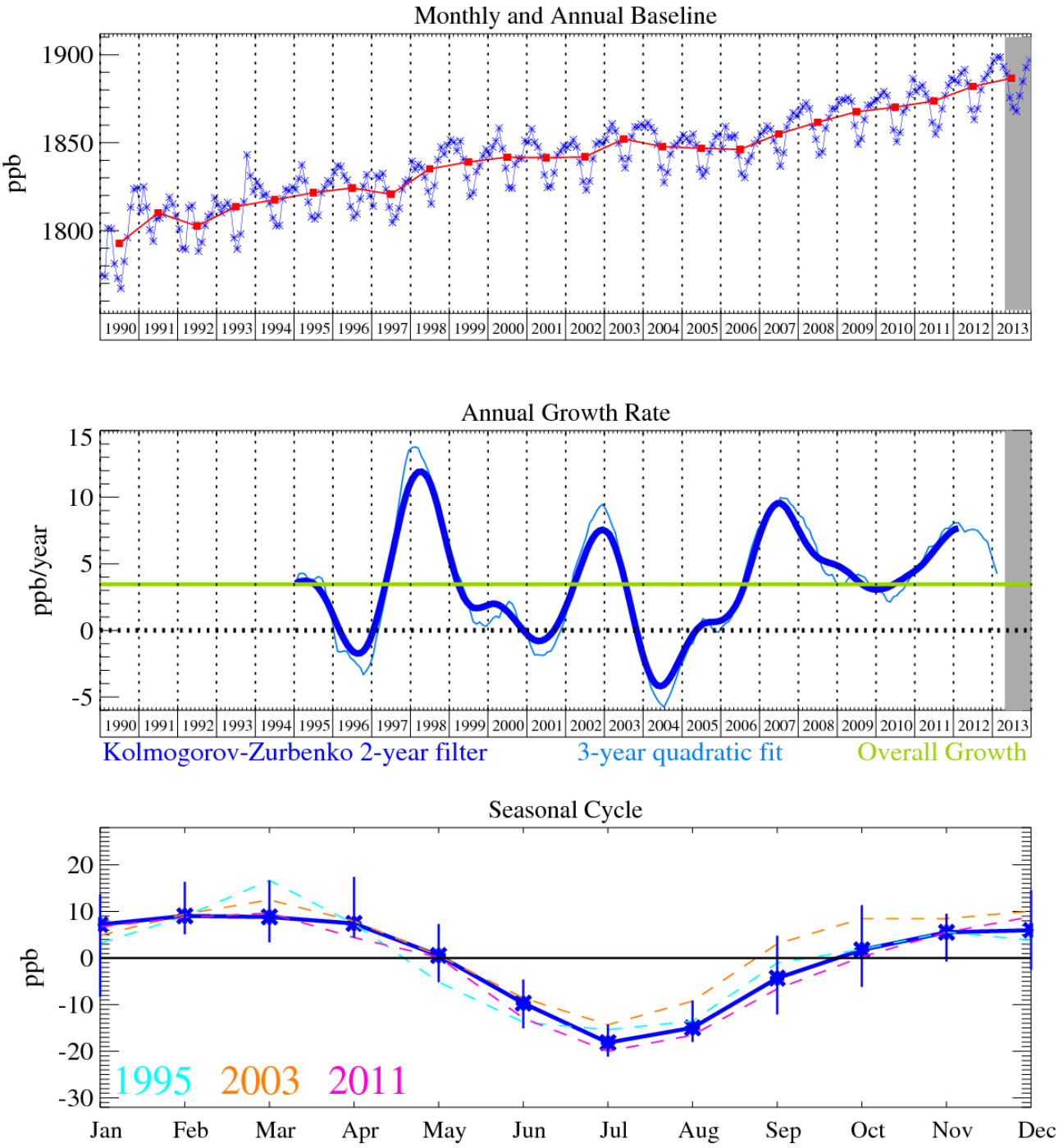

Figure 22: Methane: Monthly (blue) and annual (red) baseline mole fractions (top plot). Annual (blue) and overall average growth rate (green) (middle plot). Seasonal cycle (de-trended) with year-to-year variability (lower plot). Grey area covers un-ratified and therefore provisional data.

The long term trend for CH_4, shown in Figure 22, is of particular interest with a steep rise up to about 2000 followed by a flat period with almost no growth and then most recently a steep rise of up to 9 ppb/yr over the period 2007-2008. Recent growth is estimated to be 4.2 ppb/yr with a mixing ratio of 1897 ppb in December 2013. The growth rate anomaly in 2007-2008 is unusual in that it occurred almost simultaneously in both hemispheres.

In 2007-2008 and 2010-2012 the mole fraction of CH_4 in the atmosphere rose faster than its long-term average growth rate. Several theories are postulated:

- Increased emissions from the high latitudes in the Northern hemisphere related to wetlands and reduced permafrost/snow cover.

- Increased emissions in the tropics due to increased emissions from wetlands/rice production or biomass burning due to El Niño conditions.
- Reduced levels of OH in the atmosphere. OH is the major sink for atmospheric CH_4.

However each of these theories in isolation does not seem to completely fit the evidence gathered so far. For example, there is no evidence for any link to large scale biomass burning (i.e. no concomitant increase in carbon monoxide), as was the case in 1998 - driven by the largest ever El Niño drought.

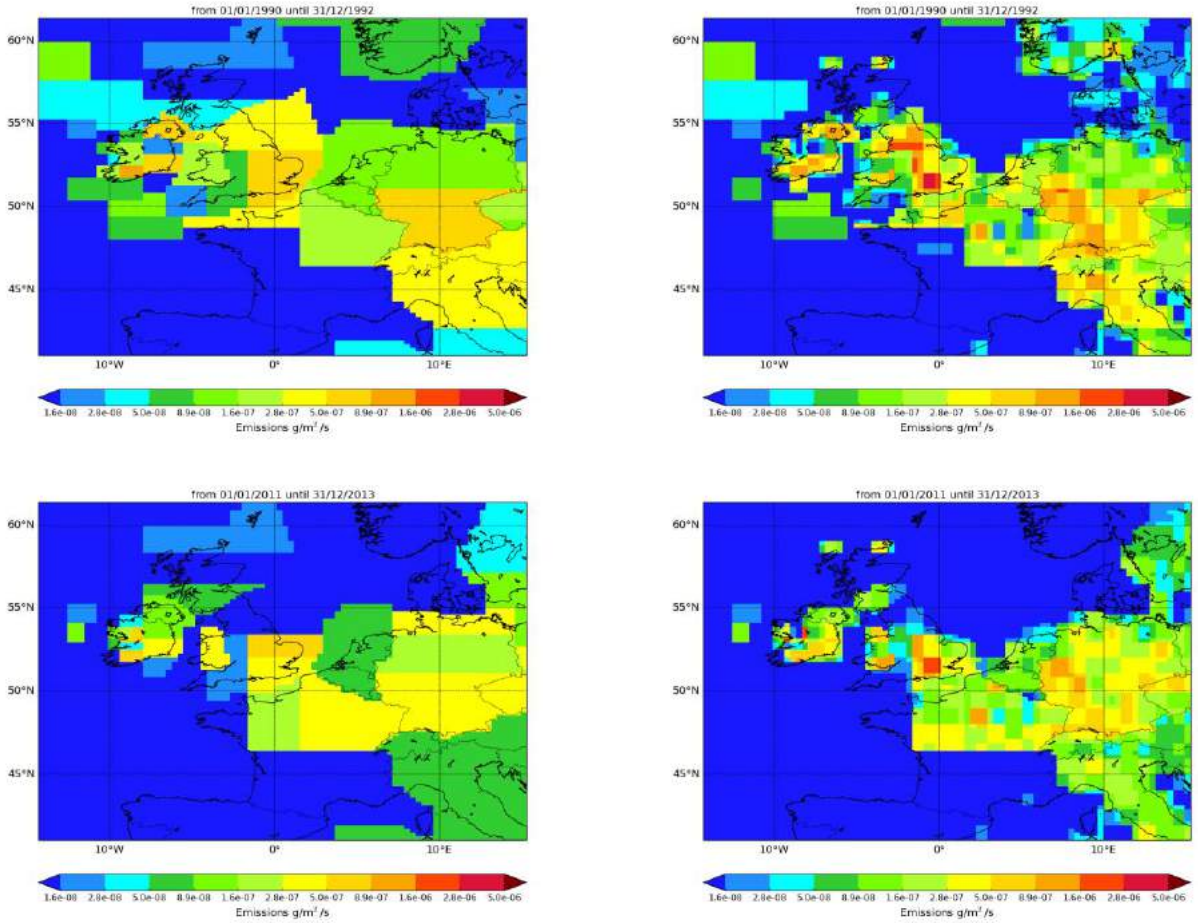

Figure 23: NAME-inversion emission estimates for 1990-1992 (upper) and 2011-2013 (lower). On the right hand side the emissions per grid box have been re-distributed based on population.

The inferences drawn from the observations were that the CH_4 increase is driven by wetland emissions in the boreal region (driven by a temperature anomaly) and in the tropics (possibly driven by a precipitation anomaly) with a small role for OH changes a possibility in the tropics but not statistically significant. Satellite observations have also detected an increase in global mixing ratios in recent years [Bloom *et al*., 2010] and identified increased wetland emissions as a potential cause, consistent with *in situ* measurements. The mole fractions of CH_4 reported from Mace Head (and other AGAGE stations) in 2009 indicate that the rapid rise in CH_4 mole fractions slowed (as shown in Figure 22). Future trends of CH_4 are uncertain but very important as CH_4 has a strong influence on radiative forcing and stratospheric ozone depletion.

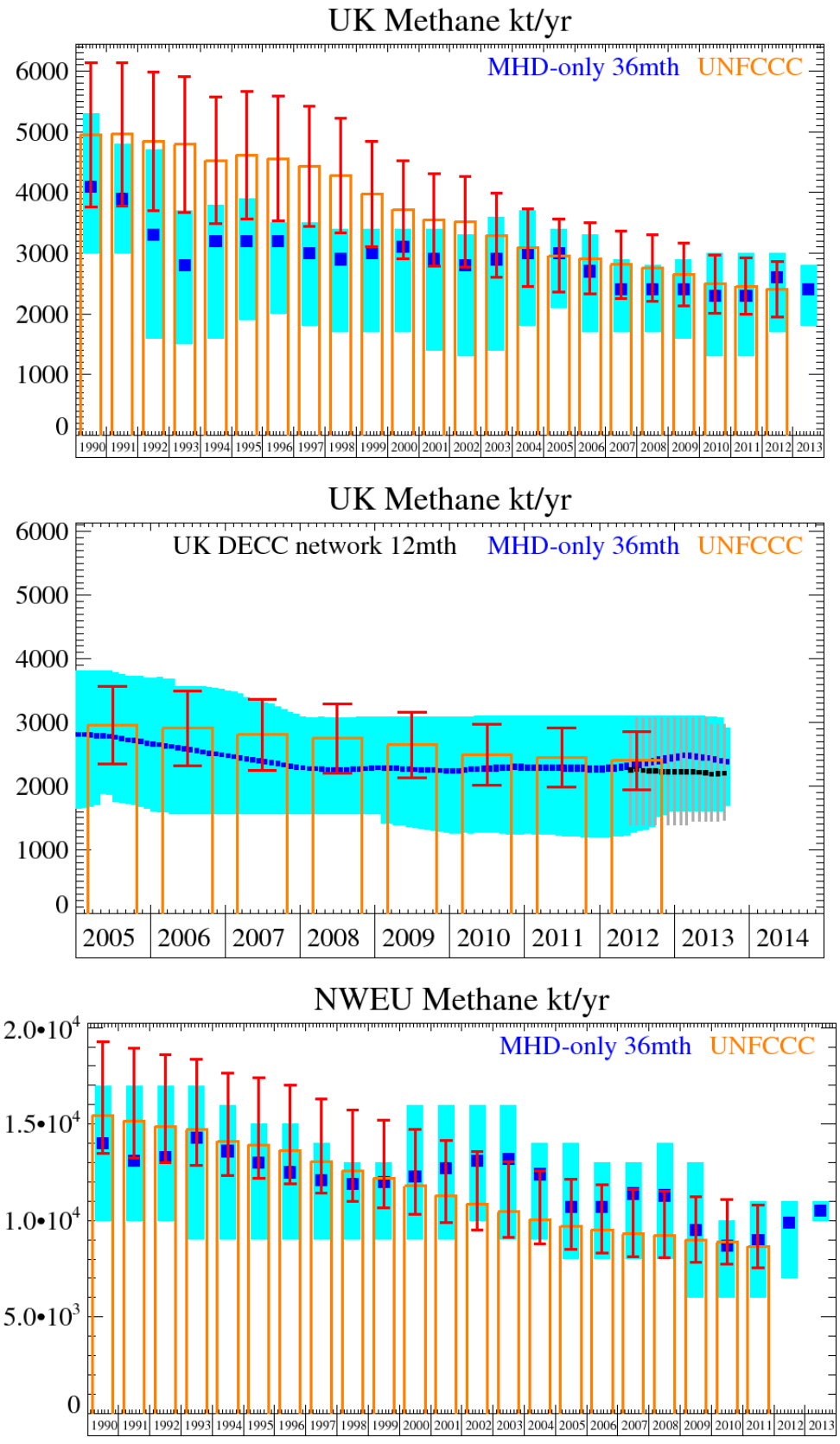

Figure 24: Emission (kt/y) estimates for UK (MHD-only and DECC network) and North West European (NWEU). The uncertainty bars represent the 5th and 95th percentiles.

The inventory and InTEM emission estimates for the UK are similar from 2000 onwards. In the early to late 1990s the InTEM estimates for the UK were markedly lower than the inventory values. For the NWEU the two methods agree very well 1990 – 1999, from 2000 onwards the InTEM estimates are higher but the uncertainty bars strongly overlap throughout. The pollution events seen at Mace Head are regular and strong and the statistical match between the modelled time-series and the

observations is good. The results from the DECC network InTEM inversion agree extremely well to both the MHD-only and the inventory estimates.

Unit	Year	UK	(5th-95th)	NWEU	(5th-95th)
Mt/y	1990	4.1	(3.0- 5.3)	14.0	(10. -17.)
Mt/y	1991	3.9	(3.0- 4.8)	13.1	(10. -17.)
Mt/y	1992	3.3	(1.6- 4.7)	13.3	(10. -17.)
Mt/y	1993	2.8	(1.5- 3.7)	14.3	(9. -17.)
Mt/y	1994	3.2	(1.6- 3.8)	13.6	(9. -16.)
Mt/y	1995	3.2	(1.9- 3.9)	13.0	(9. -15.)
Mt/y	1996	3.2	(2.0- 3.5)	12.5	(9. -15.)
Mt/y	1997	3.0	(1.8- 3.5)	12.1	(9. -14.)
Mt/y	1998	2.9	(1.7- 3.4)	11.9	(9. -13.)
Mt/y	1999	3.0	(1.7- 3.4)	12.0	(9. -13.)
Mt/y	2000	3.1	(1.7- 3.4)	12.3	(9. -16.)
Mt/y	2001	2.9	(1.4- 3.4)	12.7	(9. -16.)
Mt/y	2002	2.8	(1.3- 3.3)	13.1	(10. -16.)
Mt/y	2003	2.9	(1.4- 3.6)	13.2	(9. -16.)
Mt/y	2004	3.0	(1.8- 3.7)	12.4	(9. -14.)
Mt/y	2005	3.0	(2.1- 3.4)	10.7	(8. -14.)
Mt/y	2006	2.7	(1.7- 3.3)	10.7	(8. -13.)
Mt/y	2007	2.4	(1.7- 2.9)	11.4	(8. -13.)
Mt/y	2008	2.4	(1.7- 2.8)	11.3	(8. -14.)
Mt/y	2009	2.4	(1.6- 2.9)	9.5	(6. -13.)
Mt/y	2010	2.3	(1.3- 3.0)	8.7	(6. -10.)
Mt/y	2011	2.3	(1.3- 3.0)	9.0	(6. -11.)
Mt/y	2012	2.6	(1.7- 3.0)	9.9	(7. -11.)
Mt/y	2013	2.4	(1.8- 2.8)	10.5	(10. -11.)

Table 6: Emission (Mt/y) estimates for UK and NWEU with uncertainty (5^{th} – 95^{th} %ile).

Region	Unit	Emission	Range	GHGI (2010)
England	kt/yr	1800	(1320 - 2320)	1320
Scotland	kt/yr	193	(2 - 500)	270
Wales	kt/yr	99	(1 - 249)	190
N.Ireland	kt/yr	139	(0.2 - 347)	140

Table 7: Emission (t/y) estimates for the UK Devolved Administrations using the UK DECC network for July 2012-2013.

The InTEM uncertainty for each of the DA regions overlaps the GHGI estimates, the median results are within a factor of two of the average GHGI results. It is interesting to note that the GHGI estimates for England are at the extreme lower end of the InTEM uncertainty range whereas for Wales and Scotland the GHGI estimates are higher than the median InTEM estimates. It must be noted that the time periods of the estimates do not overlap (GHGI 2010 Vs. InTEM 2012/13).

5.3 Nitrous oxide (N_2O)

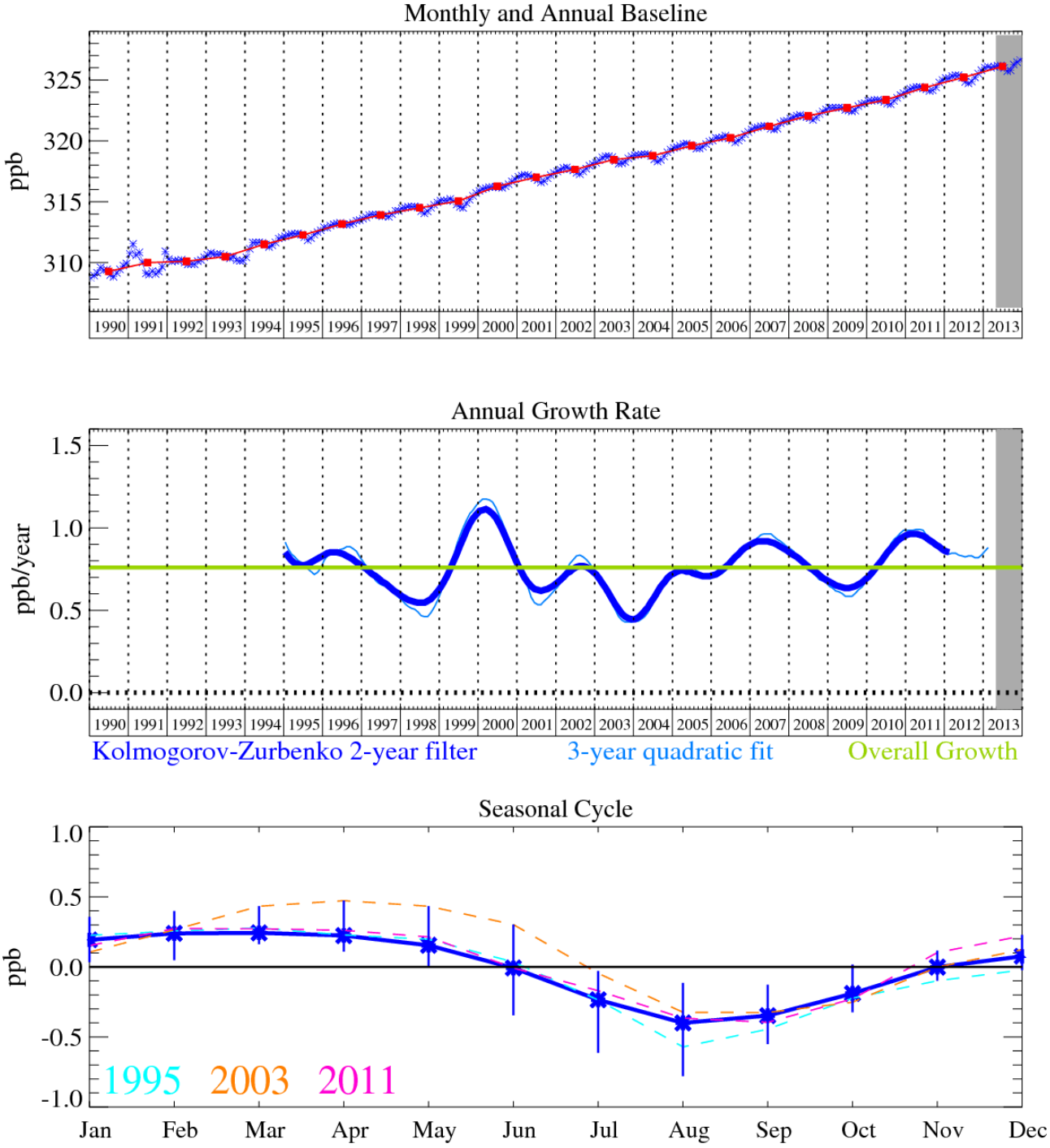

Figure 25: Nitrous oxide: Monthly (blue) and annual (red) baseline mole fractions (top). Annual (blue) and overall growth rate (green) (middle). Seasonal cycle (de-trended) with year-to-year variability (lower plot). Grey area covers un-ratified and therefore provisional data.

Figure 25 shows the baseline monthly means and trend for N_2O with an almost linear upwards average trend of 0.7 ppb/yr. The most recent growth rate is estimated to be 0.8 ppb/yr. The mixing ratio in December 2013 was 326.6 ppb at Mace Head. The N_2O increase is attributable to human activities, such as fertilizer use and fossil fuel burning, although it is also emitted through natural processes occurring in soils and oceans. There are large uncertainties associated with quantifying the sources of this gas. The global growth anomaly in N_2O is of particular interest with a very substantial increase in 2010-2011. At Mace Head the average historical growth rate of about 0.7 ppb/year has increased to over 0.8 ppb/year. Similarly in the Southern Hemisphere at Cape Grim, Tasmania the growth rate has increased from about 0.6 ppb/year in 2003 to about 1 ppb/year in 2011. Increases in N_2O emissions may also be linked to the tropics where 'wet and warm' microbes in soil can produce bursts in N_2O production, although this is contrary to reports where very

saturated soils can decrease N_2O emissions, however, as noted by Dr R. Weiss of Scripps Institution of Oceanography, there may be different spatial distributions of “wetness” with increased N_2O emissions in some regions and decreases in others. Interestingly, hydrogen has also exhibited a growth spurt in 2011. Here wet soils tend to reduce the normal H_2 deposition velocities due to a reduction in diffusivity. At this stage more global sites need to be carefully assessed to confirm these increases in the N_2O growth rate. We expect AGAGE, in collaboration with NOAA, to address these issues.

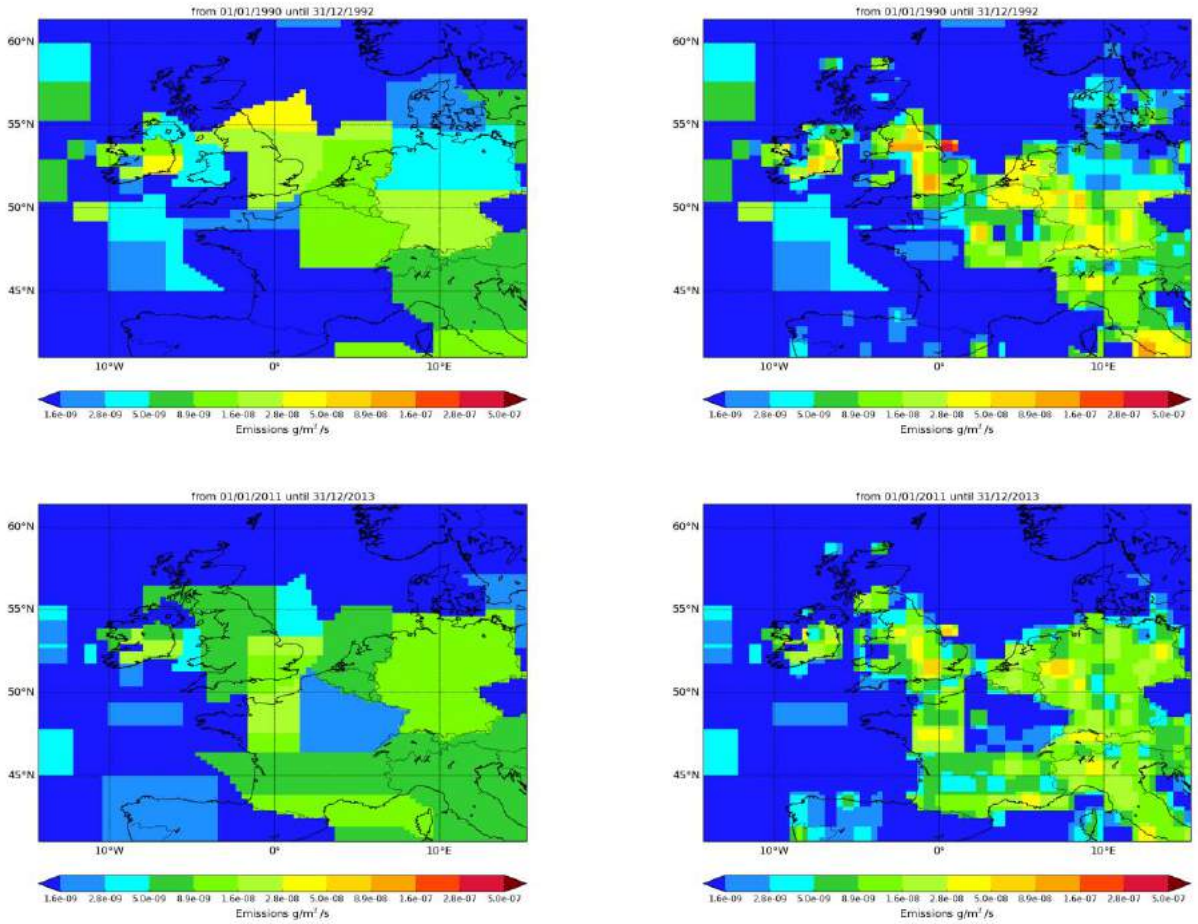

Figure 26: NAME-inversion emission estimates for 1990-1992 (upper) and 2011-2013 (lower). On the right hand side the emissions per grid box have been re-distributed based on population.

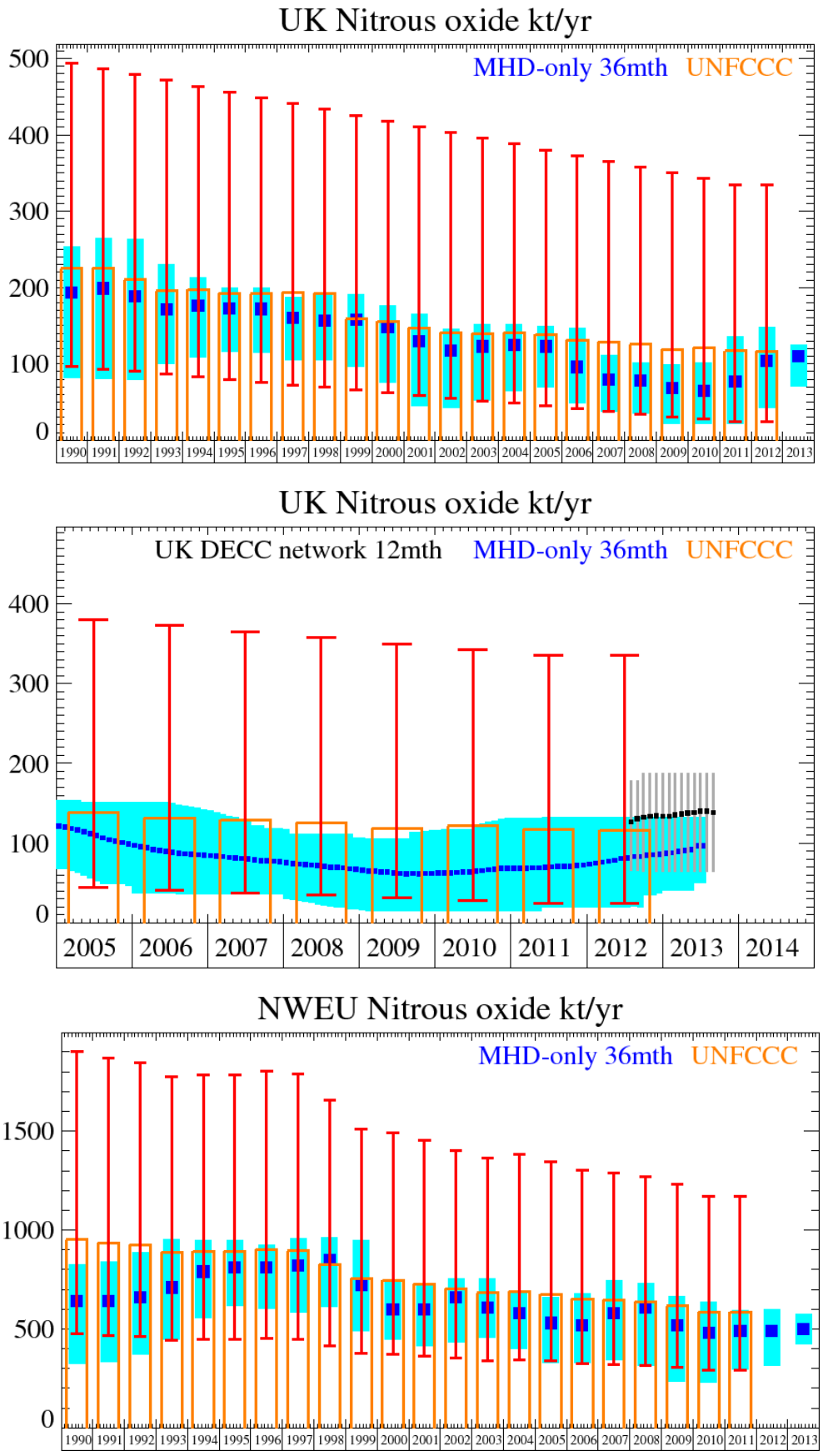

Figure 27: Emission (kt/y) estimates for UK (MHD-only and DECC network) and NWEU. The uncertainty bars represent the 5th and 95th percentiles.

The UK GHGI and InTEM estimates are broadly in agreement. The uncertainty of the GHGI is very significant compared to the uncertainty estimated for the InTEM results. Both the 3-yr Mace Head (MHD) -only and the extended DECC network 1-yr InTEM estimates are showing a positive trend in

the latter period. The difference between the MHD-only and the DECC network results show the value of moving to a higher temporal resolution. It will be important to see whether this positive InTEM trend continues and whether the GHGI shows an upturn in 2013.

Unit	Year	UK	(5th-95th)	NWEU	(5th-95th)
kt/y	1990	193.	(82.- 254.)	640.	(320. -830.)
kt/y	1991	199.	(80.- 265.)	640.	(330. -840.)
kt/y	1992	189.	(79.- 264.)	660.	(370. -890.)
kt/y	1993	171.	(100.- 231.)	710.	(450. -960.)
kt/y	1994	176.	(109.- 213.)	790.	(560. -950.)
kt/y	1995	173.	(116.- 200.)	810.	(620. -950.)
kt/y	1996	172.	(115.- 200.)	810.	(600. -930.)
kt/y	1997	160.	(105.- 188.)	820.	(590. -960.)
kt/y	1998	157.	(105.- 190.)	850.	(610. -960.)
kt/y	1999	158.	(96.- 191.)	720.	(490. -950.)
kt/y	2000	148.	(75.- 176.)	600.	(450. -740.)
kt/y	2001	130.	(45.- 165.)	600.	(420. -720.)
kt/y	2002	117.	(42.- 146.)	660.	(430. -760.)
kt/y	2003	123.	(52.- 152.)	610.	(460. -760.)
kt/y	2004	125.	(64.- 152.)	580.	(400. -690.)
kt/y	2005	123.	(69.- 149.)	530.	(330. -660.)
kt/y	2006	96.	(49.- 147.)	520.	(330. -680.)
kt/y	2007	79.	(37.- 112.)	580.	(340. -750.)
kt/y	2008	78.	(35.- 102.)	610.	(310. -730.)
kt/y	2009	68.	(21.- 99.)	520.	(240. -670.)
kt/y	2010	65.	(21.- 102.)	480.	(230. -640.)
kt/y	2011	77.	(22.- 136.)	490.	(300. -590.)
kt/y	2012	104.	(42.- 148.)	490.	(310. -600.)
kt/y	2013	110.	(71.- 125.)	500.	(420. -580.)

Table 8: Emission (kt/y) estimates for UK and NWEU with uncertainty (5^{th} – 95^{th} %ile).

Region	Unit	Emission	Range	GHGI (2010)
England	kt/yr	98.5	(52.7 - 128.6)	79.2
Scotland	kt/yr	14.4	(0.1 - 32.9)	16.2
Wales	kt/yr	18.5	(6.1 - 31.9)	9.9
N.Ireland	kt/yr	3.9	(0.0 - 12.6)	8.3

Table 9: Emission (t/y) estimates for the UK Devolved Administrations using the UK DECC network for July 2012-2013 compared with the 2010 GHGI (submitted 2012).

The InTEM uncertainty for each of the DA regions overlaps the GHGI estimates, the median results are within a factor of two of the average GHGI results. The GHGI for the DAs will have a similar (probably higher) level of uncertainty as for the UK as a whole. These results are therefore very encouraging.

5.4 Carbon dioxide (CO_2)

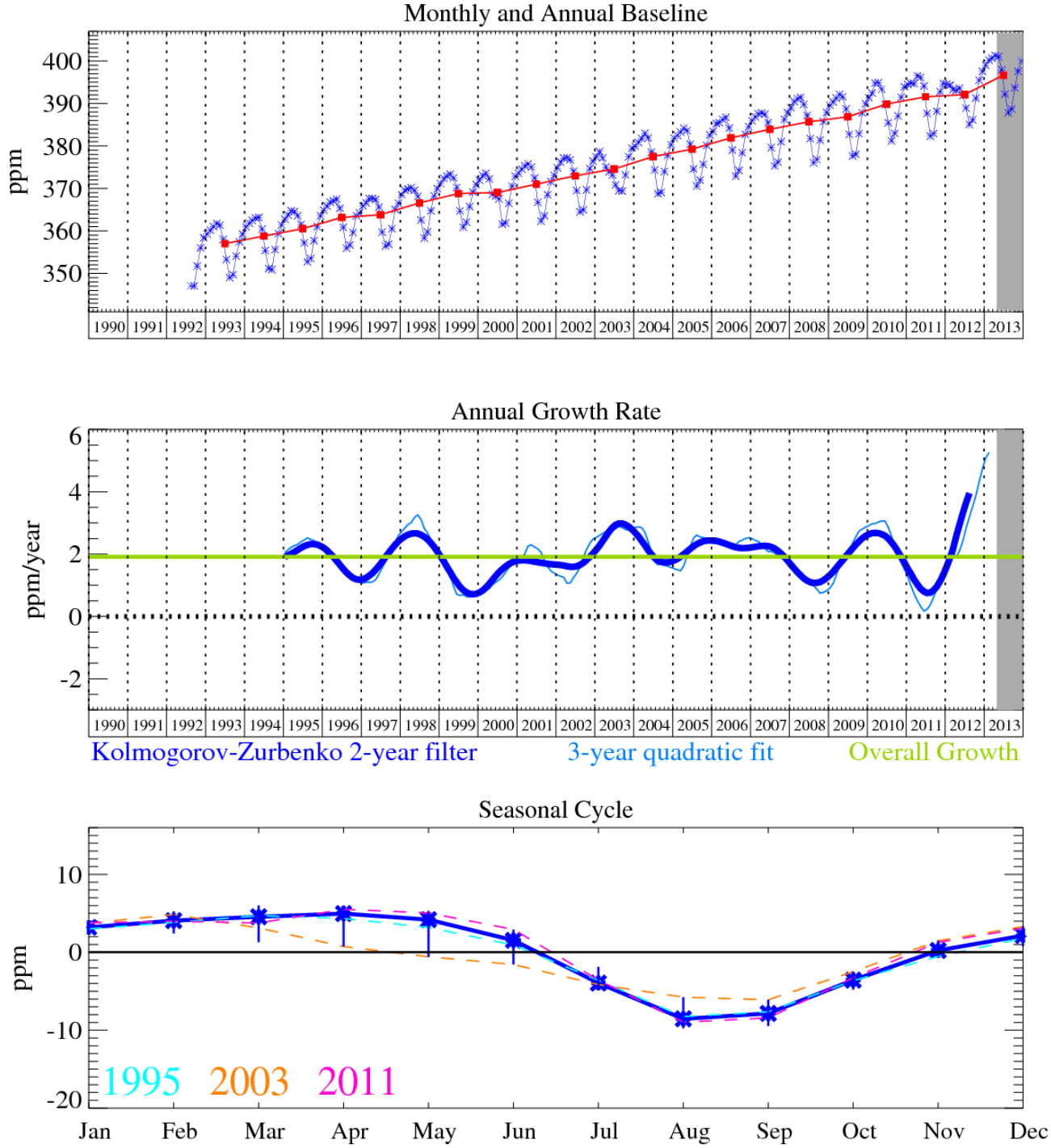

Figure 28: Carbon dioxide (CO_2): Monthly (blue) and annual (red) baseline mole fractions (top plot). Annual (blue) and overall average growth rate (green) (middle plot). Seasonal cycle (de-trended) with year-to-year variability (lower plot). Grey area covers un-ratified and therefore provisional data.

CO_2 (Figure 28) is the most important greenhouse gas, and has steadily grown at an annual average rate of 1.9 ppm/yr, calculated from the baseline-selected monthly means. The most recent growth rate is estimated to be over 4 ppm/yr but this is likely to be strongly influenced by only a few months of data at the end of the time-series and will probably reduce rapidly to its long-term rate. It has now reached a mixing ratio of 401 ppm (April 2013) which is the highest yet recorded at Mace Head, Ireland, and has shown significant growth rate anomalies in 1998/99 and 2002/03, which we suggest are a result of the global biomass burning events in those years.

Plants both respire CO_2 and absorb it through photosynthesis. Therefore the CO_2 flux from vegetation has a diurnal and seasonal cycle and switches from positive to negative on a daily basis. This unknown natural (biogenic) component of the observed CO_2 is significant when compared to the anthropogenic (man-made) component and cannot be assumed negligible (except during the winter months). From the CO_2 mole fractions it is impossible to distinguish between biogenic and anthropogenic CO_2. Therefore it is difficult to use the CO_2 mole fractions directly in an inversion to estimate anthropogenic emissions because the diurnally varying biogenic CO_2 flux is contrary to the inversion method assumption of temporally invariant emissions. Methods are under development to attempt to over-come these challenges, such as the use of isotopic observations, through ratios with respect to anthropogenic CO and other tracers. The uncertainties associated with each of these methods are predicted to be significant.

However there is an important policy requirement to verify the published man-made CO_2 emission inventories using the UK DECC network CO_2 observations. Several surrogate species have been considered such that the InTEM inversions for the surrogate can be utilised to estimate the man-made source strength of CO_2. To illustrate the methodology, carbon monoxide (CO) has been employed as an example surrogate.

The NAEI presents the spatially-disaggregated emission inventory for CO with a resolution of 1 km x 1 km for the UK for the year 2011. This inventory is split into various sectors, the most useful of which for this study being that for area sources, which are predominantly represented by road transport. The NAEI also usefully provides the corresponding emission inventory for CO_2 area sources in units of CO_2 as C. A scatter plot of the individual 1 km x 1 km estimates of area source emissions of CO_2 versus CO shows a simple linear relationship between the two emissions which can be characterised by linear regression, the gradient of which can be used as the ratio to scale CO to CO_2 emissions.

We can apply this relationship to the InTEM inversions for CO of 2.0 (1.6-2.7) Tg/year for 2011 for the UK to estimate the man-made area source emissions of CO_2. Using this approach, we estimate an area source emission of CO_2 from man-made sources of the order of 290 (232-392) Tg CO_2/year for 2011. The UK power stations emit little CO as there are active processes to remove (oxidise) it, therefore this proportion of the inventory is not covered by the CO:CO2 ratio scaling. Therefore the area emission is then uplifted by the reported power station emissions for 2011 (145 Tg CO_2/year) to give a total UK CO_2 InTEM emission estimate of 436 (377-537) Tg CO_2/year. This compares well with the published GHGI estimate of 473 Tg CO_2/year. All years 1995-2011 have been assessed and the results are shown in the figure and table below.

The InTEM CO_2 uncertainty estimates have been propagated from the InTEM CO uncertainty estimates. The CO_2 power station estimates from the inventory that are added to the man-made area source estimates were assumed to have negligible uncertainty compared to the InTEM uncertainty. This analysis could be completed with ethane and/or propane rather than CO as the surrogate anthropogenic gas, such extra analysis would increase the robustness of this approach.

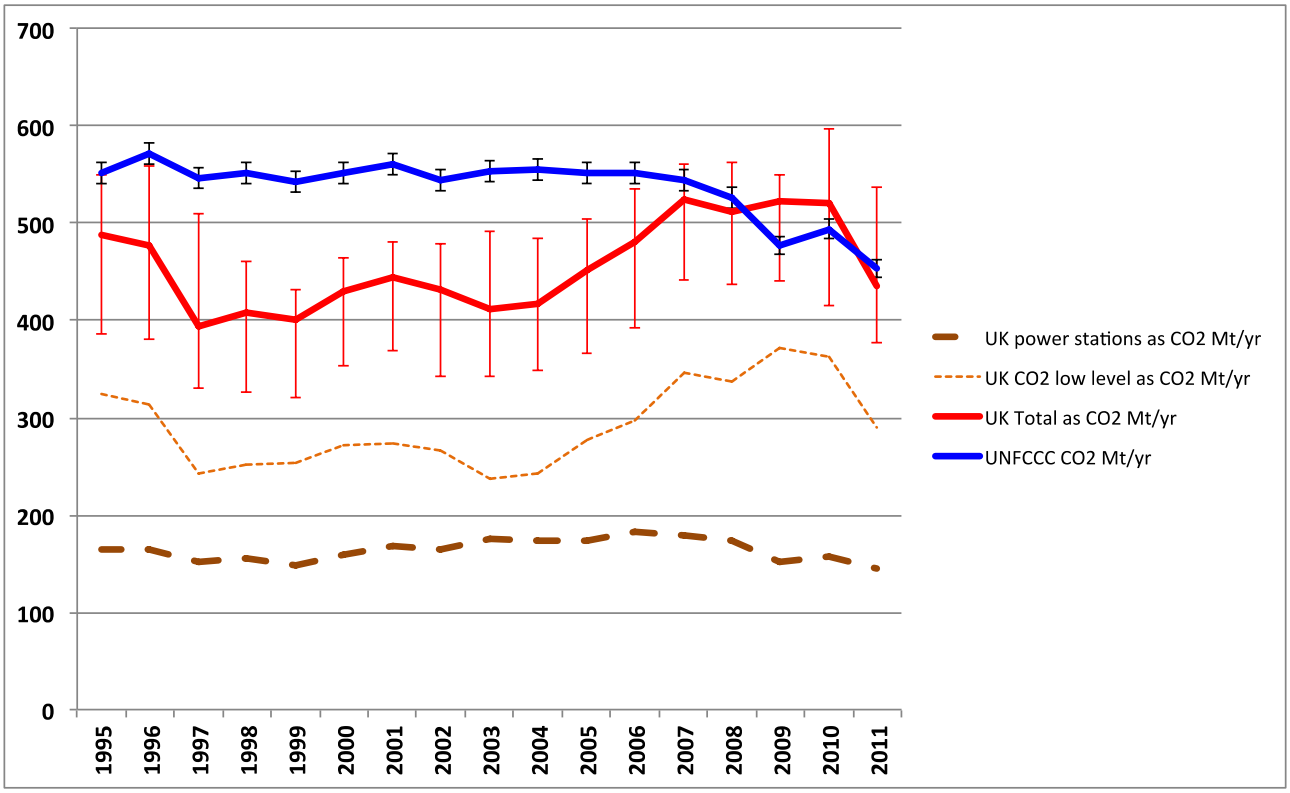

Figure 29: InTEM emission estimates for the UK for CO_2 (red) based on the CO ratio method compared to the UNFCCC estimates (blue). The area (low level) InTEM CO_2 emissions and the power station (inventory) estimates are shown separately.

Unit	Year	UK CO million tonnes /yr	CO_2 as CO_2/CO ratio by mass	UK power stations as CO_2 million tonnes /yr	UK CO_2 low level as CO_2 million tonnes /yr	UK Total as CO_2 million tonnes /yr
Mt/y	1995	6.3 (4.3-7.5)	51.5	164	324	488 (385-550)
Mt/y	1996	5.8 (4.0-7.3)	54.1	164	314	478 (380-559)
Mt/y	1997	4.6 (3.4-6.8)	52.8	151	243	394 (331-510)
Mt/y	1998	4.3 (2.9-5.2)	58.6	156	252	408 (326-461)
Mt/y	1999	4.1 (2.8-4.6)	61.7	148	253	401 (321-432
Mt/y	2000	3.9 (2.8-4.4)	69.5	159	271	430 (354-465
Mt/y	2001	3.7 (2.7-4.2)	74.1	169	274	444 (369-480
Mt/y	2002	3.3 (2.2-3.9)	80.5	165	266	431 (342-479
Mt/y	2003	2.7 (1.9-3.6)	87.8	175	237	412 (342-491
Mt/y	2004	2.5 (1.8-3.2)	97.1	174	243	417 (349-485
Mt/y	2005	2.6 (1.8-3.1)	106.6	174	277	451 (366-504
Mt/y	2006	2.7 (1.9-3.2)	110.3	183	298	481 (393-536
Mt/y	2007	2.9 (2.2-3.2)	119.4	179	346	525 (442-561
Mt/y	2008	2.7 (2.1-3.1)	125.3	174	338	512 (437-562
Mt/y	2009	2.7 (2.1-2.9)	137.4	152	371	523 (441-550
Mt/y	2010	2.4 (1.7-2.9)	151.2	158	363	521 (415-596
Mt/y	2011	2.0 (1.6-2.7)	145.1	145	290	436 (377-537)

Table 10: InTEM CO emission estimates for the UK and how they are converted to InTEM CO_2 emission estimates for the UK using the ratio method.

5.5 HFC-125

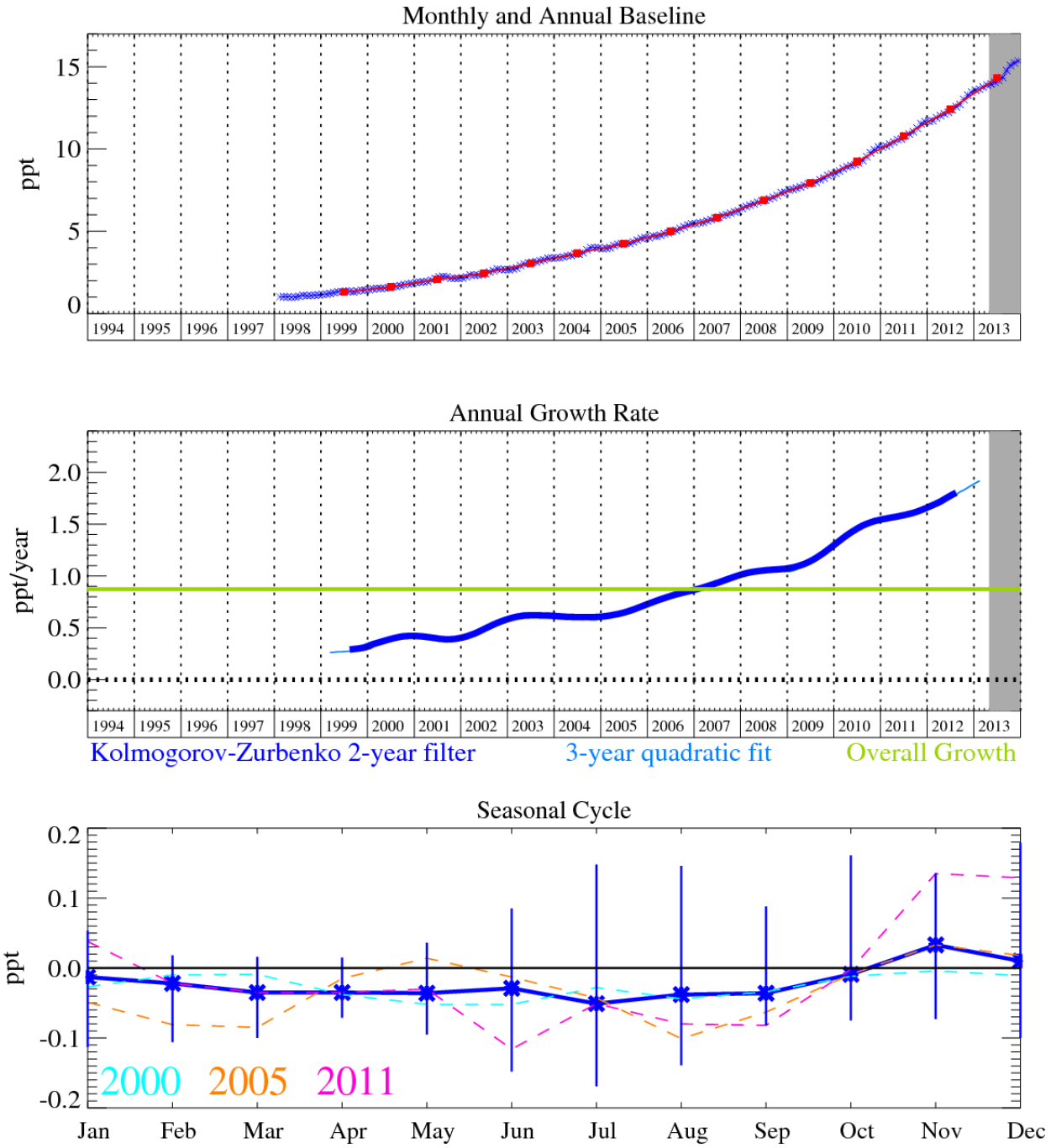

Figure 30: HFC-125 (CHF_2CF_3): Monthly (blue) and annual (red) baseline mole fractions (top plot). Annual (blue) and overall average growth rate (green) (middle plot). Seasonal cycle (de-trended) with year-to-year variability (lower plot). Grey area covers un-ratified provisional data.

Hydrofluorocarbons (HFCs) are replacement chemicals for the long-lived ozone depleting substances in various applications such as refrigeration, fire extinguishers, propellants, and foam blowing. The most recent measurements of the HFCs at the UK DECC network indicate that the mixing ratios of all HFC compounds continue to grow, as is consistent with sustained emissions of these replacement compounds into the atmosphere. The baseline monthly mean, mixing ratios for all the HFCs are shown in Figures 30-48 and the growth rates of these compounds, calculated from the data, are presented in Table 1c.

HFC-125 (CHF_2CF_3): This compound is used in refrigeration blends and for fire suppression. It has a GWP_{100} of 3420 and an atmospheric lifetime of 30.5 years. [Ko *et al.*, 2013]. This compound is growing rapidly in the atmosphere reaching an annual level of 14.3 ppt in 2013 with a current growth rate of 1.8 ppt/yr.

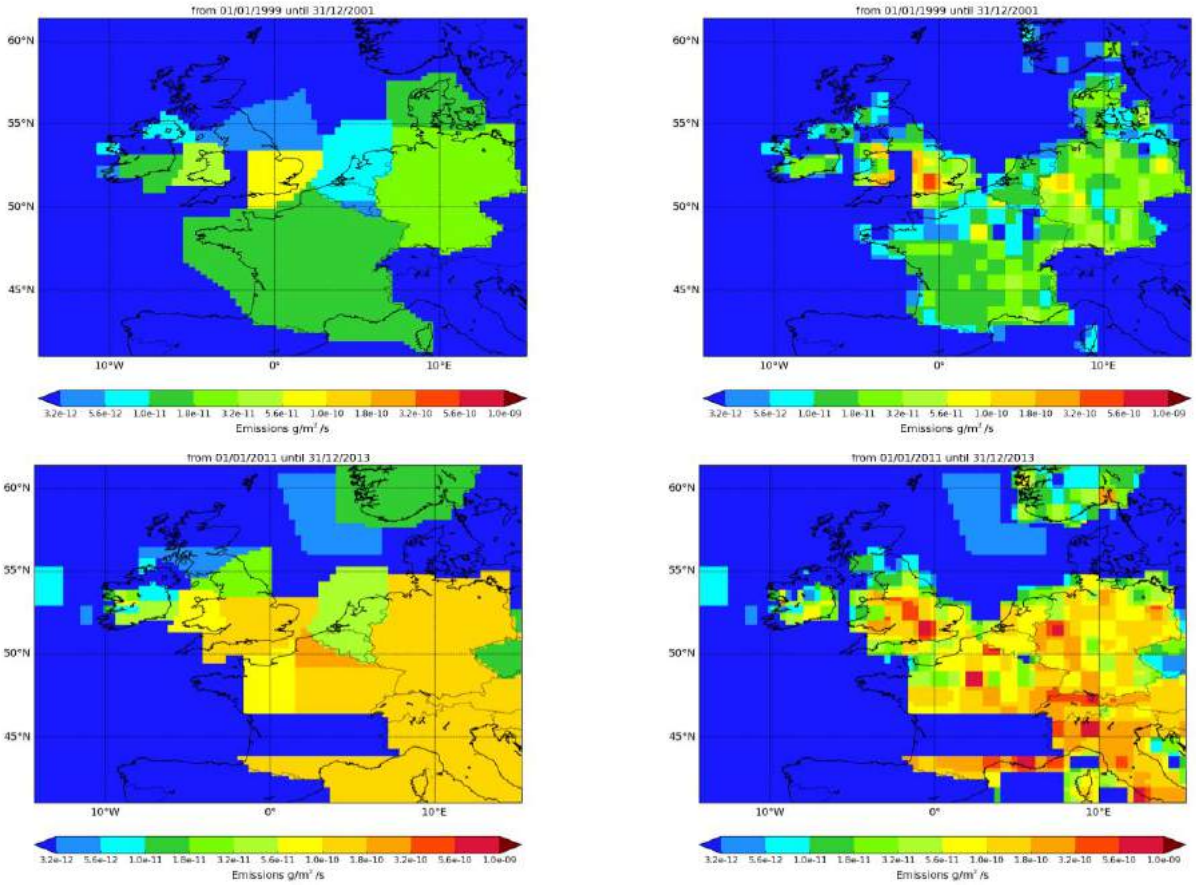

Figure 31: NAME-inversion emission estimates for 1999-2001 (upper) and 2011-2013 (lower). On the right hand side the emissions per grid box have been re-distributed based on population.

Relative to the magnitude of the baseline (growing rapidly but still currently less than 16 ppt) the pollution events are very significant. Therefore InTEM has plenty of clear information on which to base the emission estimates. The agreement between the inventory and InTEM for the UK is excellent up until 2009 with a strong overlap of the uncertainty bars from both methods. It is interesting to note that with InTEM the UK estimates have remained broadly constant from 2010 onwards in contrast to the inventory that continues to grow strongly. However, it is also noticeable that the NWEU InTEM estimates have continued to grow, and at a stronger rate than the inventory. The inclusion of Tacolneston data in the InTEM analysis supports the MHD-only analysis.

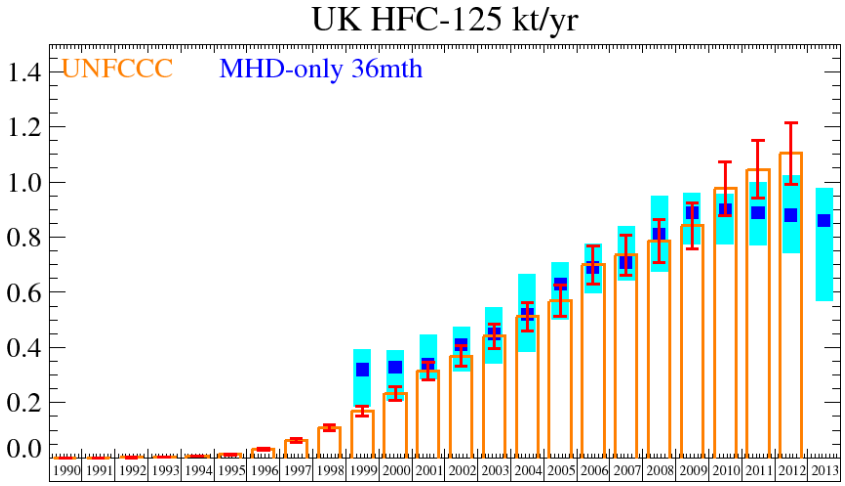

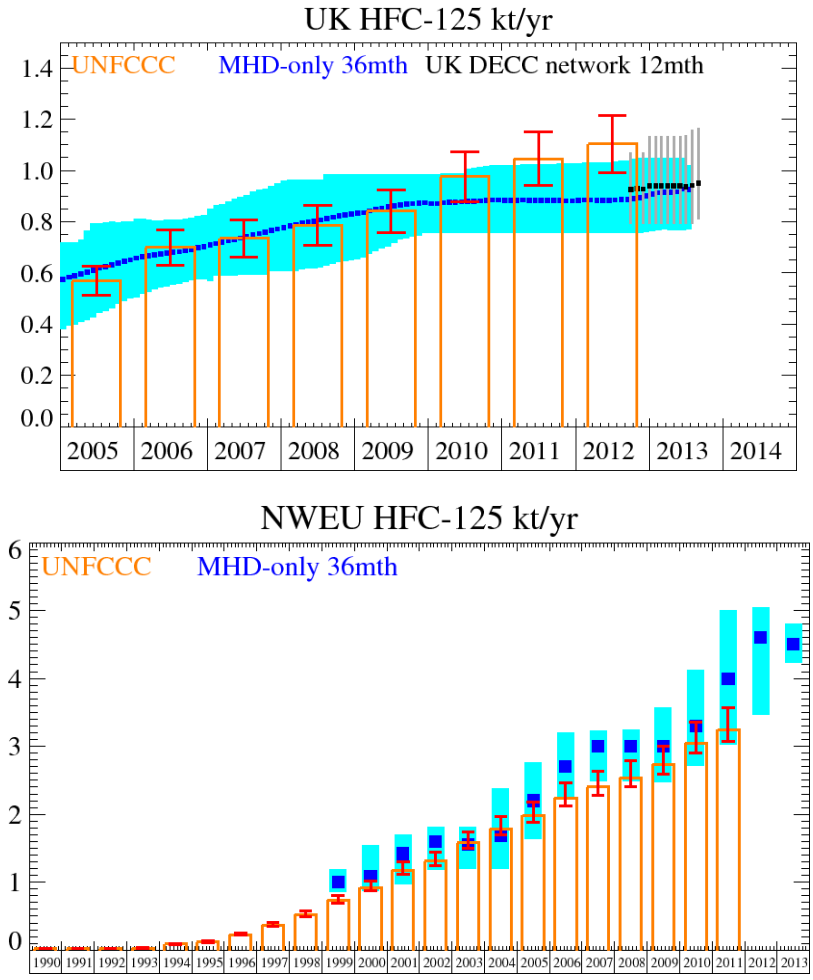

Figure 32: Emission (kt/y) estimates for UK (MHD-only and DECC network) and NWEU. The uncertainty bars represent the 5th and 95th percentiles.

Unit	Year	UK	(5th-95th)	NWEU	(5th-95th)
t/y	1999	320.	(180.- 390.)	1000.	(860.-1190.)
t/y	2000	330.	(210.- 390.)	1090.	(870.-1540.)
t/y	2001	340.	(290.- 450.)	1420.	(970.-1700.)
t/y	2002	410.	(310.- 470.)	1600.	(1180.-1810.)
t/y	2003	450.	(340.- 550.)	1560.	(1190.-1810.)
t/y	2004	520.	(390.- 670.)	1690.	(1200.-2390.)
t/y	2005	630.	(500.- 710.)	2200.	(1630.-2770.)
t/y	2006	690.	(600.- 780.)	2700.	(2240.-3200.)
t/y	2007	710.	(650.- 840.)	3000.	(2490.-3240.)
t/y	2008	810.	(670.- 950.)	3000.	(2480.-3250.)
t/y	2009	890.	(780.- 960.)	3000.	(2470.-3570.)
t/y	2010	900.	(770.- 960.)	3300.	(2710.-4120.)
t/y	2011	890.	(770.- 1000..)	4000.	(3030.-5010.)
t/y	2012	880.	(740.-1020.)	4600.	(3470.-5050.)
t/y	2013	860.	(570.- 980.)	4500.	(4230.-4810.)

Table 11: Emission (t/y) estimates for UK and NWEU with uncertainty (5th – 95th %ile).

Region	Unit	Emission	Range
England	t/yr	827	(684 - 973)
Scotland	t/yr	23	(0.0 - 77)
Wales	t/yr	85	(2.0 - 170)
N.Ireland	t/yr	2	(0.0 - 18)

Table 12: Emission (t/y) estimates for the UK Devolved Administrations using the UK DECC network for July 2012-2013.

5.6 HFC-134a

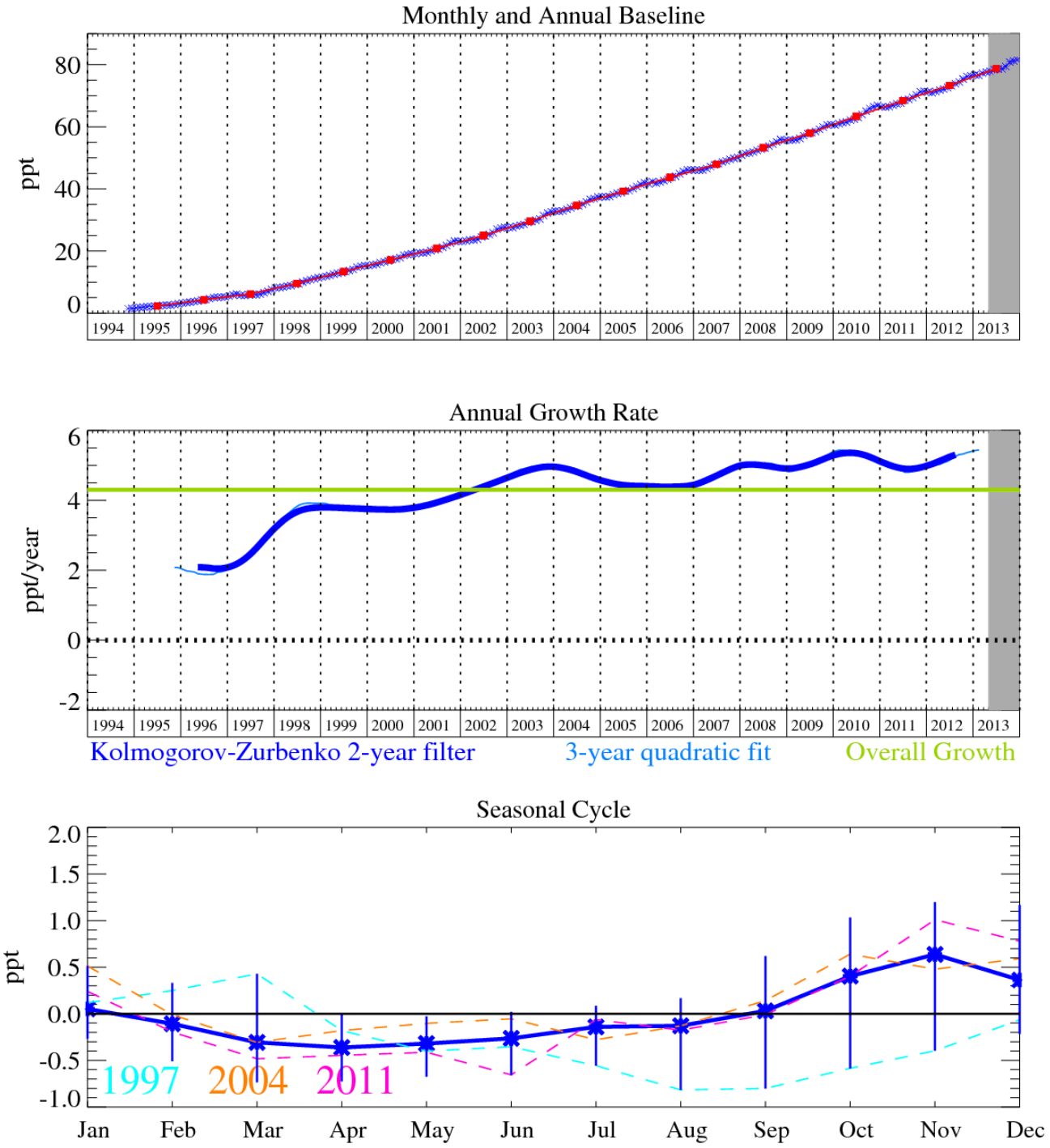

Figure 33: HFC-134a (CH_2FCF_3): Monthly (blue) and annual (red) baseline mole fractions (top plot). Annual (blue) and overall average growth rate (green) (middle plot). Seasonal cycle (de-trended) with year-to-year variability (lower plot). Grey area covers un-ratified and therefore provisional data.

HFC-134a (CH_2FCF_3): Globally HFC-134a is the most abundant HFC present in the atmosphere and is used predominantly in refrigeration and mobile air conditioning (MAC). Due to its long lifetime, 13.5 years, and relatively high GWP_{100} 1370 [Forster *et al.*, 2007], the use of HFC-134a (and any other HFCs with a GWP_{100} >150) is being phased out in Europe between 2011 and 2017. It is proposed that a very gradual phase-out of the use of HFC-134a in cars will also take place outside Europe because of the global nature of the car industry. However in developing countries the potential for growth of HFC-134a is still large [Velders *et al.*, 2009]. As of December 2012 the atmospheric mole fraction of HFC-134a was 81.5 ppt and recent growth is estimated to be 5.1 ppt/yr.

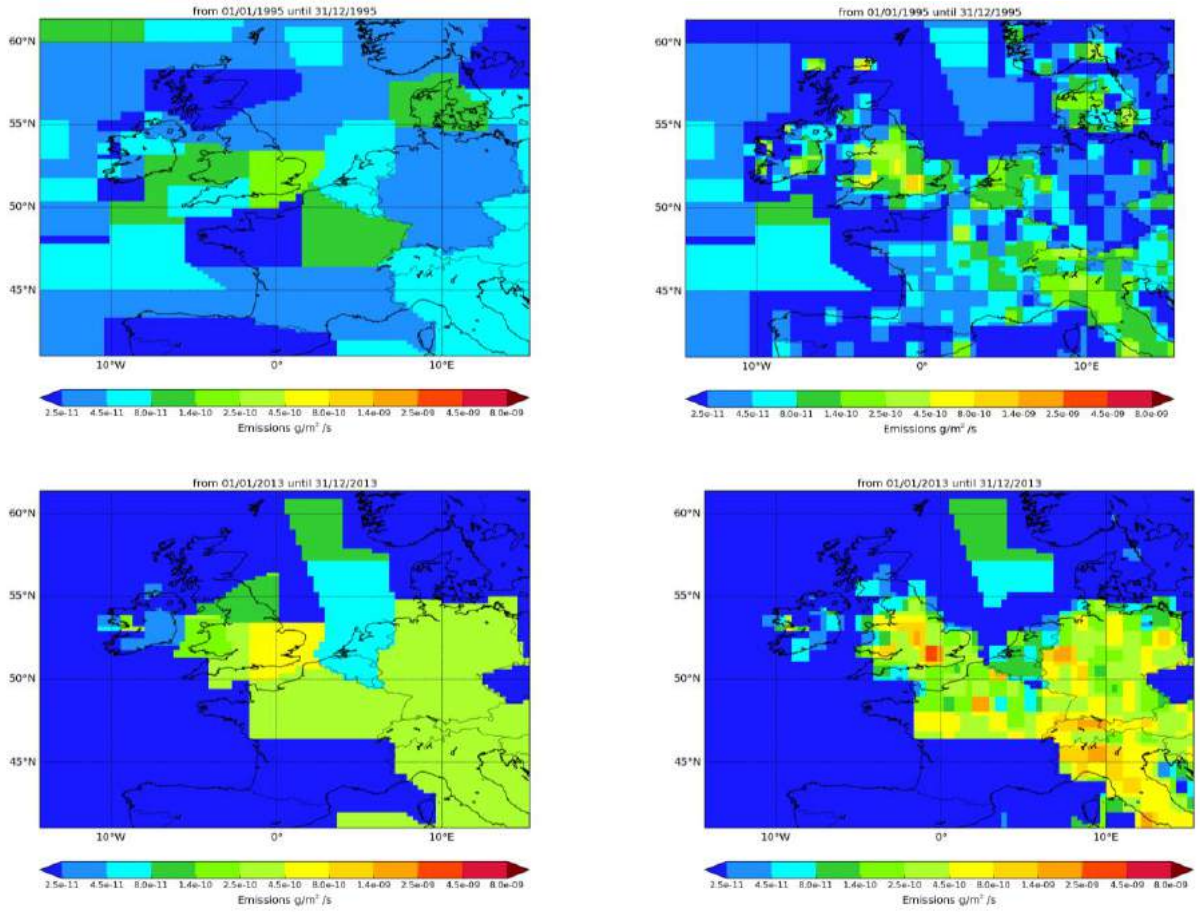

Figure 34: NAME-inversion emission estimates for 1995-1997 (upper) and 2011-2013 (lower). On the right hand side the emissions per grid box have been re-distributed based on population.

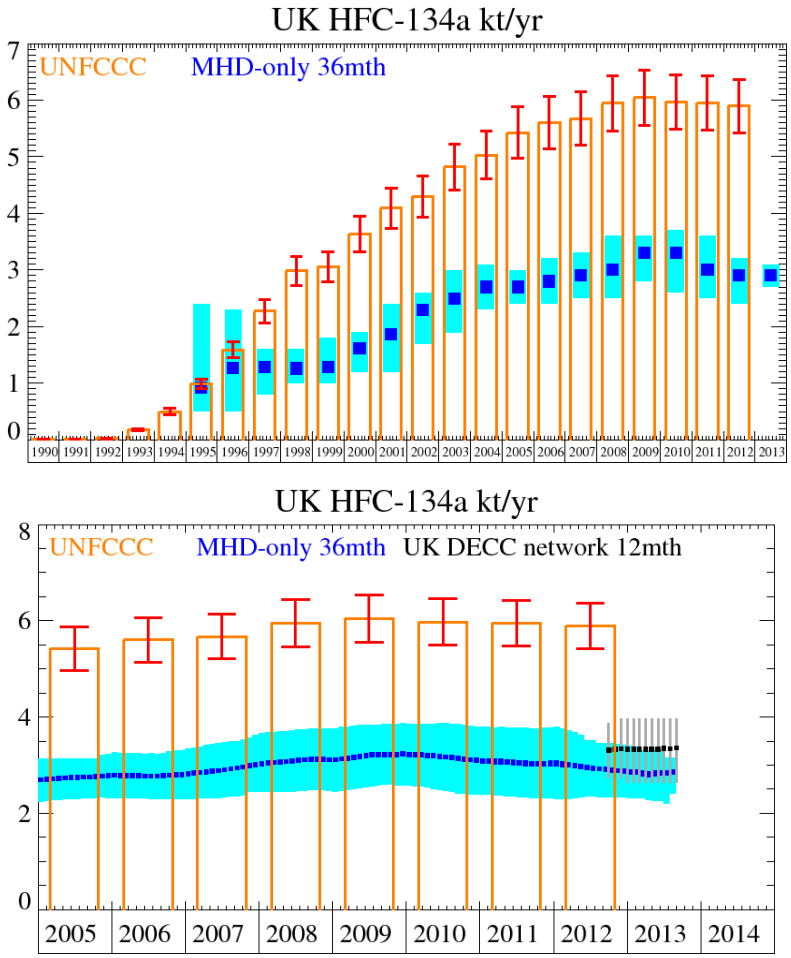

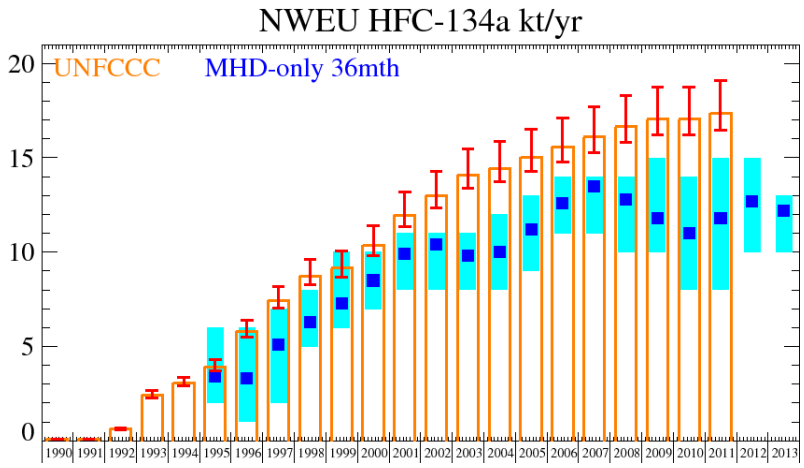

Figure 35: Emission (kt/y) estimates for UK (MHD-only and DECC network) and NWEU. The uncertainty bars represent the 5th and 95th percentiles.

The UK inventory and InTEM estimates increased between the mid-1990s until 2009. Since then the UK inventory and InTEM have very slightly decreased. The InTEM estimates for the UK are consistently around half to two thirds of the inventory estimates. A different picture emerges in NWEU as a whole, the inventory shows increasing emissions in recent years whereas InTEM has a flatter profile. The statistical fit between the measurements and the modelling is relatively good throughout the time-series. A significant proportion of the HFC-134a emitted is estimated to come from in-use vehicles (it is used in mobile air conditioning units). Inspection of the inventory shows that different countries across the EU use surprisingly different values for the leakage rates from in-use vehicles.

Unit	Year	UK	(5th-95th)	NWEU	(5th-95th)
kt/y	1995	0.92	(0.5- 2.4)	3.4	(2. - 6.)
kt/y	1996	1.27	(0.5- 2.3)	3.3	(1. - 6.)
kt/y	1997	1.28	(0.8- 1.6)	5.1	(2. - 7.)
kt/y	1998	1.26	(1.0- 1.6)	6.3	(5. - 8.)
kt/y	1999	1.28	(1.0- 1.8)	7.3	(6. -10.)
kt/y	2000	1.62	(1.2- 1.9)	8.5	(7. -10.)
kt/y	2001	1.86	(1.2- 2.4)	9.9	(8. -11.)
kt/y	2002	2.3	(1.7- 2.6)	10.4	(8. -11.)
kt/y	2003	2.5	(1.9- 3.0)	9.8	(8. -11.)
kt/y	2004	2.7	(2.3- 3.1)	10.0	(8. -12.)
kt/y	2005	2.7	(2.4- 3.0)	11.2	(9. -13.)
kt/y	2006	2.8	(2.4- 3.2)	12.6	(11. -14.)
kt/y	2007	2.9	(2.5- 3.3)	13.5	(11. -14.)
kt/y	2008	3.0	(2.5- 3.6)	12.8	(10. -14.)
kt/y	2009	3.3	(2.8- 3.6)	11.8	(10. -15.)
kt/y	2010	3.3	(2.6- 3.7)	11.0	(8. -14.)
kt/y	2011	3.0	(2.5- 3.6)	11.8	(8. -15.)
kt/y	2012	2.9	(2.4- 3.2)	12.7	(10. -15.)
kt/y	2013	2.9	(2.7- 3.1)	12.2	(10. -13.)

Table 13: Emission (kt/y) estimates for UK and NWEU with uncertainty (5th – 95th %ile).

Region	Unit	Emission	Range
England	t/yr	2750	(2200 - 3200)
Scotland	t/yr	152	(0 - 426)
Wales	t/yr	374	(74 - 654)
N.Ireland	t/yr	63	(0 - 217)

Table 14: Emission (t/y) estimates for the UK Devolved Administrations using the UK DECC network for July 2012-2013.

5.7 HFC-143a

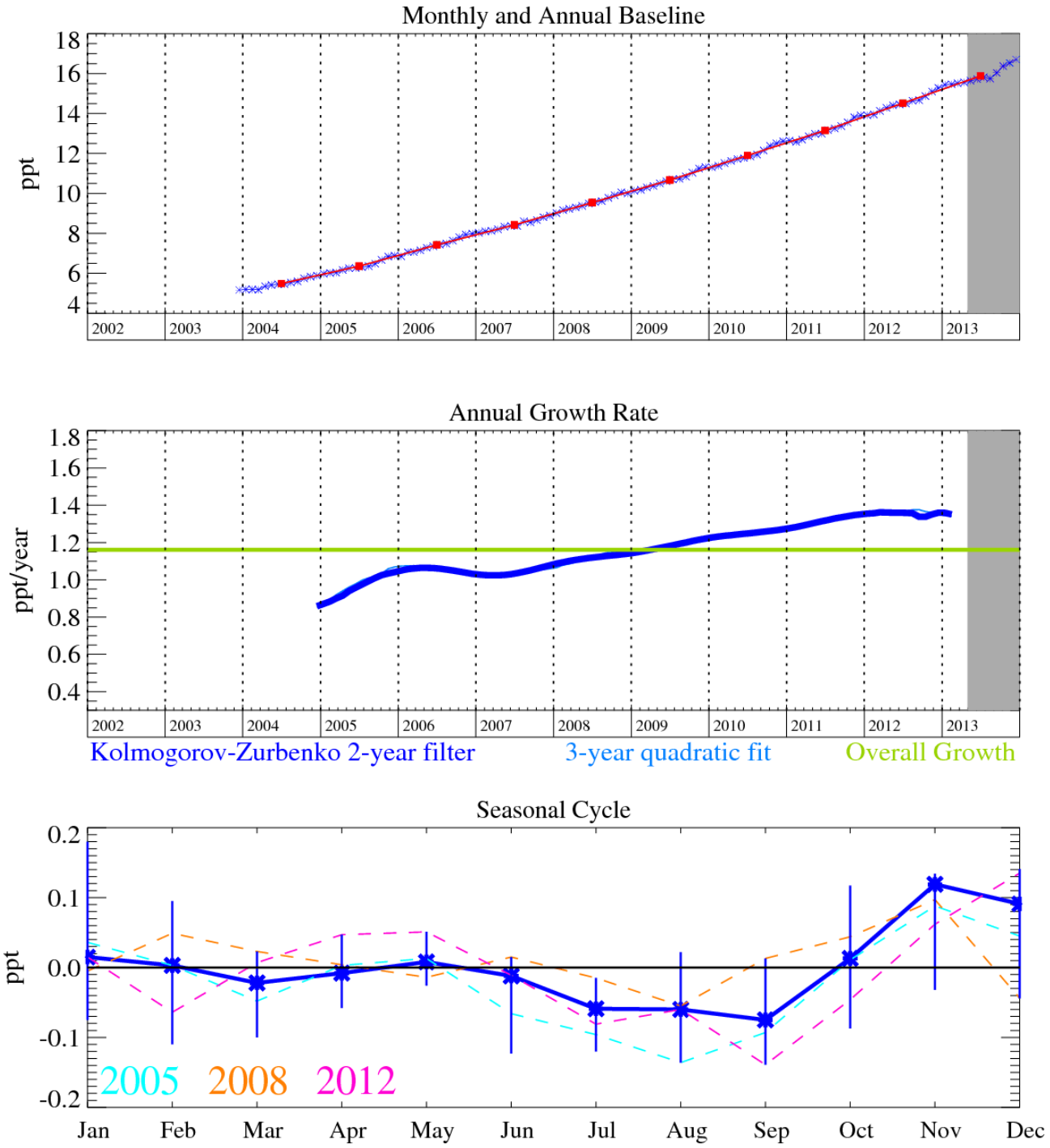

Figure 36: HFC-143a (CH_3CF_3): Monthly (blue) and annual (red) baseline mole fractions (top plot). Annual (blue) and overall average growth rate (green) (middle plot). Seasonal cycle (de-trended) with year-to-year variability (lower plot). Grey area covers un-ratified and therefore provisional data.

HFC-143a (CH_3CF_3): is used mainly as a working fluid in refrigerant blends (R-404A and R-507A) for low and medium temperature commercial refrigeration systems. In December 2013 it reached 16.7 ppt. These levels have increased dramatically from the low levels in 1997 with an increasing growth rate, currently estimated to be 1.3 ppt/yr. It has a relatively long atmospheric lifetime of 51.4 years and a significant radiative forcing value (third largest of all the HFCs) with a GWP_{100} of 4400.

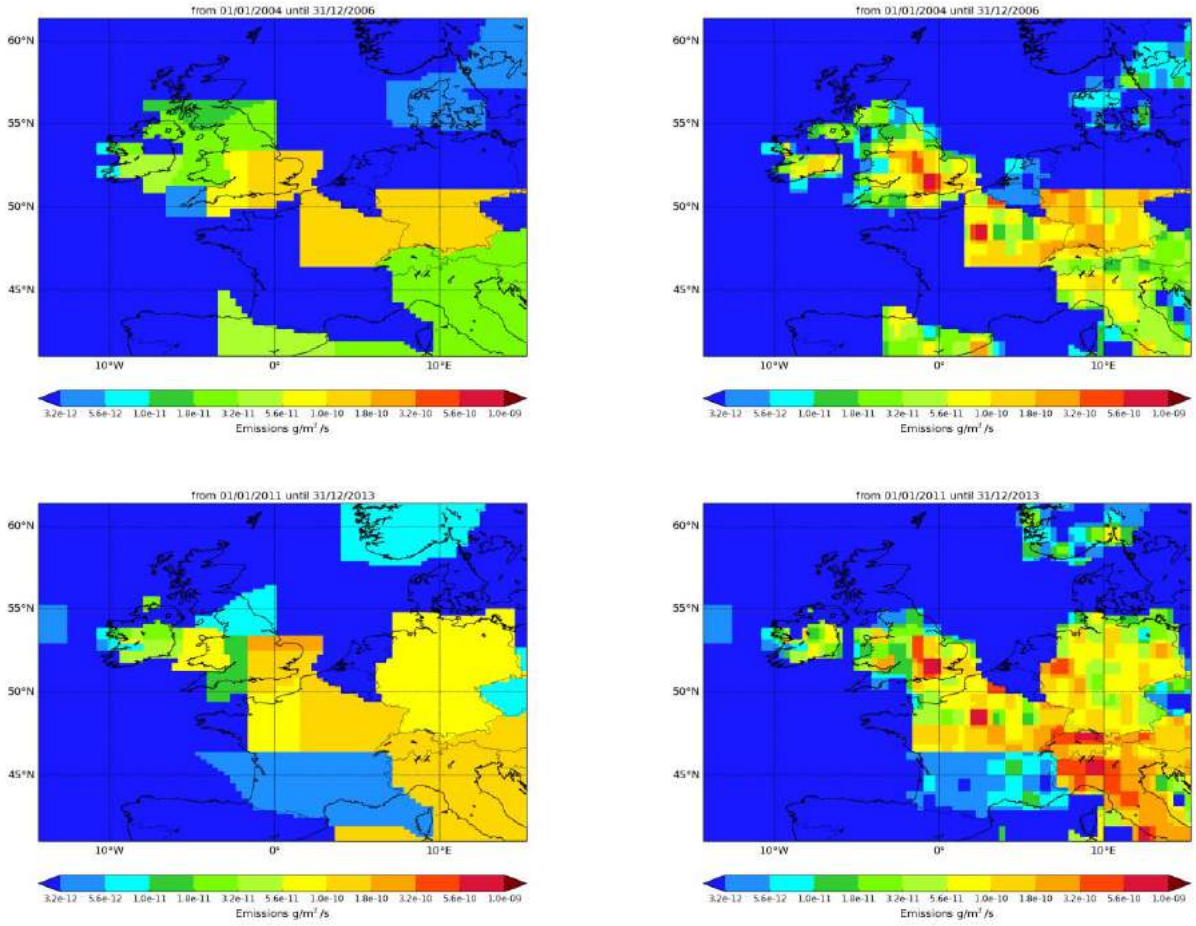

Figure 37: NAME-inversion emission estimates for 2004-2006 (upper) and 2011-2013 (lower). On the right hand side the emissions per grid box have been re-distributed based on population.

The InTEM emission estimates for the UK show a maximum was reached in 2008-09 after which they have started to decline. The inventory estimates an increase across the years. The higher frequency (1-year) DECC network InTEM estimates also show a declining UK total but are lower than the MHD-only estimates although the uncertainty bars strongly overlap. It will be important to investigate this gas further to understand why the UK inventory shows an increase in contrast to the observations. The NWEU estimates for both InTEM and the inventory are increasing although the InTEM estimates are significantly above the inventory estimates.

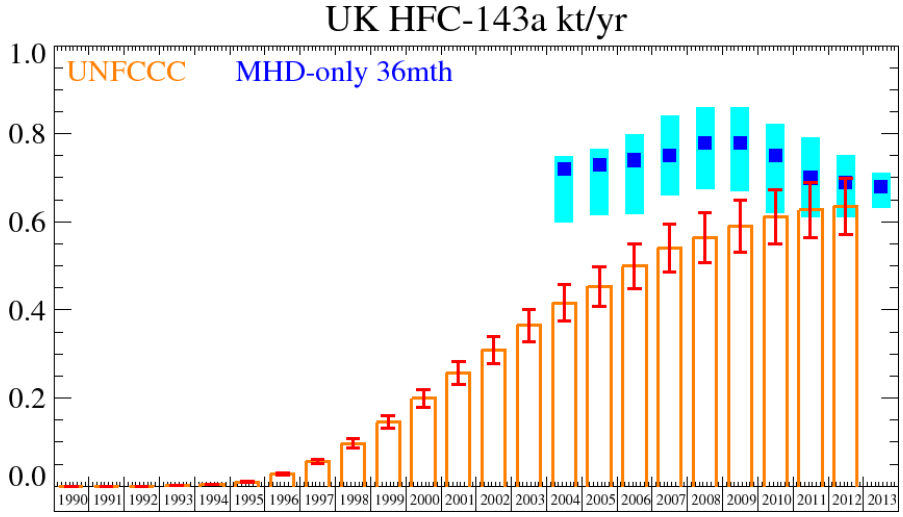

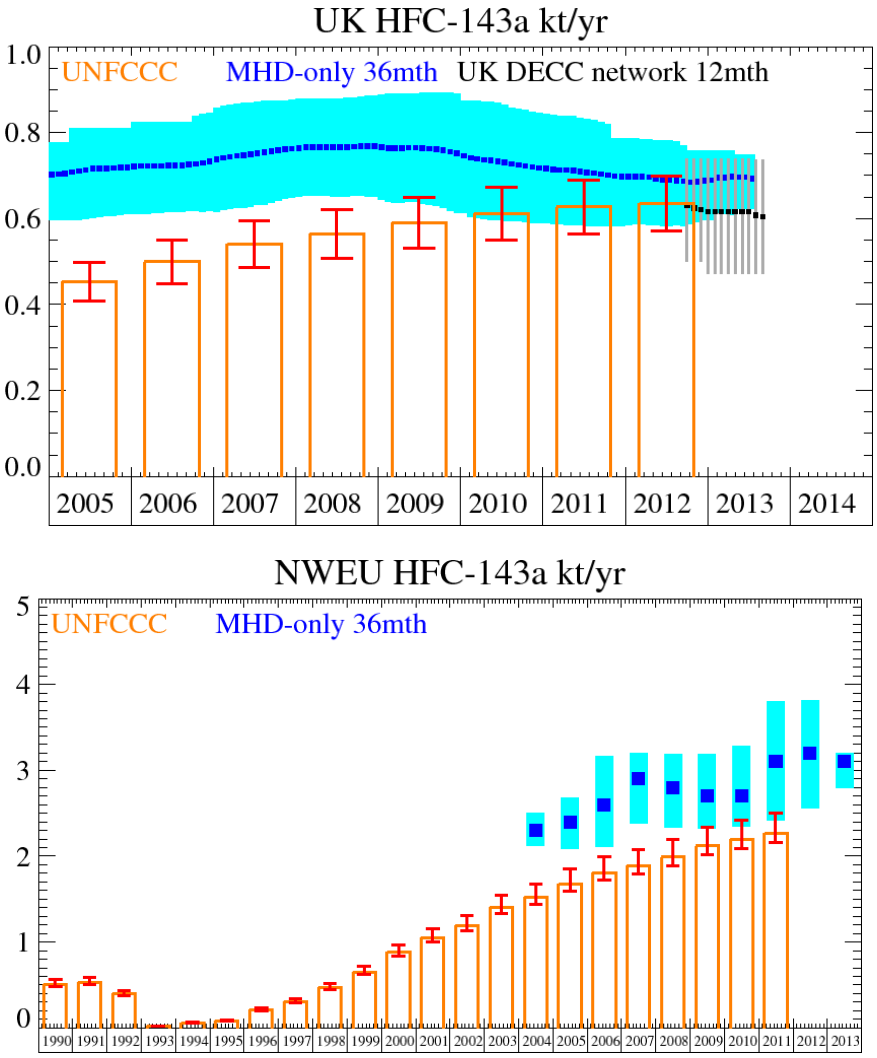

Figure 38: Emission (kt/y) estimates for UK (MHD-only and DECC network) and NWEU. The uncertainty bars represent the 5th and 95th percentiles.

Unit	Year	UK	(5th-95th)	NWEU	(5th-95th)
t/y	2004	720.	(600.- 750.)	2300.	(2120.-2500.)
t/y	2005	730.	(620.- 770.)	2400.	(2090.-2680.)
t/y	2006	740.	(620.- 800.)	2600.	(2110.-3170.)
t/y	2007	750.	(660.- 840.)	2900.	(2380.-3200.)
t/y	2008	780.	(680.- 860.)	2800.	(2330.-3190.)
t/y	2009	780.	(670.- 860.)	2700.	(2320.-3190.)
t/y	2010	750.	(620.- 820.)	2700.	(2350.-3280.)
t/y	2011	700.	(610.- 790.)	3100.	(2410.-3800.)
t/y	2012	690.	(610.- 750.)	3200.	(2560.-3820.)
t/y	2013	680.	(630.- 710.)	3100.	(2790.-3210.)

Table 15: Emission (t/y) estimates for UK and NWEU with uncertainty (5th – 95th %ile).

Region	Unit	Emission	Range
England	t/yr	562	(414. - 677.)
Scotland	t/yr	15	(0.0 - 59.0)
Wales	t/yr	39	(0.0 - 127.)
N.Ireland	t/yr	1.4	(0.0 - 13.0)

Table 16: Emission (t/y) estimates for the UK Devolved Administrations using the UK DECC network for July 2012-2013.

5.8 HFC-152a

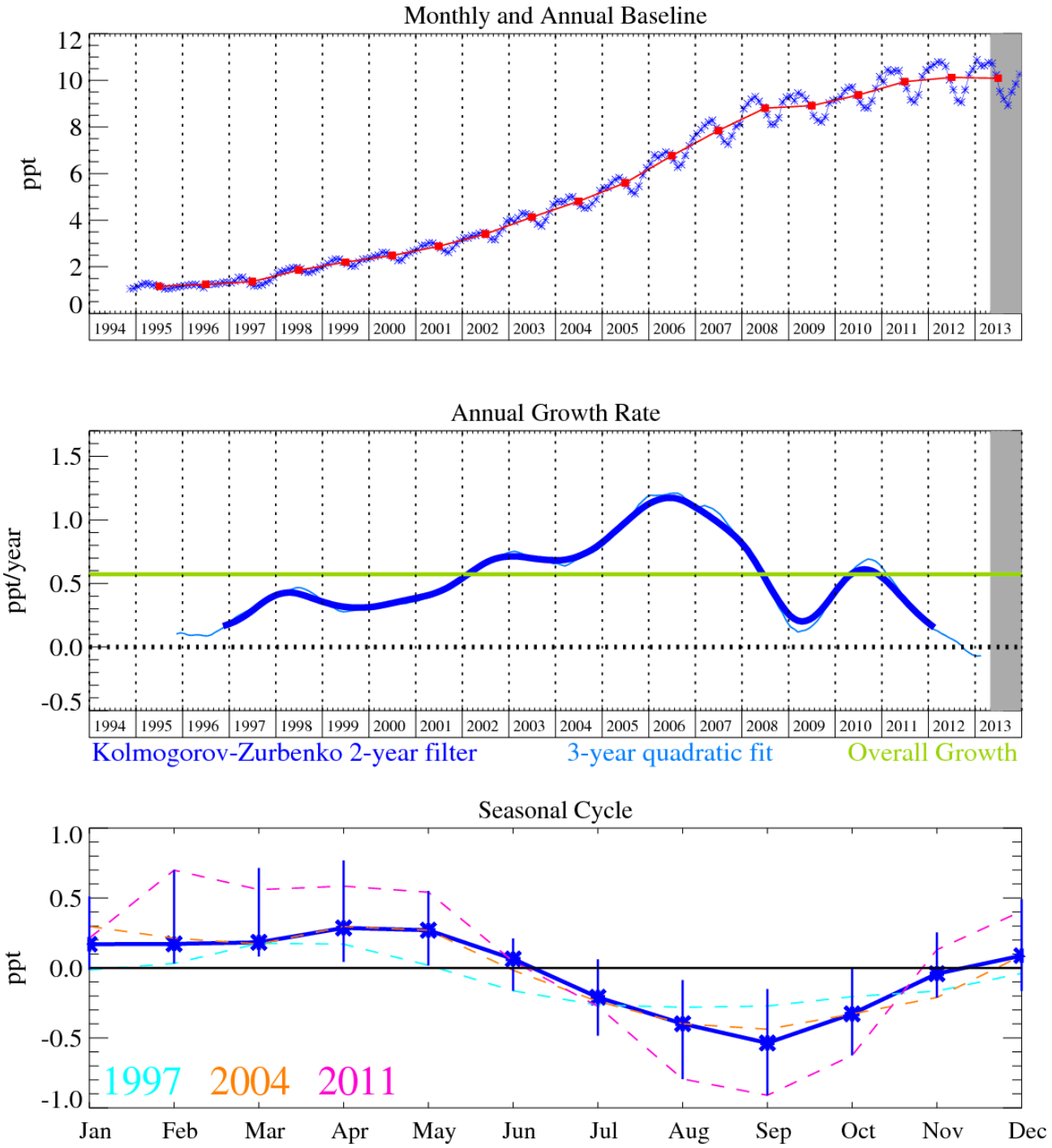

Figure 39: HFC-152a (CH_3CHF_2): Monthly (blue) and annual (red) baseline mole fractions (top plot). Annual (blue) and overall average growth rate (green) (middle plot). Seasonal cycle (de-trended) with year-to-year variability (lower plot). Grey area covers un-ratified and therefore provisional data.

HFC-152a (CH_3CHF_2): has a relatively short lifetime of 1.6 years due to its efficient removal by OH oxidation in the troposphere, consequently it has the smallest GWP_{100} at 133, of all of the major HFCs. It is used as a foam-blowing agent and aerosol propellant, and given its short lifetime has exhibited substantial growth in the atmosphere since measurement began in 1994, implying a substantial increase in emissions in these years. However, in the last few years the rate of growth has slowed somewhat to ~0.4 ppt/yr, reaching a mixing ratio in Dec 2013 of 10.3 ppt.

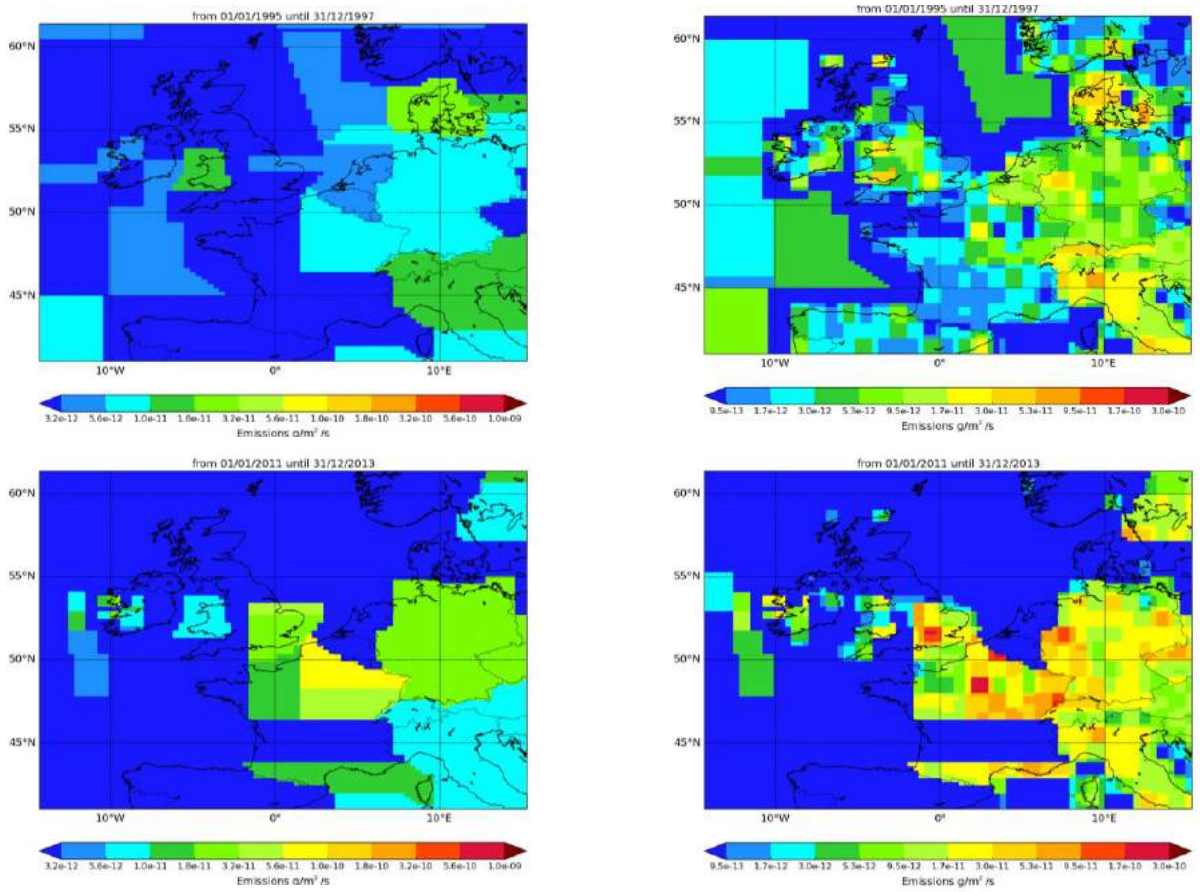

Figure 40: NAME-inversion emission estimates for 1995-1997 (upper) and 2011-2013 (lower). On the right hand side the emissions per grid box have been re-distributed based on population.

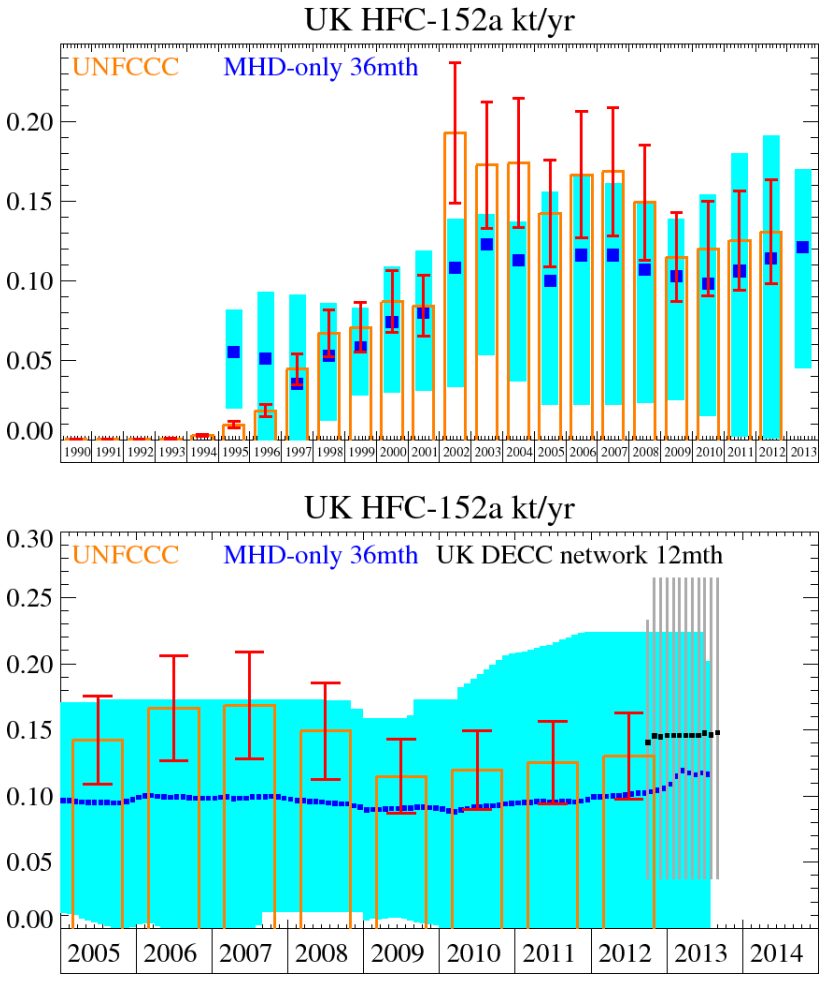

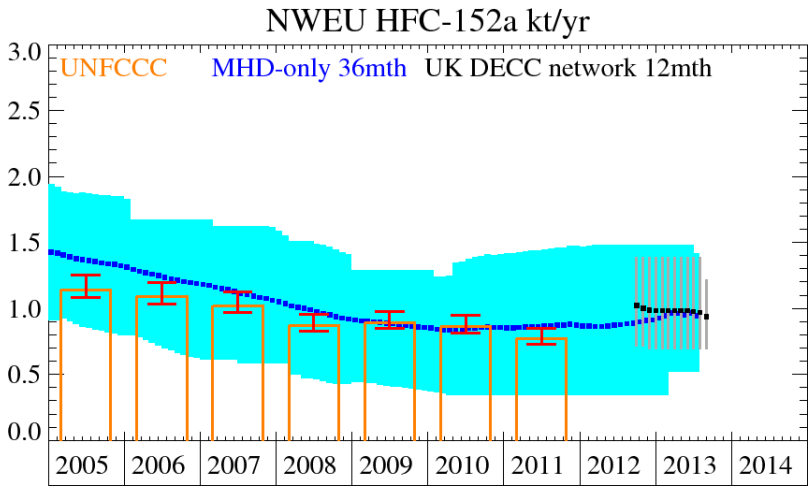

Figure 41: Emission (kt/y) estimates for UK (MHD-only and DECC network) and NWEU. The uncertainty bars represent the 5th and 95th percentiles.

The NWEU emission estimates from both InTEM and the inventory match very well. The comparison for the UK is less well matched between 2002-2008, when the inventory exhibited a substantial increase in emissions compared to InTEM. The UK comparison either side of this time window is good. This difference in a specific time window is very interesting and DECC may like to consider further investigation into this in collaboration with the inventory compilers.

Unit	Year	UK	(5th-95th)	NWEU	(5th-95th)
t/y	1995	55.	(20.- 82.)	410.	(280.- 840.)
t/y	1996	51.	(0.- 93.)	290.	(10.- 600.)
t/y	1997	35.	(0.- 91.)	440.	(30.- 570.)
t/y	1998	53.	(12.- 86.)	480.	(360.- 570.)
t/y	1999	58.	(28.- 83.)	550.	(440.- 840.)
t/y	2000	74.	(30.- 109.)	840.	(510.-1360.)
t/y	2001	80.	(31.- 119.)	1300.	(780.-1790.)
t/y	2002	108.	(33.- 139.)	1600.	(1170.-1870.)
t/y	2003	123.	(53.- 142.)	1610.	(1330.-1910.)
t/y	2004	113.	(37.- 137.)	1500.	(1170.-1910.)
t/y	2005	100.	(22.- 156.)	1460.	(890.-1700.)
t/y	2006	116.	(22.- 167.)	1410.	(870.-1580.)
t/y	2007	116.	(22.- 161.)	1150.	(650.-1540.)
t/y	2008	107.	(23.- 149.)	1040	.(620.-1270.)
t/y	2009	103.	(25.- 139.)	950.	(450.-1180.)
t/y	2010	98.	(15.- 154.)	930.	(410.-1070.)
t/y	2011	106.	(2.- 180.)	980.	(400.-1360.)
t/y	2012	114.	(1.- 191.)	1030.	(400.-1400.)
t/y	2013	121.	(45.- 170.)	910.	(450.-1230.)

Table 17: Emission (t/y) estimates for UK and NWEU with uncertainty (5th – 95th %ile).

Region	Unit	Emission	Range
England	t/yr	134	(37 - 249)
Scotland	t/yr	6.5	(0.0 - 29.5)
Wales	t/yr	0	(0.0 - 0.2)
N.Ireland	t/yr	5.6	(0.0 - 22)

Table 18: Emission (t/y) estimates for the UK Devolved Administrations using the UK DECC network for July 2012-2013.

5.9 HFC-23

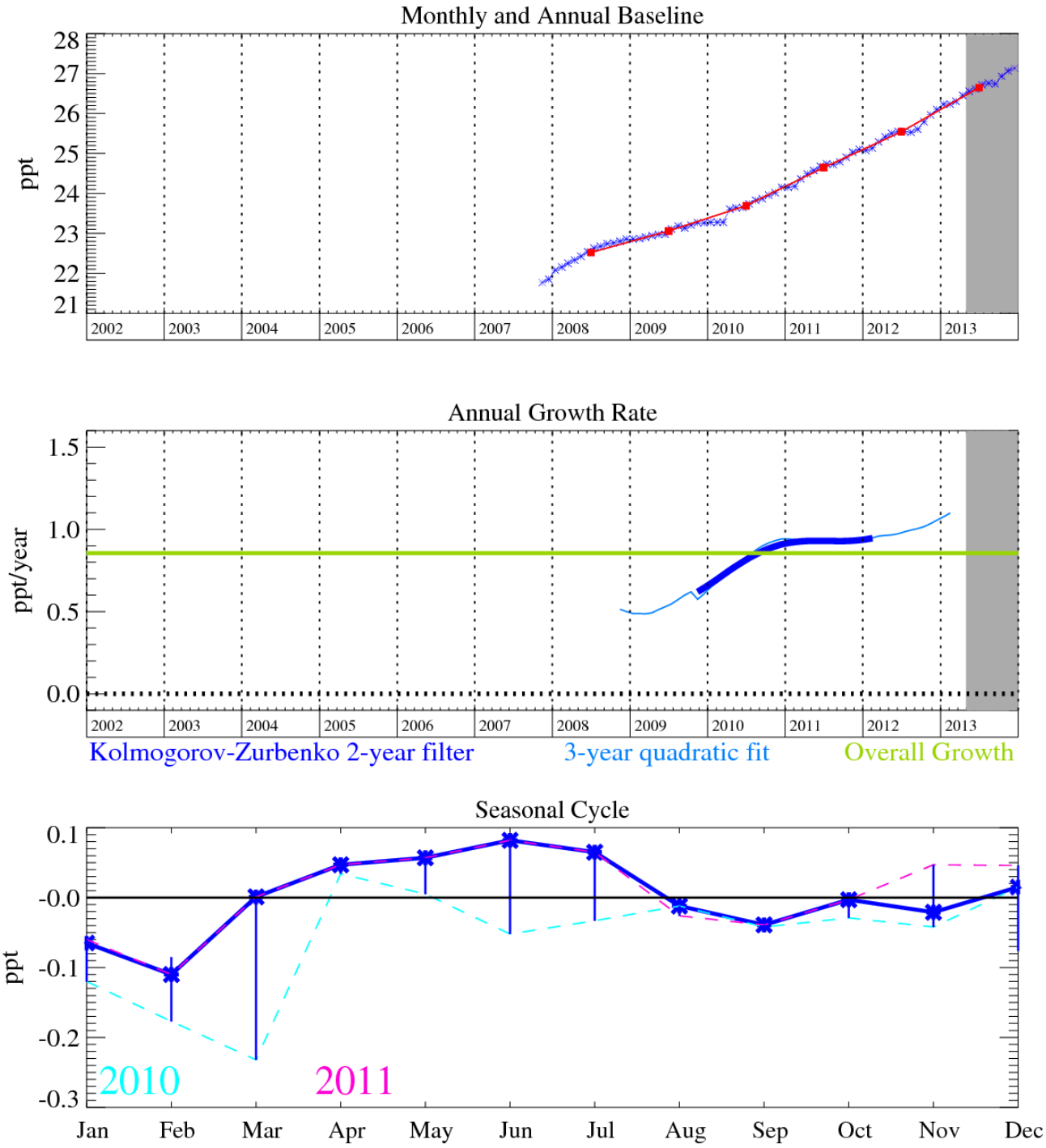

Figure 42: HFC-23 (CHF_3): Monthly (blue) and annual (red) baseline mole fractions. Annual (blue) and overall average growth rate (green) (lower plot). Grey area covers un-ratified and therefore provisional data.

HFC-23 (CHF_3): is primarily a by-product formed by the over fluorination of chloroform during the production of HCFC-22, other minor emissions arise from the electronic industry and fire extinguishers. For this reason it has grown at an average rate of 1.1 ppt/yr and by December 2013 had reached a mixing ratio of 27.1 ppt. It is the second most abundant HFC in the atmosphere after HFC-134a; this combined with a long atmospheric lifetime of 228 years makes this compound a potent GHG. Emissions of HFC-23 in developed countries has declined due to the Montreal Protocol phase-out schedule for HCFC-22, however, emissions from developing countries continues to drive global mixing ratios up, and will continue to do so until implementation of HFC-23 incineration through the Clean Development Mechanism is more widely used.

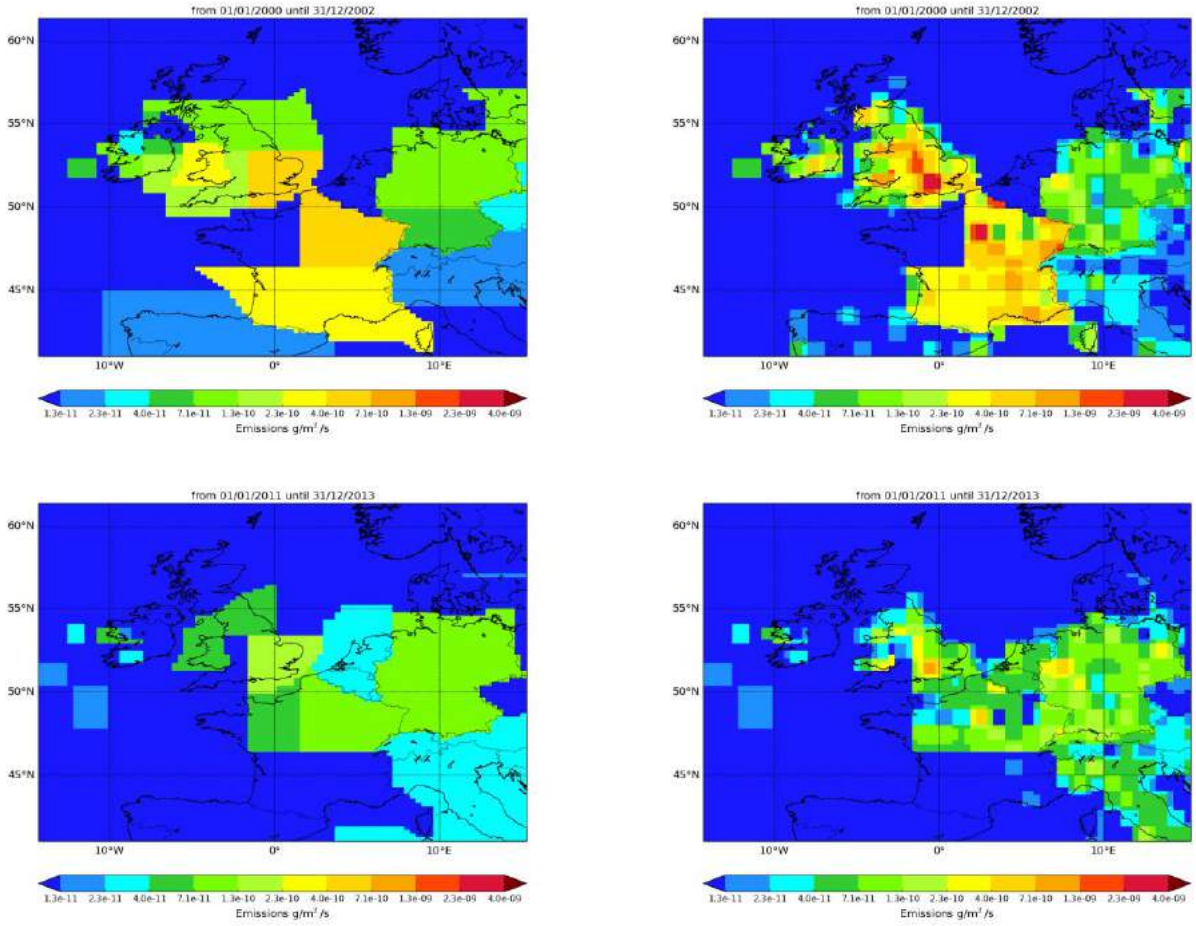

Figure 43: NAME-inversion emission estimates for 2008-2010 (upper) and 2011-2013 (lower). On the right hand side the emissions per grid box have been re-distributed based on population.

The statistical fit between the model time-series and the observations is not strong and this is reflected in the significant uncertainty bars for the InTEM emission estimates. Although the InTEM estimates on average are higher than the inventory estimates, the uncertainty ranges entirely overlap for the UK. The baseline uncertainty is of a similar magnitude to the pollution events and so the emission estimates are very uncertain. The use of the Mace Head baseline at Tacolneston is a particular issue for this gas because of this issue, hence the even larger uncertainty when the DECC network observations are included.

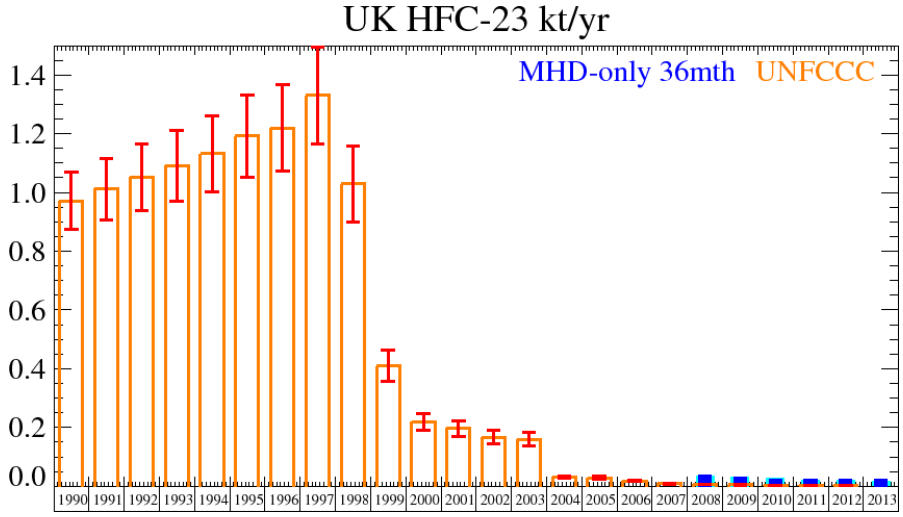

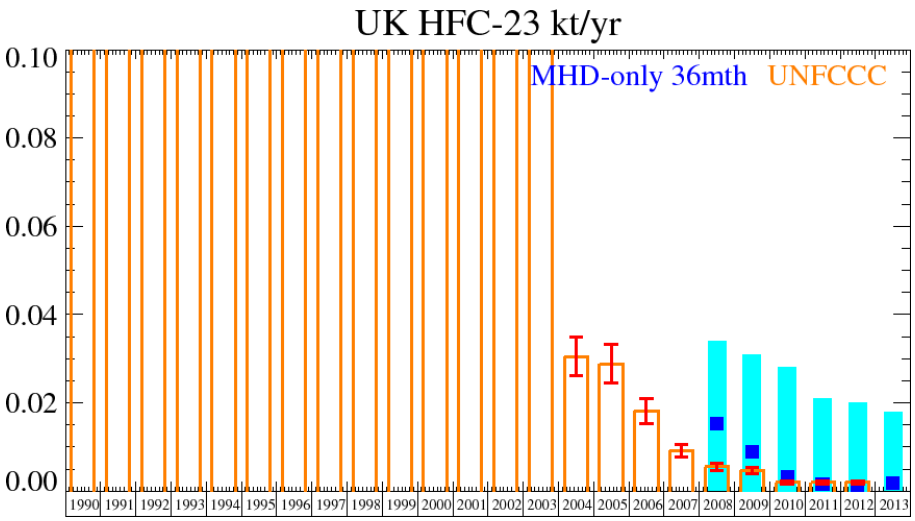
UK HFC-23 kt/yr
MHD-only 36mth
UNFCCC
0.10
0.08
0.06
0.04
0.02
0.00
1990 1991 1992 1993 1994 1995 1996 1997 1998 1999 2000 2001 2002 2003 2004 2005 2006 2007 2008 2009 2010 2011 2012 2013

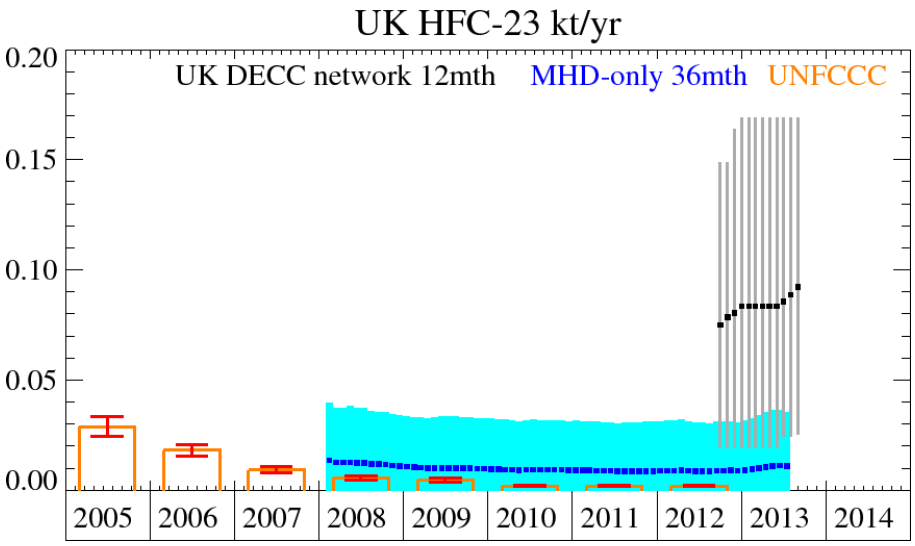
UK HFC-23 kt/yr
UK DECC network 12mth
MHD-only 36mth
UNFCCC
0.20
0.15
0.10
0.05
0.00
2005 2006 2007 2008 2009 2010 2011 2012 2013 2014

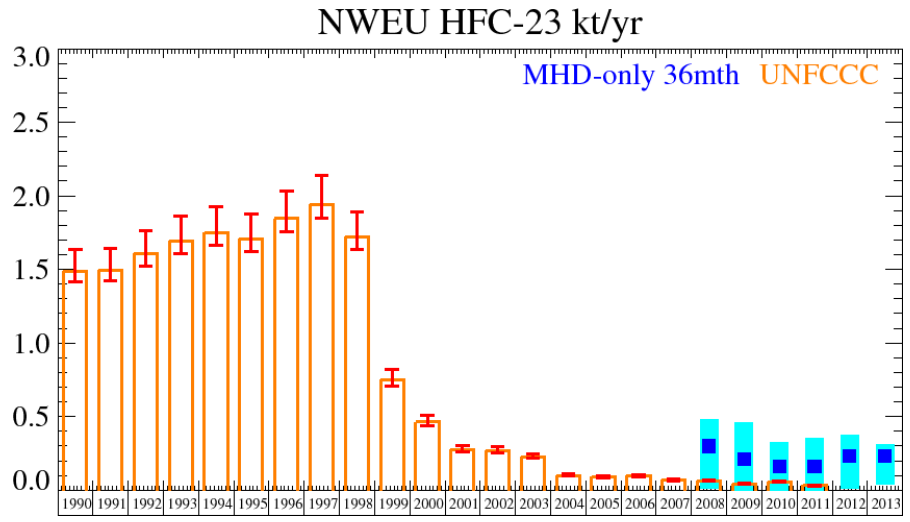
NWEU HFC-23 kt/yr
MHD-only 36mth
UNFCCC
3.0
2.5
2.0
1.5
1.0
0.5
0.0
1990 1991 1992 1993 1994 1995 1996 1997 1998 1999 2000 2001 2002 2003 2004 2005 2006 2007 2008 2009 2010 2011 2012 2013

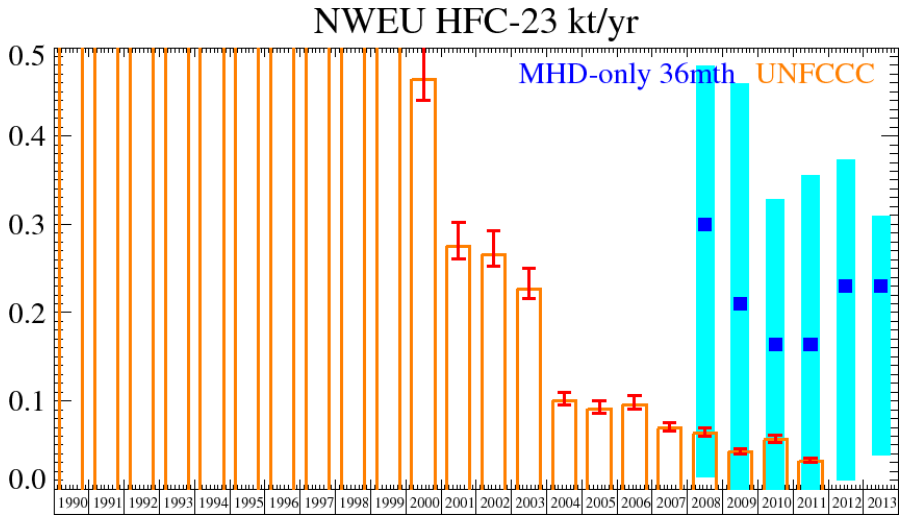

Figure 44: Emission (kt/y) estimates for UK (MHD-only and DECC network and NWEU. The uncertainty bars represent the 5th and 95th percentiles.

Unit	Year	UK	(5th-95th)	NWEU	(5th-95th)
t/y	2008	15.4	(0.03- 34.)	300.	(14. -480.)
t/y	2009	9.0	(0.00- 31.)	210.	(0. -460.)
t/y	2010	3.2	(0.00- 28.)	164.	(0. -330.)
t/y	2011	1.56	(0.01- 21.)	164.	(0. -360.)
t/y	2012	1.04	(0.01- 20.)	230.	(10. -370.)
t/y	2013	1.89	(0.22- 18.)	230.	(39. -310.)

Table 19: Emission (t/y) estimates for UK and NWEU with uncertainty (5th – 95th %ile).

Region	Unit	Emission	Range
England	t/yr	60	(21 - 111)
Scotland	t/yr	23	(0.0 - 72)
Wales	t/yr	0	(0.0 - 0.0)
N.Ireland	t/yr	0.5	(0.0 - 3.9)

Table 20: Emission (t/y) estimates for the UK Devolved Administrations using the UK DECC network for July 2012-2013.

5.10 HFC-32

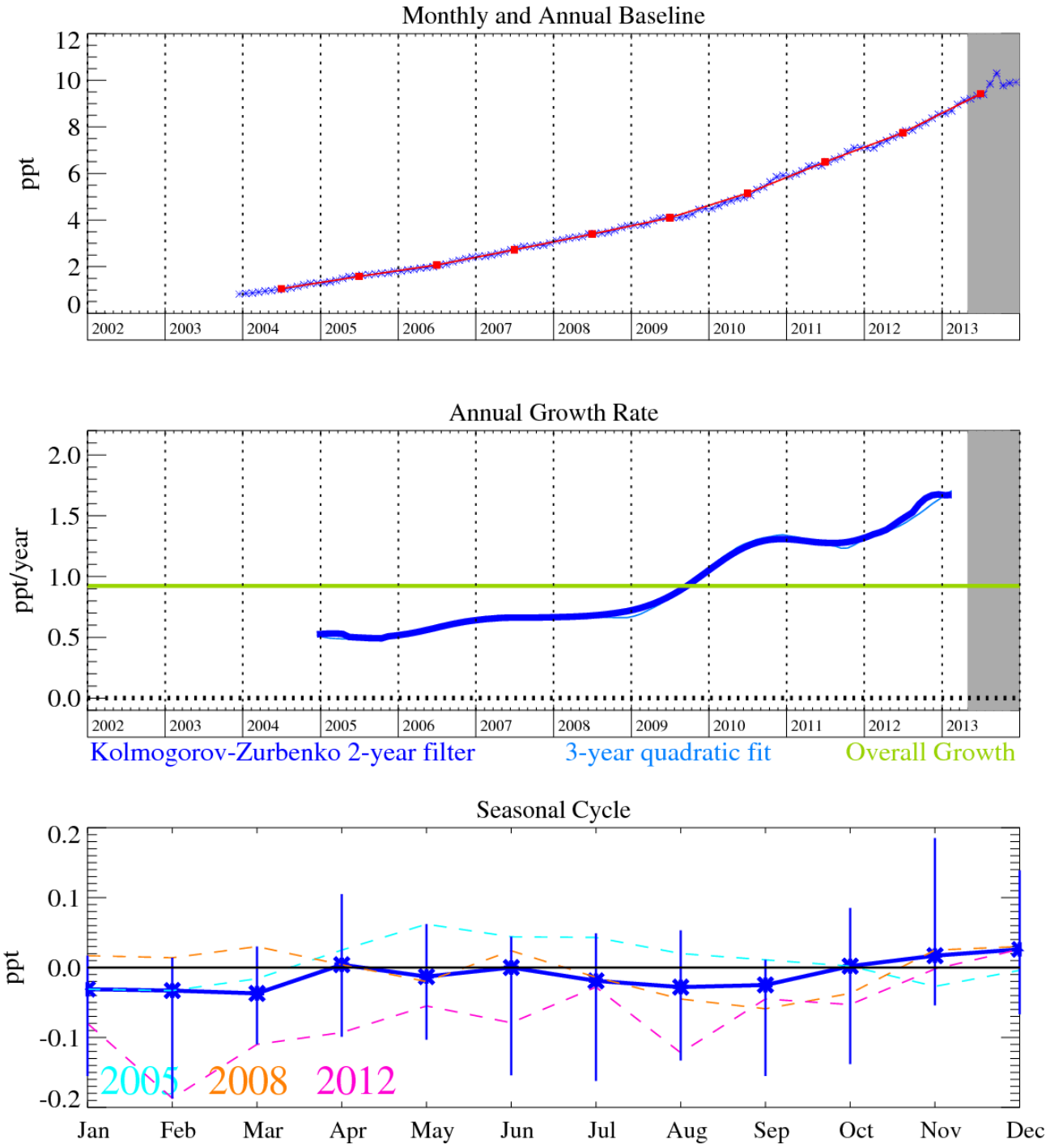

Figure 45: HFC-32 (CH_2F_2): Monthly (blue) and annual (red) baseline mole fractions (top plot). Annual (blue) and overall average growth rate (green) (middle plot). Seasonal cycle (de-trended) with year-to-year variability (lower plot). Grey area covers un-ratified and therefore provisional data.

HFC-32 (CH_2F_2): has an atmospheric lifetime of 5.4 years and a GWP_{100} of 716. It is used in air conditioning and refrigeration applications; azeotropic R-410A (50% HFC-32, 50% HFC-125 by weight) and R-407C (23% HFC-32, 52% HFC-134a, 25% HFC-125 by weight) are used to replace HCFC-22. As the phase-out of HCFC-22 gains momentum it might be expected that demand for these refrigerant blends will increase. The pollution events measured at Mace Head are highly correlated with that of HFC-125, and is used as a diagnostic for leakages in the on-site air conditioners.

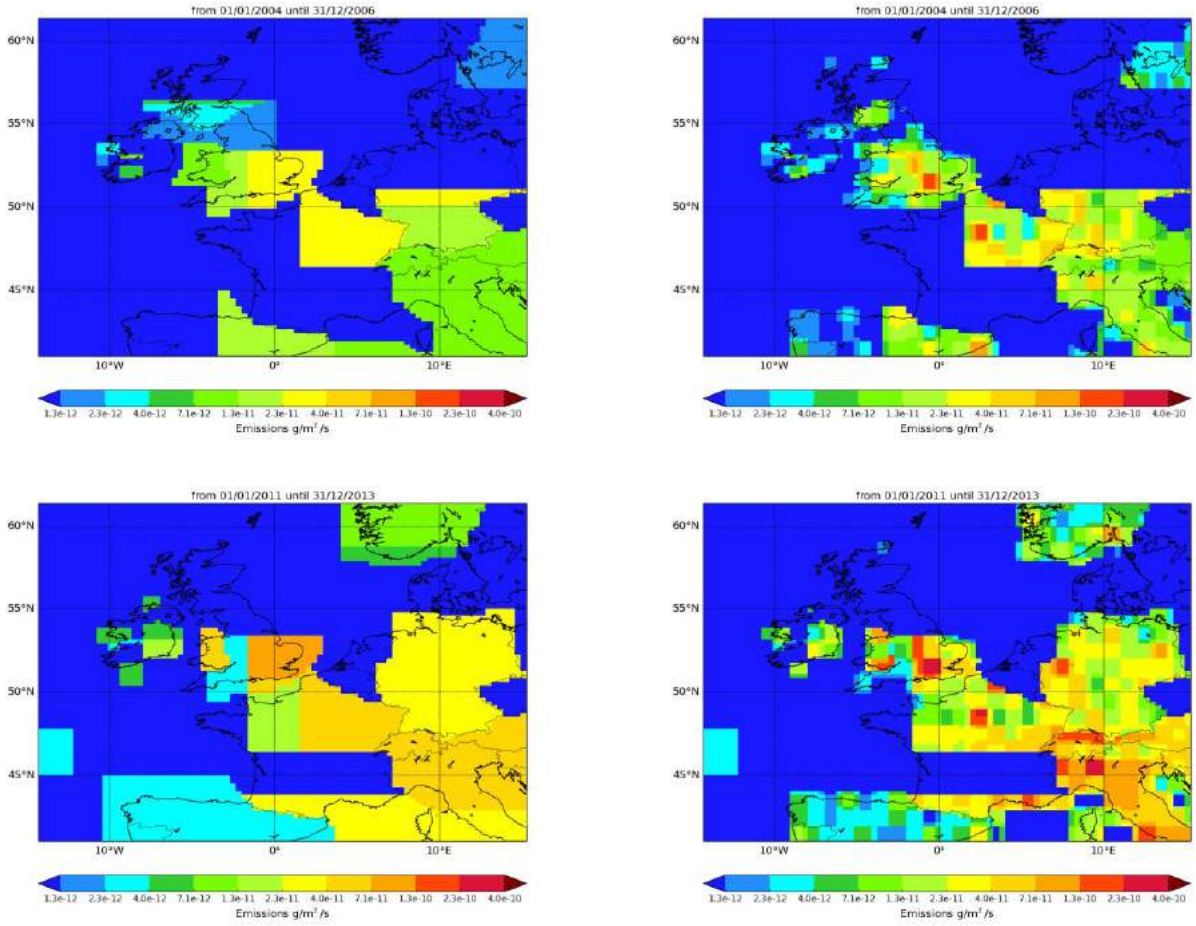

Figure 46: NAME-inversion emission estimates for 2004-2006 (upper) and 2011-2013 (lower). On the right hand side the emissions per grid box have been re-distributed based on population.

The UK emission estimates from the inventory and InTEM are both growing but the inventory is growing faster than the InTEM estimates. The UK emission estimates when the Tacolneston data are included are higher than the MHD-only estimates, although the uncertainties overlap. The NWEU estimates from InTEM are very similar to the inventory estimates.

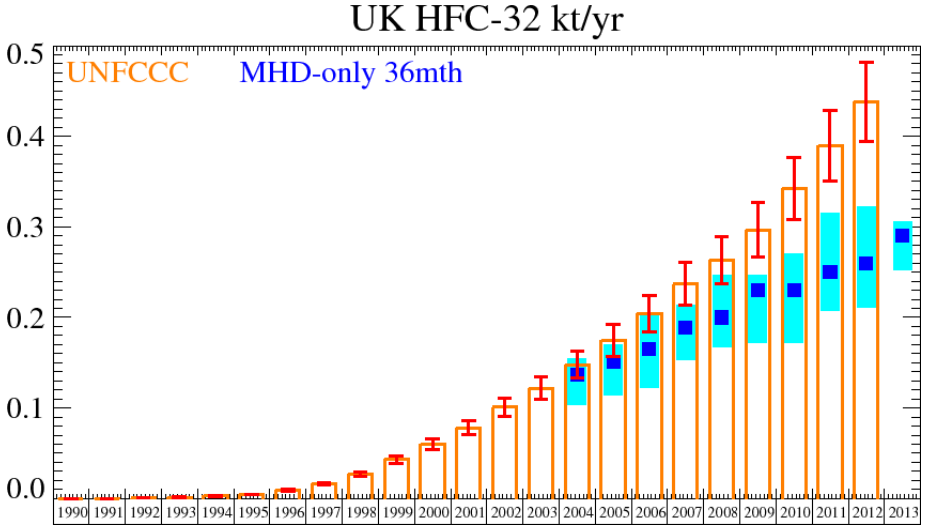

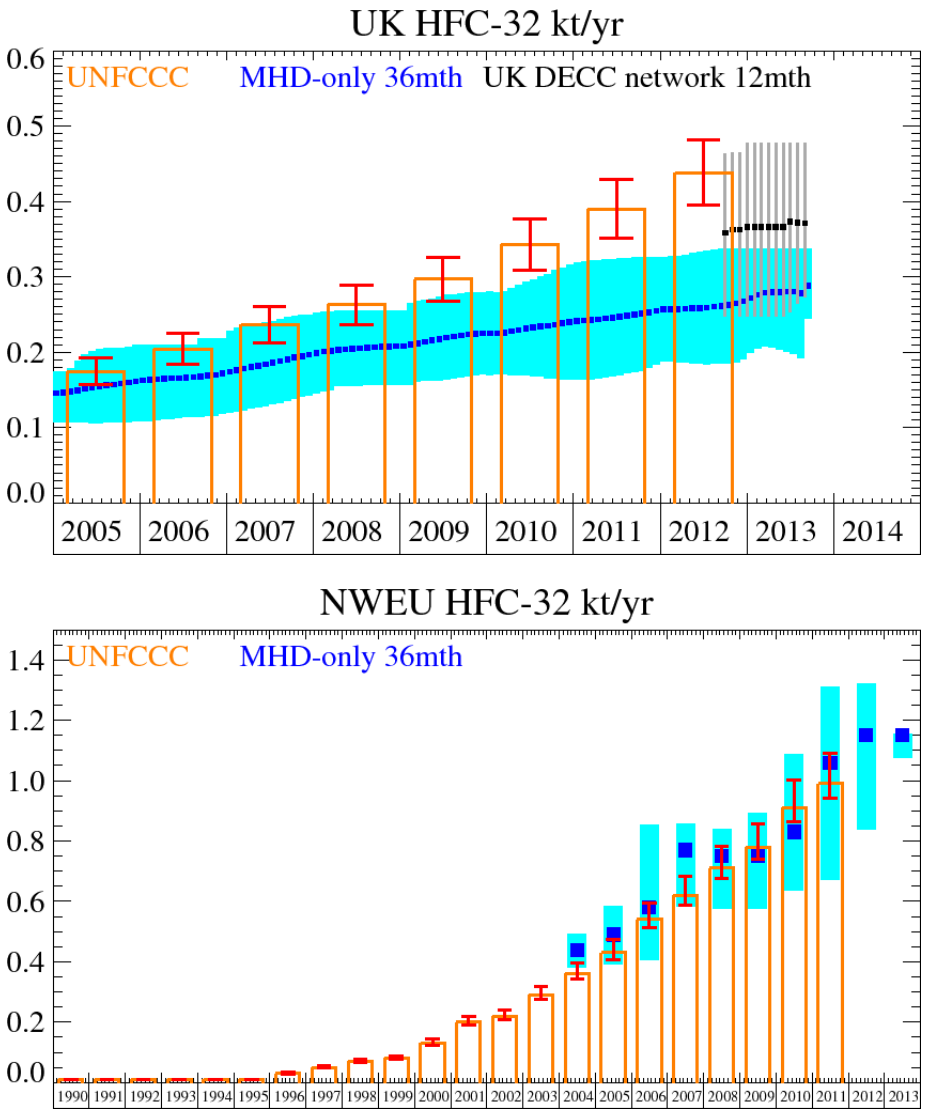

Figure 47: Emission (kt/y) estimates for UK (MHD-only and DECC network) and NWEU. The uncertainty bars represent the 5th and 95th percentiles.

Unit	Year	UK	(5th-95th)	NWEU	(5th-95th)
t/y	2004	137.	(103.- 155.)	440.	(380.- 490.)
t/y	2005	151.	(114.- 170.)	490.	(390.- 590.)
t/y	2006	165.	(122.- 205.)	580.	(410.- 860.)
t/y	2007	189.	(153.- 214.)	770.	(580.- 860.)
t/y	2008	200.	(167.- 247.)	750.	(580.- 840.)
t/y	2009	230.	(172.- 247.)	750.	(580.- 890.)
t/y	2010	230.	(172.- 271.)	830.	(640.-1090.)
t/y	2011	250.	(207.- 315.)	1060.	(670.-1310.)
t/y	2012	260.	(211.- 323.)	1150.	(840.-1320.)
t/y	2013	290.	(252.- 306.)	1150.	(1080.-1160.)

Table 21: Emission (t/y) estimates for UK and NWEU with uncertainty (5th – 95th %ile).

Region	Unit	Emission	Range
England	t/yr	284.46	(201. - 382.)
Scotland	t/yr	27.22	(0.0 - 88.6)
Wales	t/yr	49.48	(26.5 - 66.8)
N.Ireland	t/yr	5.77	(0.0 - 23.3)

Table 22: Emission (t/y) estimates for the UK Devolved Administrations using the UK DECC network for July 2012-2013.

5.11 HFC-227ea

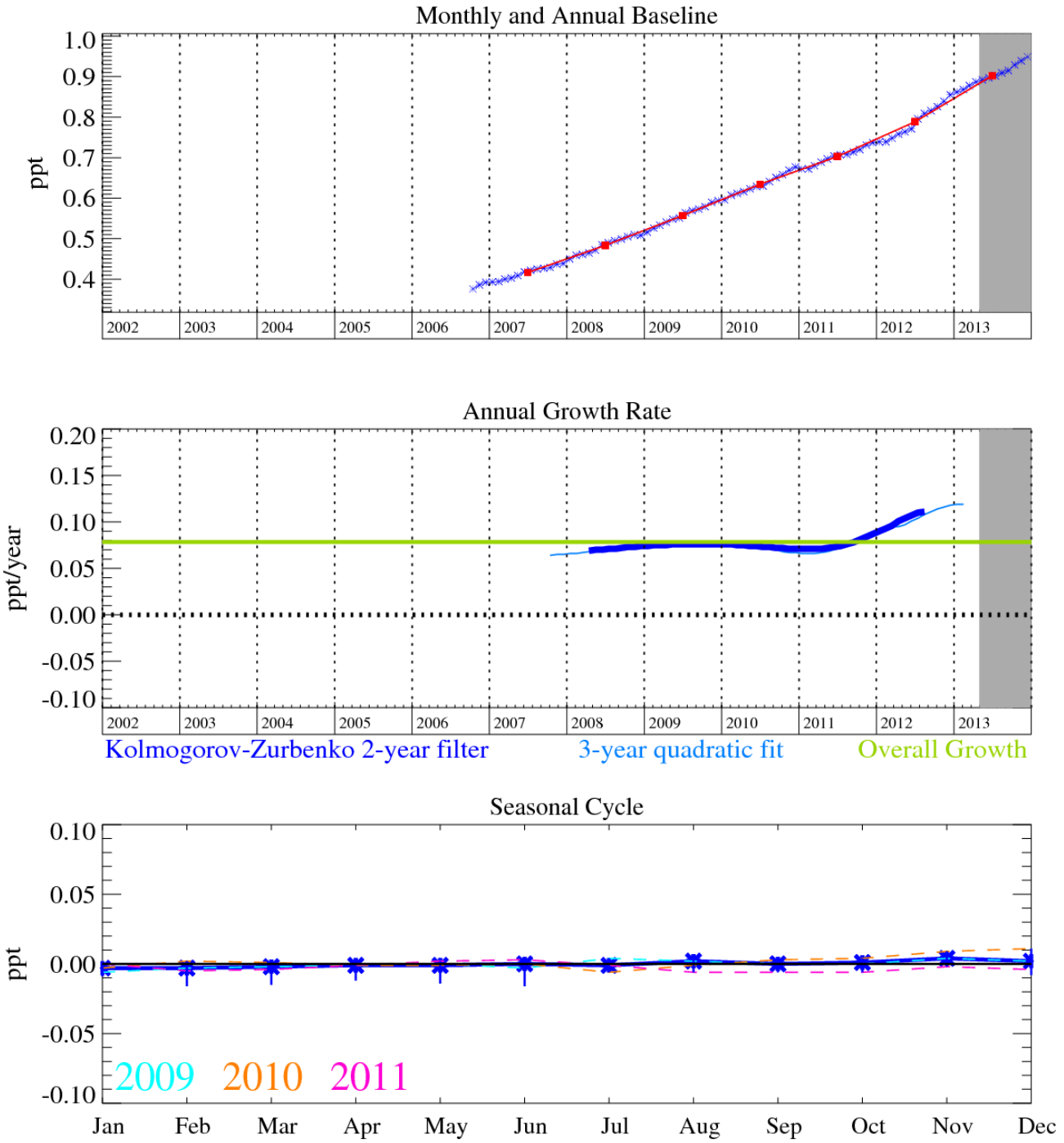

Figure 48: HFC-227ea (C_3HF_7): Monthly (blue) and annual (red) baseline mole fractions (top plot). Annual (blue) and overall average growth rate (green) (middle plot). Seasonal cycle (de-trended) with year-to-year variability (lower plot). Grey area covers un-ratified and therefore provisional data.

HFC-227ea (C_3HF_7): was added to the Medusa analysis in January 2008. HFC-227ea is used as a propellant for medical aerosols and a fire-fighting agent and to a lesser extent in metered-dose inhalers, and foam blowing (atmospheric lifetime 35.8 years and GWP_{100} of 3580). It has reached a mole fraction of 0.95 ppt (Dec. 2012) with a growth rate of 0.11 ppt/yr.

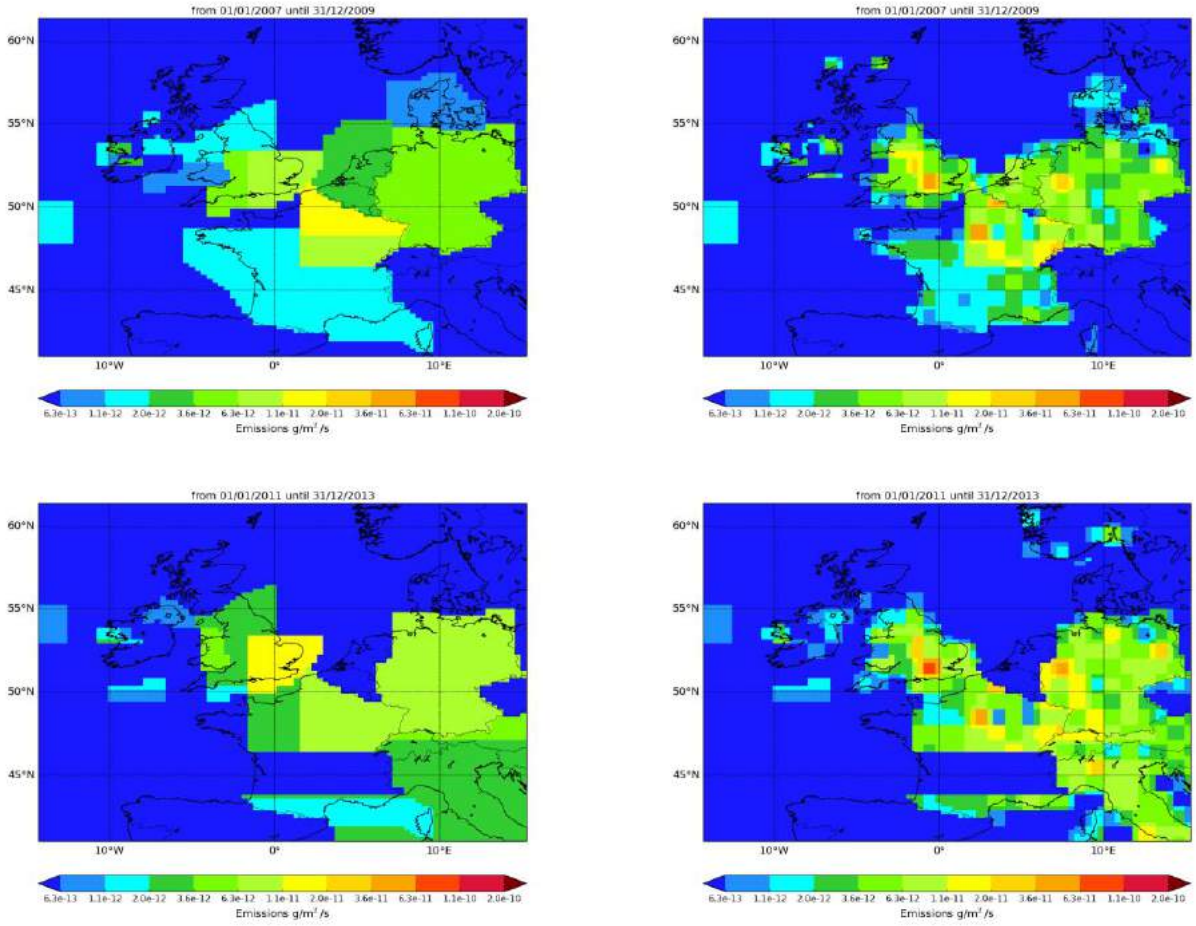

Figure 49: NAME-inversion emission estimates for 2007-2009 (upper) and 2011-2013 (lower). On the right hand side the emissions per grid box have been re-distributed based on population.

The InTEM results are significantly lower (50%) than the inventory estimates. The reason for this difference is unknown. The results when the new observations from Tacolneston are incorporated are similar to the Mace Head only InTEM results. DECC may like to consider further investigation into this in collaboration with the inventory compilers to understand this significant mis-match. The statistical match between the model time-series and the observations is reasonable.

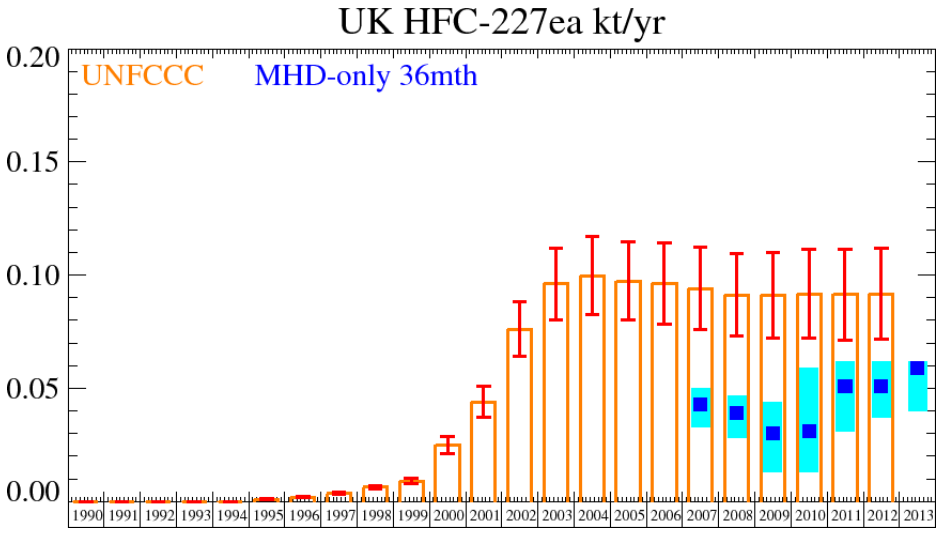

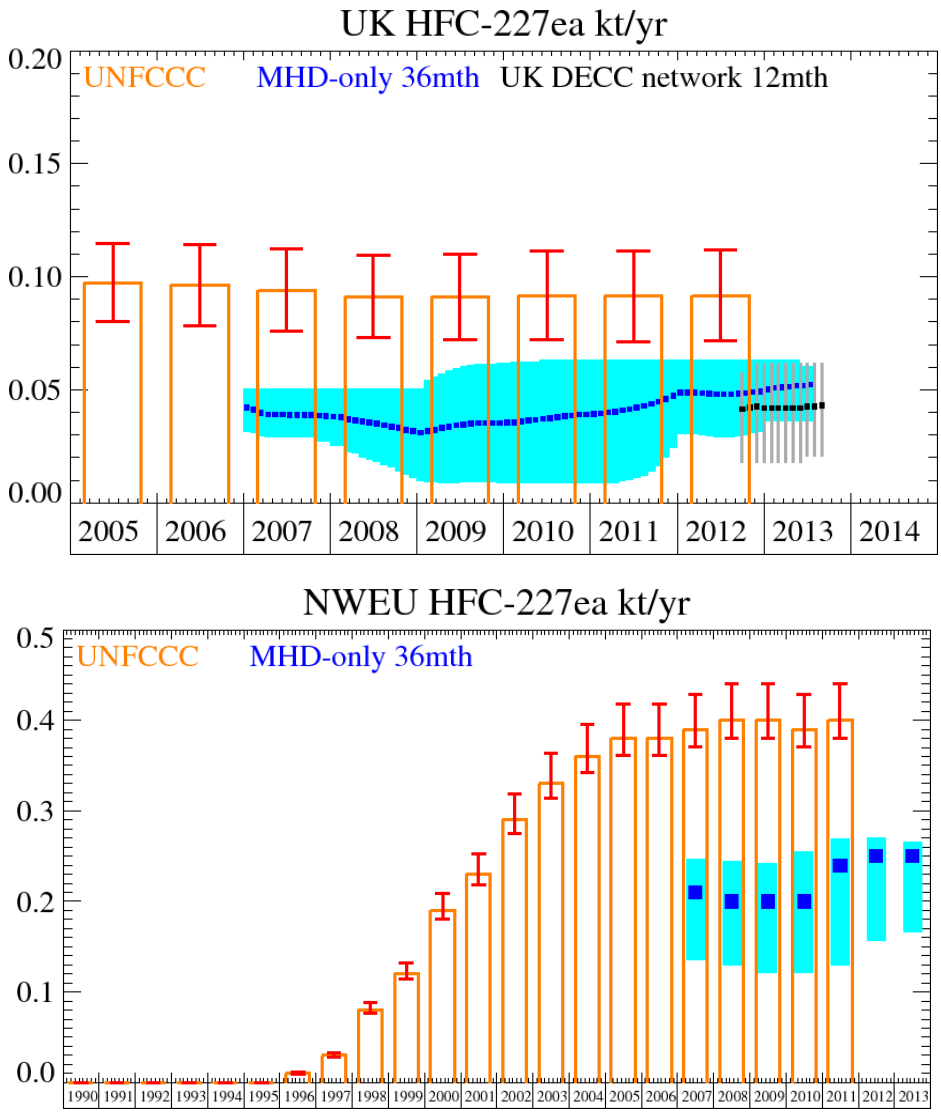

Figure 50: Emission (kt/y) estimates for UK (MHD-only and DECC network) and NWEU. The uncertainty bars represent the 5th and 95th percentiles.

Unit	Year	UK	(5th-95th)	NWEU	(5th-95th)
t/y	2007	43.	(33.- 50.)	210.	(135. -247.)
t/y	2008	39.	(28.- 47.)	200.	(130. -245.)
t/y	2009	30.	(13.- 44.)	200.	(121. -242.)
t/y	2010	31.	(13.- 59.)	200.	(121. -255.)
t/y	2011	51.	(31.- 62.)	240.	(130. -269.)
t/y	2012	51.	(37.- 62.)	250.	(157. -271.)
t/y	2013	59.	(40.- 62.)	250.	(166. -266.)

Table 23: Emission (t/y) estimates for UK and NWEU with uncertainty (5th – 95th %ile).

Region	Unit	Emission	Range
England	t/yr	36	(15 - 56)
Scotland	t/yr	1.3	(0.0 - 6.0)
Wales	t/yr	3.9	(0.0 - 8.9)
N.Ireland	t/yr	0.7	(0.0 - 3.1)

Table 24: Emission (t/y) estimates for the UK Devolved Administrations using the UK DECC network for July 2012-2013.

5.12 HFC-43-10mee

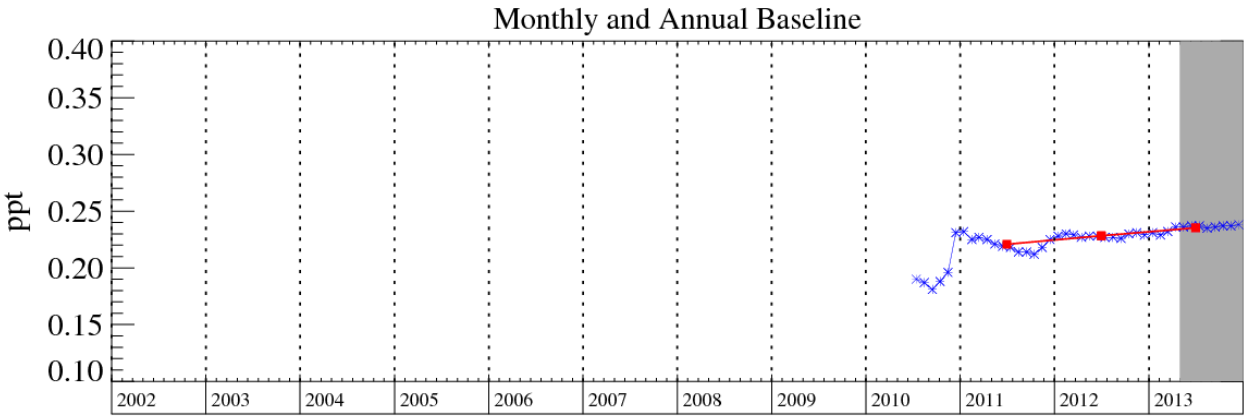

Figure 51: HFC-43-10mee ($C_5H_2F_{10}$): Monthly (blue) and annual (red) baseline mole fractions.

HFC-43-10mee ($C_5H_2F_{10}$): Introduced in the mid 1990s as a replacement for CFC-113. It meets many requirements in the electronics industries and replaces PFCs in some uses such as a carrier fluid for lubricants applied to computer hard disks. It has an atmospheric lifetime of 15.9 years, a GWP_{100} of 1,640 and a radiative efficiency of 0.4 W m^{-2} ppb^{-1}.

As yet it is too early to calculate growth rates for this gas, but this information will be included once 3 years of data have been acquired. The first inversion results for HFC-43-10mee show that there is significant disagreement between the inventory and the InTEM results. The median InTEM results are a factor of eight smaller albeit the emissions from either method are small.

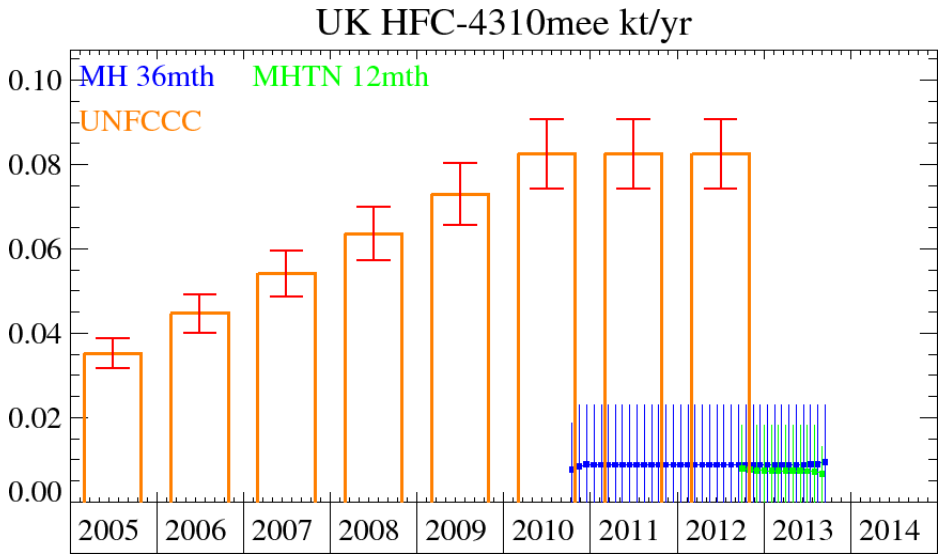

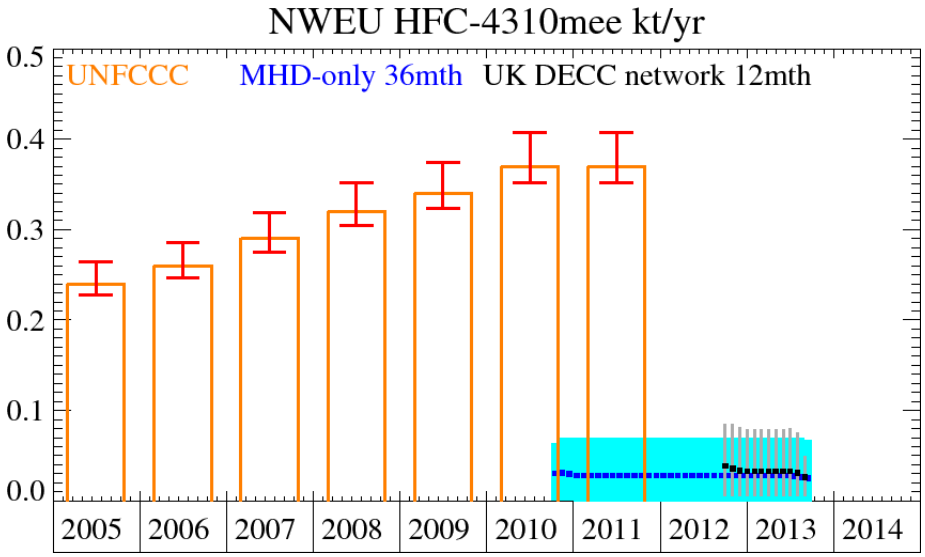

Figure 52: Emission (kt/y) estimates for UK and NWEU (UK DECC network). The uncertainty bars represent the 5th and 95th percentiles.

Unit	Year	UK	(5th-95th)	NWEU	(5th-95th)
t/y	2011	9.3	(0.01- 23.)	28	(0.1 -64.)
t/y	2012	9.3	(0.01- 23.)	28	(0.1 -64.)
t/y	2013	9.5	(0.96- 14.)	26	(2.6 -28.)

Table 25: Emission (t/y) estimates for UK and NWEU with uncertainty (5th – 95th %ile).

Region	Unit	Emission	Range
England	t/yr	4.7	(0.0 - 11.0)
Scotland	t/yr	1.1	(0.0 - 3.8)
Wales	t/yr	0.9	(0.0 - 3.5)
N.Ireland	t/yr	0.7	(0.0 - 2.6)

Table 26: Emission (t/y) estimates for the UK Devolved Administrations using the UK DECC network for July 2012-2013.

5.13 PFC-14 (CF_4)

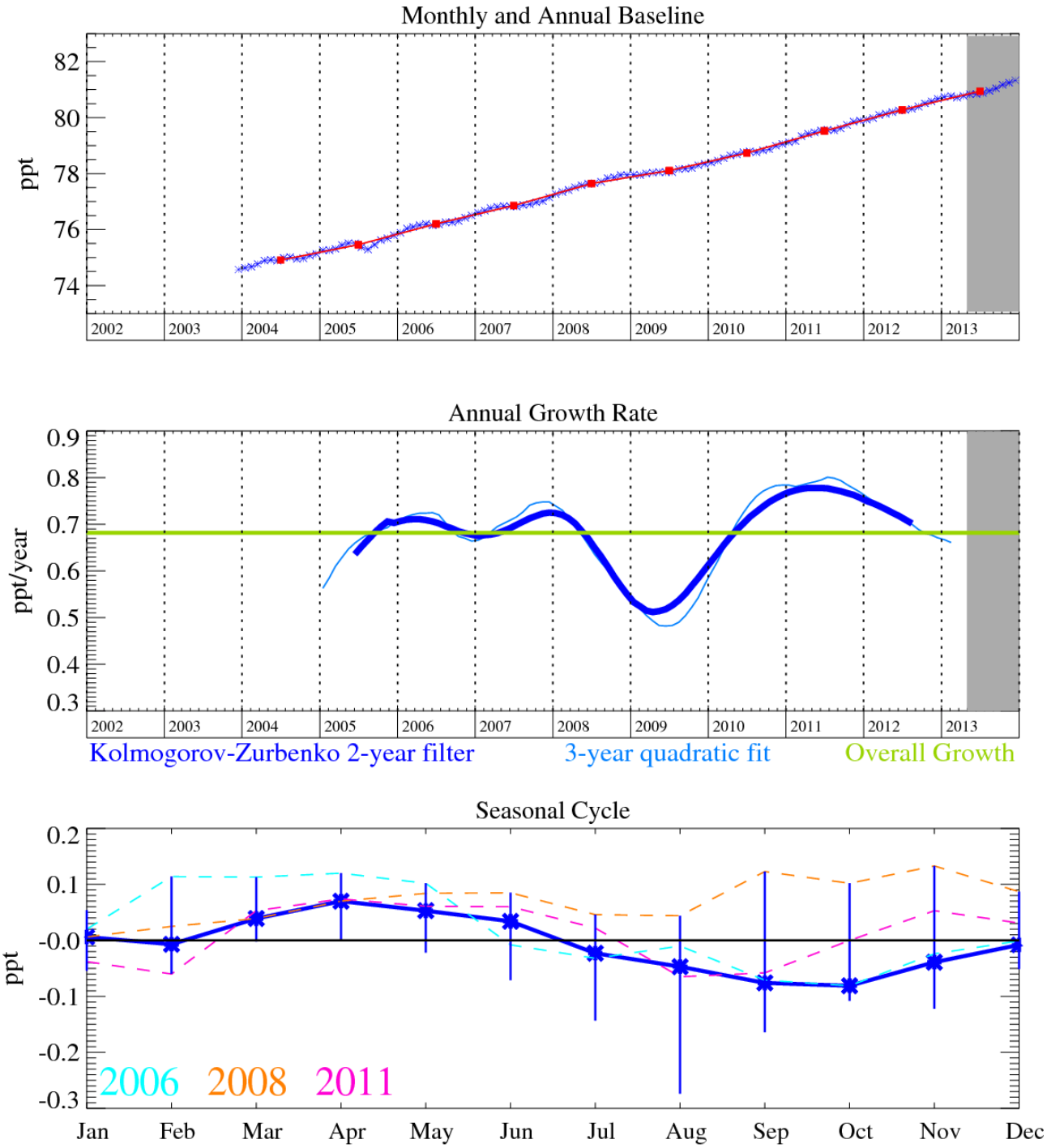

Figure 53: PFC-14 (CF_4): Monthly (blue) and annual (red) baseline mole fractions (top plot). Annual (blue) and overall average growth rate (green) (middle plot). Seasonal cycle (de-trended) with year-to-year variability (lower plot). Grey area covers un-ratified and therefore provisional data.

PFC-14 (CF_4) possesses the longest known lifetime of anthropogenic molecules (>50,000 yrs), which, when coupled with its high absolute radiative forcing (0.08 W m^{-2} ppb^{-1}) gives rise to a high GWP_{100} of 5,820 and can equate to upwards of 1% of total radiative forcing. Its primary emission source is as an unwanted by-product of aluminium smelting during a fault condition known as the Anode Effect. Thus the frequency of occurrence and duration of an anode effect event will determine the regional and global CF_4 emission. CF_4 has some additional minor applications in the semiconductor industry (as a source of F radicals), but industry has shied away from using CF_4 knowing that its GWP is so high. The aluminium industry has recognised the CF_4 (and C_2F_6) emission problem and has been undergoing processes of replacement of older, less efficient aluminium production cells with more efficient designs, and automated and quicker intervention

policies to prevent the occurrence of these anode effects. It is also thought that CF_4 has a natural source from crustal degassing.

The current growth rate of atmospheric CF_4 is 0.7 ppt/yr. This compound will continue to accumulate in the atmosphere due to its very long atmospheric lifetime. In December 2013 the mole fraction of CF_4 was 81.3 ppt.

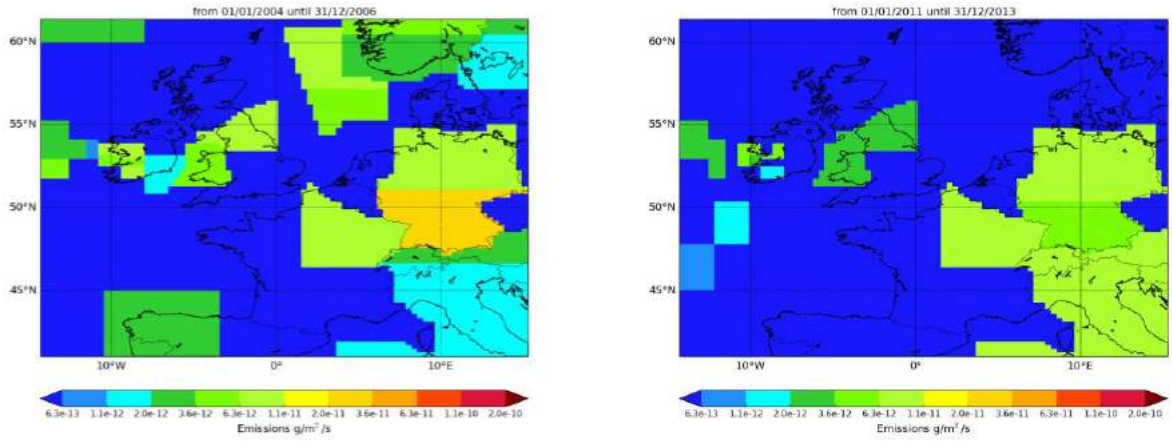

Figure 54: NAME-inversion emission estimates for 2003-2005 (left) and 2011-2013 (lright). As the primary emissions are from aluminium production the emissions have not been re-distributed based on population.

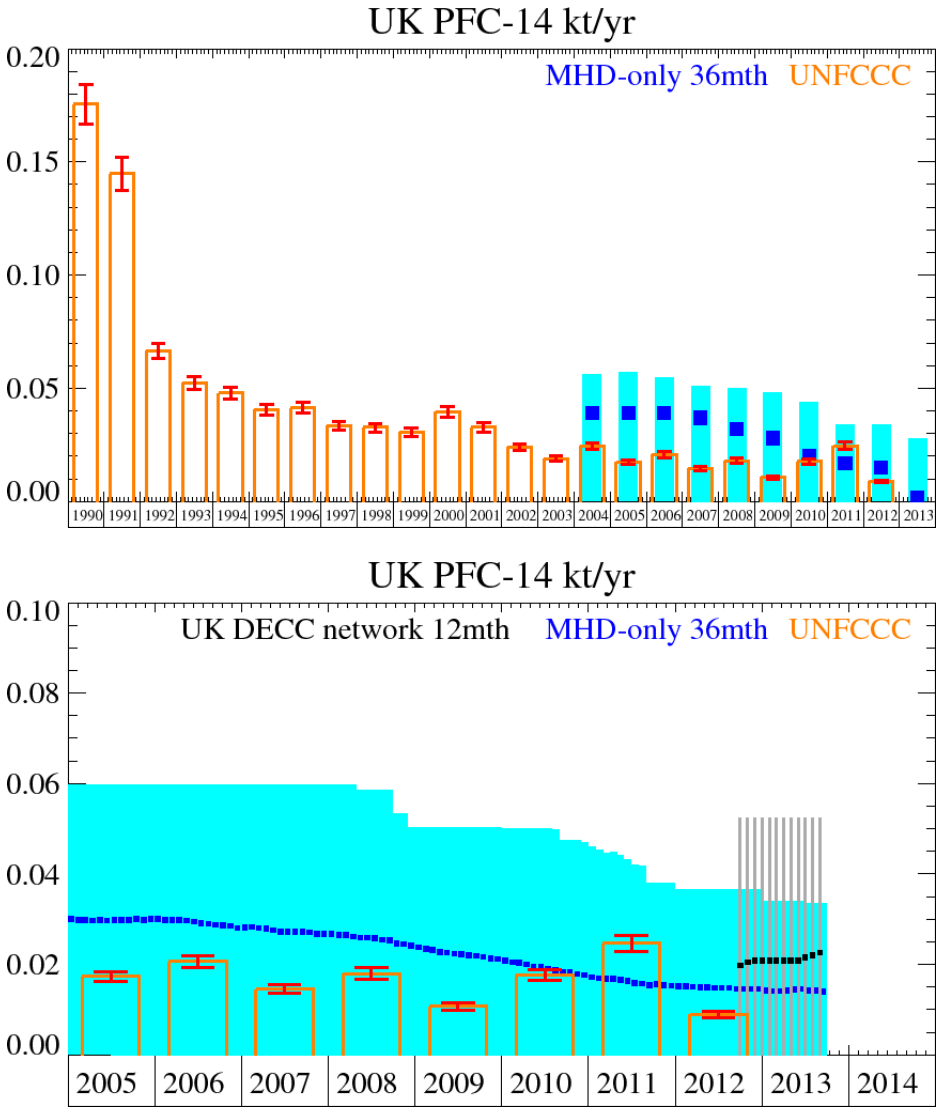

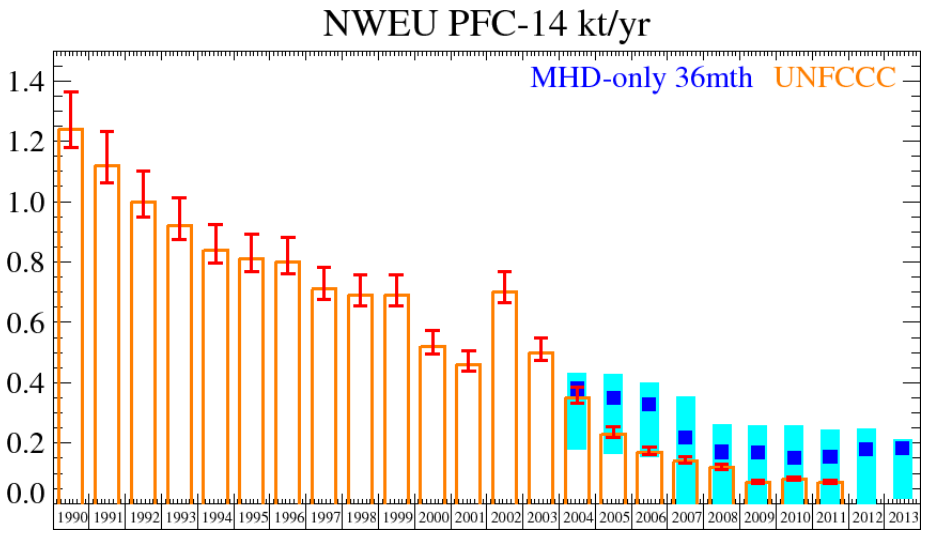

Figure 55: Emission (kt/y) estimates for UK (MHD-only and DECC network) and NWEU. The uncertainty bars represent the 5th and 95th percentiles.

The significant uncertainties in the InTEM results entirely overlap with the inventory estimates although the median results are consistently higher. In the standard InTEM inversion, the statistical match between the model time-series and the observations is weak. This is because the emissions are principally from point sources (aluminium smelters). If the locations of the smelters are included and solved for as single grid cells (25 km) then the agreement between model and observation is much improved. The largest smelter in the UK, at Lynemouth on the north east coast of England ceased operations in March 2012. This is very clearly seen in the modelled emissions when the smelter locations are included as prior information.

Unit	Year	UK	(5th-95th)	NWEU	(5th-95th)
t/y	2004	39.	(0.12- 56.)	380.	(180. -430.)
t/y	2005	39.	(0.08- 57.)	350.	(160. -430.)
t/y	2006	39.	(0.08- 55.)	330.	(160. -400.)
t/y	2007	37.	(0.02- 51.)	220.	(0. -360.)
t/y	2008	32.	(0.01- 50.)	171.	(0. -260.)
t/y	2009	28.	(0.01- 48.)	169.	(0. -260.)
t/y	2010	20.	(0.01- 44.)	153.	(0. -260.)
t/y	2011	16.8	(0.02- 34.)	156.	(0. -240.)
t/y	2012	15.2	(0.03- 34.)	179.	(0. -250.)
t/y	2013	1.68	(0.17- 28.)	183.	(18. -210.)

Table 27: Emission (t/y) estimates for UK and NWEU with uncertainty (5th – 95th %ile).

Region	Unit	Emission	Range
England	t/yr	13.94	(0.0 - 33.2)
Scotland	t/yr	0.73	(0.0 - 3.9)
Wales	t/yr	6.37	(0.0 - 17.1)
N.Ireland	t/yr	0	(0.0 - 0.0)

Table 28: Emission (t/y) estimates for the UK Devolved Administrations using the UK DECC network for July 2012-2013.

5.13.1 InTEM using prior information emissions

The table below details the PFC-14 emissions (t/y) for 2011 per significant sector as submitted the UNFCCC (2013). As can be seen, the emission from aluminium production in most countries is the most significant sector. Italy has the largest reported emissions in Europe and it is from neither aluminium production or from the semi-conductor industry. The tabulated emissions have been used to generate a prior emission map for use within InTEM. The locations of the aluminium smelters are known, as is the approximate amount of aluminium produced per site, so the emissions per smelter

can be estimated. The locations of the emissions from the other sectors are not known so these emissions are spread evenly across the relevant country. The prior map produced is shown in Figure 56.

Country	Location	Aluminium Produced (kt/y) 2012	% Aluminium per country	Estimated emission of PFC-14 (t/y) 2004
UK	Anglesey			4.5
UK	Lynemouth			14.7
UK	Lochaber			0.7
Germany	Essen	170	27	20.5
Germany	Hamburg	135	22	16.7
Germany	Neuss	230	36	27.4
Germany	Voerde	96	15	11.4
France	Dunkirk	273	66	143.9
France	St Jean de M	141	34	74.1
Netherlands	Delfzijl	170	100	14.0
Norway	Aardal	233	16.7	20.37
Norway	Hoyanger	60	4.3	5.25
Norway	Husnes	185	13.2	16.10
Norway	Karmoy	170	12.2	14.88
Norway	Lista	127.5	9.1	11.10
Norway	Mosjoen	221.5	15.9	19.40
Norway	Sunndalsora	400	28.6	34.89
Spain	Aviles	93	21.6	5.40
Spain	La Coruna	87	20.2	5.05
Spain	San Ciprian	250	58.2	14.55
Total				476

Table 29: Aluminium produced (kt/y) in 2012 per smelter in Western Europe and the estimated emissions of PFC-14 of each individual smelter.

Country	Semi-Conductor	Aluminium Prod.	Other	Total
UK	2.48	21.14	1.05	24.7
Germany	9.35	10.71	0.02	20.1
Belgium	0.49		0.82	1.3
Switzerland	0.65		2.82	3.5
Denmark			0.2	0.2
Spain		8.71		8.7
France	12.65	11.68	0.53	24.9
Ireland	0.86			0.9
Italy	9.93	10.70	194.7	215.3
Netherlands		10.73		10.7
Norway		29.90		29.9
Poland		5.17		5.2
Sweden			23.49	23.5

Table 30: UNFCCC emissions (t/y) for 2011 (UNFCCC 2013 submissions) per country per significant sector

InTEM was re-run using the prior emission distribution with a Bayesian cost function. The prior uncertainty was defined as 100% for each grid. InTEM was run for each 1-year time period both using MHD-only and DECC network observations, an example of the posteriori solution is shown in Figure 57. The emission estimates for the Lynemouth aluminium smelter and the whole UK are shown in Figure 58. The Lynemouth smelter closed in March 2012 in excellent agreement with the InTEM results. The inclusion of the Tacolneston observations compliments the Mace Head only InTEM results. Due to the closure of the largest smelter in the UK, the overall UK estimates show a very significant reduction in very good agreement to the inventory (Table 27).

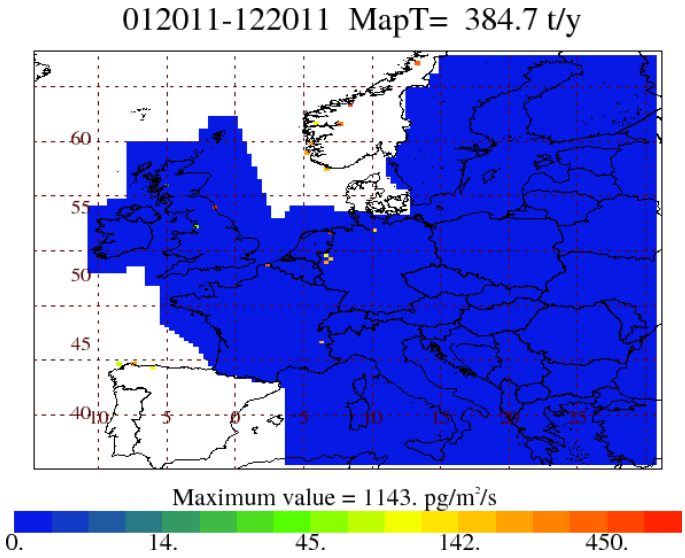

Figure 56: PFC-14 prior emission distribution (UNFCCC 2011) with aluminium smelters as point sources and the remaining country emissions spread evenly across each country.

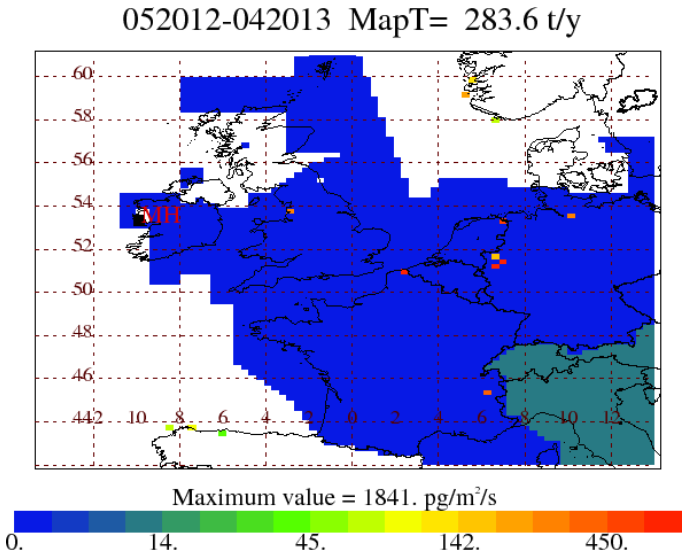

Figure 57: PFC-14 posteriori emission distribution (InTEM) when prior emissions are used.

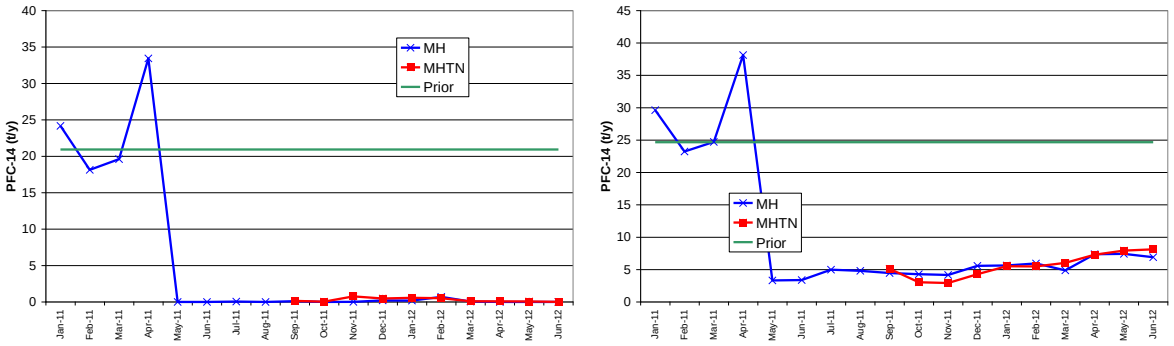

(a) (b)

Figure 58: (a) InTEM emission estimation at Lynemouth aluminium smelter, UK (MHD-only and DECC network), (b) InTEM emission estimate for the whole UK (MHD-only and DECC network).

5.14 PFC-116

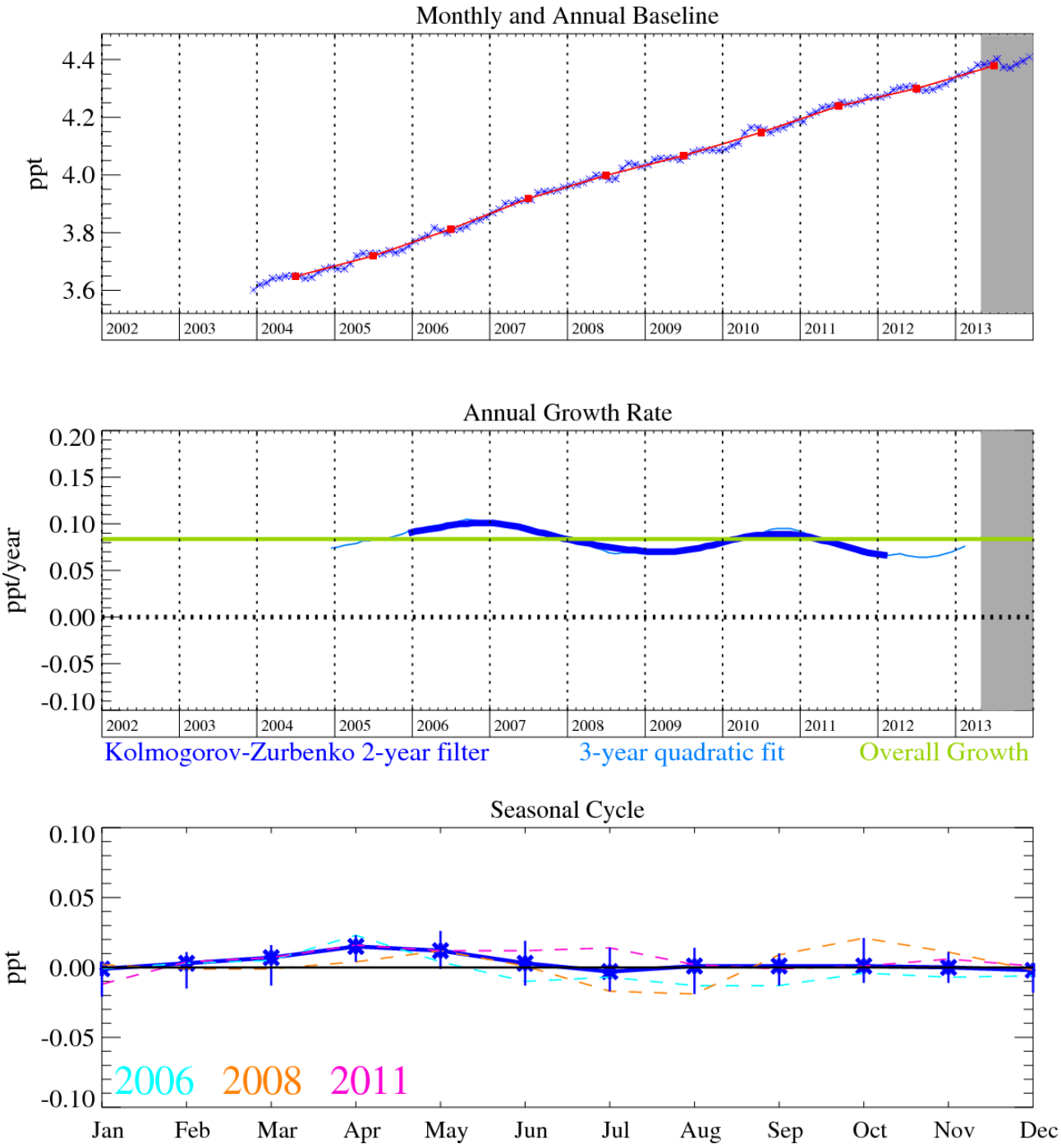

Figure 59: PFC-116 (C_2F_6): Monthly (blue) and annual (red) baseline mole fractions (top plot). Annual (blue) and overall average growth rate (green) (middle plot). Seasonal cycle (de-trended) with year-to-year variability (lower plot). Grey area covers un-ratified and therefore provisional data.

PFC-116 (C_2F_6) is also a potent greenhouse gas with an atmospheric lifetime of >10,000 years. It has common sources to CF_4, this serves to help explain why all of the CF_4 above-baseline (pollution) events are usually correlated with those of C_2F_6. However, we note that there are many more frequent and greater magnitude emissions of C_2F_6 relative to CF_4. This is due to the dominant source of C_2F_6 being from semiconductor industries (plasma etching).

The current growth rate of atmospheric C_2F_6 is 0.08 ppt/yr. This compound will continue to accumulate in the atmosphere due to its very long atmospheric lifetimes. In December 2013 the mole fraction of C_2F_6 was 4.4 ppt.

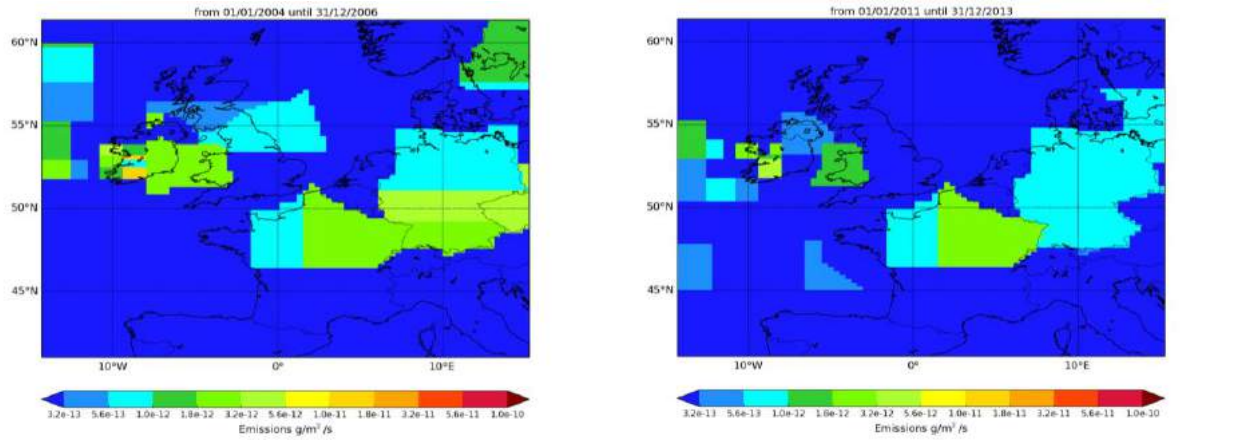

Figure 60: NAME-inversion emission estimates for 2004-2006 (left) and 2011-2013 (right).

The InTEM uncertainty ranges for the regional emissions are large but consistently overlap the inventory estimates. The statistical match between the estimated model time-series and the observations is fair to weak.

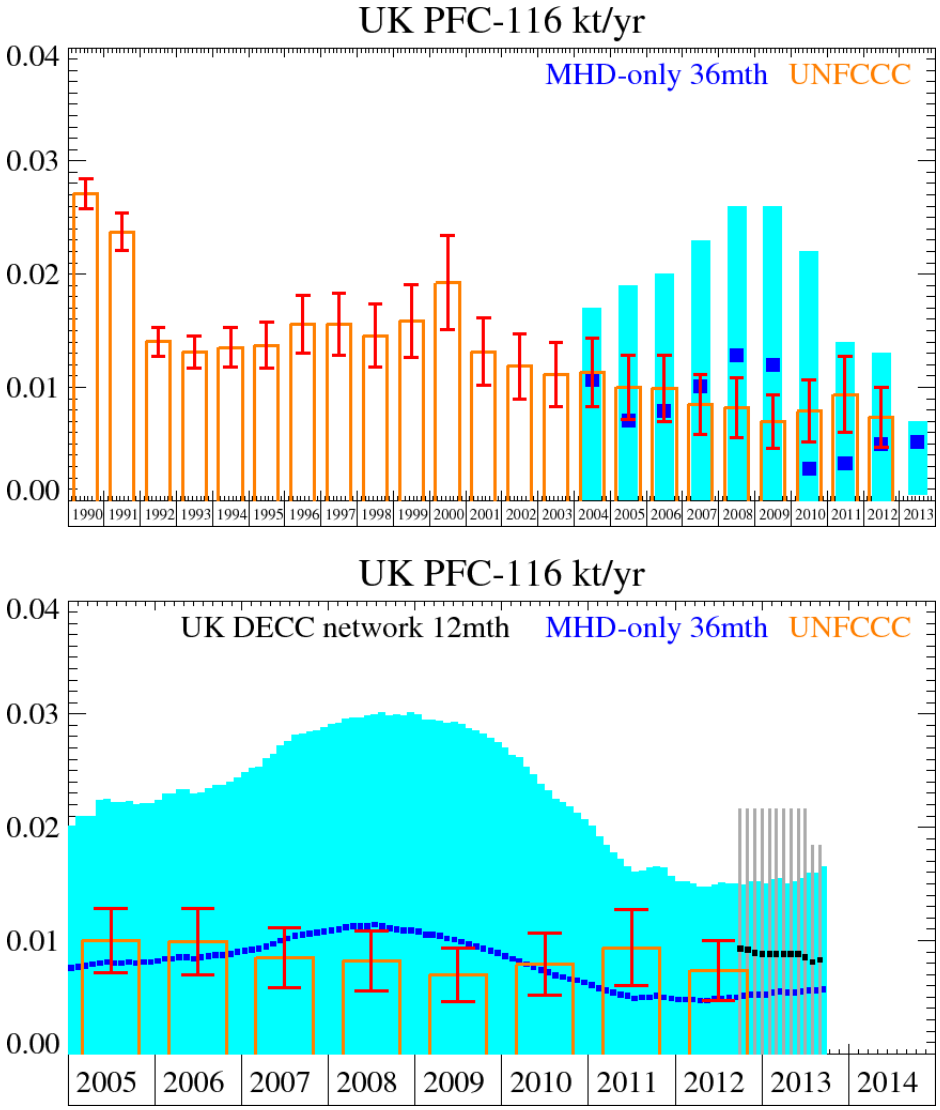

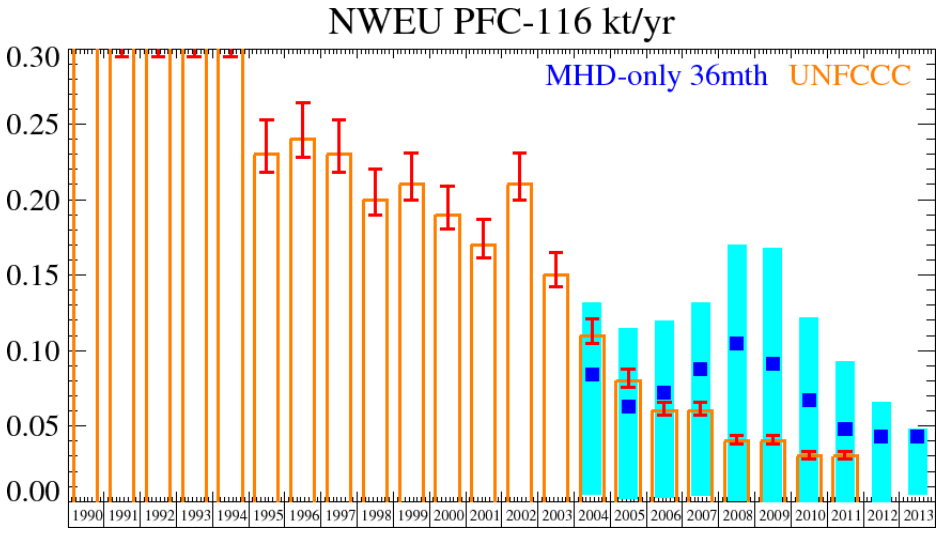

Figure 61: Emission (kt/y) estimates for UK (MHD-only and DECC network) and NWEU. The uncertainty bars represent the 5th and 95th percentiles.

Unit	Year	UK	(5th-95th)	NWEU	(5th-95th)
t/y	2004	10.7	(0.03- 17.)	84.	(4.9 -132.)
t/y	2005	7.1	(0.03- 19.)	63.	(1.8 -115.)
t/y	2006	7.9	(0.03- 20.)	72.	(2.5 -120.)
t/y	2007	10.1	(0.03- 23.)	88.	(3.9 -132.)
t/y	2008	12.8	(0.01- 26.)	105.	(0.1 -170.)
t/y	2009	12.0	(0.01- 26.)	91.	(0.0 -168.)
t/y	2010	2.8	(0.00- 22.)	67.	(0.0 -122.)
t/y	2011	3.3	(0.00- 14.)	48.	(0.0 - 93.)
t/y	2012	5.0	(0.00- 13.)	43.	(0.0 - 66.)
t/y	2013	5.2	(0.55- 7.)	43.	(4.4 - 48.)

Table 31: Emission (t/y) estimates for UK and NWEU with uncertainty (5th – 95th %ile).

Region	Unit	Emission	Range
England	t/yr	5.5	(0.0 - 14.0)
Scotland	t/yr	0.01	(0.0 - 0.2)
Wales	t/yr	3.2	(0.0 - 8.1)
N.Ireland	t/yr	0	(0.0 - 0.0)

Table 32: Emission (t/y) estimates for the UK Devolved Administrations using the UK DECC network for July 2012-2013.

5.15 PFC-218

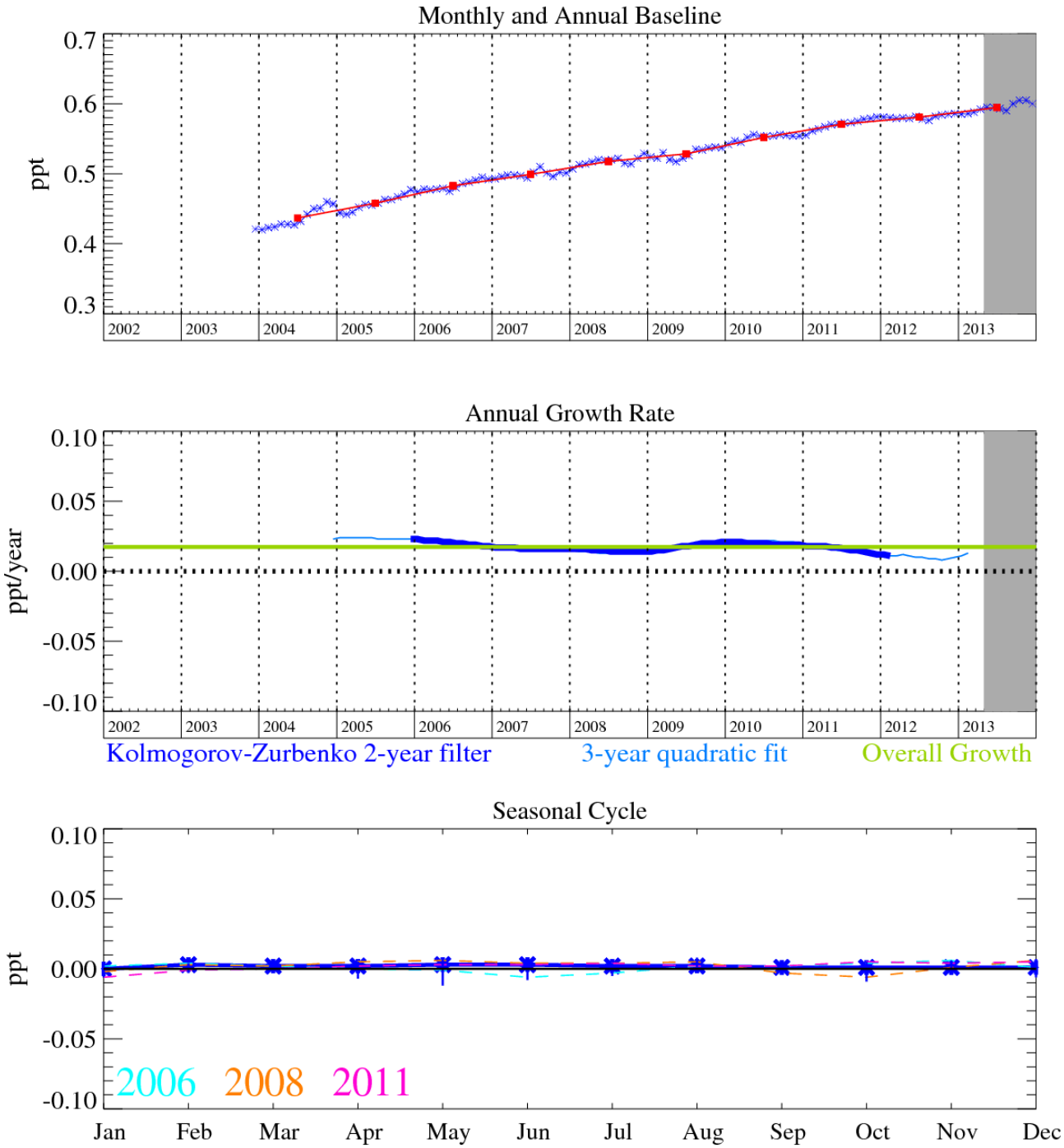

Figure 62: PFC-218 (C_3F_8): Monthly (blue) and annual (red) baseline mole fractions (top plot). Annual (blue) and overall average growth rate (green) (middle plot). Seasonal cycle (de-trended) with year-to-year variability (lower plot). Grey area covers un-ratified and therefore provisional data.

PFC-218 (C_3F_8) has an atmospheric lifetime of 2600 years and a GWP_{100} of 8690. It is also used in semiconductor manufacturing, but to a lesser extent than C_2F_6. It also has a very small contribution from aluminium smelting and has an increasing contribution from refrigeration use. Observations of above-baseline C_3F_8 emissions are less frequent than those of C_2F_6 but are of a higher relative magnitude.

The current growth rate of atmospheric C_3F_8 is very low at 0.01 ppt/yr. This compound will tend to accumulate in the atmosphere due to its very long atmospheric lifetime. In December 2013 the mixing ratio of C_3F_8 was 0.6 ppt.

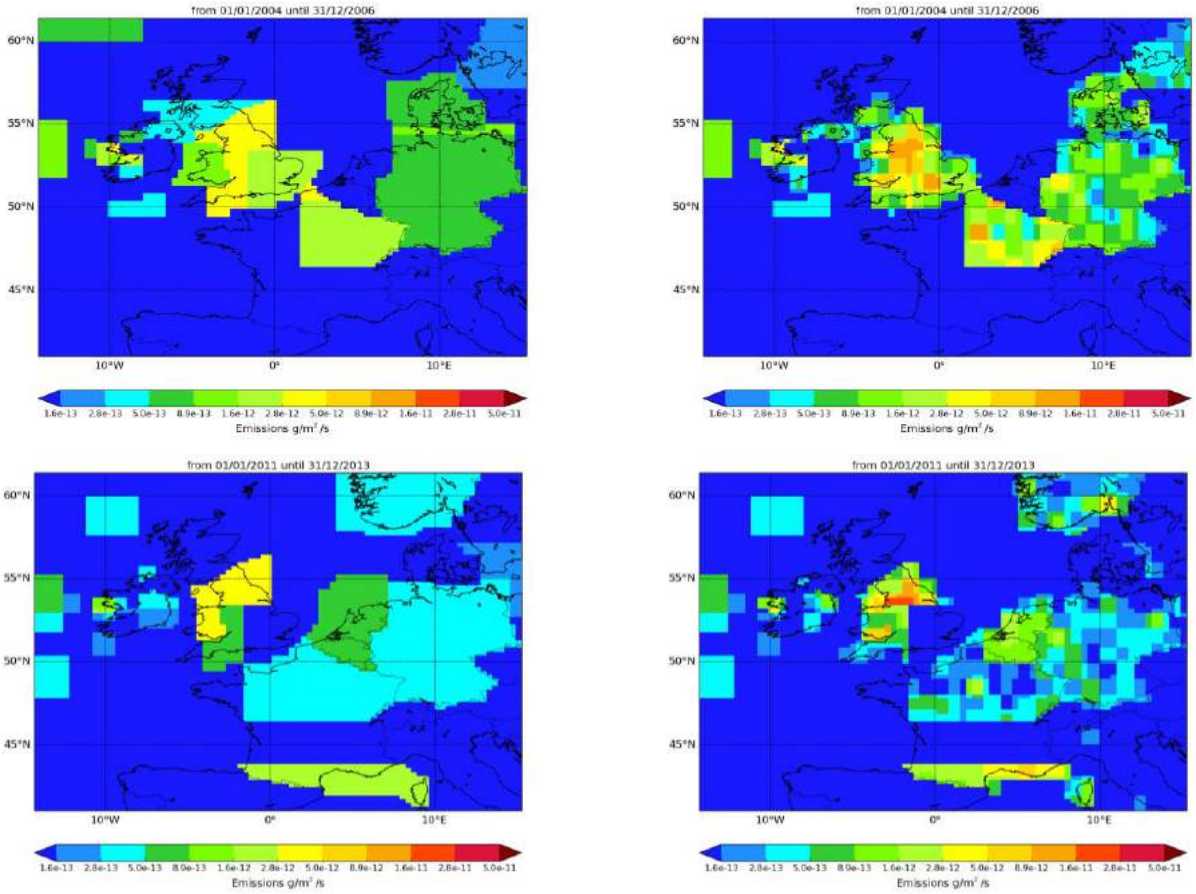

Figure 63: NAME-inversion emission estimates for 2004-2006 (upper) and 2011-2013 (lower). On the right hand side the emissions per grid box have been re-distributed based on population.

There is a large uncertainty in the InTEM emission estimates because the pollution events are relatively difficult to model because the significant sources are probably specific point sources that cannot be readily resolved by the large inversion grids used. Prior knowledge is required to pin-point the significant point sources in a similar analysis as conducted for PFC-14. Within the InTEM and inventory uncertainty the results are consistent.

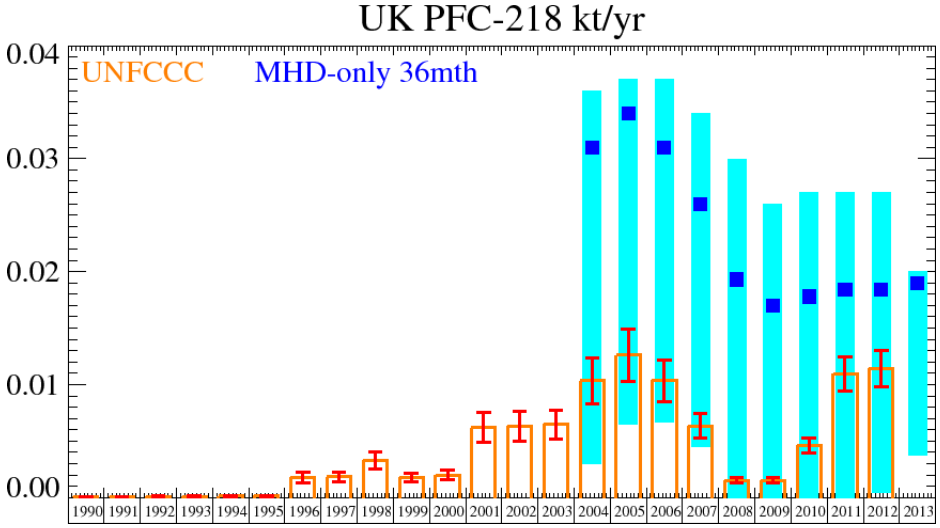

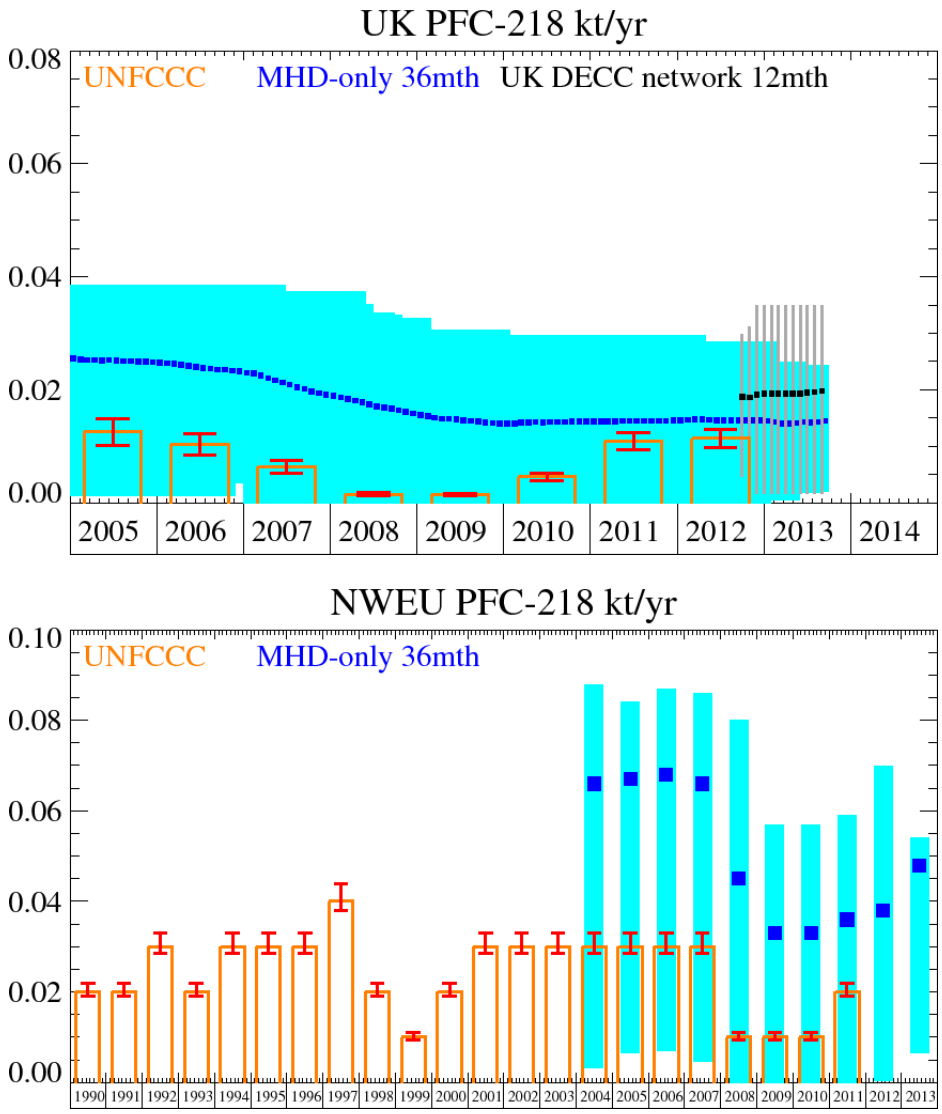

Figure 64: Emission (kt/y) estimates for UK (MHD-only and DECC network) and NWEU. The uncertainty bars represent the 5th and 95th percentiles.

Unit	Year	UK	(5th-95th)	NWEU	(5th-95th)
t/y	2004	31.	(3.- 36.)	66.	(3.2 -88.)
t/y	2005	34.	(7- 37.)	67.	(6.6 -84.)
t/y	2006	31.	(7.- 37.)	68.	(6.9 -87.)
t/y	2007	26.	(5.- 34.)	66.	(4.6 -86.)
t/y	2008	19.	(0.- 30.)	45.	(0.0 -80.)
t/y	2009	17.	(0.- 26.)	33.	(0.0 -57.)
t/y	2010	18	(0.- 27.)	33.	(0.0 -57.)
t/y	2011	18.	(0.- 27.)	36.	(0.0 -59.)
t/y	2012	18.	(0.- 27.)	38.	(0.4 -70.)
t/y	2013	19.	(4.- 20.)	48.	(6.6 -54.)

Table 33: Emission (t/y) estimates for UK and NWEU with uncertainty (5th – 95th %ile).

Region	Unit	Emission	Range
England	t/yr	5.54	(0.0 - 14.0)
Scotland	t/yr	0.01	(0.0 - 0.2)
Wales	t/yr	3.19	(0.0 - 8.1)
N.Ireland	t/yr	0	(0.0 - 0.0)

Table 34: Emission (t/y) estimates for the UK Devolved Administrations using the UK DECC network for July 2012-2013.

5.16 PFC-318

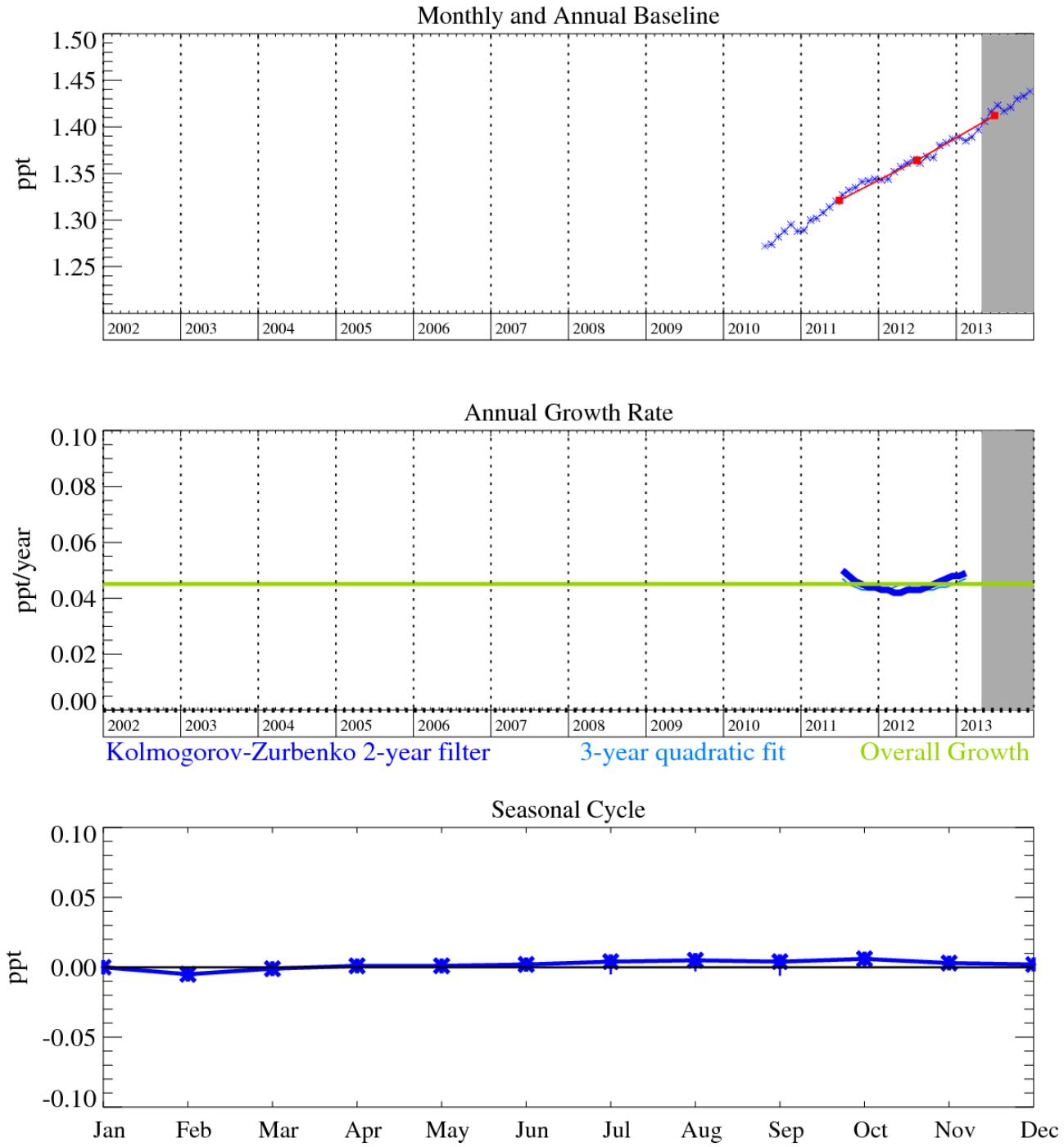

Figure 65: PFC-318 (C_4F_8): Monthly (blue) and annual (red) baseline mole fractions (top plot). Annual (blue) and overall average growth rate (green) (middle plot). Seasonal cycle (de-trended) with year-to-year variability (lower plot). Grey area covers un-ratified and therefore provisional data.

This gas is increasingly used in the semiconductor and electronics industries for cleaning, plasma etching and deposition gas, also it has more minor use in aerolyzed foods, retinal detachment surgery, size estimation of natural gas and oil reservoirs, specialist military applications, tracer experiments and may also replace SF_6 as an electrically insulating gas. It has an atmospheric lifetime of 3,200 years, a GWP_{100} of 10,300 and a radiative efficiency of 0.32 W m^{-2} ppb^{-1}.

The reported inventory emissions of PFC-318 are very small compared to the median InTEM emission estimates. However the InTEM estimates have significant uncertainty, it is likely that significant amounts of this gas are released intermittently thereby challenging one of the InTEM assumptions of uniform emissions in time in the inversion time-window.

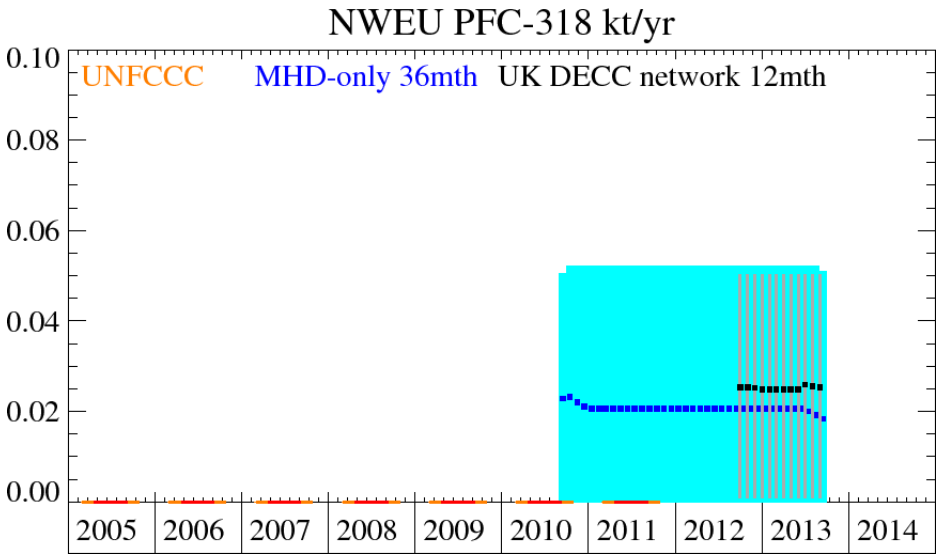

Figure 66: Emission (kt/y) estimates for NWEU (MHD-only and DECC network). The uncertainty bars represent the 5th and 95th percentiles

Unit	Year	UK	(5th-95th)	NWEU	(5th-95th)
t/y	2011-2013	3.3	(0.- 14.)	22.	(0.0 - 50.)

Table 35: Emission (t/y) estimates for UK and NWEU (MHD-only) for 2011-2013 with uncertainty (5th – 95th %ile).

Region	Unit	Emission	Range
England	t/yr	11.1	(0.8 - 24.5)
Scotland	t/yr	6.4	(0.0 - 13.5)
Wales	t/yr	0.3	(0.0 - 2.2)
N.Ireland	t/yr	0	(0.0 - 0.0)

Table 36: Emission (t/y) estimates for the UK Devolved Administrations using the UK DECC network for July 2012-2013.

5.17 SF_6

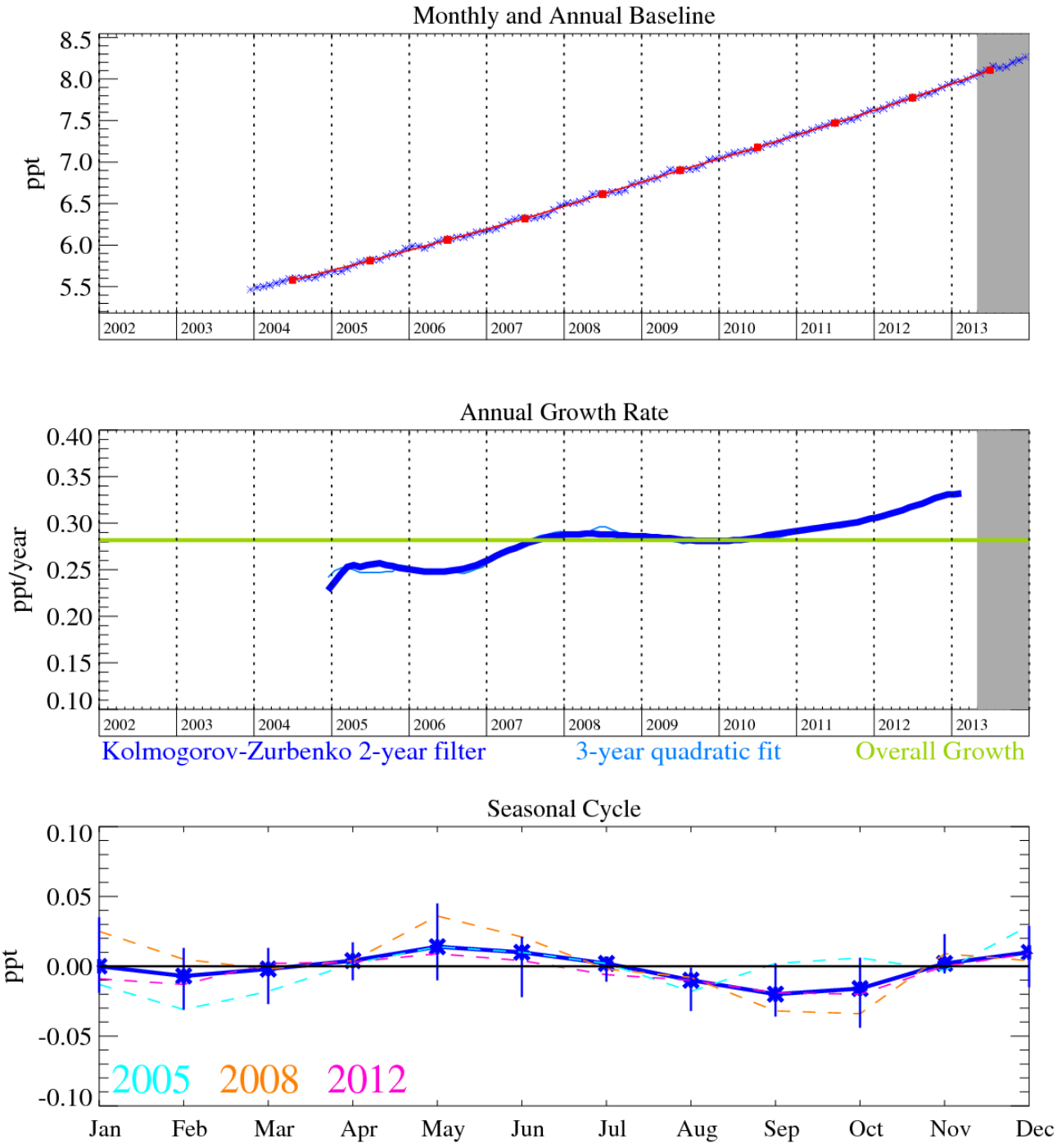

Figure 67: SF_6: Monthly (blue) and annual (red) baseline mole fractions (top plot). Annual (blue) and overall average growth rate (green) (middle plot). Seasonal cycle (de-trended) with year-to-year variability (lower plot). Grey area covers un-ratified and therefore provisional data.

SF_6 is an important greenhouse gas since it has a long atmospheric lifetime of 3,200 years and a high radiative efficiency; giving rise to a GWP_{100} of 22,800. It has an atmospheric trend of 0.33 ppt/yr and reached a mixing ratio of 8.3 ppt by December 2013. Although having minor usage in the semiconductor industry, it is predominantly used in electrical circuit breakers, heavy-duty gas-insulated switchgear (GIS) for systems with voltages from 5,000-38,000 volts, and other switchgear used in the electrical transmission systems to manage high voltages (>38 kV). The electrical power industry uses roughly 80% of all SF_6 produced worldwide. Although the units themselves are hermetically sealed and pressurised, aging equipment, breakdown and disposal, alongside leakage from wear-and-tear will cause this sector to emit SF_6. A minor use of this gas is also reported in its

use as a blanketing (i.e. oxygen inhibiting inert gas) agent during magnesium production. Hence SF_6 will have many, and more diffuse, sources relative to the other perfluorinated species. Its atmospheric trend has been predicted to rise at a rate faster than linear, as older electrical switchgear is switched to higher efficiency units.

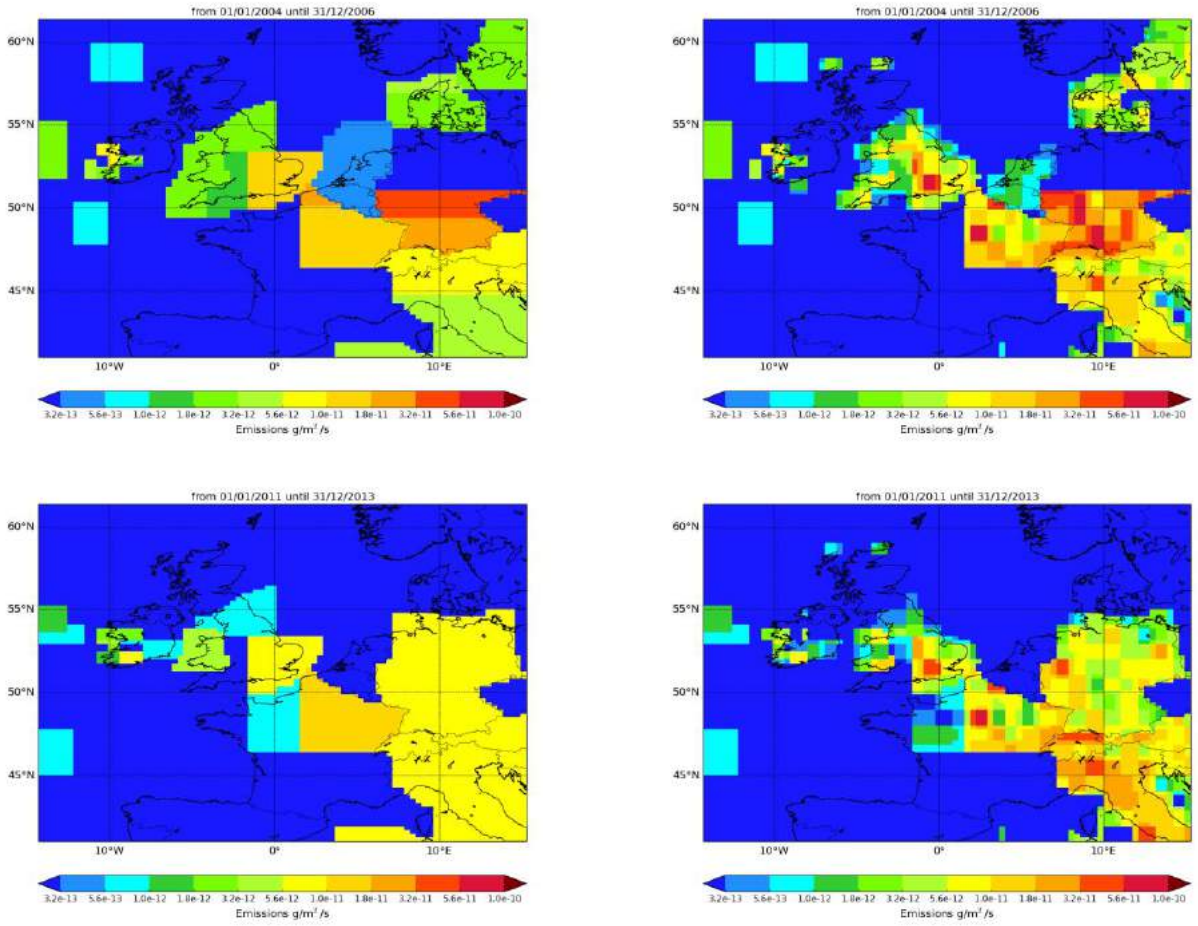

Figure 68: NAME-inversion emission estimates for 2004-2006 (upper) and 2011-2013 (lower). On the right hand side the emissions per grid box have been re-distributed based on population.

The UK InTEM estimates are consistently elevated compared to the inventory, however, the InTEM uncertainty ranges do encompass the inventory estimates. The NWEU InTEM estimates are higher than the inventory until 2010 after which the agreement is good. The statistical match between the model time-series and the observations is reasonable.

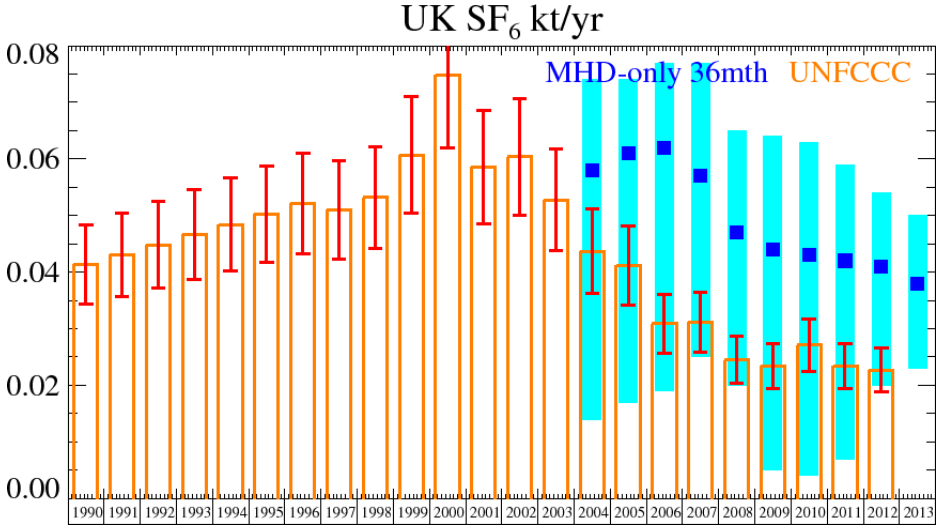

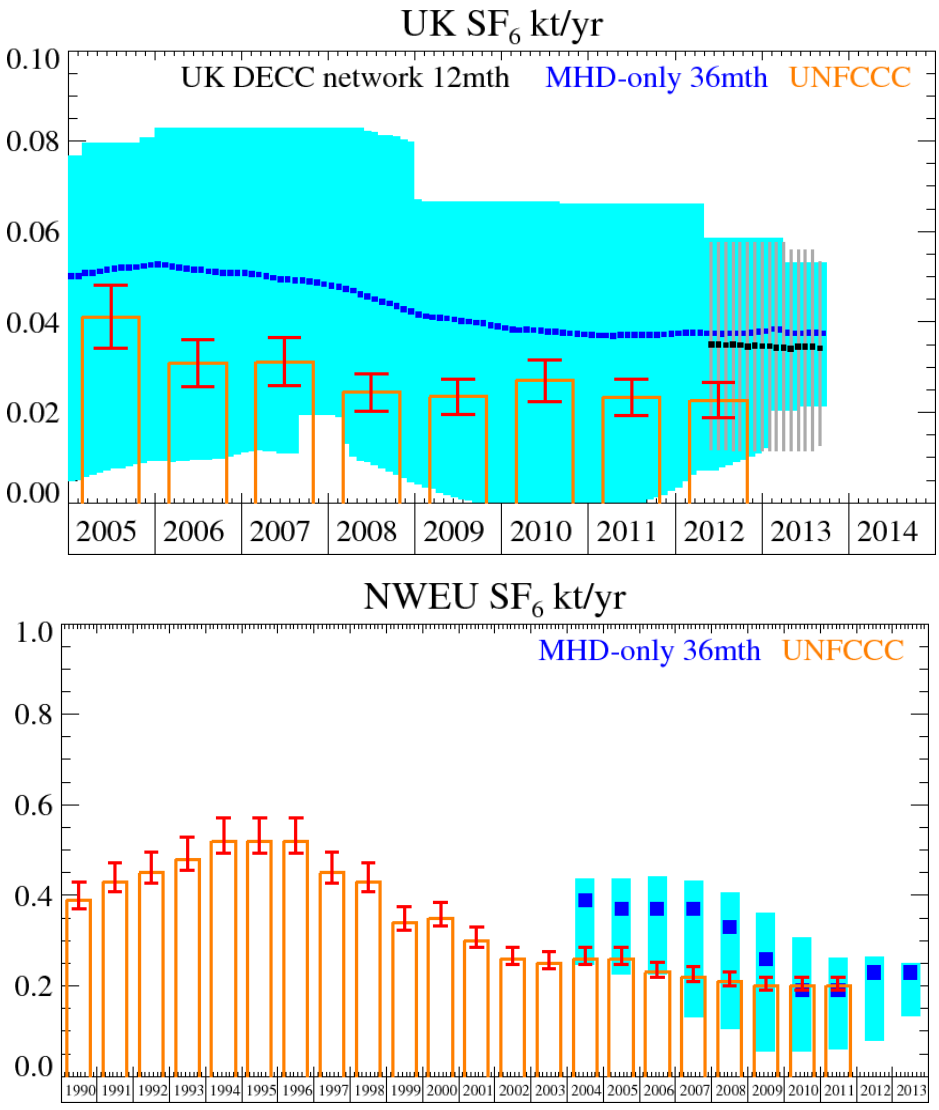

Figure 69: Emission (kt/y) estimates for UK (MHD-only and DECC network) and NWEU. The uncertainty bars represent the 5th and 95th percentiles.

Unit	Year	UK	(5th-95th)	NWEU	(5th-95th)
t/y	2004	58.	(14.- 74.)	390.	(250. -440.)
t/y	2005	61.	(17.- 74.)	370.	(230. -440.)
t/y	2006	62.	(19.- 77.)	370.	(230. -440.)
t/y	2007	57.	(25.- 77.)	370.	(130. -430.)
t/y	2008	47.	(20.- 65.)	330.	(110. -410.)
t/y	2009	44.	(5.- 64.)	260.	(60. -360.)
t/y	2010	43.	(4.- 63.)	191.	(60. -310.)
t/y	2011	42.	(7.- 59.)	191.	(60. -260.)
t/y	2012	41.	(20.- 54.)	230.	(80. -260.)
t/y	2013	38.	(23.- 50.)	230.	(130. -250.)

Table 37: Emission (t/y) estimates for UK and NWEU with uncertainty (5th – 95th %ile).

Region	Unit	Emission	Range
England	t/yr	27.7	(11.4 - 44.2)
Scotland	t/yr	1.7	(0.0 - 6.6)
Wales	t/yr	5.1	(0.0 - 11.5)
N.Ireland	t/yr	0.2	(0.0 - 1.2)

Table 38: Emission (t/y) estimates for the UK Devolved Administrations using the UK DECC network for July 2012-2013.

6 Results and analysis of additional gases

6.1 Introduction

This section discusses the atmospheric trends and regional emissions of the other gases that are measured at Mace Head. The table below describes, if applicable, the principle uses of each of the gases, their radiative efficiency, atmospheric lifetime, global warming potential in a 100-year framework (GWP_{100}) and ozone depleting potential (ODP). In the following sections each of these gases are discussed. The amount of detail provided per gas is dependant on their relative importance as a greenhouse gas (GHG) or ozone-depleting substance.

Gas	Primary use	Radiative Efficiency (W m^{-2} ppb^{-1})	Atmospheric Lifetime (years)	GWP_{100}	ODP
CFC-11	Widespread – discontinued	0.25	53	4,750	1
CFC-12	Refrigerant	0.32	111	10,900	0.82
CFC-113	Coolant, electronics	0.30	109	6,130	0.85
CFC-115	Refrigerant	0.18	1,020	7,230	0.57
HCFC-124	Refrigerant, fire suppression	0.22	5.9	619	0.02
HCFC-141b	Foam blowing	0.14	9.4	717	0.12
HCFC-142b	Chem. synthesis/foam blowing	0.20	17.7	2,220	0.06
HCFC-22	Propellant, air conditioning	0.2	12.4	1,790	0.04
HFC-236fa	Fire extinguisher	0.28	242	9,820	
HFC-245fa	Foam blowing	0.28	7.9	1,020	
HFC-365mfc	Foam blowing	0.22	8.7	842	
HFC-4310mee	Electronics industry	0.40	15.9	1,640	
SO_2F_2	Fumigant		36		
CH_3Cl	Natural, refrigerant	0.01	1	13	0.02
CH_2Cl_2	Foam plastic, solvent, natural		144 days		
$CHCl_3$	Bi-product, natural		149 days		
CCl_4	Fire suppression, precursor	0.13	26	1,400	0.82
CH_3CCl_3	Solvent	0.06	5.04	146	0.16
$CHClCCl_2$	Degreasing solvent		5 days	5	
CCl_2CCl_2	Solvent, dry cleaning		90 days	15	
CH_3Br	Natural (seaweed), fumigant		0.8		
CH_2Br_2	Natural (seaweed)		123 days		
$CHBr_3$	Natural (seaweed)		24 days		0.66
$CBrClF_2$	Fire suppression (military)	0.3	16	1,890	7.9
$CBrF_3$	Fire suppression	0.32	65	7,140	15.9
$C_2Br_2F_4$	Fire suppression	0.33	20	1,640	13.0
CH_3I	Natural (seaweed)		7 days		
C_2H_6	Combustion, gas leakage				
CO	Combustion		30-90 days		
O_3	Reactions in atmosphere				
H_2	Combustion, photolysis				

Table 39: The principle uses of the gases observed at Mace Head, their radiative efficiency, atmospheric lifetime, global warming potential in a 100 year framework (GWP_{100}) and ozone depleting potential (ODP). The gases listed in red are specifically covered by the Montreal Protocol. All of the gases with a GWP are GHGs but not all GHGs are covered by the Kyoto Protocol.

6.2 CFC-11

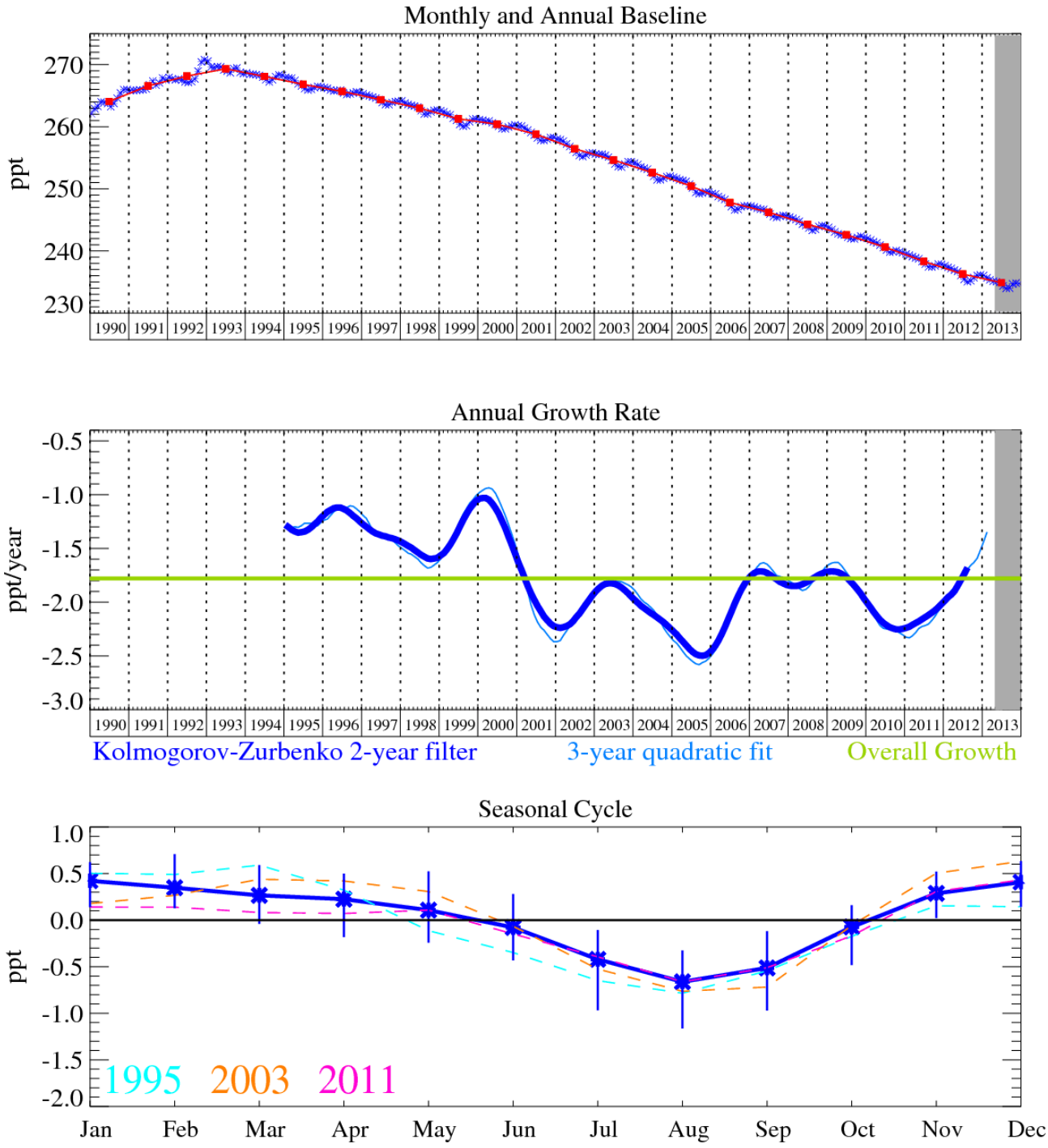

The grey area on each plot contains data that are unratified and therefore provisional.

Figure 70: CFC-11 (CCl_3F): Monthly (blue) and annual (red) baseline (top plot). Annual (blue) and overall average growth rate (green) (middle plot). Seasonal cycle (de-trended) with year-to-year variability (lower plot). The grey area covers un-ratified and therefore provisional data.

The time series of mid-latitude northern hemisphere baseline (i.e. pollution, local and southerly events removed) monthly means for atmospheric CFC-11 is shown in Figure 70.

The emissions of all of the CFC compounds have decreased substantially in response to the Montreal Protocol on Substances that Deplete the Ozone Layer, the rate of removal of these compounds by their sinks is limited by their long atmospheric lifetimes.

CFC-11 (53 year lifetime) has declined from its peak year in 1993. Its current rate of decline is 1.5 ppt/yr and by December 2013 its mole fraction at Mace Head was 234.7 ppt (Figure 70).

It was reported in the 2010 WMO Ozone Assessment, that the decline of CFC-11 and CFC-12 has been smaller than projected. This is most likely due to releases of these compounds from banks being fairly constant over time rather than declining over time as was originally expected. It is also possible that the atmospheric lifetime of these compounds is potentially longer than reported; this aspect is discussed in the latest SPARC lifetimes assessment, and is dealt with in a publication by Rigby *et al.* [2013].

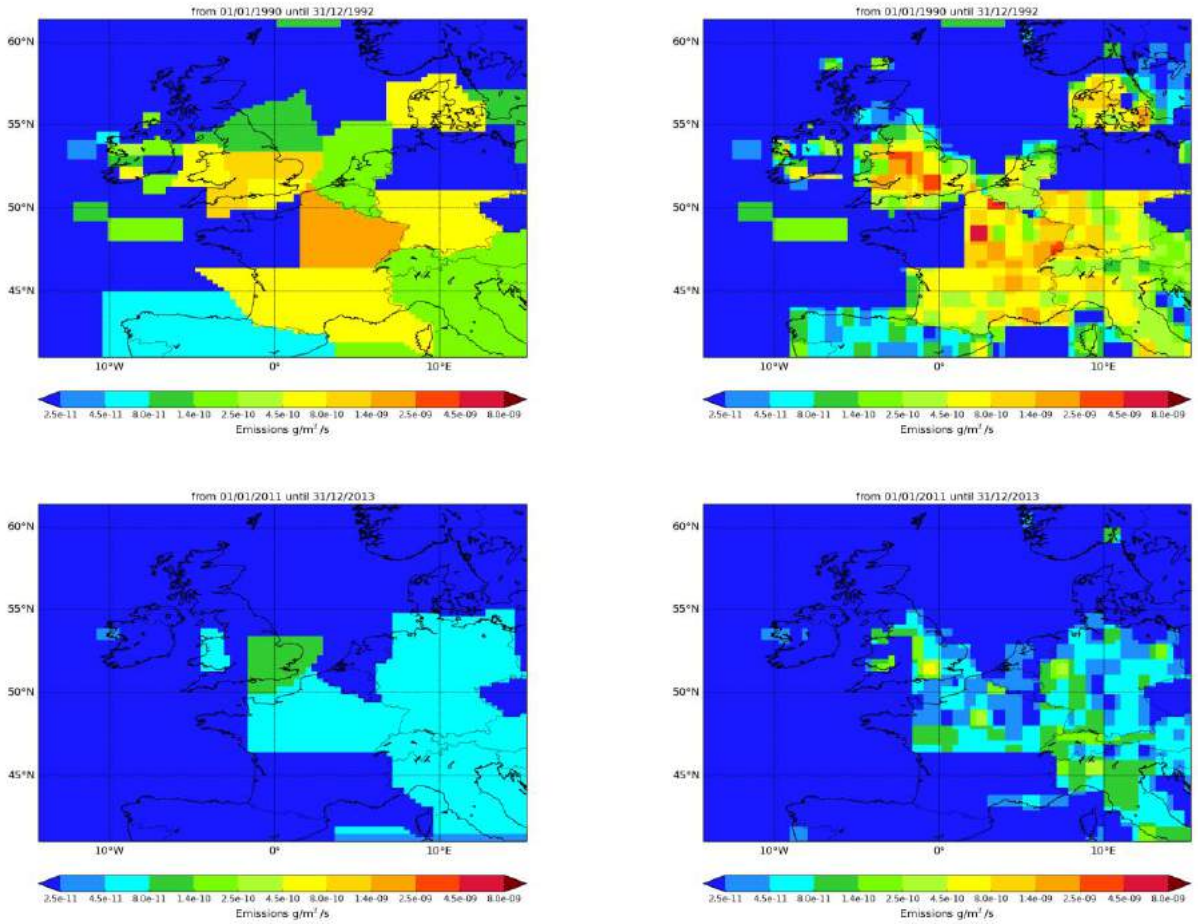

Figure 71: NAME-inversion emission estimates for 1990-1992 (upper) and 2011-2013 (lower). On the right hand side the emissions per grid box have been re-distributed based on population.

The emissions of CFC-11 in both the UK and NWEU as a whole fell very significantly between 1990 and the late 1990s. This clearly shows the impact of the Montreal Protocol, which banned the use of this gas in developed countries from 1995 onwards. The residual emissions reflect the leakage from old appliances e.g. fridges.

In 1990 there were significant pollution events, some events reaching more than 80 ppt above baseline, by 2013 they were barely discernible above baseline.

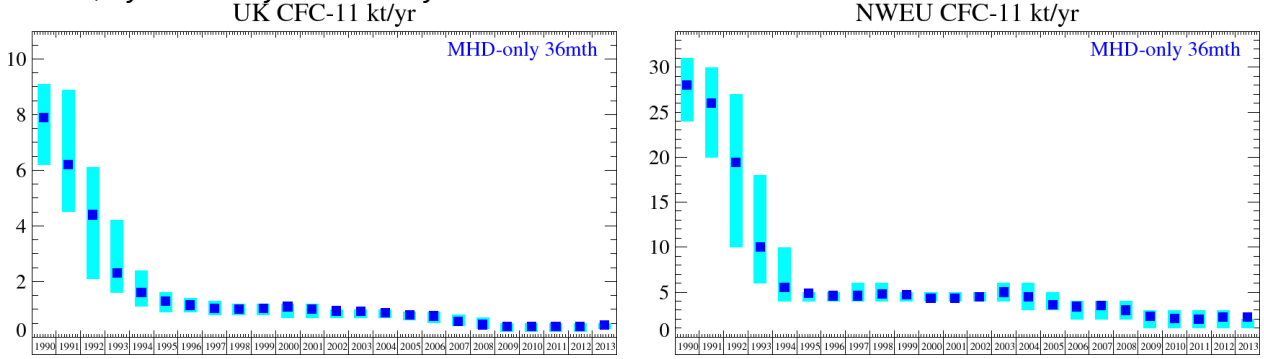

Figure 72: Emission estimates for UK and NWEU (MHD-only). The uncertainty bars represent the 5th and 95th percentiles.

Unit	Year	UK	(5th-95th)	NWEU	(5th-95th)
kt/y	1990	7.9	(6.2- 9.1)	28.	(24. -31.)
kt/y	1991	6.2	(4.5- 8.9)	26.	(20. -30.)
kt/y	1992	4.4	(2.1- 6.1)	19.4	(10. -27.)
kt/y	1993	2.3	(1.6- 4.2)	10.0	(6. -18.)
kt/y	1994	1.6	(1.1- 2.4)	5.5	(4. -10.)
kt/y	1995	1.3	(0.9- 1.6)	4.9	(4. - 5.)
kt/y	1996	1.2	(0.9- 1.4)	4.6	(4. - 5.)
kt/y	1997	1.0	(0.8- 1.3)	4.6	(4. - 6.)
kt/y	1998	1.0	(0.8- 1.2)	4.8	(4. - 6.)
kt/y	1999	1.0	(0.8- 1.2)	4.7	(4. - 5.)
kt/y	2000	1.1	(0.7- 1.2)	4.3	(4. - 5.)
kt/y	2001	1.0	(0.7- 1.2)	4.3	(4. - 5.)
kt/y	2002	0.9	(0.7- 1.0)	4.5	(4. - 5.)
kt/y	2003	0.9	(0.7- 1.0)	5.0	(4. - 6.)
kt/y	2004	0.9	(0.7- 1.0)	4.5	(3. - 6.)
kt/y	2005	0.8	(0.6- 0.9)	3.6	(3. - 5.)
kt/y	2006	0.8	(0.5- 0.9)	3.4	(2. - 4.)
kt/y	2007	0.6	(0.4- 0.8)	3.5	(2. - 4.)
kt/y	2008	0.5	(0.3- 0.7)	3.0	(2. - 4.)
kt/y	2009	0.4	(0.2- 0.5)	2.3	(1. - 3.)
kt/y	2010	0.4	(0.2- 0.5)	2.1	(1. - 3.)
kt/y	2011	0.4	(0.2- 0.5)	2.0	(1. - 3.)
kt/y	2012	0.4	(0.2- 0.5)	2.2	(1. - 3.)
kt/y	2013	0.4	(0.3- 0.5)	2.2	(1. - 2.)

Table 40: Emission estimates for UK and NWEU with uncertainty (5th – 95th %ile).

6.3 CFC-12

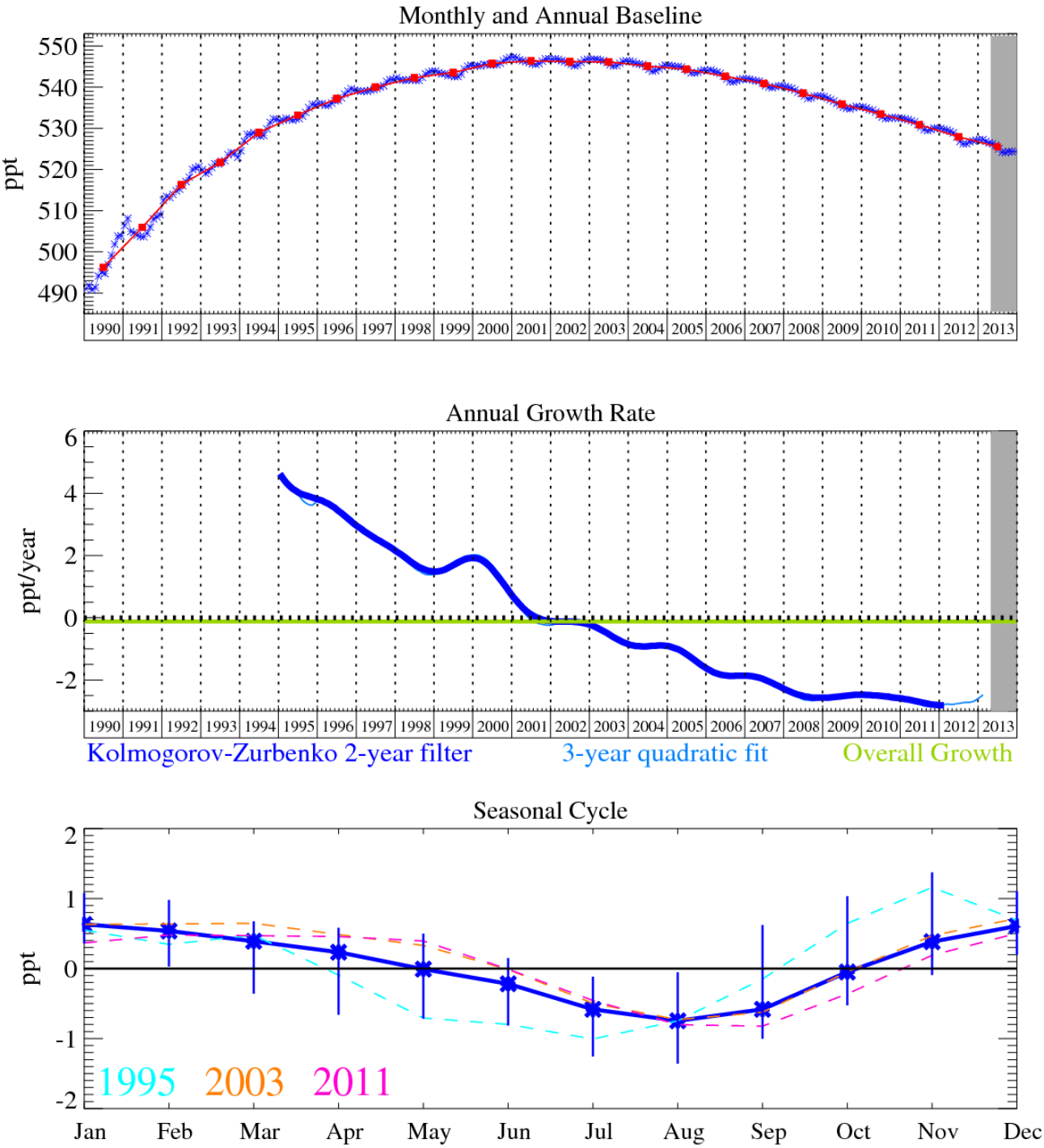

The grey area on each plot contains data that are unratified and therefore provisional.

Figure 73: CFC-12 (CCl_2F_2): Monthly (blue) and annual (red) baseline (top plot). Annual (blue) and overall average growth rate (green) (middle plot). Seasonal cycle (de-trended) with year-to-year variability (lower plot). The grey area covers un-ratified and therefore provisional data.

CFC-12, which has a 111-year lifetime, is currently declining at a rate of 2.5 ppt/yr reaching a mixing ratio in December 2013 of 524.3 ppt (Figure 73).

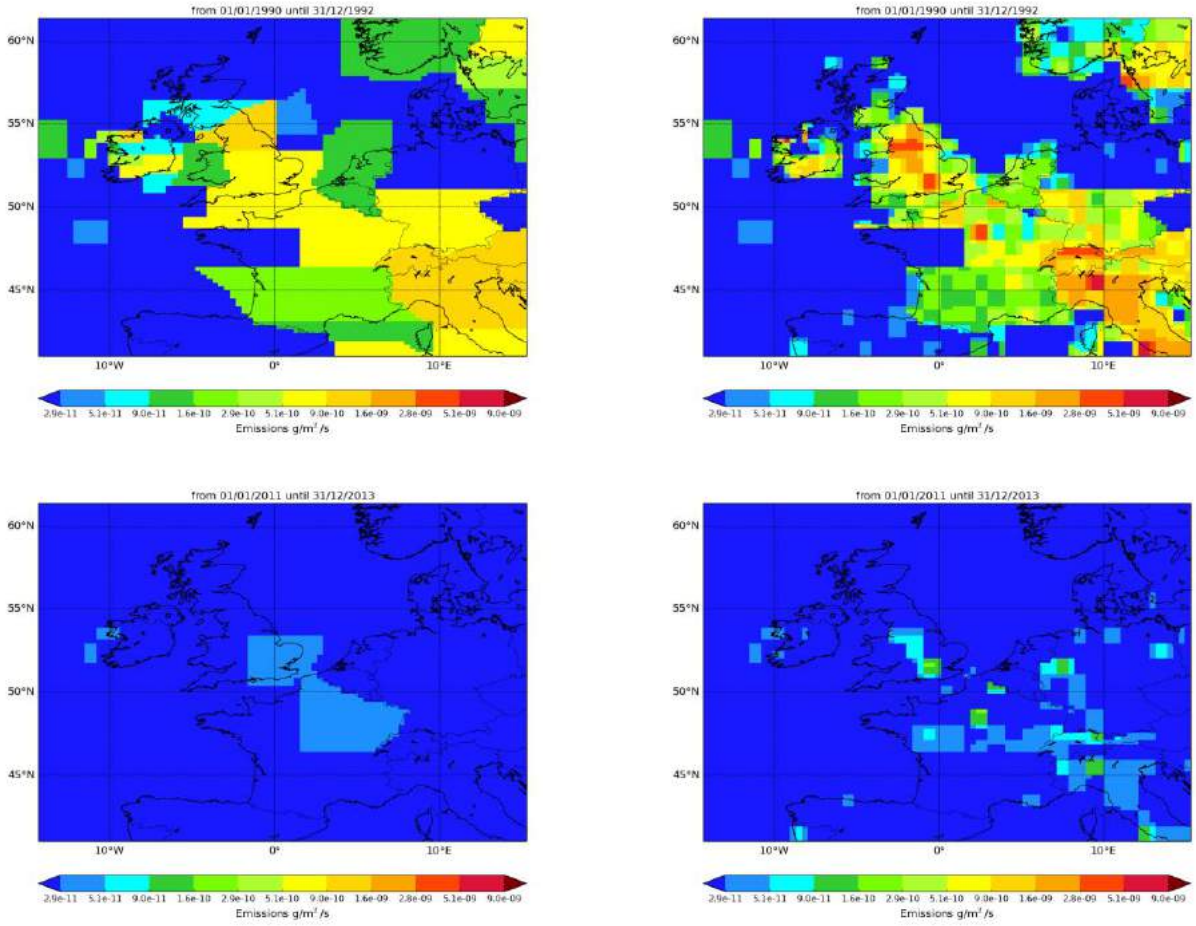

Figure 74: NAME-inversion emission estimates for 1990-1992 (upper) and 2011-2013 (lower). On the right hand side the emissions per grid box have been re-distributed based on population.

The emissions of CFC-12 in both the UK and NWEU as a whole fell very significantly between 1990 and the late 1990s, for the same reasons detailed with CFC-11.

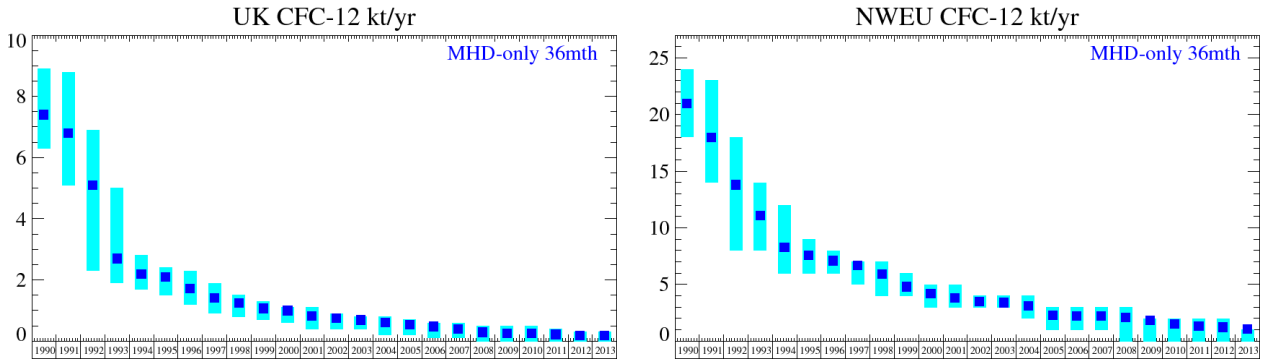

Figure 75: Emission estimates for UK and NWEU (MHD-only). The uncertainty bars represent the 5th and 95th percentiles.

Unit	Year	UK	(5th-95th)	NWEU	(5th-95th)
kt/y	1990	7.4	(6.3- 8.9)	21.	(18. -24.)
kt/y	1991	6.8	(5.1- 8.8)	18.0	(14. -23.)
kt/y	1992	5.1	(2.3- 6.9)	13.8	(8. -18.)
kt/y	1993	2.7	(1.9- 5.0)	11.1	(8. -14.)
kt/y	1994	2.2	(1.7- 2.8)	8.3	(6. -12.)
kt/y	1995	2.1	(1.5- 2.4)	7.6	(6. - 9.)
kt/y	1996	1.7	(1.2- 2.3)	7.1	(6. - 8.)
kt/y	1997	1.4	(0.9- 1.9)	6.7	(5. - 7.)
kt/y	1998	1.2	(0.8- 1.5)	5.9	(4. - 7.)
kt/y	1999	1.1	(0.7- 1.3)	4.8	(4. - 6.)
kt/y	2000	1.0	(0.6- 1.1)	4.2	(3. - 5.)
kt/y	2001	0.8	(0.4- 1.1)	3.8	(3. - 5.)
kt/y	2002	0.8	(0.4- 0.9)	3.5	(3. - 4.)
kt/y	2003	0.7	(0.4- 0.8)	3.4	(3. - 4.)
kt/y	2004	0.6	(0.2- 0.8)	3.1	(2. - 4.)
kt/y	2005	0.5	(0.2- 0.7)	2.3	(1. - 3.)
kt/y	2006	0.5	(0.1- 0.6)	2.2	(1. - 3.)
kt/y	2007	0.4	(0.1- 0.6)	2.2	(1. - 3.)
kt/y	2008	0.3	(0.0- 0.5)	2.1	(0. - 3.)
kt/y	2009	0.3	(0.0- 0.5)	1.83	(0. - 2.)
kt/y	2010	0.3	(0.0- 0.5)	1.52	(0. - 2.)
kt/y	2011	0.2	(0.0- 0.4)	1.35	(0. - 2.)
kt/y	2012	0.2	(0.0- 0.3)	1.23	(0. - 2.)
kt/y	2013	0.2	(0.0- 0.3)	1.09	(0. - 1.)

Table 41: Emission estimates for UK and NWEU with uncertainty (5^{th} – 95^{th} %ile).

6.4 CFC-113

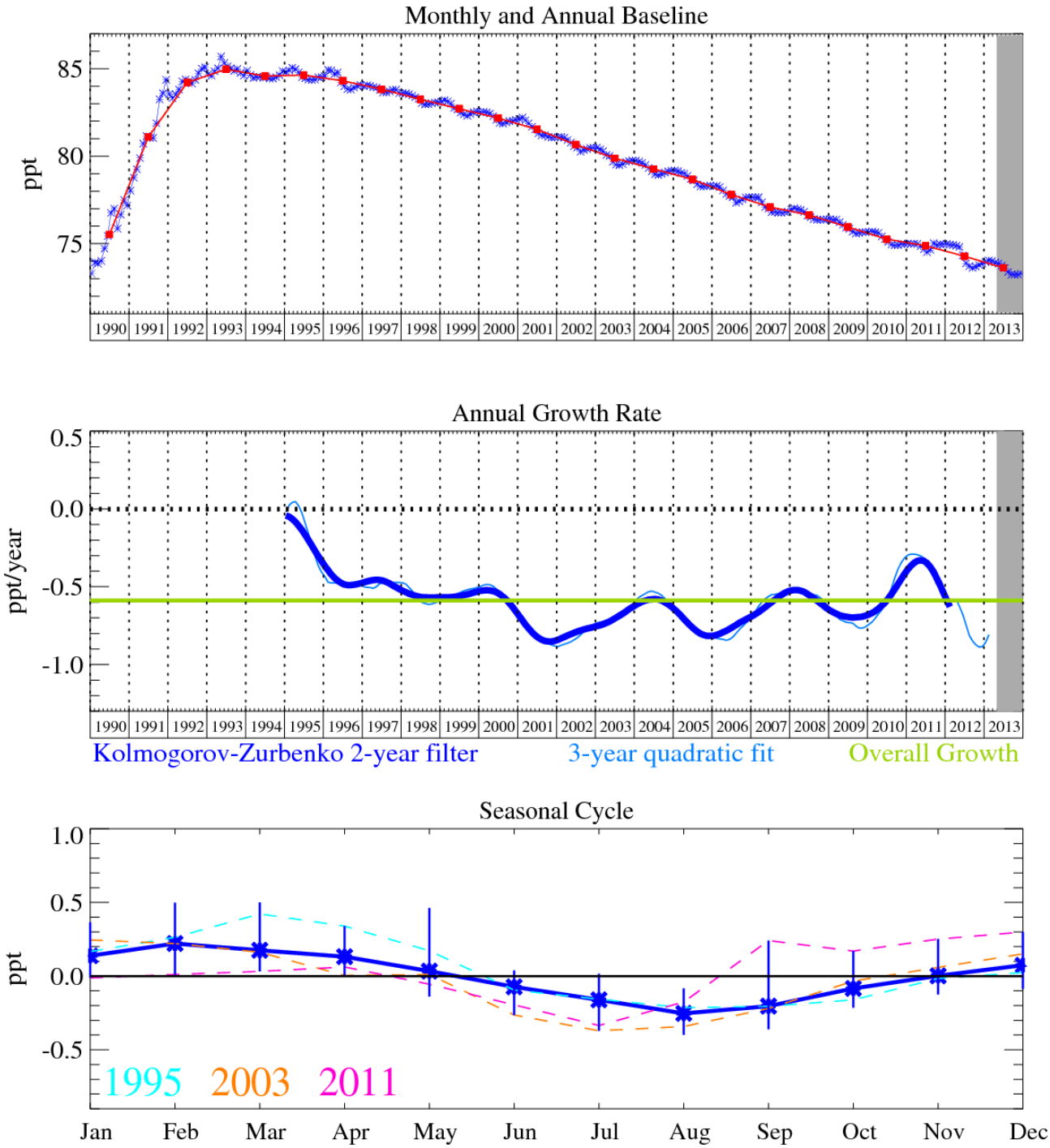

The grey area on each plot contains data that are unratified and therefore provisional.

Figure 76: CFC-113 ($C_2Cl_3F_3$): Monthly (blue) and annual (red) baseline (top plot). Annual (blue) and overall average growth rate (green) (middle plot). Seasonal cycle (de-trended) with year-to-year variability (lower plot). The grey area covers un-ratified and therefore provisional data.

As shown in Figure 76, CFC-113 ($C_2Cl_3F_3$): (109 year lifetime) is currently declining at a rate of 0.8 ppt/yr, by December 2013 it had fallen to 73.3 ppt. Again the decline is less than had been projected and is most likely due to the potential presence of small residual emissions.

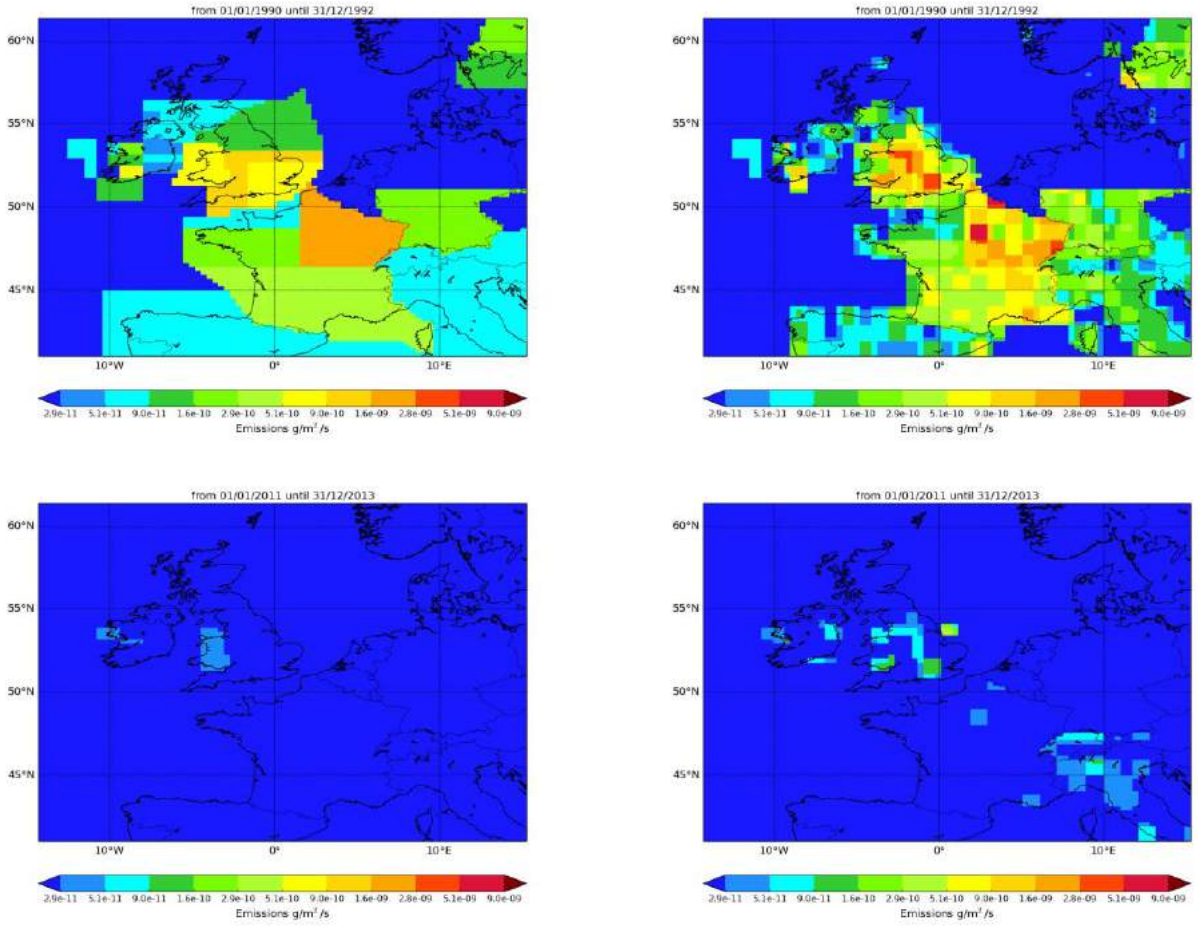

Figure 77: NAME-inversion emission estimates for 1990-1992 (upper) and 2011-2013 (lower). On the right hand side the emissions per grid box have been re-distributed based on population.

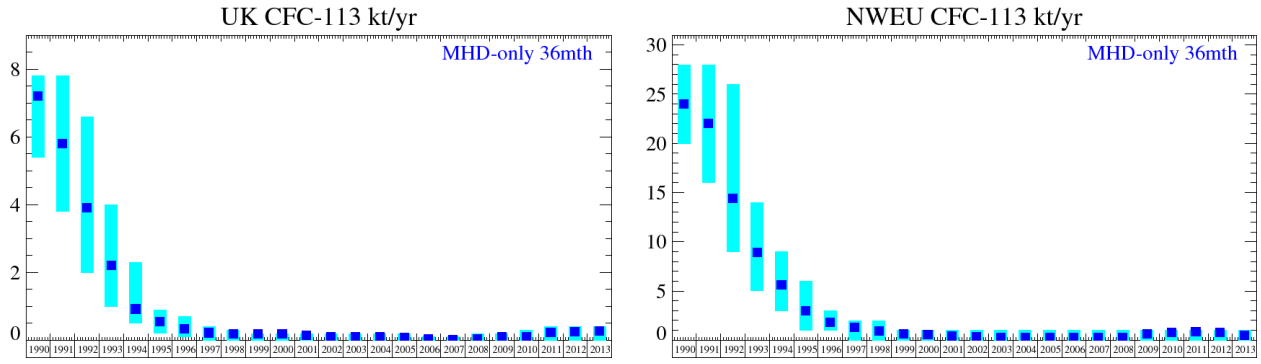

Figure 78: Emission estimates for UK and NWEU. The uncertainty bars represent the 5th and 95th percentiles. Grey line represents the emission estimates presented in last year's report.

The emissions of CFC-113 in both the UK and NWEU as a whole fell very significantly between 1990 and the late 1990s. This again shows the impact of the Montreal Protocol.

Unit	Year	UK	(5th-95th)	NWEU	(5th-95th)
kt/y	1990	7.2	(5.4- 7.8)	24.	(20. -28.)
kt/y	1991	5.8	(3.8- 7.8)	22.	(16. -28.)
kt/y	1992	3.9	(2.0- 6.6)	14.4	(9. -26.)
kt/y	1993	2.2	(1.0- 4.0)	8.9	(5. -14.)
kt/y	1994	0.9	(0.5- 2.3)	5.6	(3. - 9.)
kt/y	1995	0.7	(0.2- 0.9)	3.0	(1. - 6.)
kt/y	1996	0.3	(0.1- 0.7)	1.83	(1. - 3.)
kt/y	1997	0.2	(0.0- 0.4)	1.32	(0. - 2.)
kt/y	1998	0.2	(0.0- 0.3)	0.96	(0. - 2.)
kt/y	1999	0.2	(0.0- 0.2)	0.65	(0. - 1.)
kt/y	2000	0.2	(0.0- 0.2)	0.57	(0. - 1.)
kt/y	2001	0.2	(0.0- 0.2)	0.40	(0. - 1.)
kt/y	2002	0.1	(0.0- 0.2)	0.31	(0. - 1.)
kt/y	2003	0.1	(0.0- 0.2)	0.28	(0. - 1.)
kt/y	2004	0.1	(0.0- 0.2)	0.28	(0. - 1.)
kt/y	2005	0.1	(0.0- 0.2)	0.28	(0. - 1.)
kt/y	2006	0.0	(0.0- 0.1)	0.24	(0. - 1.)
kt/y	2007	0.0	(0.0- 0.1)	0.24	(0. - 1.)
kt/y	2008	0.0	(0.0- 0.2)	0.30	(0. - 1.)
kt/y	2009	0.1	(0.0- 0.2)	0.64	(0. - 1.)
kt/y	2010	0.1	(0.0- 0.3)	0.77	(0. - 1.)
kt/y	2011	0.2	(0.0- 0.4)	0.84	(0. - 1.)
kt/y	2012	0.3	(0.0- 0.4)	0.80	(0. - 1.)
kt/y	2013	0.3	(0.0- 0.4)	0.48	(0. - 1.)

Table 42: Emission estimates for UK and NWEU with uncertainty (5^{th} – 95^{th} %ile).

6.5 CFC-115

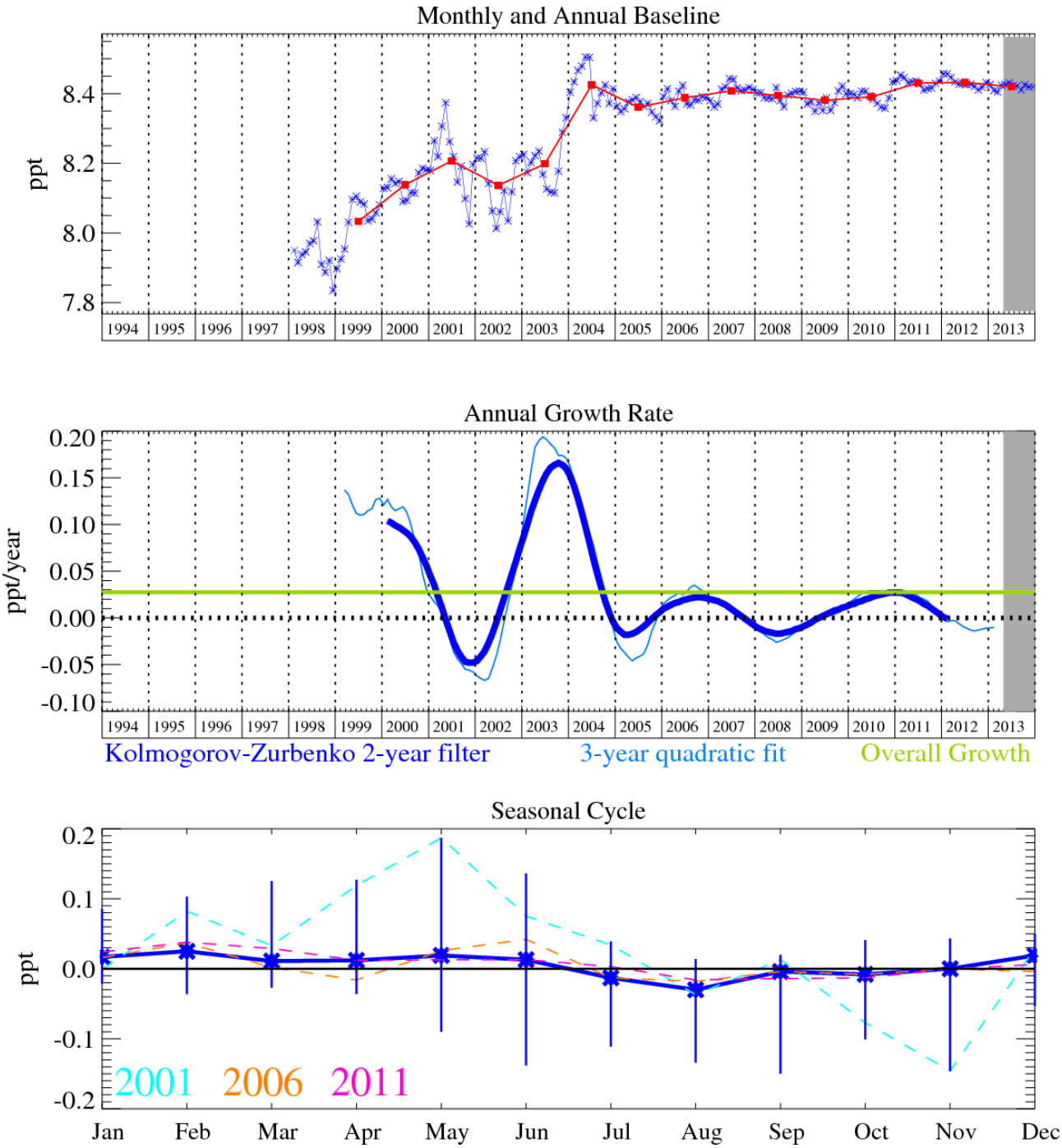

The grey area on each plot contains data that are unratified and therefore provisional.

Figure 79: CFC-115 (C_2ClF_5): Monthly (blue) and annual (red) baseline (top plot). Annual (blue) and overall average growth rate (green) (middle plot). Seasonal cycle (de-trended) with year-to-year variability (lower plot). The grey area covers un-ratified and therefore provisional data.

The mixing ratios of the substantially less abundant CFC-115 (C_2ClF_5), has not changed appreciably since 2006. Its atmospheric abundance and current growth rate are 8.4 ppt and -0.01 ppt/yr respectively.

6.6 HCFC-124

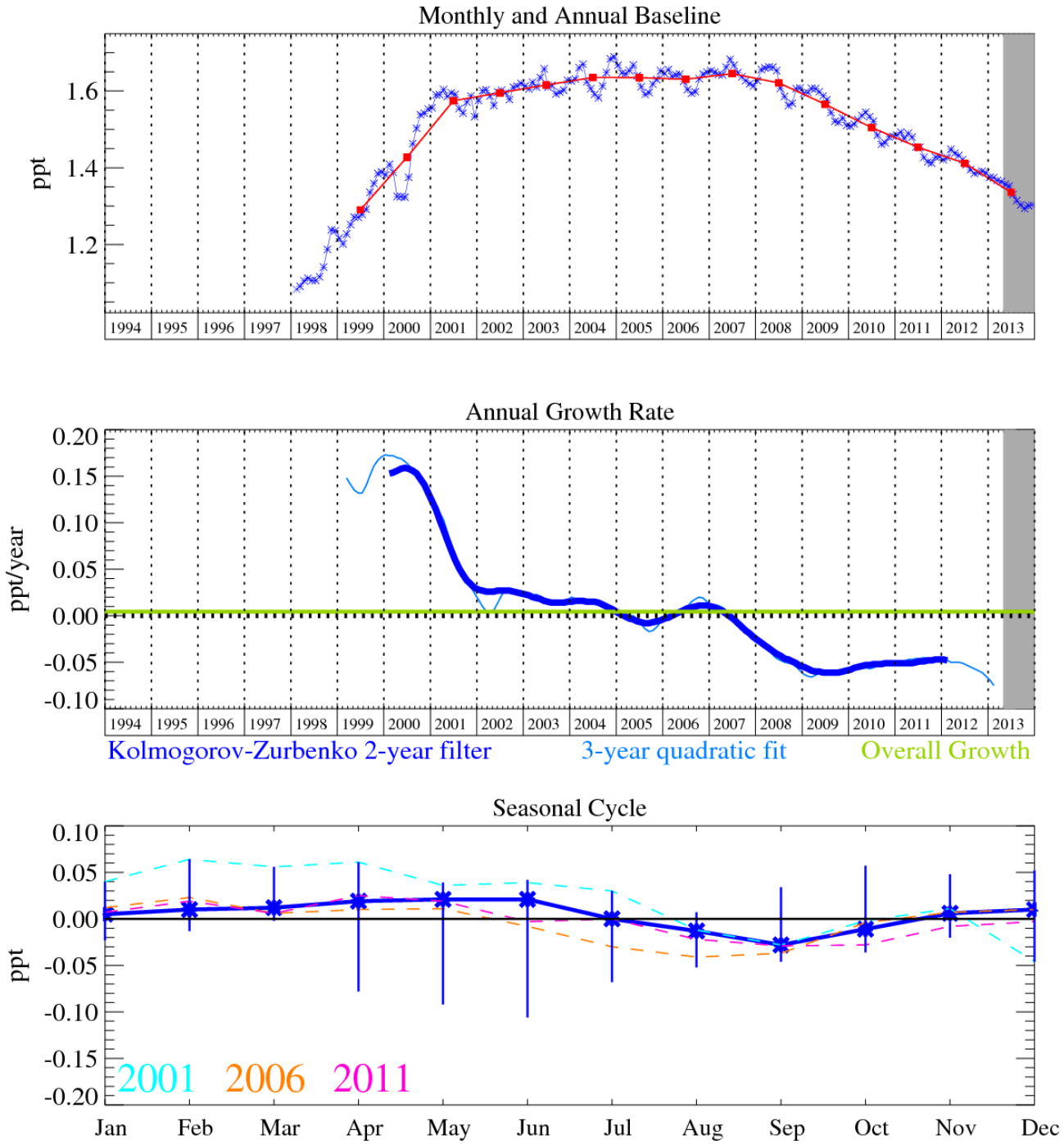

The grey area on each plot contains data that are unratified and therefore provisional.

Figure 80: HCFC-124 (C_2HClF_4): Monthly (blue) and annual (red) baseline (top plot). Annual (blue) and overall average growth rate (green) (middle plot). Seasonal cycle (de-trended) with year-to-year variability (lower plot). The grey area covers un-ratified and therefore provisional data.

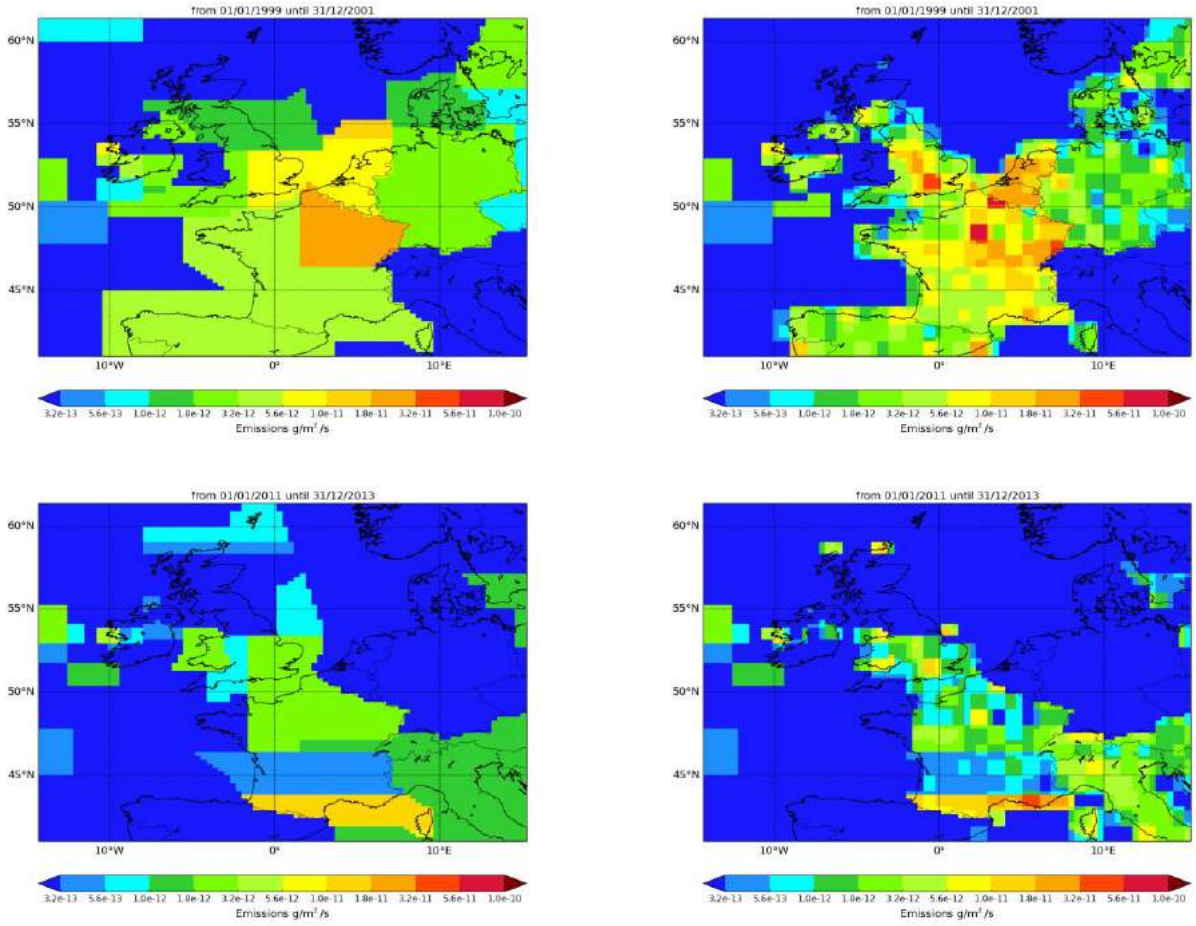

Figure 81: NAME-inversion emission estimates for 1999-2001 (upper) and 2011-2013 (lower). On the right hand side the emissions per grid box have been re-distributed based on population.

The measured pollution events for HCFC-124 (C_2HClF_4) have always been small and have slowly declined since 1999. The estimated regional emissions are therefore small and have significant uncertainty.

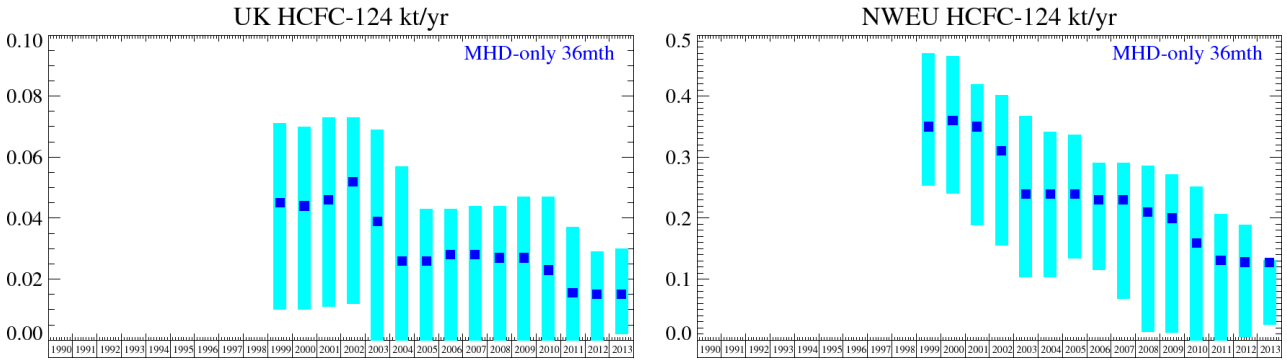

Figure 82: Emission estimates for UK and NWEU (MHD_only). The uncertainty bars represent the 5th and 95th percentiles. Grey line represents the emission estimates presented in last year's report.

Unit	Year	UK	(5th-95th)	NWEU	(5th-95th)
t/y	1999	45.	(10.- 71.)	350.	(254. -470.)
t/y	2000	44.	(10.- 70.)	360.	(240. -465.)
t/y	2001	46.	(11.- 73.)	350.	(188. -419.)
t/y	2002	52.	(12.- 73.)	310.	(155. -402.)
t/y	2003	39.	(0.- 69.)	240.	(103. -367.)
t/y	2004	26.	(0.- 57.)	240.	(104. -341.)
t/y	2005	26.	(0.- 43.)	240.	(134. -337.)
t/y	2006	28.	(0.- 43.)	230.	(115. -291.)
t/y	2007	28.	(0.- 44.)	230.	(68. -291.)
t/y	2008	27.	(0.- 44.)	210.	(14. -286.)
t/y	2009	27.	(0.- 47.)	200.	(13. -272.)
t/y	2010	23.	(0.- 47.)	160.	(0. -252.)
t/y	2011	16.	(0.- 37.)	130.	(0. -207.)
t/y	2012	15.	(0.- 29.)	130.	(5. -189.)
t/y	2013	15.	(2.- 30.)	130.	(25. -131.)

Table 43: Emission estimates for UK and NWEU with uncertainty (5^{th} – 95^{th} %ile).

6.7 HCFC-141b

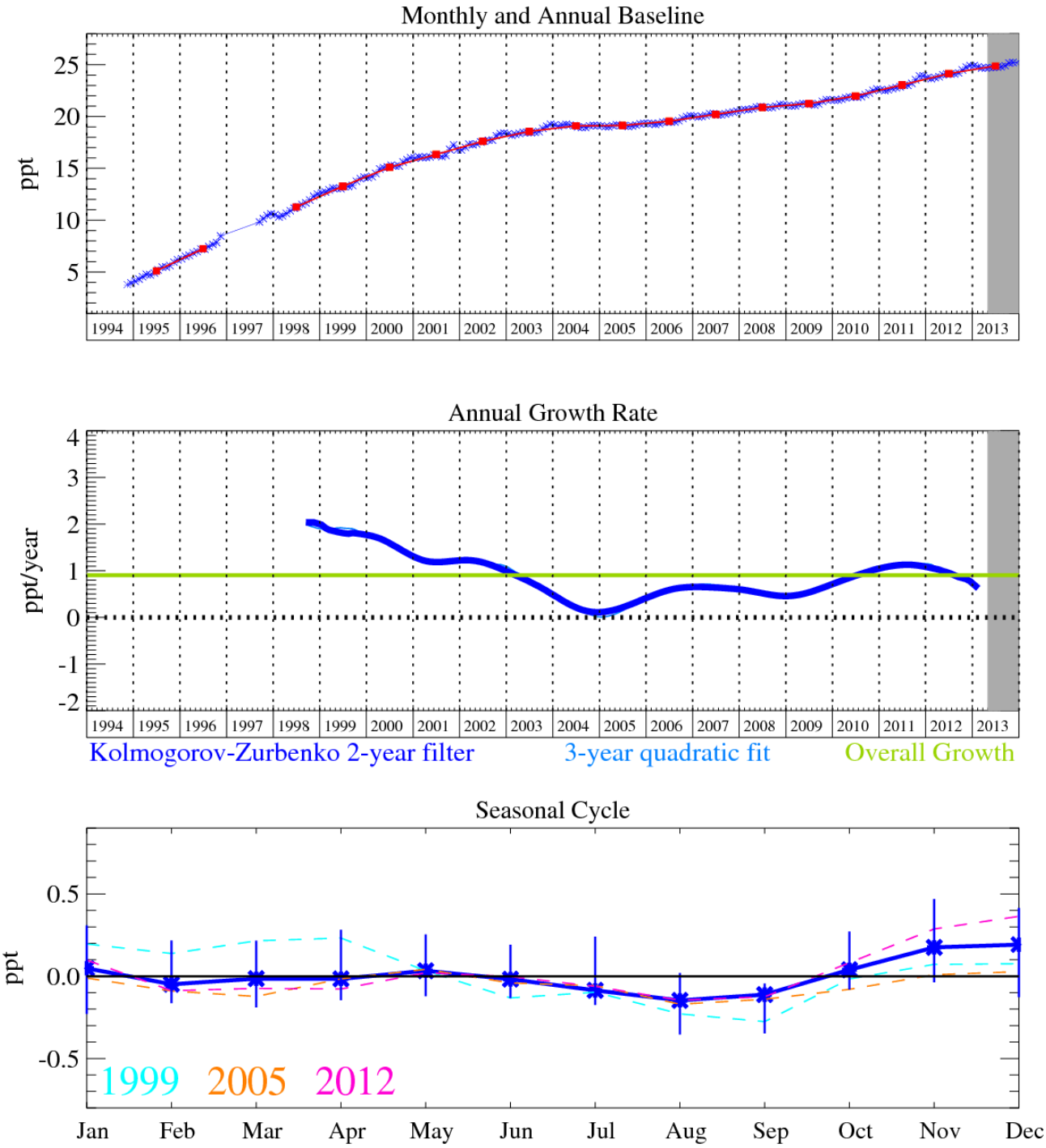

The grey area on each plot contains data that are unratified and therefore provisional.

Figure 83: HCFC-141b ($C_2H_3Cl_2F$): Monthly (blue) and annual (red) baseline (top). Annual (blue) and overall average growth rate (green) (middle plot). Seasonal cycle (de-trended) with year-to-year variability (lower plot). The grey area covers un-ratified and therefore provisional data.

HCFC-142b ($C_2H_3ClF_2$), HCFC-141b ($C_2H_3Cl_2F$) and HCFC-22 ($CHClF_2$) have continued to grow in the atmosphere. The rate of growths for all three gases peaked in 2007/08, but, unlike the other two, the growth rate for HCFC-141b increased again before starting to decline once again in 2012. Prior to 2005, HCFC-142b and HFCF-141b showed reduced growth in the atmosphere in line with their expected phase-out (90% phase-out of production and consumption by 2015 for Article 2 parties and 10% phase-out by Article 5 parties).

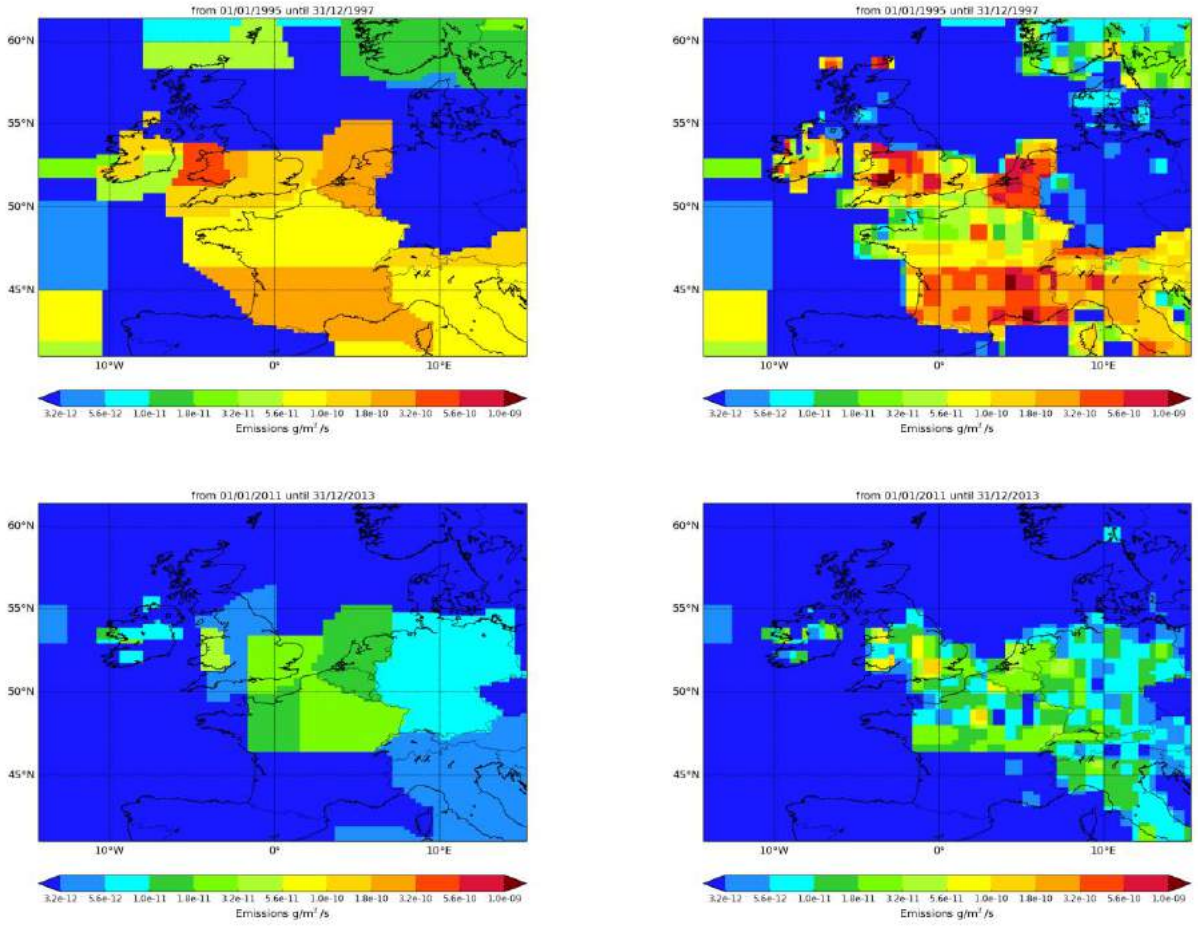

Figure 84: NAME-inversion emission estimates for 1995-1997 (upper) and 2011-2013 (lower). On the right hand side the emissions per grid box have been re-distributed based on population.

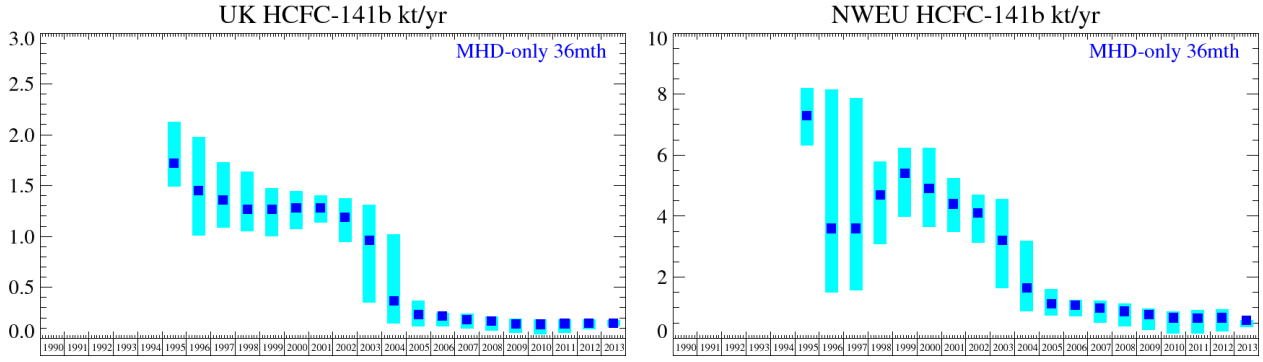

Figure 85: Emission estimates for UK and NWEU (MHD-only). The uncertainty bars represent the 5th and 95th percentiles. Grey line represents the emission estimates presented in last year's report.

Analysis of the HCFC content of regionally-polluted air arriving at Mace Head from the European continent shows that European emissions peaked during the 1990s but declined significantly between 2003 and 2005 following the phase-out in their usage. Before 2005 there were significant pollution events, by 2013 they had considerably reduced in magnitude. The reductions are consistent with the phase-out of HCFC production and use from the year 2001 onwards mandated by European regulations designed to exceed the requirements of the Montreal Protocol. In the US implementation of HCFC phase-out through the Clean Air Act Regulations, 2004 resulted in no production or importation of HCFC-141b since 2003, these restrictions did not apply to HCFC-142b until 2010. Increasing evidence indicates that increased emissions of these compounds from Asia, in particular China are now offsetting the phase-out in developed countries. The current growth rates of HCFC-141b and HCFC-142b are 0.8 and 0.2 ppt/yr respectively. The growth rates of these

compounds, calculated from the baseline mole fractions, are shown in Figures 83 and 86, are also presented in Table 1c.

Unit	Year	UK	(5th-95th)	NWEU	(5th-95th)
t/y	1995	1720.	(1490.-2120.)	7300.	(6330.-8200.)
t/y	1996	1450.	(1010.-1980.)	3600.	(1500.-8160.)
t/y	1997	1360.	(1090.-1730.)	3600.	(1570.-7860.)
t/y	1998	1270.	(1060.-1630.)	4700.	(3090.-5790.)
t/y	1999	1270.	(1000.-1470.)	5400.	(3980.-6250.)
t/y	2000	1280.	(1080.-1440.)	4900.	(3640.-6250.)
t/y	2001	1280.	(1140.-1400.)	4400.	(3480.-5250.)
t/y	2002	1190.	(950.-1370.)	4100.	(3130.-4700.)
t/y	2003	960.	(350.-1310.)	3200.	(1650.-4550.)
t/y	2004	370.	(150.-1020.)	1640.	(890.-3190.)
t/y	2005	230.	(120.- 370.)	1130.	(750.-1610.)
t/y	2006	220.	(120.- 250.)	1080.	(720.-1240.)
t/y	2007	180.	(100.- 240.)	990.	(500.-1230.)
t/y	2008	170.	(70.- 210.)	880.	(390.-1140.)
t/y	2009	140.	(50.- 190.)	770.	(270.- 970.)
t/y	2010	140.	(40.- 190.)	670.	(160.- 870.)
t/y	2011	140.	(50.- 190.)	650.	(170.- 920.)
t/y	2012	150.	(90.- 180.)	670.	(240.- 950.)
t/y	2013	150.	(120.- 180.)	590.	(370.- 600.)

Table 44: Emission estimates for UK and NWEU with uncertainty (5^{th} – 95^{th} %ile).

6.8 HCFC-142b

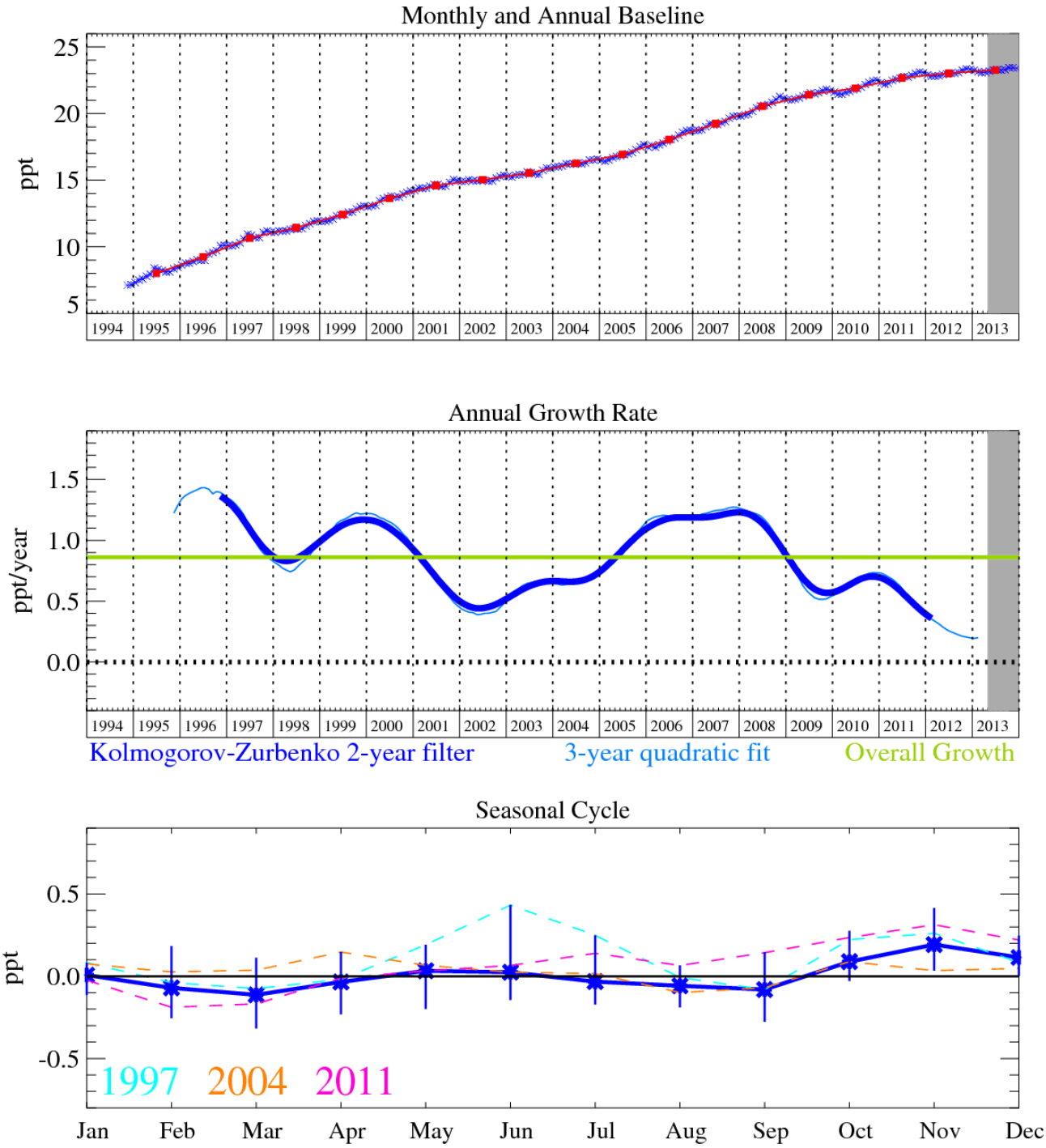

The grey area on each plot contains data that are unratified and therefore provisional.

Figure 86: HCFC-142b ($C_2H_3ClF_2$): Monthly (blue) and annual (red) baseline (top). Annual (blue) and overall average growth rate (green) (middle plot). Seasonal cycle (de-trended) with year-to-year variability (lower plot). The grey area covers un-ratified and therefore provisional data.

The emissions of HCFC-142b in both the UK and NWEU as a whole fell very significantly between 2000 and 2005. Like HCFC-141b, this clearly shows the impact of the Montreal Protocol, which banned the use of this gas in developed countries from 2005 onwards. Before 2002 there were significant pollution events, by 2013 they had considerably reduced in magnitude.

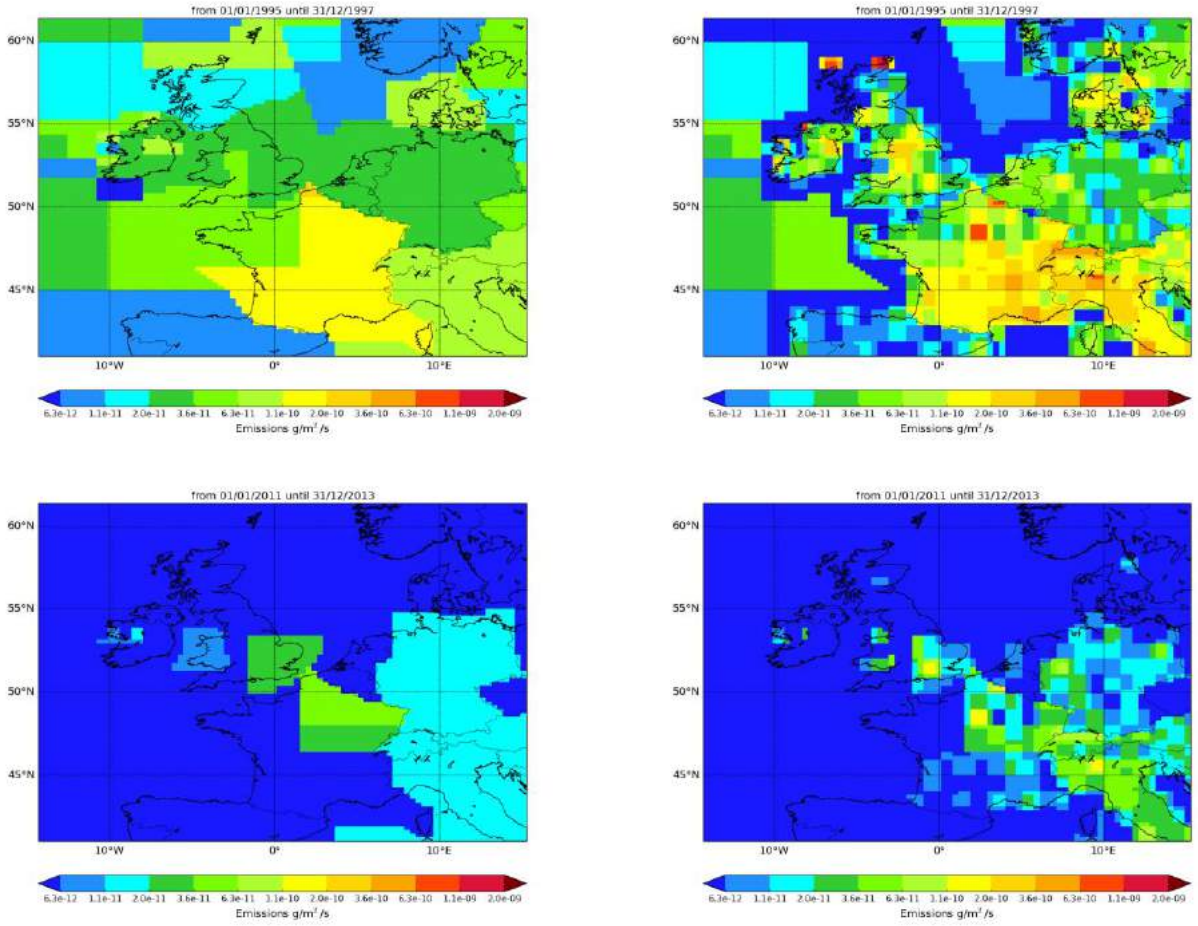

Figure 87: NAME-inversion emission estimates for 1995-1997 (upper) and 2011-2013 (lower). On the right hand side the emissions per grid box have been re-distributed based on population.

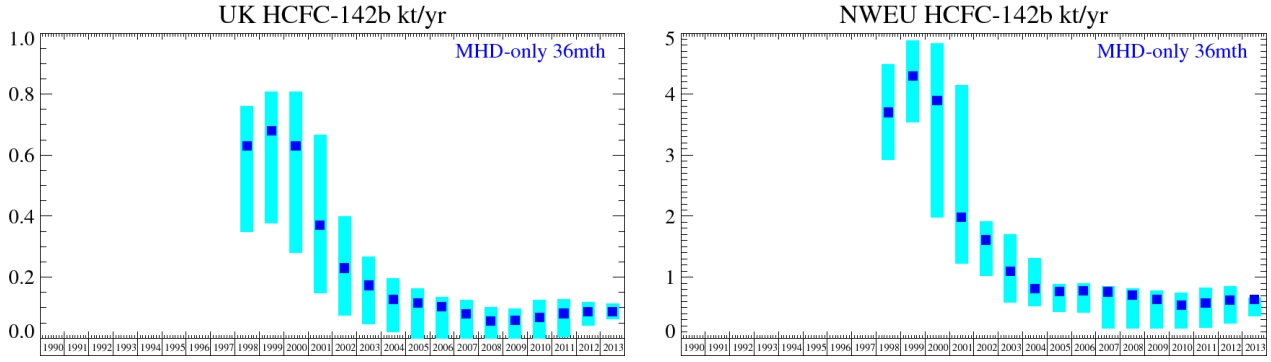

Figure 88: Emission estimates for UK and NWEU (MHD-only). The uncertainty bars represent the 5th and 95th percentiles. Grey line represents the emission estimates presented in last year's report.

Unit	Year	UK	(5th-95th)	NWEU	(5th-95th)
t/y	1998	630.	(349.- 760.)	3700.	(2930.-4490.)
t/y	1999	680.	(377.- 807.)	4300.	(3540.-4880.)
t/y	2000	630.	(279.- 807.)	3900.	(1980.-4830.)
t/y	2001	370.	(147.- 666.)	1980.	(1220.-4140.)
t/y	2002	230.	(74.- 400.)	1610.	(1020.-1910.)
t/y	2003	173.	(46.- 268.)	1100.	(590.-1700.)
t/y	2004	128.	(21.- 196.)	810.	(520.-1310.)
t/y	2005	115.	(0.- 162.)	770.	(440.- 880.)
t/y	2006	103.	(0.- 135.)	780.	(420.- 890.)
t/y	2007	80.	(0.- 125.)	760.	(170.- 850.)
t/y	2008	56.	(0.- 102.)	710.	(160.- 820.)
t/y	2009	59.	(0.- 98.)	640.	(160.- 780.)
t/y	2010	68.	(0.- 125.)	540.	(160.- 750.)
t/y	2011	81.	(4.- 127.)	580.	(170.- 830.)
t/y	2012	86.	(42.- 118.)	620.	(250.- 850.)
t/y	2013	86.	(63.- 114.)	640.	(360.- 670.)

Table 45: Emission estimates for UK and NWEU with uncertainty (5^{th} – 95^{th} %ile).

6.9 HCFC-22

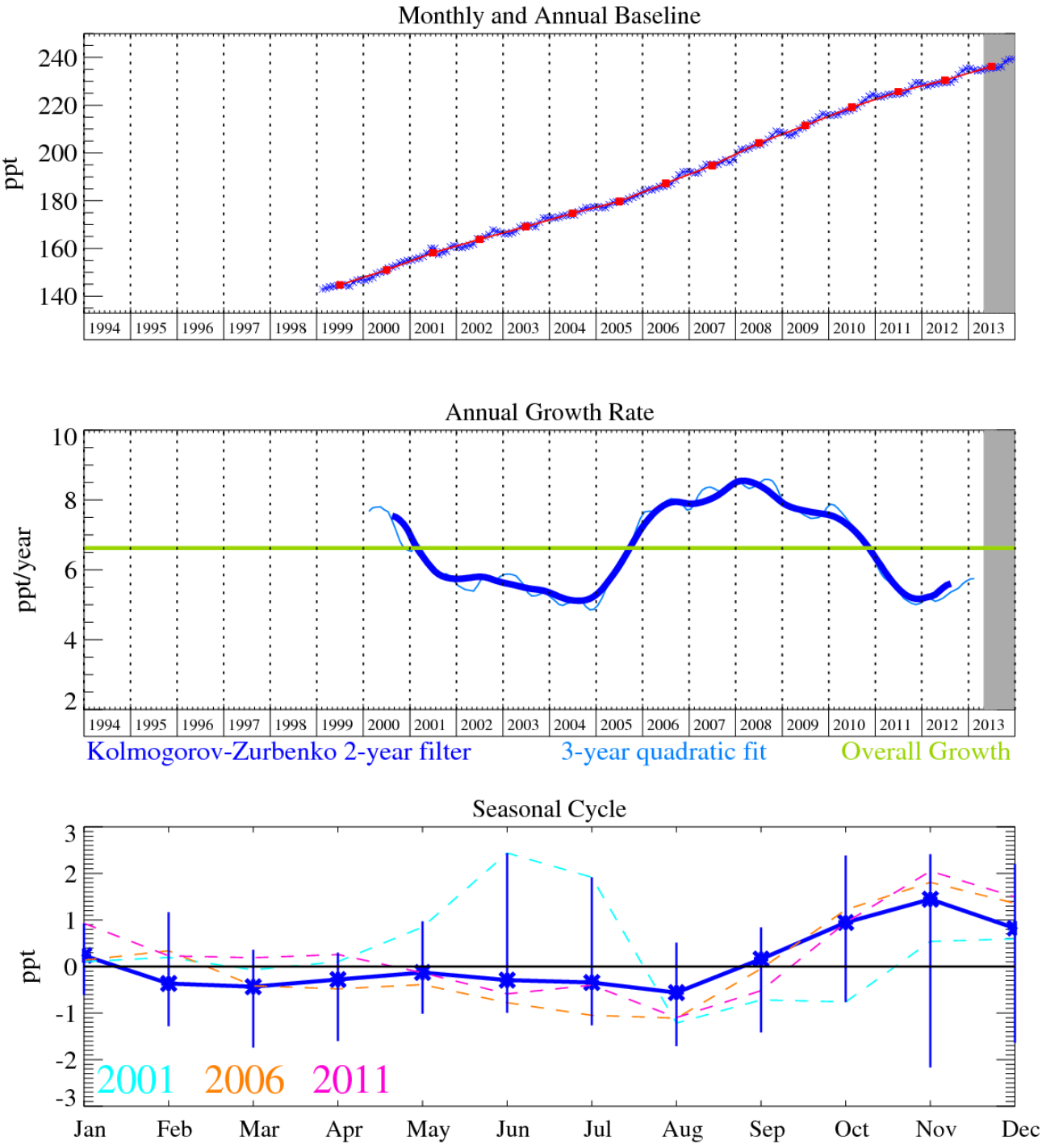

The grey area on each plot contains data that are unratified and therefore provisional.

Figure 89: HCFC-22 ($CHClF_2$): Monthly (blue) and annual (red) baseline (top plot). Annual (blue) and overall average growth rate (green) (middle plot). Seasonal cycle (de-trended) with year-to-year variability (lower plot). Grey area covers un-ratified and therefore provisional data.

Over the past 12-months HCFC-22, the dominant globally produced HCFC compound, was growing at a rate of 5.7 ppt/yr and, by December 2013, had reached a level at Mace Head of approximately 239.4 ppt. This rate of growth has steadily slowed from its maximum in 2008.

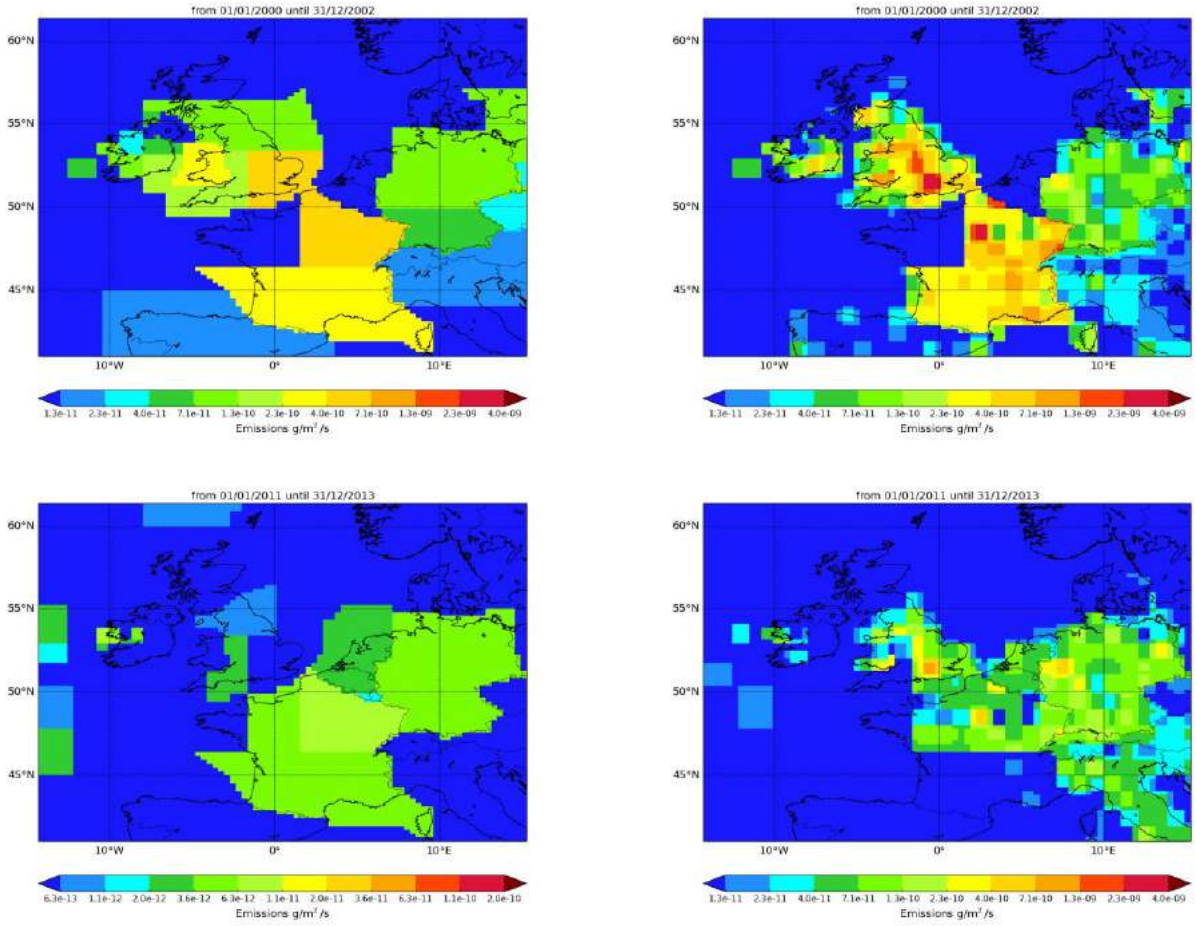

Figure 90: NAME-inversion emission estimates for 2000-2002 (upper) and 2011-2013 (lower). On the right hand side the emissions per grid box have been re-distributed based on population.

The emissions of HCFC-22 have decreased steadily over the 13 years from 2000. The magnitude of the pollution events have similarly declined.

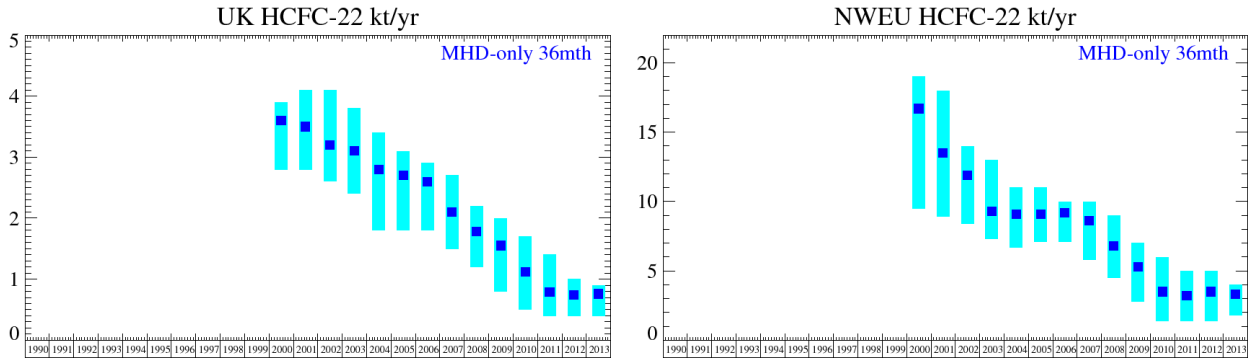

Figure 91: Emission estimates for UK and NWEU (MHD-only). The uncertainty bars represent the 5th and 95th percentiles. Grey line represents the emission estimates presented in last year's report.

Unit	Year	UK	(5th-95th)	NWEU	(5th-95th)
kt/y	2000	3.6	(2.8- 3.9)	16.7	(9.5 -19.)
kt/y	2001	3.5	(2.8- 4.1)	13.5	(8.9 -18.)
kt/y	2002	3.2	(2.6- 4.1)	11.9	(8.4 -14.)
kt/y	2003	3.1	(2.4- 3.8)	9.3	(7.3 -13.)
kt/y	2004	2.8	(1.8- 3.4)	9.1	(6.7 -11.)
kt/y	2005	2.7	(1.8- 3.1)	9.1	(7.1 -11.)
kt/y	2006	2.6	(1.8- 2.9)	9.2	(7.1 -10.)
kt/y	2007	2.1	(1.5- 2.7)	8.6	(5.8 -10.)
kt/y	2008	1.8	(1.2- 2.2)	6.8	(4.5 - 9.)
kt/y	2009	1.6	(0.8- 2.0)	5.3	(2.8 - 7.)
kt/y	2010	1.1	(0.5- 1.7)	3.5	(1.4 - 6.)
kt/y	2011	0.8	(0.4- 1.4)	3.2	(1.4 - 5.)
kt/y	2012	0.7	(0.4- 1.0)	3.5	(1.4 - 5.)
kt/y	2013	0.8	(0.4- 0.9)	3.3	(1.8 - 4.)

Table 46: Emission estimates for UK and NWEU with uncertainty (5^{th} – 95^{th} %ile).

6.10 HFC-236fa

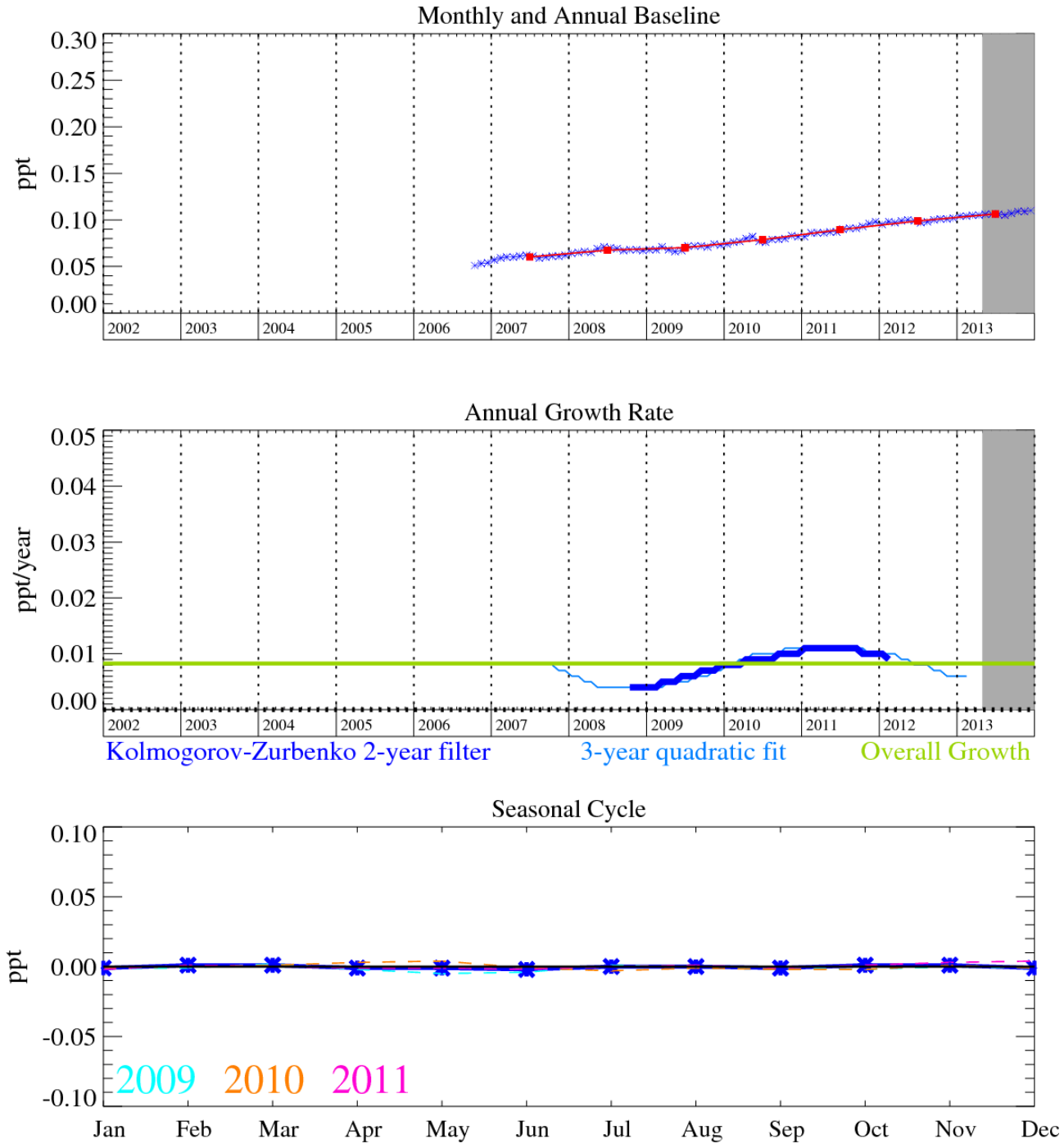

The grey area on each plot contains data that are unratified and therefore provisional.

Figure 92: HFC-236fa ($C_3H_2F_6$): Monthly (blue) and annual (red) baseline (top plot). Annual (blue) and overall average growth rate (green) (middle plot). Seasonal cycle (de-trended) with year-to-year variability (lower plot). Grey area covers un-ratified and therefore provisional data.

HFC-236fa ($C_3H_2F_6$) is used as a fire-fighting agent (atmospheric lifetime 240 years and GWP_{100} of 9500) and has reached a mixing ratio of 0.11 ppt and is growing at a rate of 0.01 ppt/yr.

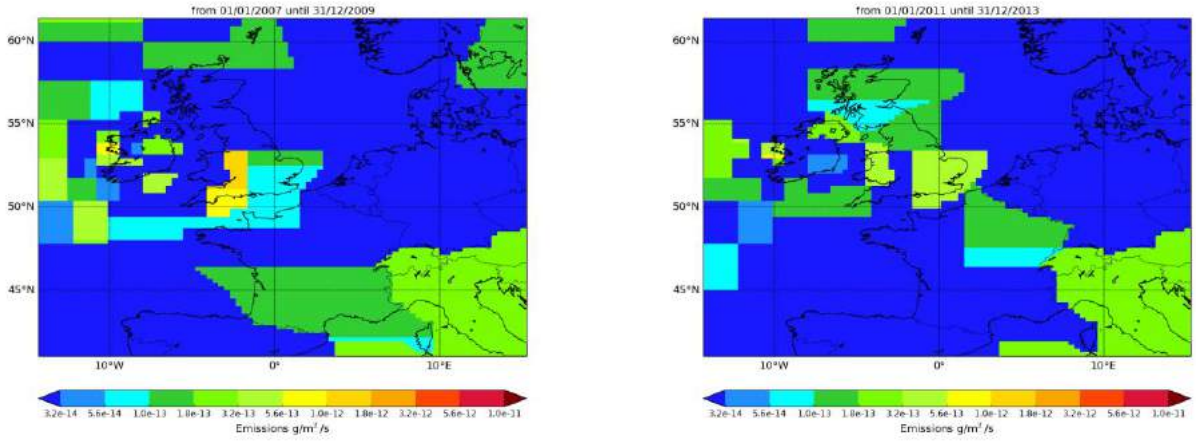

Figure 93: NAME-inversion emission estimates for 2007-2009 (left) and 2011-2013 (right).

It is clear that there are only very limited emissions of this gas across Europe. The magnitude of the pollution events are very low compared to the noise in the baseline and therefore the uncertainty in the InTEM results are significant.

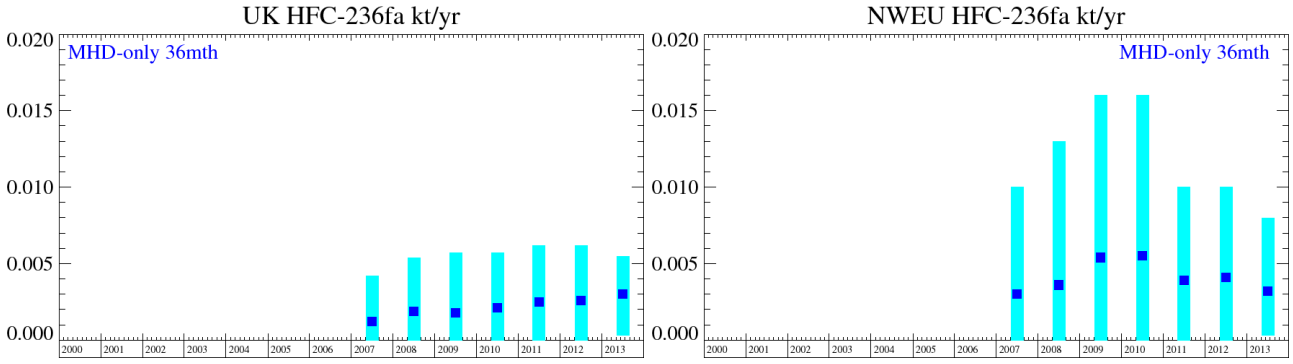

Figure 94: Emission estimates for UK and NWEU. The uncertainty bars represent the 5th and 95th percentiles.

Unit	Year	UK	(5th-95th)	NWEU	(5th-95th)
t/y	2007	1.20	(0.00- 4.2)	3.0	(0.00 -10.)
t/y	2008	1.87	(0.00- 5.4)	3.6	(0.00 -13.)
t/y	2009	1.78	(0.00- 5.7)	5.4	(0.00 -16.)
t/y	2010	2.1	(0.00- 5.7)	5.5	(0.00 -16.)
t/y	2011	2.5	(0.00- 6.2)	3.9	(0.00 -10.)
t/y	2012	2.6	(0.00- 6.2)	4.1	(0.00 -10.)
t/y	2013	3.0	(0.30- 5.5)	3.2	(0.32 - 8.)

Table 47: Emission estimates for UK and NWEU with uncertainty (5th – 95th %ile).

6.11 HFC-245fa

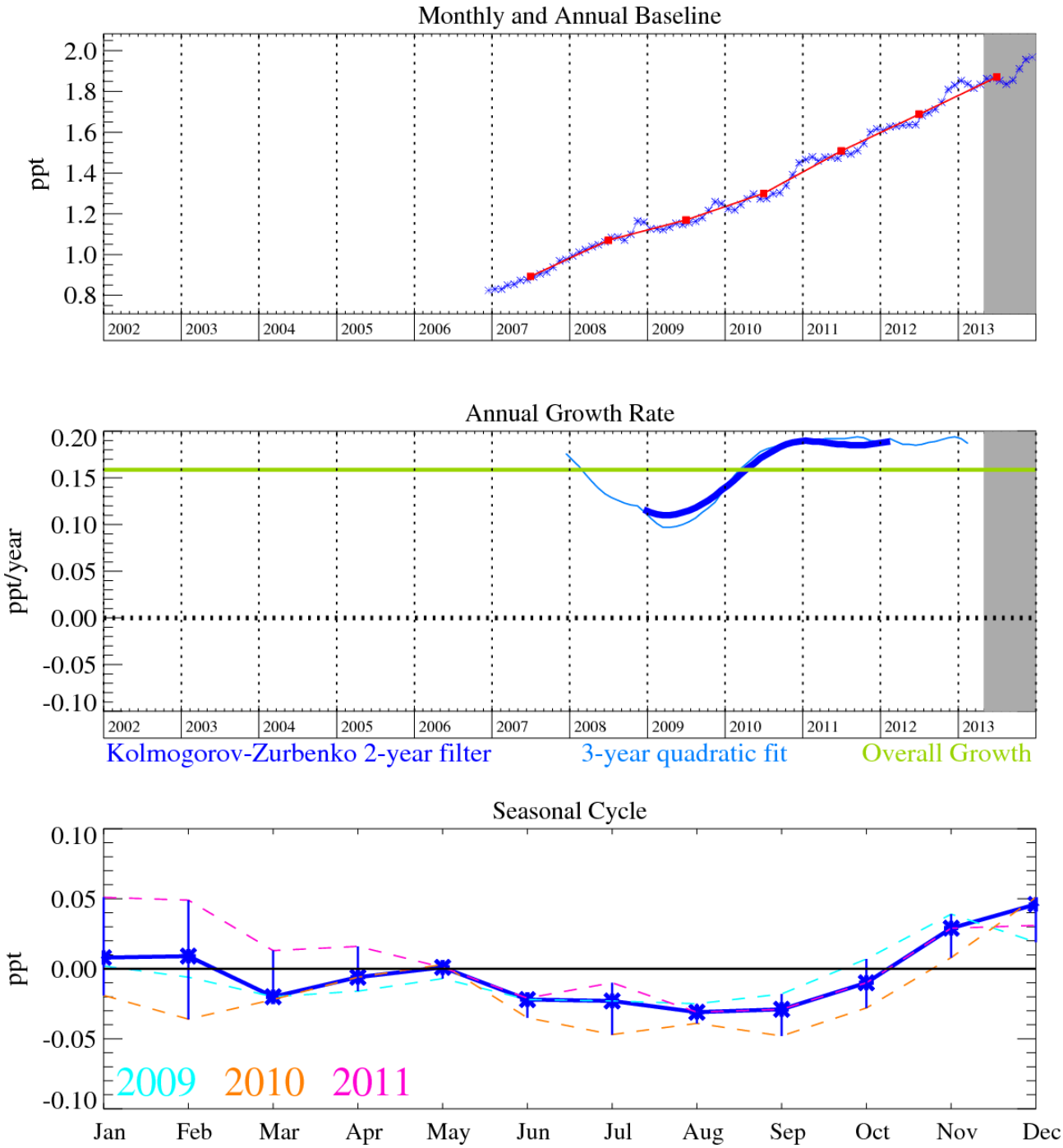

The grey area on each plot contains data that are unratified and therefore provisional.

Figure 95: HFC-245fa ($C_3H_3F_5$): Monthly (blue) and annual (red) baseline (top plot). Annual (blue) and overall average growth rate (green) (middle plot). Seasonal cycle (de-trended) with year-to-year variability (lower plot). Grey area covers un-ratified and therefore provisional data.

HFC-245fa ($C_3H_3F_5$) is used as a foam-blowing agent for polyurethane (PUR) foams. It has an atmospheric lifetime 7.9 years and GWP_{100} of 1020. In December 2013 its atmospheric mole fraction was 2.0 ppt and it is growing at a rate of 0.19 ppt/yr.

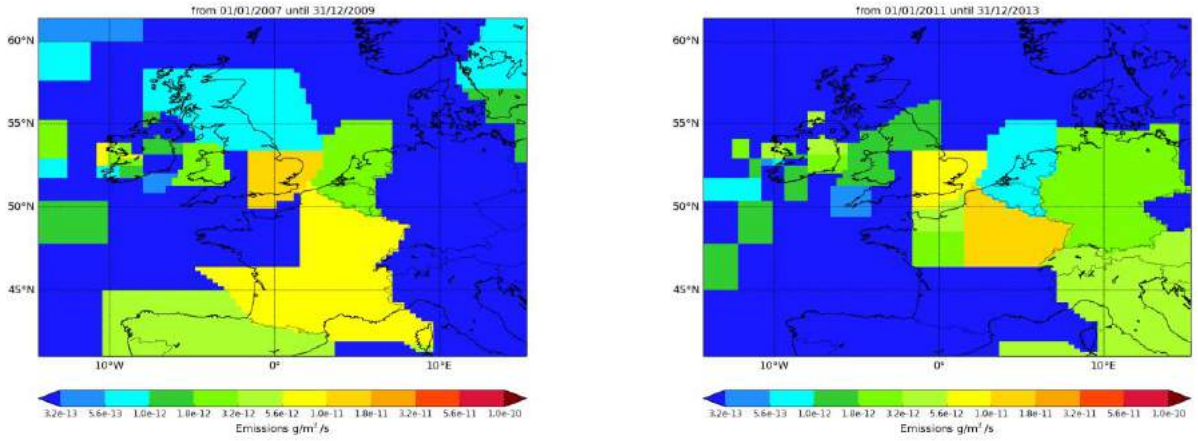

Figure 96: NAME-inversion emission estimates for 2007-2009 (left) and 2011-2013 (right

The statistical match between the modelled and observed time-series is not strong giving rise to significant uncertainty in the InTEM UK and NWEU emission estimates.

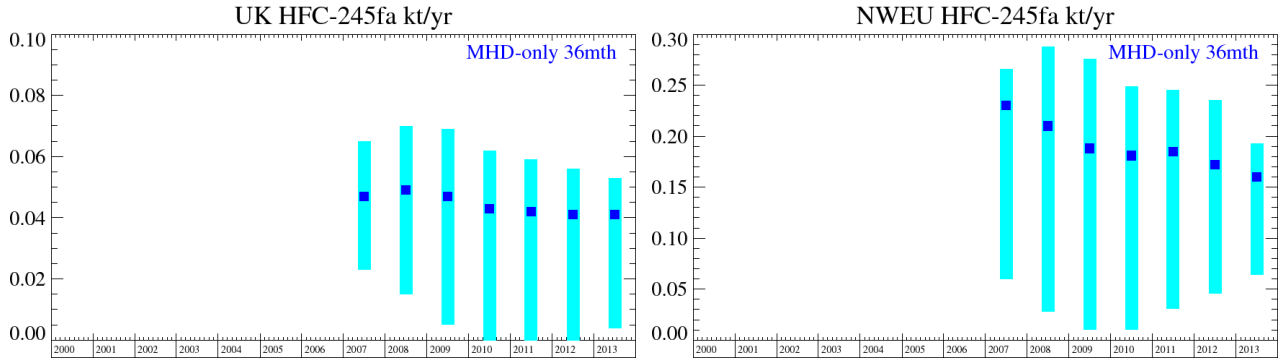

Figure 97: Emission estimates for UK and NWEU (MHD-only). The uncertainty bars represent the 5th and 95th percentiles.

Unit	Year	UK	(5th-95th)	NWEU	(5th-95th)
t/y	2007	47.	(23.- 65.)	230.	(60. -270.)
t/y	2008	49.	(15.- 70.)	210.	(30. -290.)
t/y	2009	47.	(5.- 69.)	190.	(10. -280.)
t/y	2010	43.	(0.- 62.)	180.	(10. -250.)
t/y	2011	42.	(0.- 59.)	190.	(30. -250.)
t/y	2012	41.	(0.- 56.)	170.	(50. -240.)
t/y	2013	41.	(4.- 53.)	160.	(60. -190.)

Table 48: Emission estimates for UK and NWEU with uncertainty (5th – 95th %ile).

6.12 HFC-365mfc

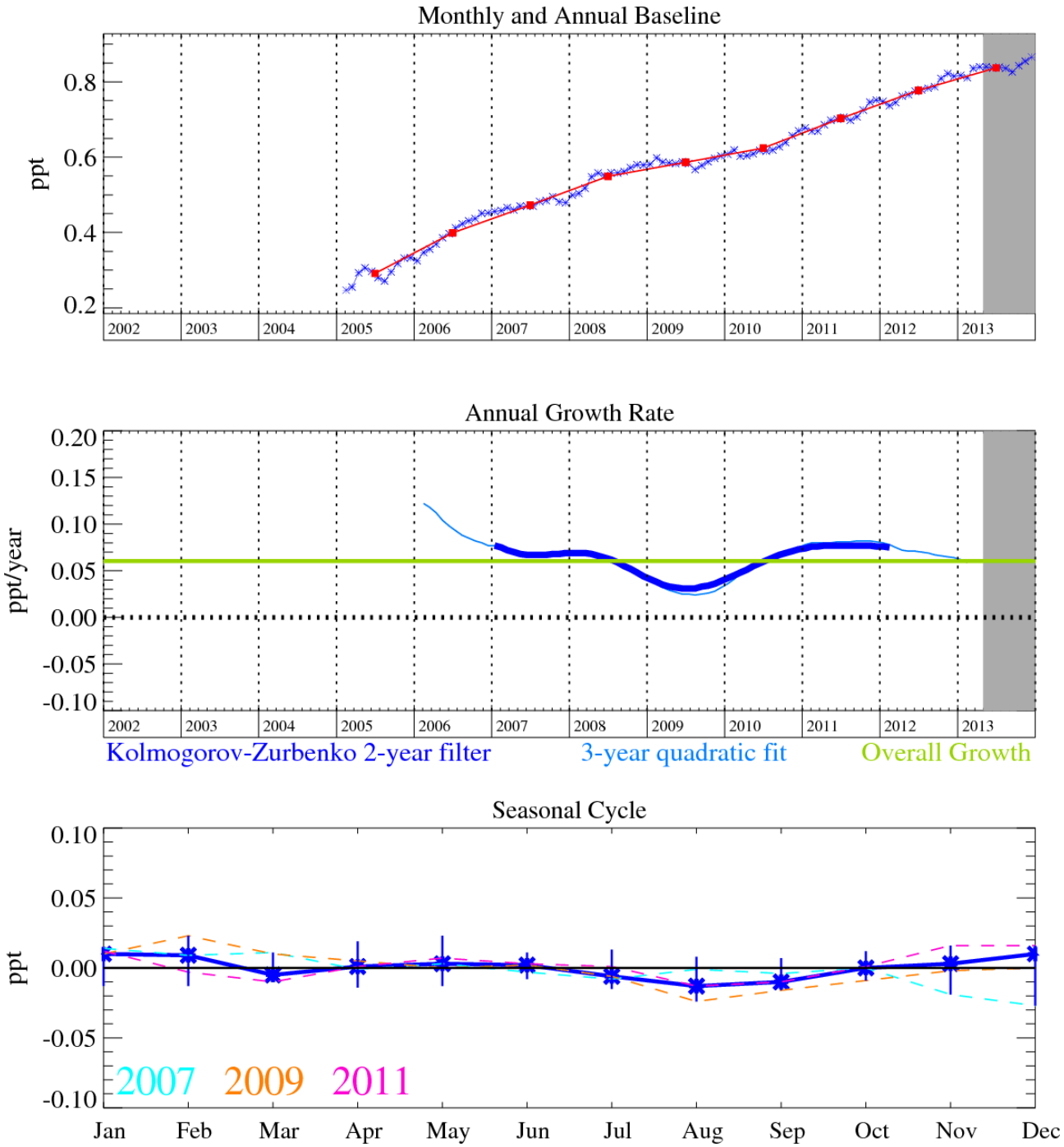

The grey area on each plot contains data that are unratified and therefore provisional.

Figure 98: HFC-365mfc ($C_4H_5F_5$): Monthly (blue) and annual (red) baseline (top plot). Annual (blue) and overall average growth rate (green) (middle plot). Seasonal cycle (de-trended) with year-to-year variability (lower plot). Grey area covers un-ratified and therefore provisional data.

HFC-365mfc ($C_4H_5F_5$) is used mainly for polyurethane structural foam blowing as a replacement for HCFC-141b, and to a minor extent as a blend component for solvents. It has an atmospheric lifetime of 8.6 years and a GWP estimated at 790-997 (100-year time horizon). It is currently growing in the atmosphere at a rate of 0.06 ppt/yr and reached a mole fraction of 0.87 ppt in 2013.

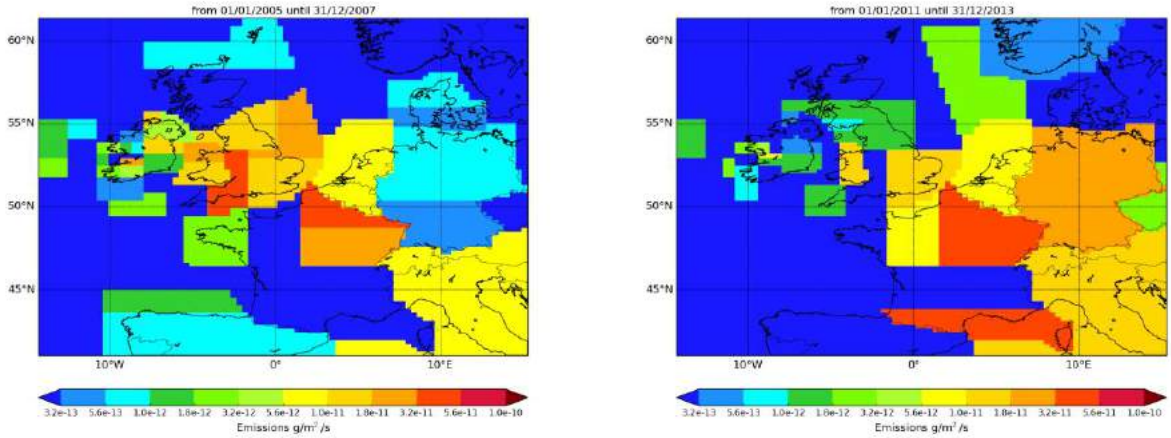

Figure 99: NAME-inversion emission estimates for 2005-2007 (left) and 2011-2013 (right).

The statistical match between the modelled and observed time-series is good. The emissions in the UK decreased significantly between 2005-2009 and then remained static, whereas those in NWEU have slowly grown over the last few years.

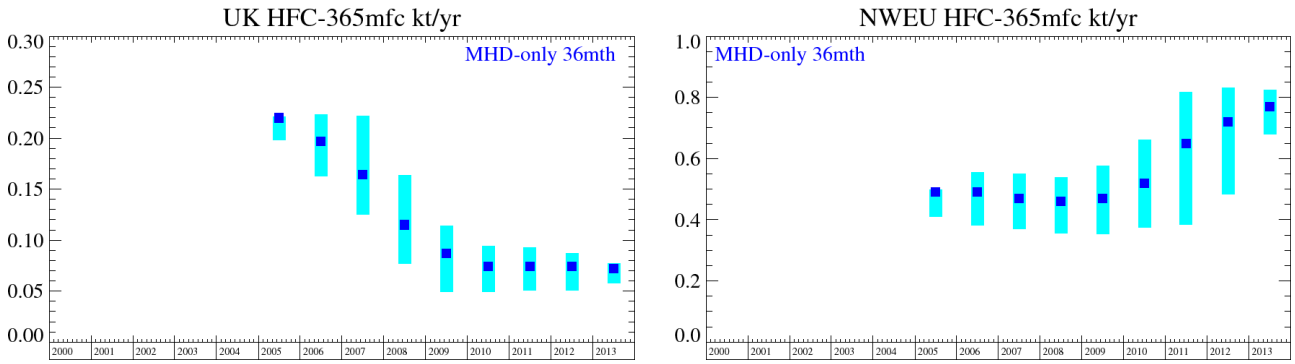

Figure 100: Emission estimates for UK and NWEU. The uncertainty bars represent the 5th and 95th percentiles.

Unit	Year	UK	(5th-95th)	NWEU	(5th-95th)
t/y	2005	220	(198.- 221.)	490	(410. -499.)
t/y	2006	197	(163.- 223.)	490	(382. -555.)
t/y	2007	164	(125.- 222.)	470	(369. -551.)
t/y	2008	115	(77.- 164.)	460	(355. -538.)
t/y	2009	87	(49.- 114.)	470	(354. -577.)
t/y	2010	74	(49.- 94.)	520	(374. -661.)
t/y	2011	74	(51.- 93.)	650	(383. -818.)
t/y	2012	74	(51.- 87.)	720	(483. -832.)
t/y	2013	72	(58.- 77.)	770	(679. -825.)

Table 49: Emission estimates for UK and NWEU with uncertainty (5th – 95th %ile).

6.13 SO_2F_2

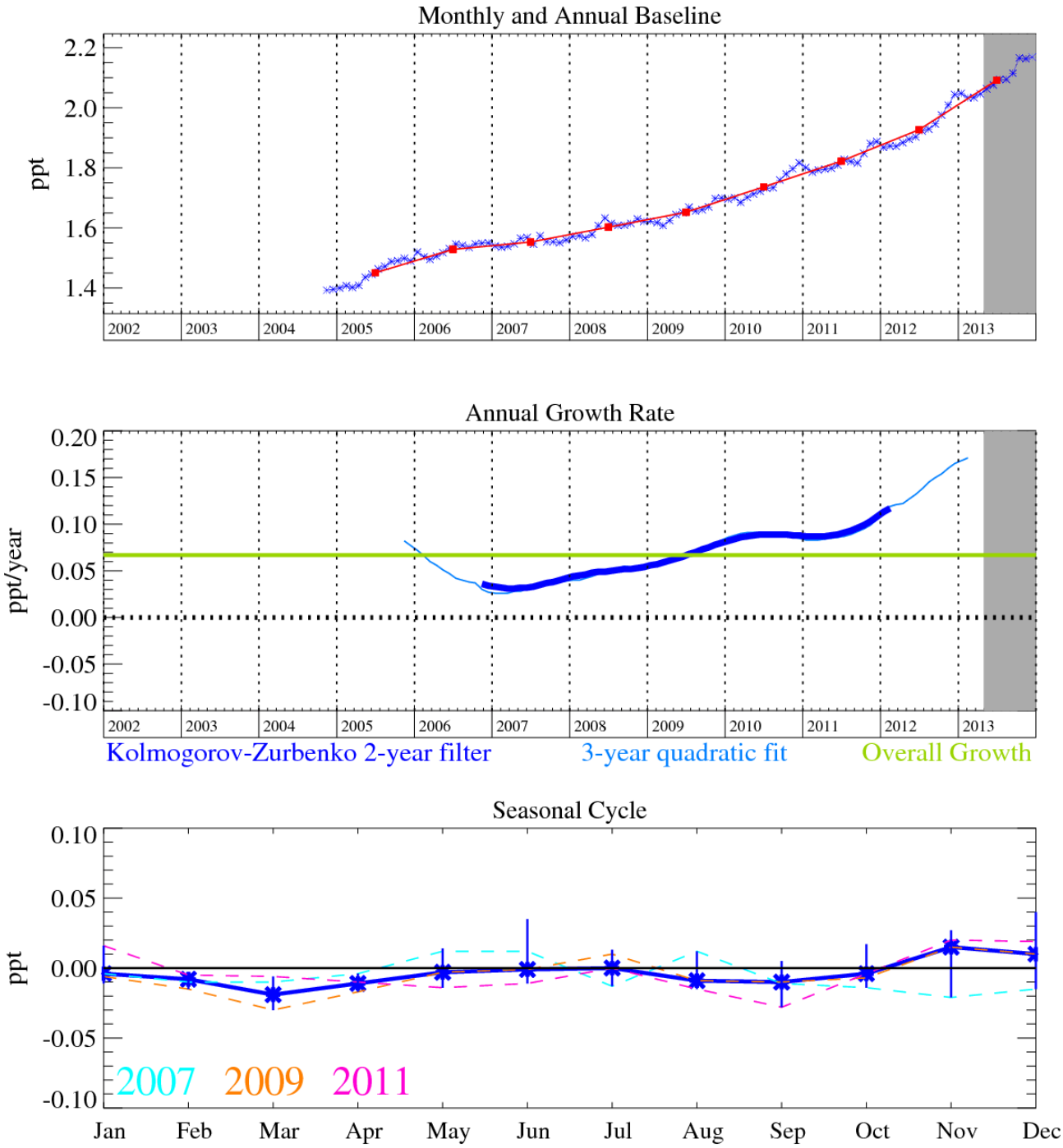

The grey area on each plot contains data that are unratified and therefore provisional.

Figure 101: SO_2F_2: Monthly (blue) and annual (red) baseline mole fractions (top plot). Annual (blue) and overall average growth rate (green) (middle plot). Seasonal cycle (de-trended) with year-to-year variability (lower plot). Grey area covers un-ratified and therefore provisional data.

6.14 CH_3Cl

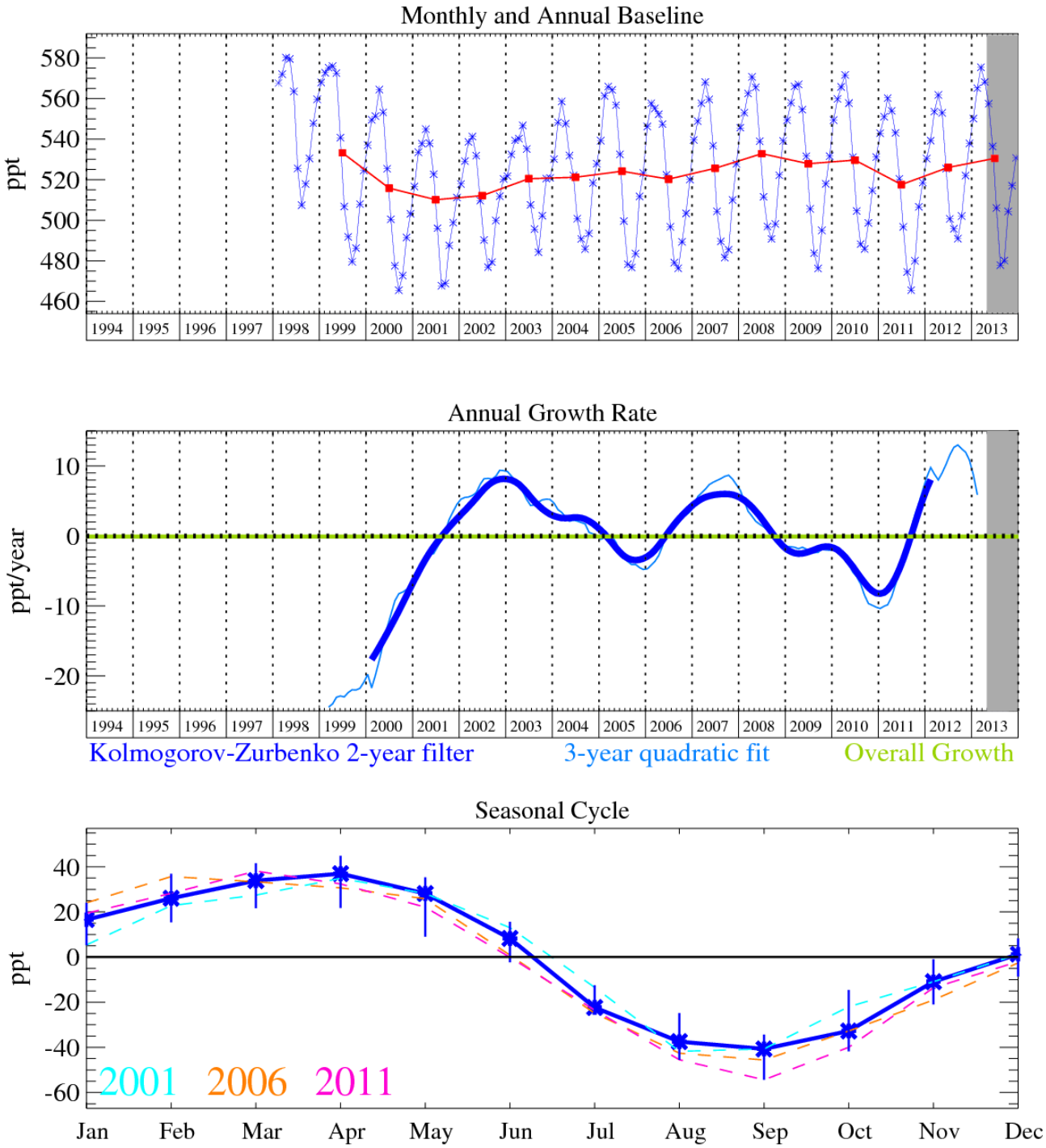

Figure 102: CH_3Cl: Monthly (blue) and annual (red) baseline mole fractions (top plot). Annual (blue) and overall growth rate (green) (middle). Seasonal cycle (de-trended) with year-to-year variability (lower plot). Grey area covers un-ratified and therefore provisional data.

A number of long lived and very short lived substances (VSLS) halocarbons are measured by the Medusa GC-MS. Previously we reported the recovery and then decline of CH_3Cl growth in the atmosphere, the growth abated in 2008, declined until 2011 and now the trend shows an increase of greater than 10 ppt/yr. At the end of 2013 its mole fraction was 531 ppt (Figure 102). Methyl chloride (CH_3Cl) is not a controlled substance and is emitted from a range of biogenic and anthropogenic sources globally. It is estimated that ~55% of CH_3Cl emissions arise from terrestrial tropical areas with emission rates dependent on global temperature changes. Other major sources are biomass burning, anthropogenic activities and oceans. The atmospheric lifetime of CH_3Cl is 1 year [*Montzka et al.*, 2011] and it has a GWP_{100} of 13 [*Forster et al.*, 2007]. CH_3Cl contributes 16% of the total

chlorine loading to the troposphere for long-lived species and is thus the most abundant chlorine containing compound in the atmosphere.

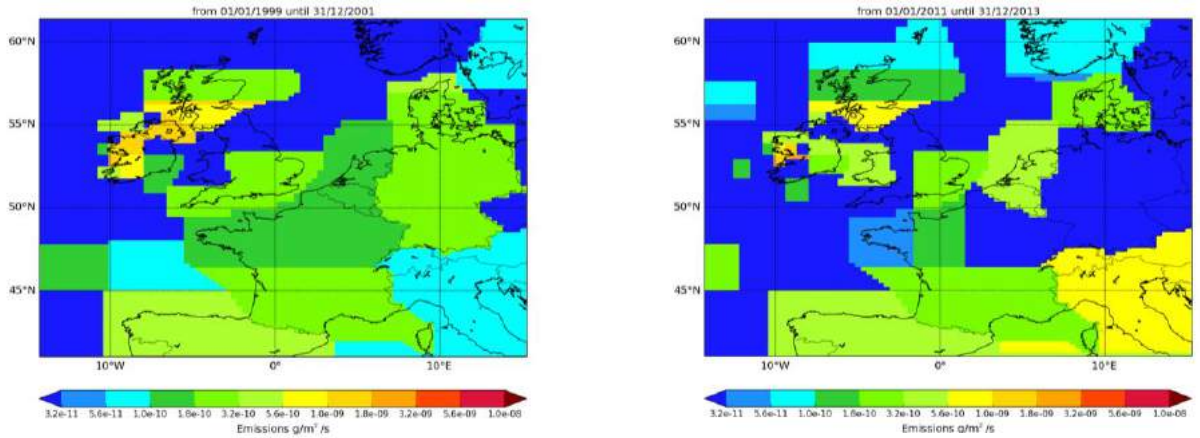

Figure 103: NAME-inversion emission estimates for 1999-2001 (left) and 2011-2013 (right).

.

For this gas the emissions have not been re-distributed based on population because given its natural releases its emissions are not well correlated with population. The statistical match between the observations and model time-series is reasonable but there is significant uncertainty in the InTEM emission estimates. The median emissions over the UK and NWEU, although uncertain, show a modest decline over the entire length of the record.

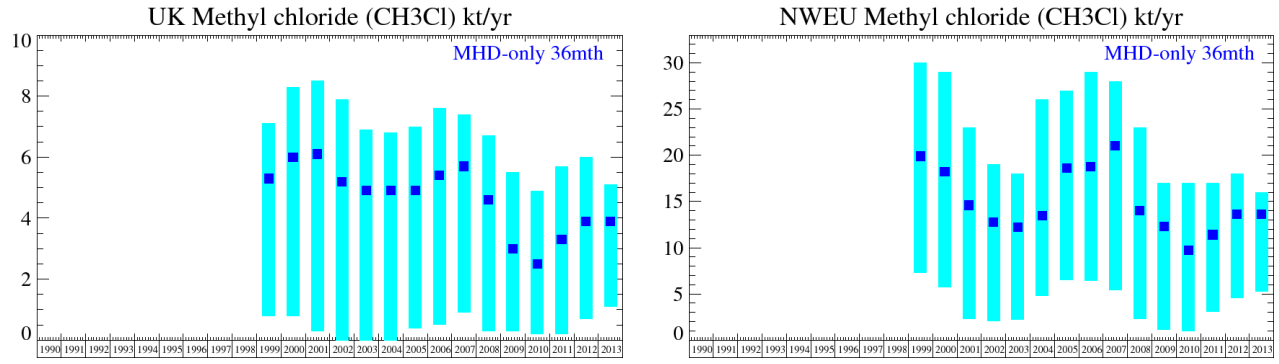

Figure 104: Emission estimates for UK and NWEU (MHD-only). The uncertainty bars represent the 5th and 95th percentiles.

Unit	Year	UK	(5th-95th)	NWEU	(5th-95th)
kt/y	1999	5.3	(0.8- 7.1)	19.9	(7.3 -30.)
kt/y	2000	6.0	(0.8- 8.3)	18.2	(5.7 -29.)
kt/y	2001	6.1	(0.3- 8.5)	14.6	(2.3 -23.)
kt/y	2002	5.2	(0.0- 7.9)	12.8	(2.1 -19.)
kt/y	2003	4.9	(0.0- 6.9)	12.2	(2.2 -18.)
kt/y	2004	4.9	(0.0- 6.8)	13.5	(4.8 -26.)
kt/y	2005	4.9	(0.4- 7.0)	18.6	(6.5 -27.)
kt/y	2006	5.4	(0.5- 7.6)	18.8	(6.4 -29.)
kt/y	2007	5.7	(0.9- 7.4)	21.	(5.4 -28.)
kt/y	2008	4.6	(0.3- 6.7)	14.0	(2.3 -23.)
kt/y	2009	3.0	(0.3- 5.5)	12.3	(1.1 -17.)
kt/y	2010	2.5	(0.2- 4.9)	9.7	(1.0 -17.)
kt/y	2011	3.3	(0.2- 5.7)	11.4	(3.1 -17.)
kt/y	2012	3.9	(0.7- 6.0)	13.6	(4.6 -18.)
kt/y	2013	3.9	(1.1- 5.1)	13.6	(5.3 -16.)

Table 50: Emission estimates for UK and NWEU with uncertainty (5th – 95th %ile).

6.15 CH_2Cl_2

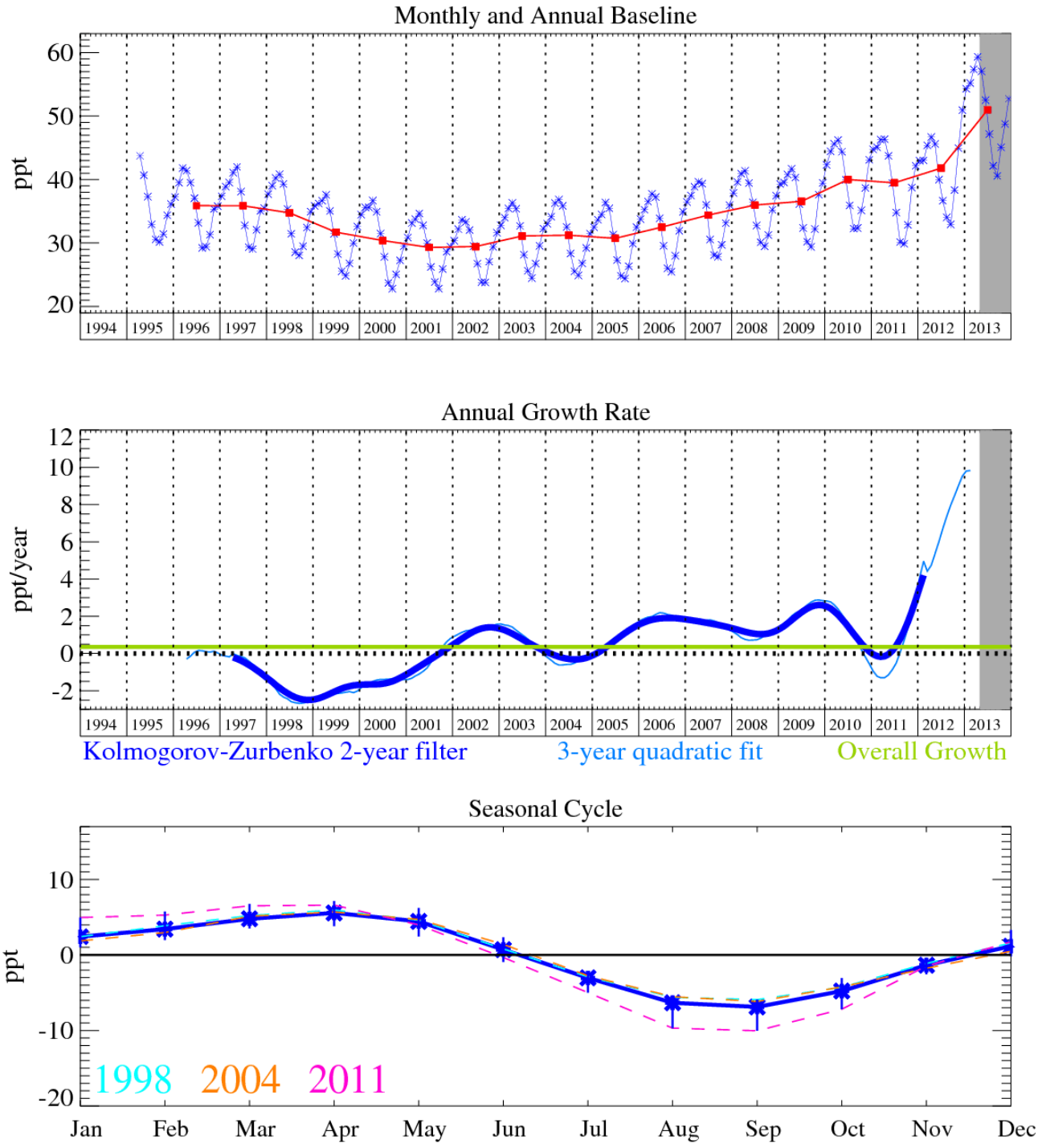

The grey area on each plot contains data that are unratified and therefore provisional.

Figure 105: CH_2Cl_2: Monthly (blue) and annual (red) baseline mole fractions (top plot). Annual (blue) and overall average growth rate (green) (middle plot). Seasonal cycle (de-trended) with year-to-year variability (lower plot). Grey area covers un-ratified and therefore provisional data.

Dichloromethane (CH_2Cl_2) global sources are thought to be 70% or greater of anthropogenic origin [*Keene et al.*, 1999; *Cox et al.*, 2003]. It is predominantly used as a paint stripper, degreaser, foam-blowing agent and in pharmaceutical production methods. Its use as a paint stripper has been banned since 2010 in the EU and there has been a reduction in the many other solvent applications for this compound, however since 2004, measurements at Mace Head have shown it to be accumulating in the atmosphere. Its recent growth rate is over 9 ppt/yr and its mole fraction at the end of 2013 was 52.7 ppt. Emission totals derived using the NAME model and the industry derived

inventory suggest that emissions from the NW Europe (and the UK) are decreasing, which implies a source of CH_2Cl_2 to the atmosphere from locations outside of Europe. CH_2Cl_2 has a lifetime of 144 days [*Montzka et al.*, 2011] and a GWP_{100} of 8.7 [*Forster et al.*, 2007].

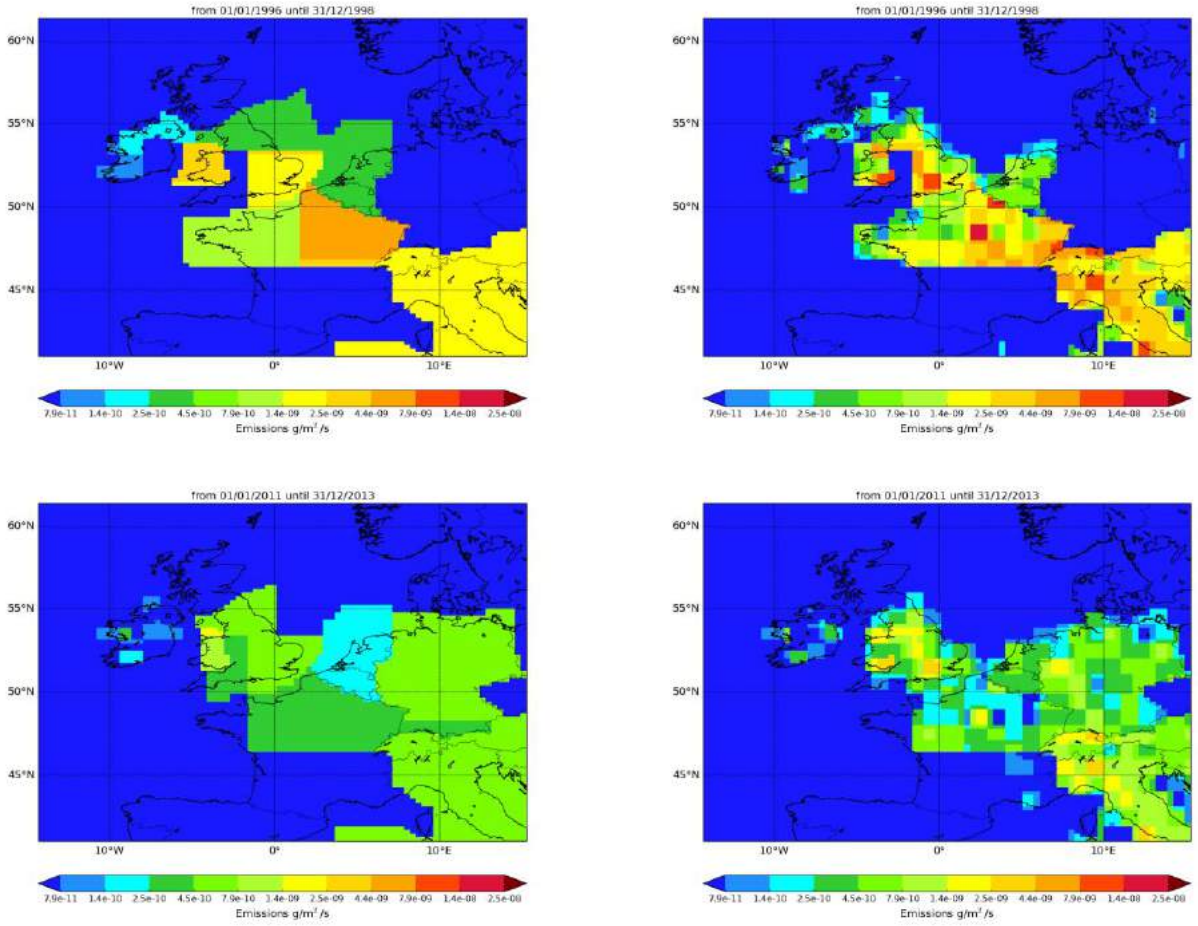

Figure 106: NAME-inversion emission estimates for 1996-1998 (upper) and 2011-2013 (lower). On the right hand side the emissions per grid box have been re-distributed based on population.

There is strong evidence across all of the metrics that UK and NWEU emissions have declined significantly since 1999 although there are still relatively strong discernible pollution events. The statistical match between the modelled and observed time-series is good.

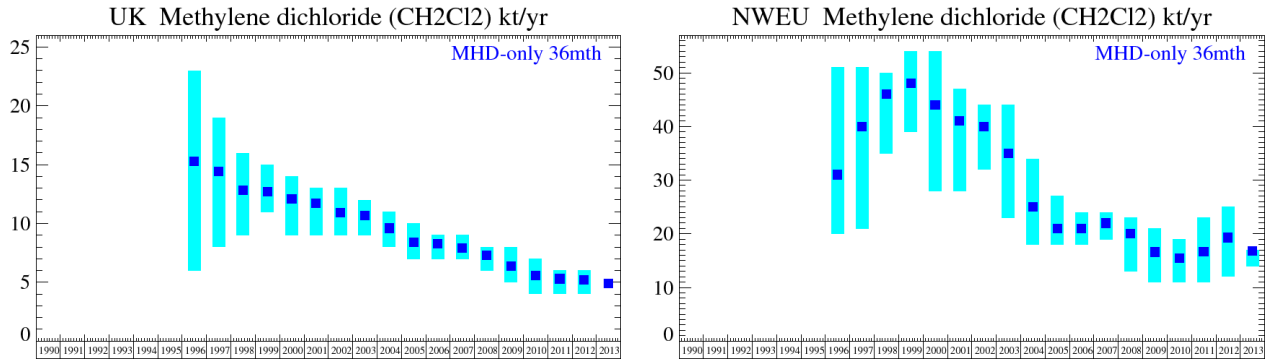

Figure 107: Emission estimates for UK and NWEU (MHD-only). The uncertainty bars represent the 5th and 95th percentiles.

Unit	Year	UK	(5th-95th)	NWEU	(5th-95th)

kt/y	1996	15.3	(6.- 23.)	31.	(20. -51.)
kt/y	1997	14.4	(8.- 19.)	40.	(21. -51.)
kt/y	1998	12.8	(9.- 16.)	46.	(35. -50.)
kt/y	1999	12.7	(11.- 15.)	48.	(39. -54.)
kt/y	2000	12.1	(9.- 14.)	44.	(28. -54.)
kt/y	2001	11.7	(9.-13.)	41.	(28.-.47)
kt/y	2002	10.9	(9.-13.)	40.	(32.-44.)
kt/y	2003	10.7	(9.-12.)	35.	(23.-44.)
kt/y	2004	9.6	(8.-11.)	25.	(18.-34.)
kt/y	2005	8.4	(7.-10.)	21.	(18.-27.)
kt/y	2006	8.3	(7.-9.)	21.	(18.-24.)
kt/y	2007	7.9	(7.-9.)	22.	(19.-24.)
kt/y	2008	7.3	(6.-8.)	20.	(13.-23.)
kt/y	2009	6.4	(5.-8.)	17.	(11.-21.)
kt/y	2010	5.6	(4.- 7.)	16.	(11. -19.)
kt/y	2011	5.3	(4.- 6.)	17.,	(11. -23.)
kt/y	2012	5.2	(4.- 6.)	19.	(12. -25.)
kt/y	2013	4.9	(5.- 5.)	17.	(14. -17.)

Table 51: Emission estimates for UK and NWEU with uncertainty (5^{th} – 95^{th} %ile).

6.16 $CHCl_3$ (chloroform)

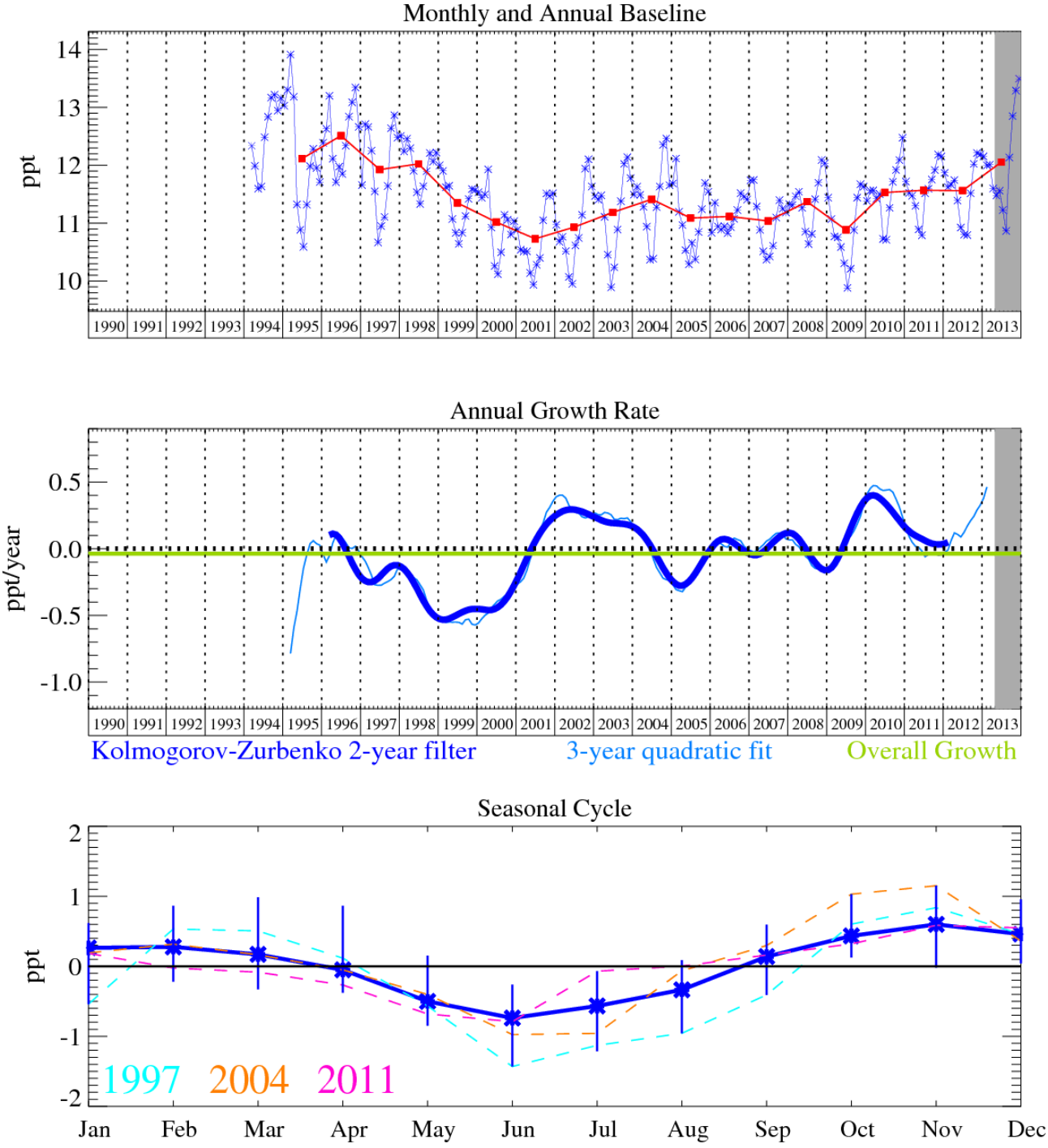

The grey area on each plot contains data that are unratified and therefore provisional.

Figure 108: $CHCl_3$: Monthly (blue) and annual (red) baseline mole fractions (top plot). Annual (blue) and overall average growth rate (green) (middle plot). Seasonal cycle (de-trended) with year-to-year variability (lower plot). Grey area covers un-ratified and therefore provisional data.

The statistical match between the modelled and observed time-series is consistently good. There has been a modest decline in emissions in the UK in line with the reduction in the magnitude of the average and maximum pollution event. NWEU emissions have remained broadly steady over the period.

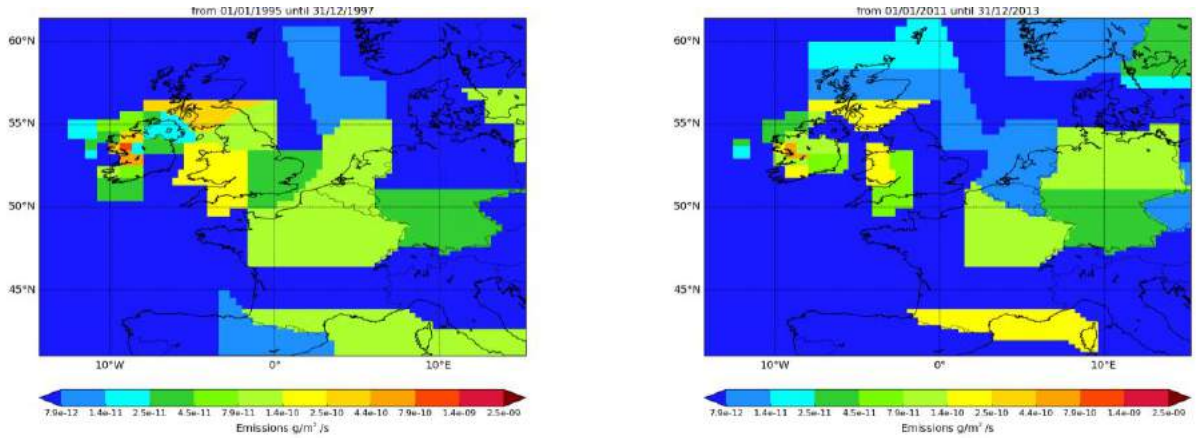

Figure 109: NAME-inversion emission estimates for 1995-1997 (left) and 2011-2013 (right). On the right hand side the emissions per grid box have been re-distributed based on population.

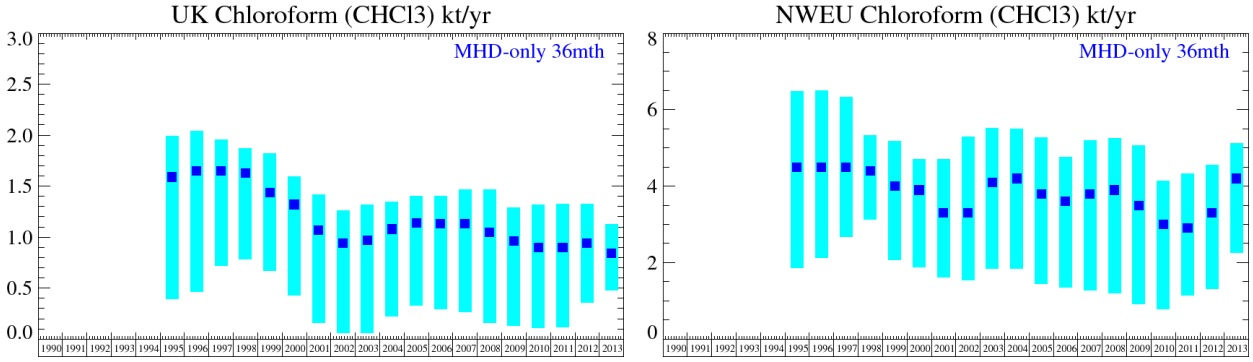

Figure 110: Emission estimates for UK and NWEU. The uncertainty bars represent the 5th and 95th percentiles.

Unit	Year	UK	(5th-95th)	NWEU	(5th-95th)
t/y	1995	1590.	(390.-1990.)	4500.	(1860.-6480.)
t/y	1996	1650.	(460.-2040.)	4500.	(2130.-6500.)
t/y	1997	1650.	(720.-1960.)	4500.	(2680.-6330.)
t/y	1998	1630.	(790.-1870.)	4400.	(3140.-5330.)
t/y	1999	1440.	(670.-1830.)	4000.	(2070.-5170.)
t/y	2000	1320.	(430.-1600.)	3900.	(1880.-4710.)
t/y	2001	1070.	(160.-1420.)	3300.	(1610.-4700.)
t/y	2002	940.	(60.-1260.)	3300.	(1530.-5300.)
t/y	2003	970.	(60.-1320.)	4100.	(1850.-5510.)
t/y	2004	1080.	(230.-1350.)	4200.	(1850.-5500.)
t/y	2005	1140.	(330.-1400.)	3800.	(1440.-5270.)
t/y	2006	1130.	(300.-1400.)	3600.	(1360.-4760.)
t/y	2007	1130.	(270.-1470.)	3800.	(1270.-5200.)
t/y	2008	1050.	(160.-1470.)	3900.	(1200.-5250.)
t/y	2009	960.	(130.-1290.)	3500.	(910.-.5060)
t/y	2010	900.	(110.-1320.)	3000.	(790.-4130.)
t/y	2011	900.	(120.-1330.)	2900.	(1150.-4330.)
t/y	2012	940.	(360.-1330.)	3300.	(1310.-4550.)
t/y	2013	840.	(480.-1130.)	4200.	(2260.-5120.)

Table 52: Emission estimates for UK and NWEU with uncertainty (5th – 95th %ile).

6.17 CCl_4 (carbon tetrachloride)

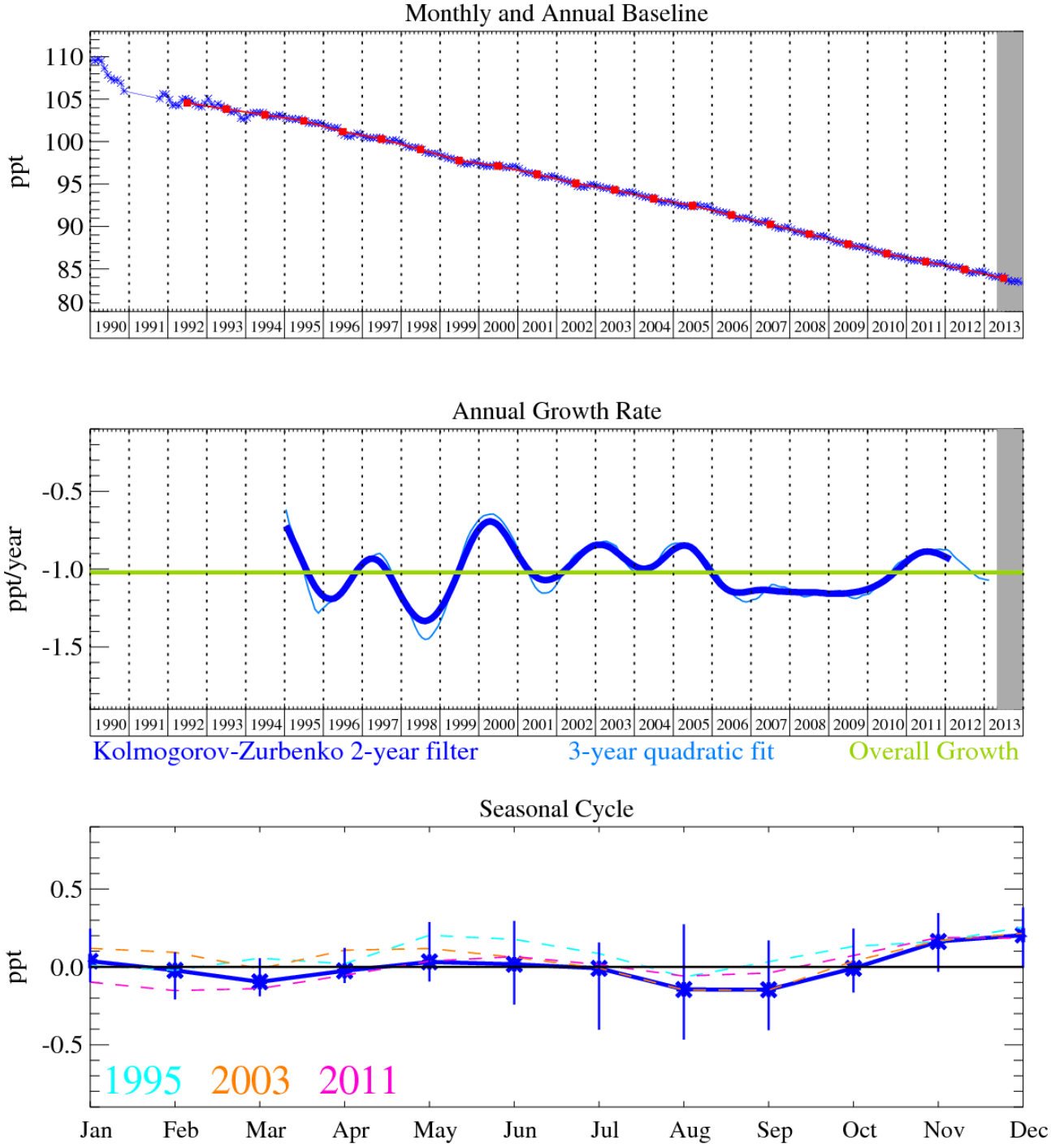

Figure 111: CCl_4: Monthly (blue) and annual (red) baseline mole fractions (top plot). Annual (blue) and overall average growth rate (green) (middle plot). Seasonal cycle (de-trended) with year-to-year variability (lower plot). Grey area covers un-ratified and therefore provisional data.

Figure 111 illustrates the steady downward trend of CCl_4 (26 year lifetime [*Montzka et al.*, 2011]), currently -1.1 ppt/yr, making this compound the second most rapidly decreasing chlorocarbon after CH_3CCl_3. The level of CCl_4 at Mace Head in December 2013 was 83.4 ppt. Its major use was as a feedstock for CFC manufacturing and unlike CH_3CCl_3 a significant inter-hemispheric CCl_4 gradient still exists, resulting from a persistence of significant northern hemisphere (NH) emissions. It is interesting that atmospheric observations for this compound are decreasing less rapidly than projected in the A1 scenario of the Ozone Assessment [Daniel and Velders *et al.*, 2007]. CCl_4 emissions derived from atmospheric observations (top-down) suggest substantially smaller emissions than those derived from bottom-up techniques using reported production, feedstock and

destruction data. The reason for this discrepancy was the subject of a study in the recent WMO SPARC report [Ko et al., 2013].

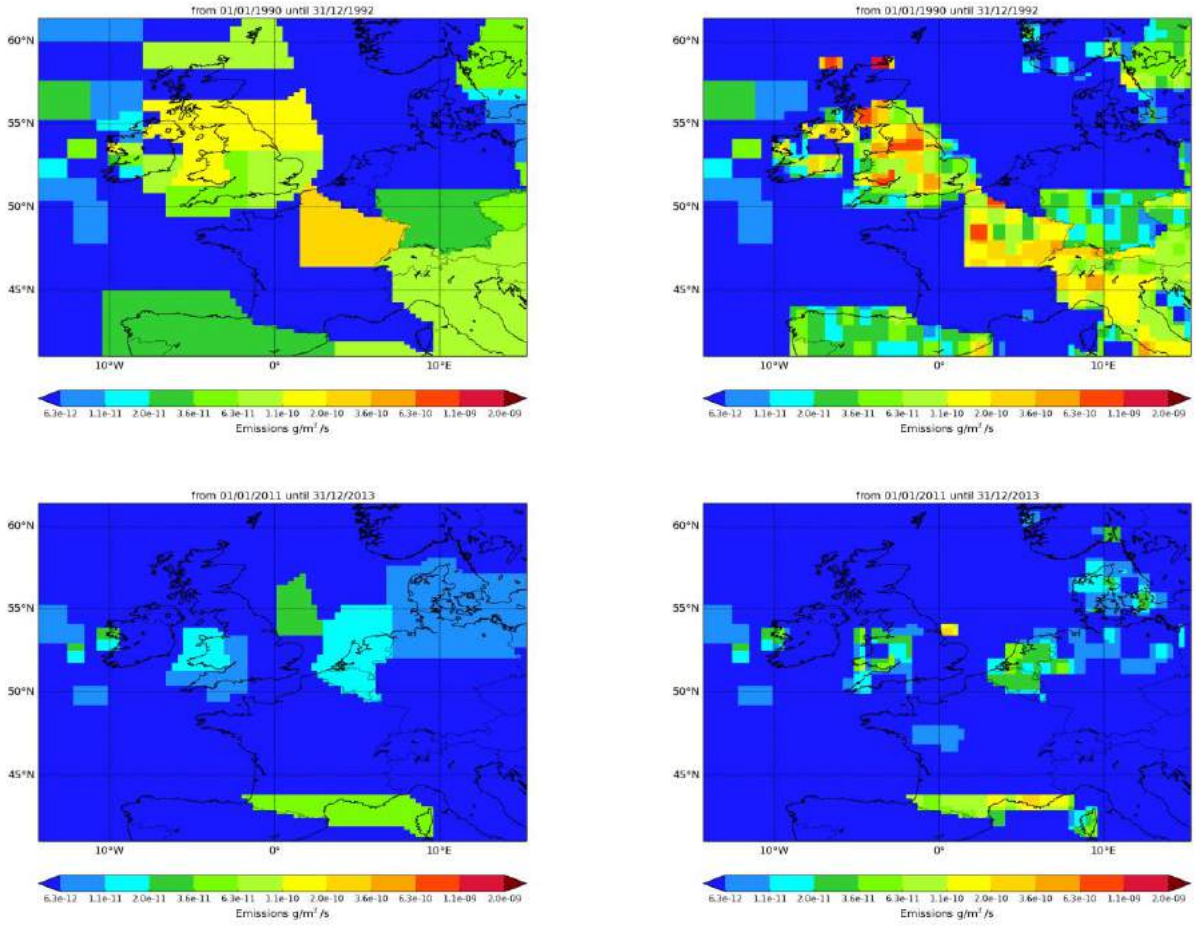

Figure 112: NAME-inversion emission estimates for 1990-1992 (upper) and 2011-2013 (lower). On the right hand side the emissions per grid box have been re-distributed based on population.

The magnitude of the pollution events reaching Mace Head have fallen very significantly from 1990 reflecting the impact of the Montreal Protocol and the strong decline in emissions across NWEU. The pollution events are now poorly resolved against the uncertainty in the baseline leading to a poor correlation between the model time-series and the observations in the latter years.

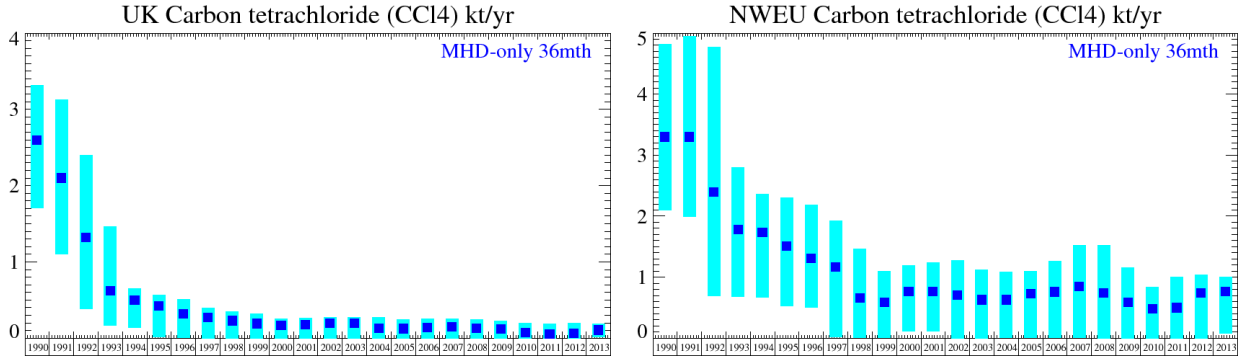

Figure 113: Emission estimates for UK and NWEU. The uncertainty bars represent the 5th and 95th percentiles.

Unit	Year	UK	(5th-95th)	NWEU	(5th-95th)
t/y	1990	2600.	(1700.-3320.)	3300.	(2100.-4820.)
t/y	1991	2100.	(1100.-3130.)	3300.	(2000.-4960.)
t/y	1992	1320.	(380.-2400.)	2400.	(690.-4770.)
t/y	1993	620.	(170.-1470.)	1780.	(680.-2790.)
t/y	1994	500.	(140.- 650.)	1730.	(670.-2360.)
t/y	1995	420.	(10.- 570.)	1510.	(530.-2310.)
t/y	1996	320.	(10.- 510.)	1310.	(510.-2180.)
t/y	1997	270.	(0.- 400.)	1170.	(20.-1930.)
t/y	1998	230.	(0.- 350.)	660.	(0.-1460.)
t/y	1999	190.	(0.- 330.)	590.	(0.-1100.)
t/y	2000	170.	(0.- 260.)	770.	(110.-1200.)
t/y	2001	180.	(0.- 260.)	770.	(110.-1240.)
t/y	2002	200.	(0.- 280.)	710.	(0.-1280.)
t/y	2003	200.	(0.- 280.)	630.	(0.-1120.)
t/y	2004	130.	(0.- 270.)	630.	(0.-1080.)
t/y	2005	130.	(0.- 240.)	730.	(0.-1100.)
t/y	2006	140.	(0.- 250.)	760.	(0.-1270.)
t/y	2007	150.	(0.- 260.)	850.	(0.-1520.)
t/y	2008	130.	(0.- 250.)	740.	(0.-1520.)
t/y	2009	120.	(0.- 230.)	590.	(0.-1150.)
t/y	2010	70.	(0.- 200.)	480.	(0.- 830)
t/y	2011	50.	(0.- 190.)	500.	(0.-1010.)
t/y	2012	60.	(0.- 200.)	740.	(0.-1040.)
t/y	2013	110.	(1.- 190.)	770.	(70.-1000.)

Table 53: Emission estimates for UK and NWEU with uncertainty (5^{th} – 95^{th} %ile).

6.18 CH_3CCl_3 (methyl chloroform)

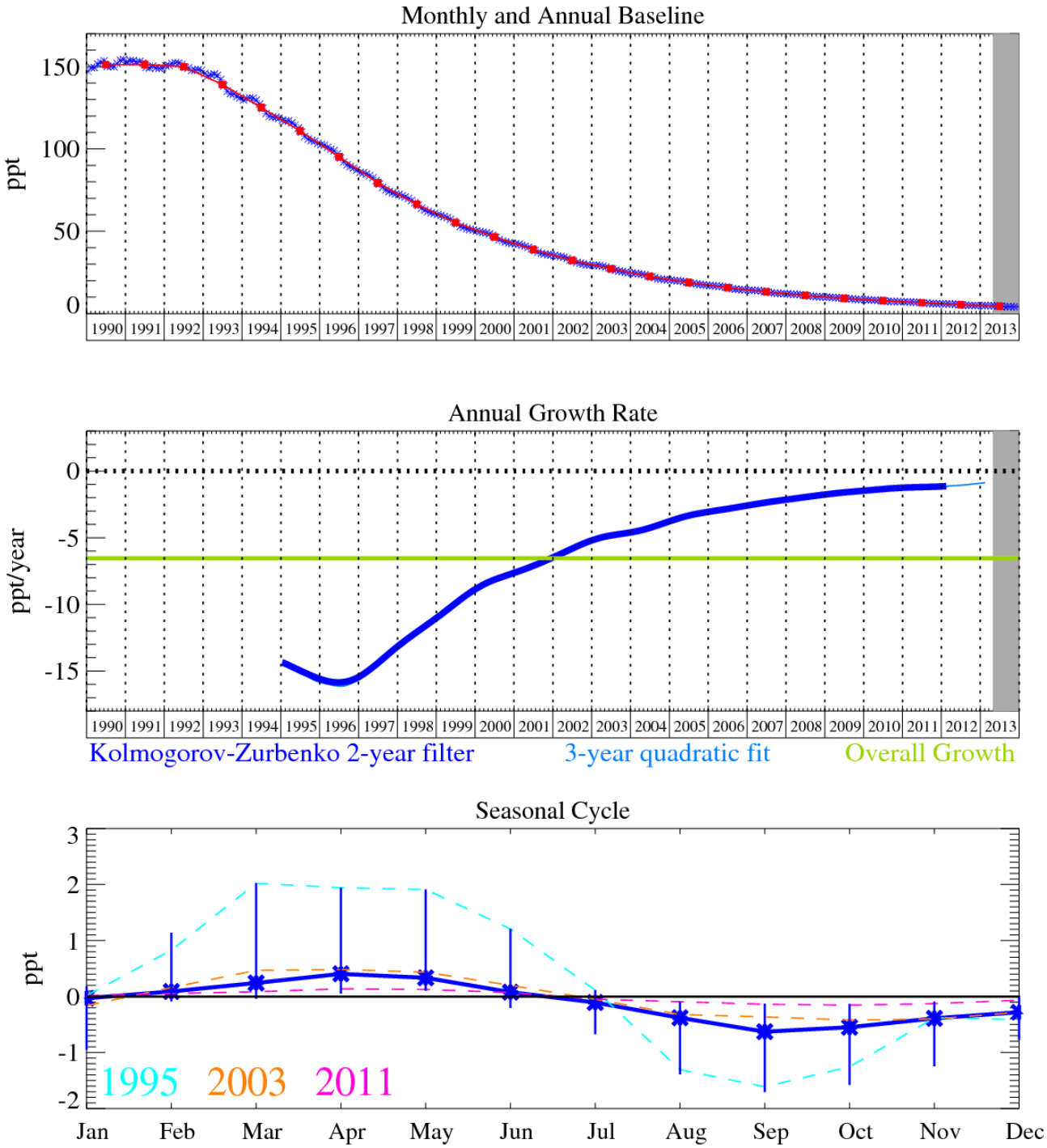

Figure 114: CH_3CCl_3: Monthly (blue) and annual (red) baseline mole fractions (top plot). Annual (blue) and overall average growth rate (green) (middle plot). Seasonal cycle (de-trended) with year-to-year variability (lower plot). Grey area covers un-ratified and therefore provisional data.

The major solvent methyl chloroform (CH_3CCl_3) is an important compound because of its use to estimate concentrations of the hydroxyl radical (OH), which is the major sink species for CH_4, HFCs and HCFCs. The global atmospheric CH_3CCl_3 concentration peaked in 1992 (Prinn *et al*., 2000) then declined in accordance with its short atmospheric lifetime (5.04 years [*Ko et al.*, 2013]) and phase out under the terms of the Montreal protocol. The baseline mole fraction of CH_3CCl_3 at Mace Head (Figure 114) is currently decreasing by 0.9 ppt/yr and reached a mixing ratio of 4.1 ppt in December 2013. The GWP_{100} of methyl chloroform is 146.

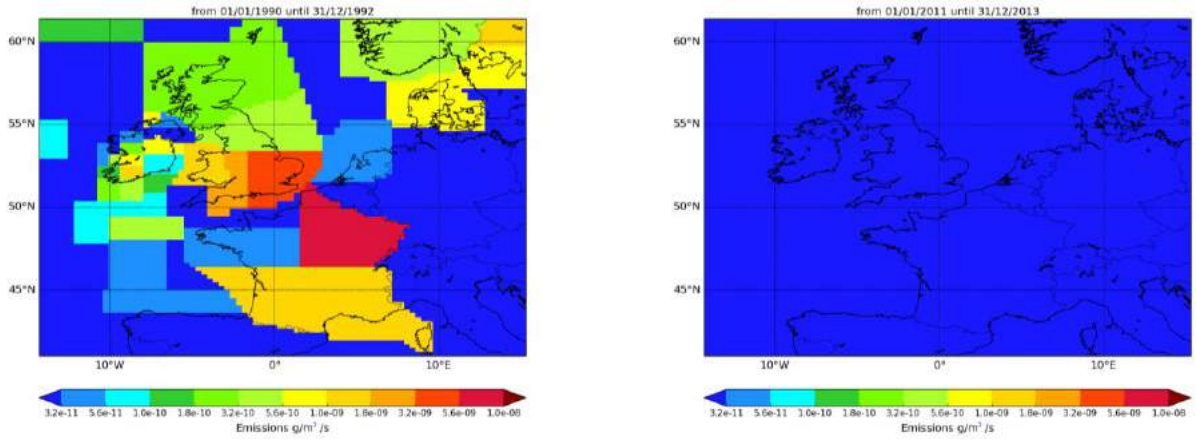

Figure 115: NAME-inversion emission estimates for 1990-1992 (left) and 2011-2013 (left).

Like carbon tetrachloride, the magnitude of the pollution events reaching Mace Head have fallen very significantly from 1990 reflecting the impact of the Montreal Protocol and the strong decline in emissions across NWEU. The pollution events are now poorly resolved against the uncertainty in the baseline leading to a poor correlation between the model time-series and the observations in the latter years.

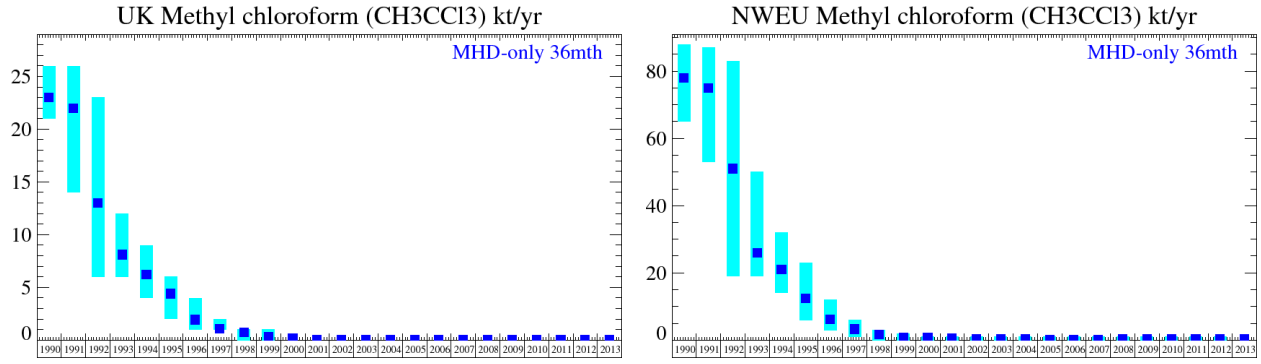

Figure 116: Emission estimates for UK and NWEU. Uncertainty bars are 5th and 95th percentiles.

Unit	Year	UK	(5th-95th)	NWEU	(5th-95th)
kt/y	1990	23.	(21.- 26.)	78.	(65. -88.)
kt/y	1991	22.	(14.- 26.)	75.	(53. -87.)
kt/y	1992	13.	6.- 23.)	51.	(19. -83.)
kt/y	1993	8.1	(6.- 12.)	26.	(19. -50.)
kt/y	1994	6.2	(4.- 9.)	21.	(14. -32.)
kt/y	1995	4.4	(2.- 6.)	12.4	(6. -23.)
kt/y	1996	1.9	(1.- 4.)	6.2	(3. -12.)
kt/y	1997	1.1	(1.- 2.)	3.3	(1. - 6.)
kt/y	1998	0.7	(0.- 1.)	1.6	(0. - 3.)
kt/y	1999	0.3	(0.- 1.)	0.8	(0. - 2.)
kt/y	2000	0.2	(0.- 0.)	0.7	(0. - 1.)
kt/y	2001 onwards	0.02- 0.07	(0.- 0.)	0.2-0.7	(0. - 1.)

Table 54: Emission estimates for UK and NWEU with uncertainty (5th – 95th %ile).

6.19 $CHClCCl_2$ (TCE)

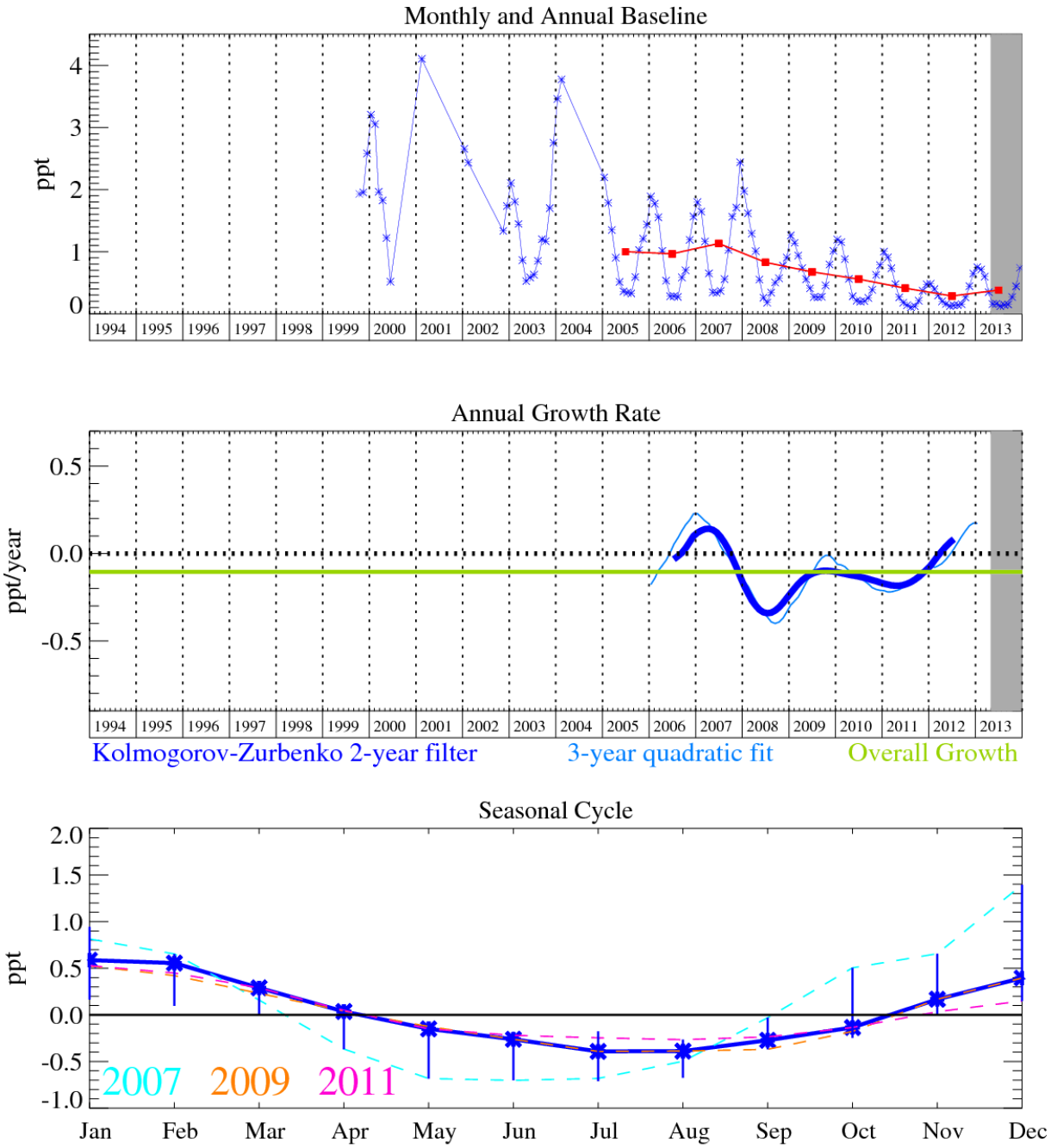

Figure 117: $CHClCCl_2$: Monthly (blue) and annual (red) baseline mole fractions (top plot). Annual (blue) and overall average growth rate (green) (middle plot). Seasonal cycle (de-trended) with year-to-year variability (lower plot). Grey area covers un-ratified and therefore provisional data.

The major source of trichloroethylene (C_2HCl_3) is from industrial usage as a degreasing agent. All but about 2% of the sales are in the NH. The main removal process is via reaction with OH. It has an atmospheric lifetime of 4.9 days [*Montzka et al.*, 2011] with this lifetime resulting in a low GWP_{100} of approximately 5 [*UNEP (United Nations Environment Program)*, 2003]. C_2HCl_3 can also undergo reductive de-chlorination to 1,2-dichloroethylene through the activity of soil microbes. Natural sources of C_2HCl_3 are from the oceans and seawater algae. It has been reported that salt lakes are also a natural source of C_2HCl_3 due to the microbial activity of halobacteria [*Weissflog et al.*, 2005]. The magnitude of pollution events at Mace Head have declined sharply since records began.

6.20 CCl_2CCl_2

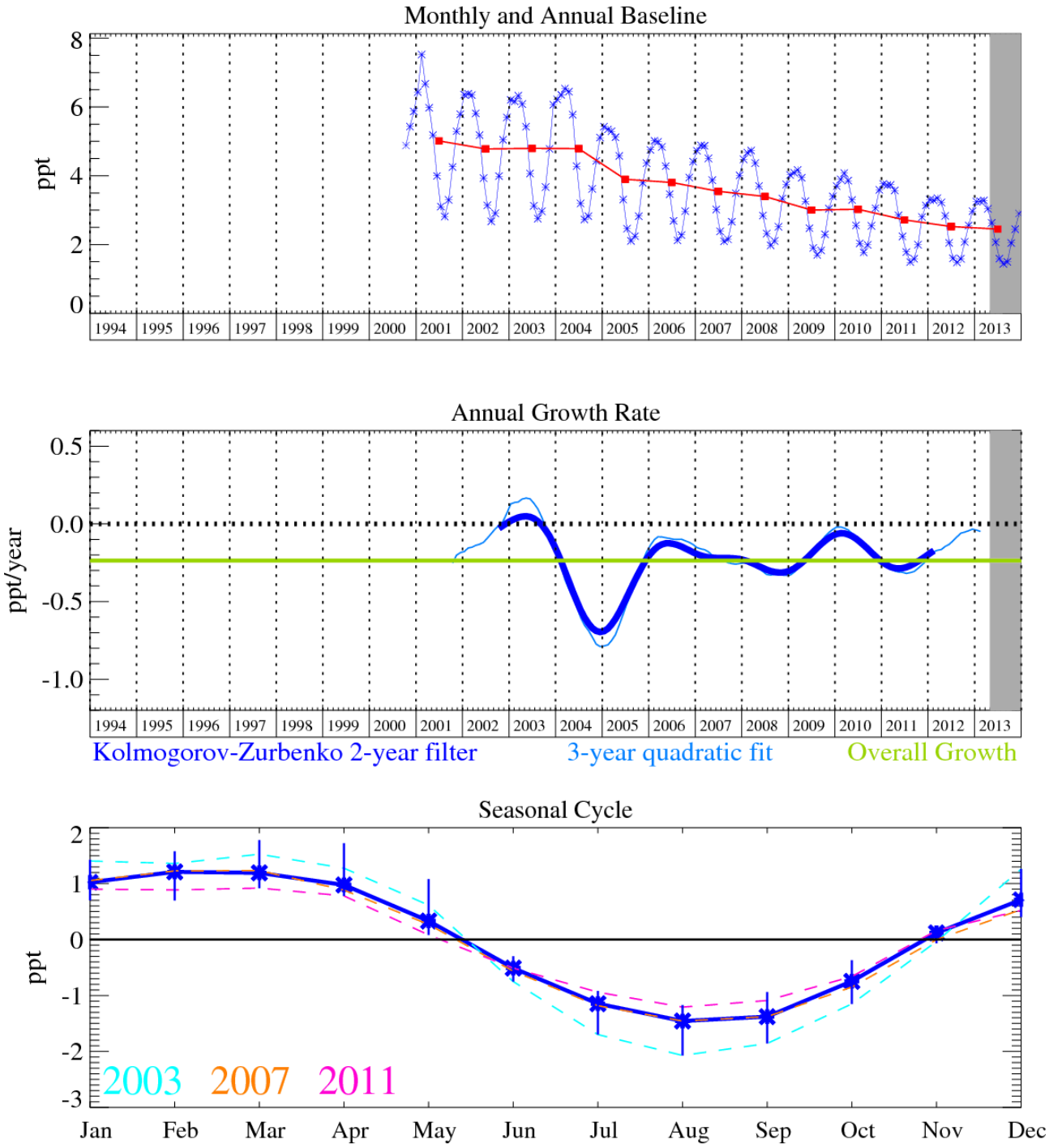

Figure 118: CCl_2CCl_2: Monthly (blue) and annual (red) baseline mole fractions (top plot). Annual (blue) and overall average growth rate (green) (middle plot). Seasonal cycle (de-trended) with year-to-year variability (lower plot). Grey area covers un-ratified and therefore provisional data.

Perchloroethylene (C_2Cl_4) is mainly used for dry cleaning and as a metal degreasing solvent. Small but significant quantities of C_2Cl_4 are emitted in the flue gas from coal-fired power plants. The atmospheric lifetime of C_2Cl_4 is 90 days [*Montzka et al.*, 2011] and its primary atmospheric sink is reaction with OH. Its December 2012 atmospheric mole fraction was 2.9 ppt with a trend currently decreasing at the rate of less than 0.1 ppt/yr (Figure 118). The short lifetime of perchloroethylene results in a GWP_{100} of approximately 12 [*UNEP (United Nations Environment Program)*, 2003].

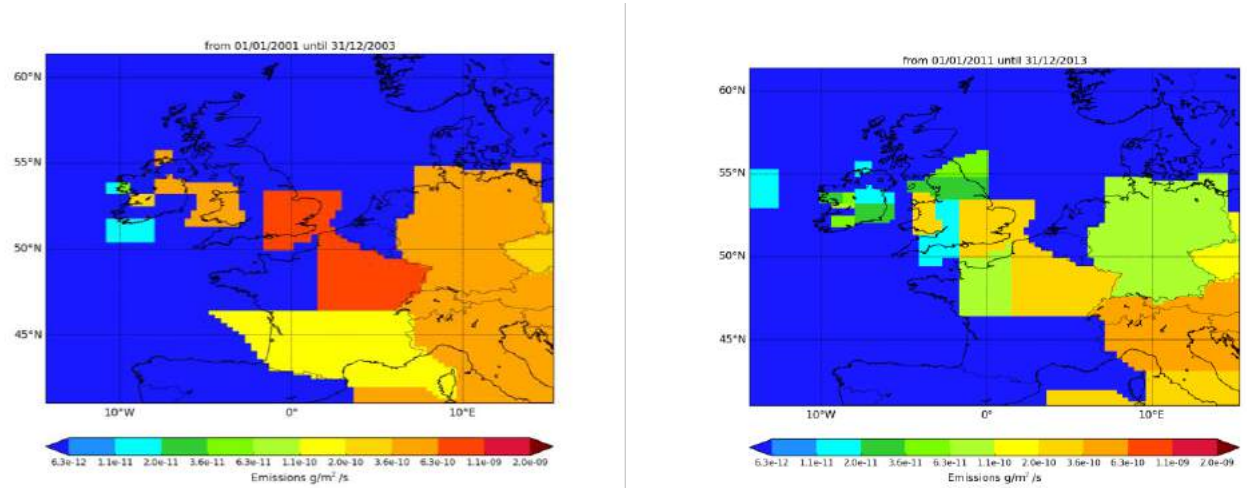

Figure 119: NAME-inversion emission estimates for 2001-2003 (left) and 2011-2013 (right).

The statistical match between the model time-series and the observations is good. The magnitude of the pollution events has declined steeply since 2001, a trend matched in the UK and NWEU estimated emissions.

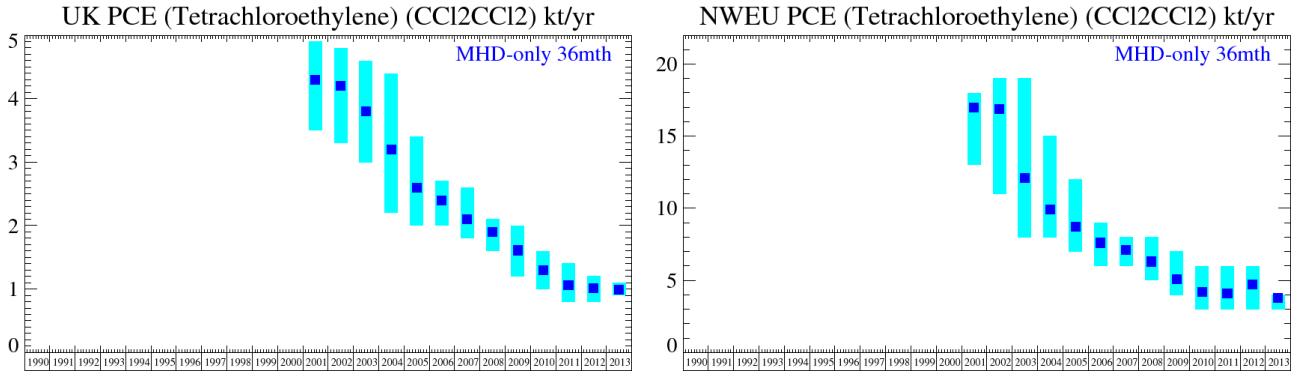

Figure 120: Emission estimates for UK and NWEU. The uncertainty bars represent the 5th and 95th percentiles.

Unit	Year	UK	(5th-95th)	NWEU	(5th-95th)
kt/y	2001	4.3	(3.5- 4.9)	17.0	(13. -18.)
kt/y	2002	4.2	(3.3- 4.8)	16.9	(11. -19.)
kt/y	2003	3.8	(3.0- 4.6)	12.1	(8. -19.)
kt/y	2004	3.2	(2.2- 4.4)	9.9	(8. -15.)
kt/y	2005	2.6	(2.0- 3.4)	8.7	(7. -12.)
kt/y	2006	2.4	(2.0- 2.7)	7.6	(6. - 9.)
kt/y	2007	2.1	(1.8- 2.6)	7.1	(6. - 8.)
kt/y	2008	1.9	(1.6- 2.1)	6.3	(5. - 8.)
kt/y	2009	1.6	(1.2- 2.0)	5.1	(4. - 7.)
kt/y	2010	1.3	(1.0- 1.6)	4.2	(3. - 6.)
kt/y	2011	1.1	(0.8- 1.4)	4.1	(3. - 6.)
kt/y	2012	1.0	(0.8- 1.2)	4.7	(3. - 6.)
kt/y	2013	1.0	(0.9- 1.1)	3.8	(3. - 4.)

Table 55: Emission estimates for UK and NWEU with uncertainty (5th – 95th %ile).

6.21 Methyl bromide (CH_3Br)

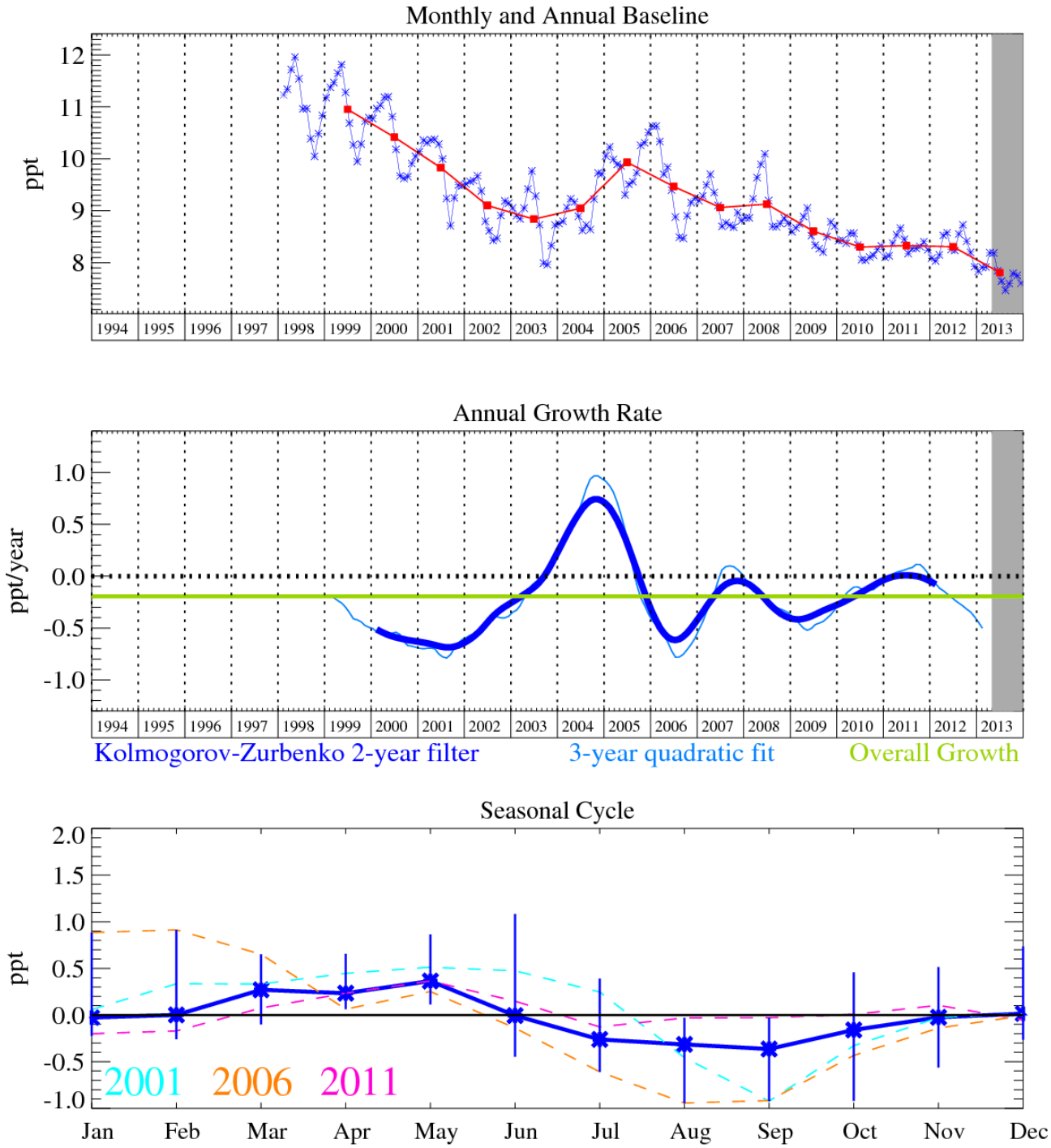

Figure 121: Methyl bromide: Monthly (blue) and annual (red) baseline (top plot). Annual (blue) and overall average growth rate (green) (middle plot). Seasonal cycle (de-trended) with year-to-year variability (lower plot). Grey area covers un-ratified and therefore provisional data.

The instrument change in 2005 to the Medusa system produced a discontinuity in the methyl bromide record and should be discounted (Figure 121).

6.22 Halon-1211

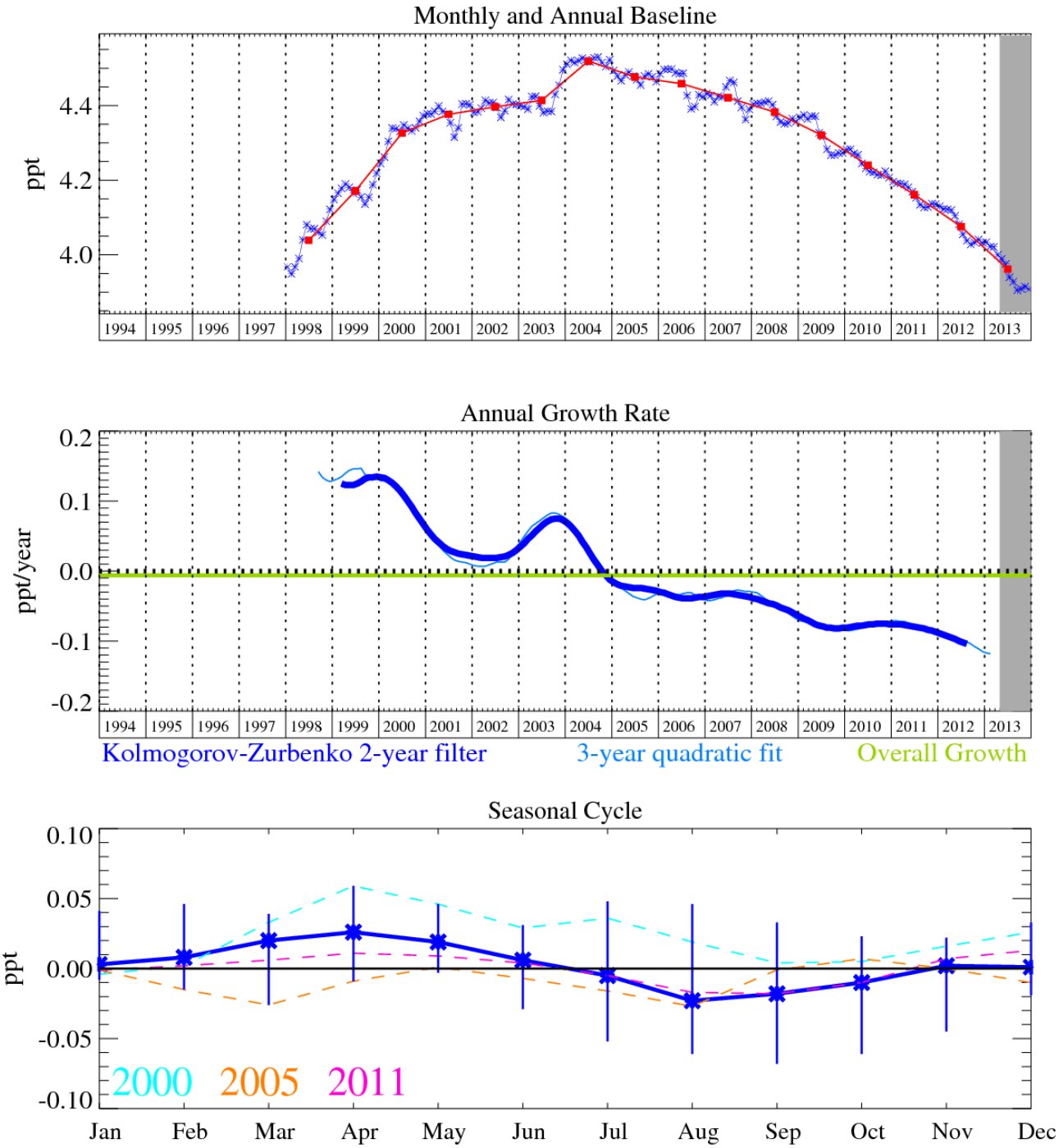

Figure 122: Halon-1211 ($CBrClF_2$): Monthly (blue) and annual (red) baseline (top plot). Annual (blue) and overall average growth rate (green) (middle plot). Seasonal cycle (de-trended) with year-to-year variability (lower plot). Grey area covers un-ratified and therefore provisional data.

Halon-1211 ($CBrClF_2$) shown in Figure 122, continues to show a current reduction of 0.11 ppt/yr due to limits imposed on halon production in developed nations. Levels of halon-1211 at Mace Head were 3.9 ppt at the end of December 2013. Halon-1211 has an atmospheric lifetime of 16 years,

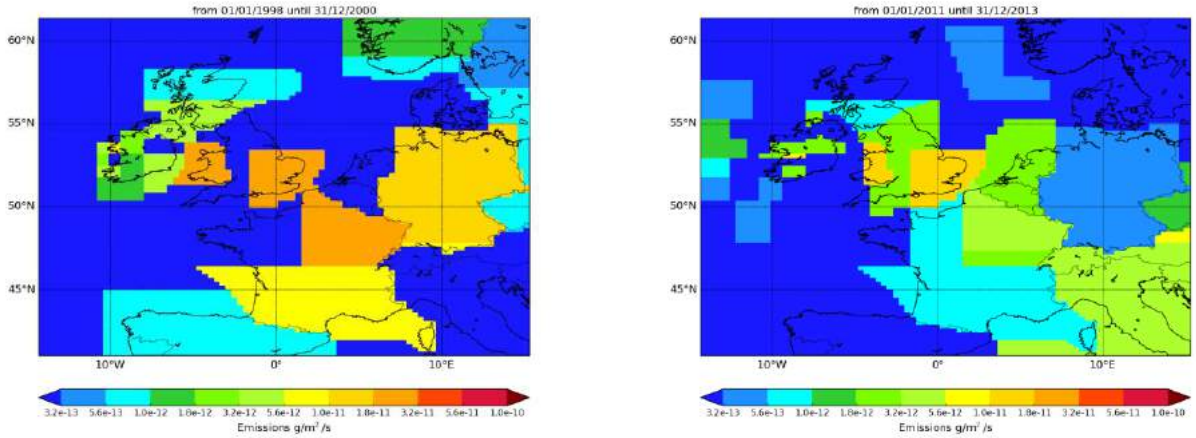

Figure 123: NAME-inversion emission estimates for 1998-2000 (left) and 2011-2013 (right).

The UK and NWEU estimated emissions of halon-1211 have declined steadily since 1998, a trend seen in the magnitude of the pollution events seen at Mace Head.

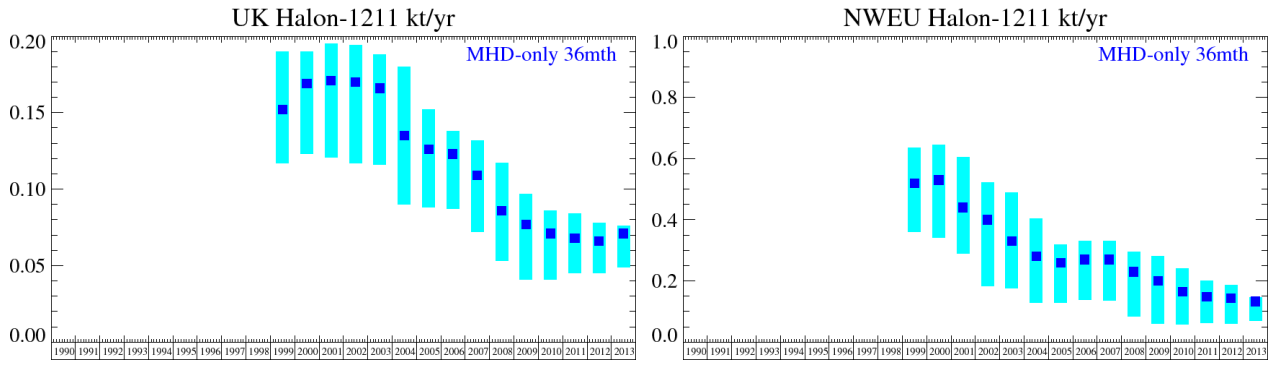

Figure 124: Emission estimates for UK and NWEU. The uncertainty bars represent the 5th and 95th percentiles.

Unit	Year	UK	(5th-95th)	NWEU	(5th-95th)
t/y	1999	152.	(117.- 190.)	520.	(361. -636.)
t/y	2000	169.	(123.- 190.)	530.	(341. -646.)
t/y	2001	171.	(121.- 195.)	440.	(289. -604.)
t/y	2002	170.	(117.- 194.)	400.	(183. -521.)
t/y	2003	166.	(116.- 188.)	330.	(176. -488.)
t/y	2004	135.	(90.- 180.)	280.	(128. -403.)
t/y	2005	126.	(88.- 152.)	260.	(128. -318.)
t/y	2006	123.	(87.- 138.)	270.	(139. -330.)
t/y	2007	109.	(72.- 132.)	270.	(136. -330.)
t/y	2008	86.	(53.- 117.)	230.	(84. -295.)
t/y	2009	77.	(41.- 97.)	200.	(60. -281.)
t/y	2010	71.	(41.- 86.)	164.	(58. -241.)
t/y	2011	68.	(45.- 84.)	148.	(63. -201.)
t/y	2012	66.	(45.- 78.)	143.	(61. -187.)
t/y	2013	71.	(49.- 76.)	133.	(70. -147.)

Table 56: Emission estimates for UK and NWEU with uncertainty (5th – 95th %ile).

6.23 Halon-1301

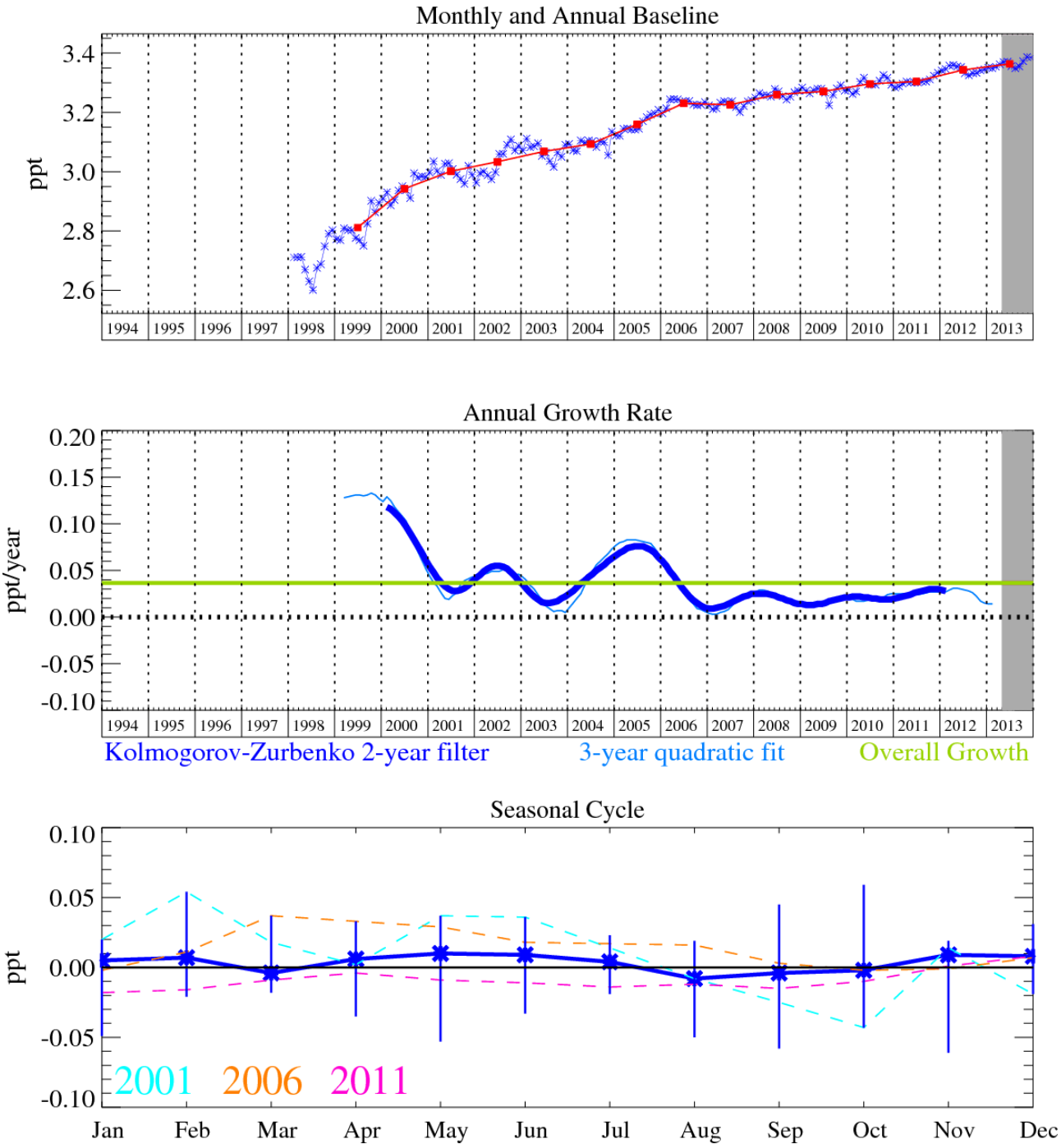

Figure 125: Halon-1301 ($CBrF_3$): Monthly (blue) and annual (red) baseline (top plot). Annual (blue) and overall average growth rate (green) (middle plot). Seasonal cycle (de-trended) with year-to-year variability (lower plot). Grey area covers un-ratified and therefore provisional data.

The halon-1301 ($CBrF_3$) mole fraction shown in Figure 125 is very slightly growing and by December 2013 had reached 3.39 ppt in the background atmosphere at Mace Head. Halon-1301 has an atmospheric lifetime of 65 years. The main source of halon emissions are from stockpiles and banks, where bank-related emissions (in-use emissions) are thought to account for a large majority of the current emissions.

The magnitude of the pollution events relative to the estimated noise in the baseline is very small and so the uncertainty in the InTEM emission estimates is very significant. The data suggests there has been a decline in emissions over the UK and NWEU, certainly the magnitude of the pollution events are smaller now than a decade ago.

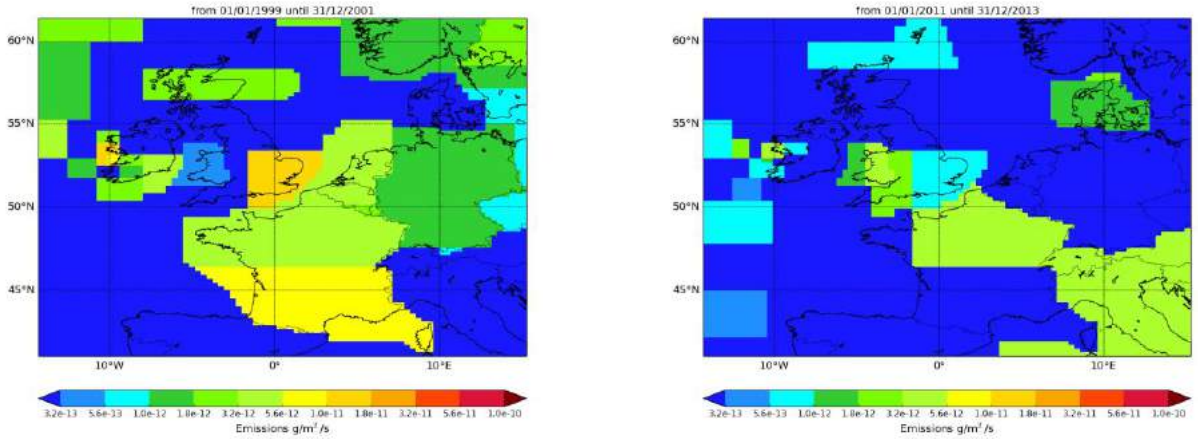

Figure 126: NAME-inversion emission estimates for 1999-2001 (left) and 2011-2013 (right).

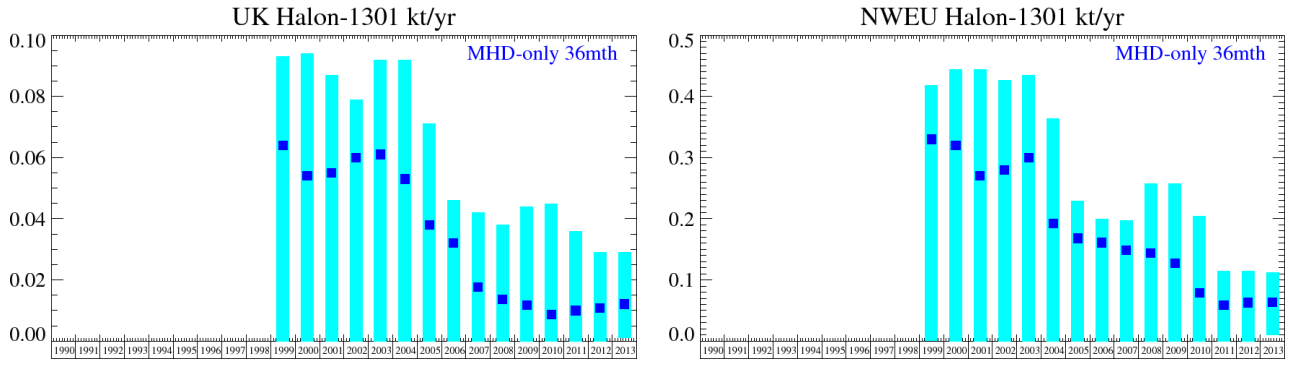

Figure 127: Emission estimates for UK and NWEU (MHD-only). The uncertainty bars represent the 5th and 95th percentiles.

Unit	Year	UK	(5th-95th)	NWEU	(5th-95th)
t/y	1999	64.	(0.- 93.)	330.	(1. -418.)
t/y	2000	54.	(0.- 94.)	320.	(0. -444.)
t/y	2001	55.	(0.- 87.)	270.	(0. -444.)
t/y	2002	60.	(0.- 79.)	280.	(0. -427.)
t/y	2003	61.	(0.- 92.)	300.	(0. -435.)
t/y	2004	53.	(0.- 92.)	192.	(0. -364.)
t/y	2005	38.	(0.- 71.)	168.	(0. -229.)
t/y	2006	32.	(0.- 46.)	161.	(0. -200.)
t/y	2007	18.	(0.- 42.)	149.	(0. -197.)
t/y	2008	14.	(0.- 38.)	144.	(0. -258.)
t/y	2009	12.	(0.- 44.)	127.	(0. -258.)
t/y	2010	9.	(0.- 45.)	79.	(0. -204.)
t/y	2011	10.	(0.- 36.)	59.	(0. -115.)
t/y	2012	11.	(0.- 29.)	63.	(0. -115.)
t/y	2013	12.	(1.- 29.)	64.	(10. -112.)

Table 57: Emission estimates for UK and NWEU with uncertainty (5th – 95th %ile).

6.24 Halon-2402

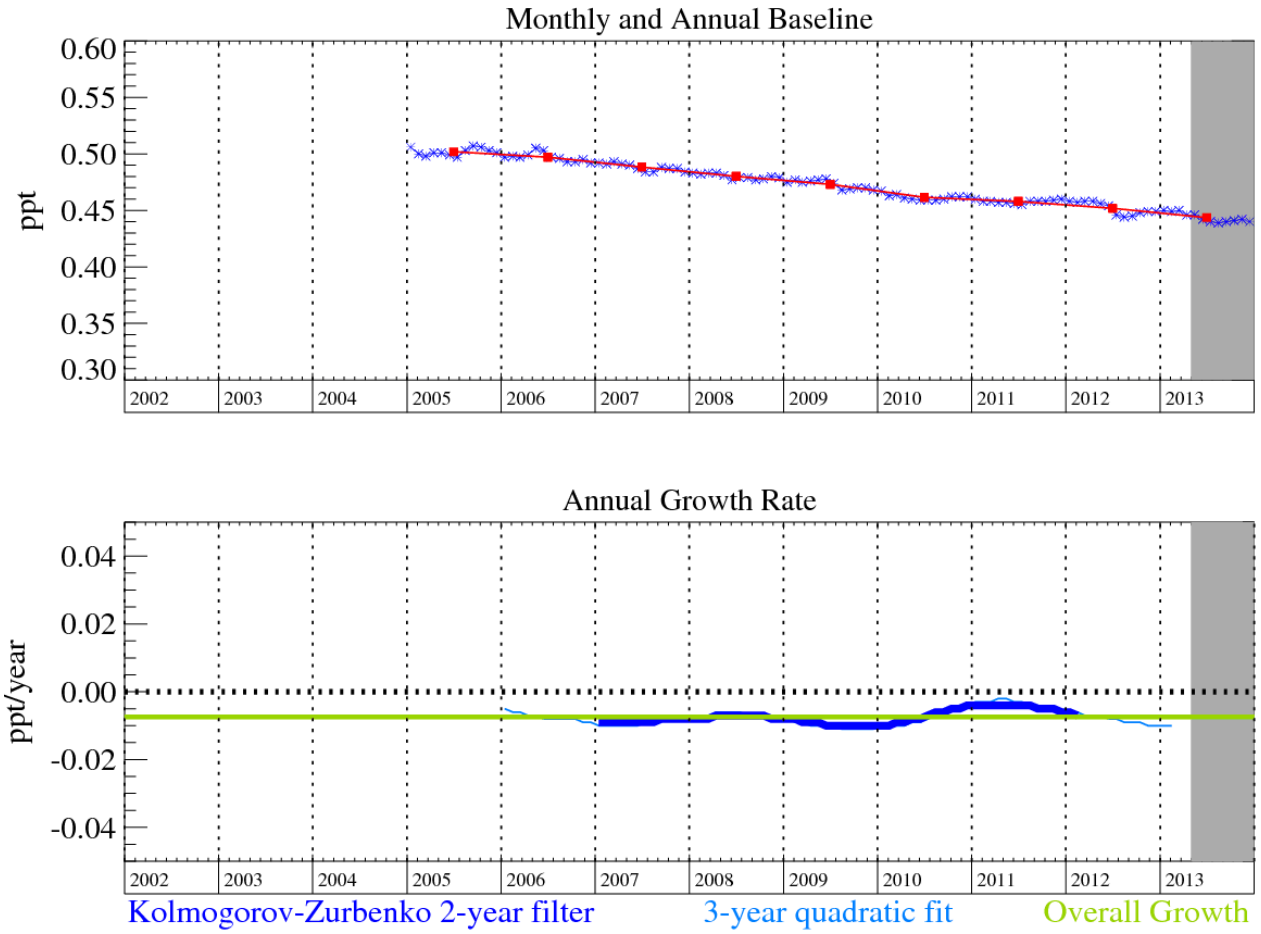

Figure 128: Halon-2402 ($C_2Br_2F_4$): Monthly (blue) and annual (red) baseline (top plot). Annual (blue) and overall average growth rate (green) (middle plot). Seasonal cycle (de-trended) with year-to-year variability (lower plot). Grey area covers un-ratified and therefore provisional data.

Halon-2402 ($C_2Br_2F_4$): (20 year lifetime) was used predominantly in the former Soviet Union. No information on the production of halon-2402 before 1986 has been found. Fraser *et al.*, (1999) developed emission projections for halon-2402 based on atmospheric measurements. They reported that the emissions grew steadily in the 1970s and 1980s, peaking in the 1988-91 timeframe at 1.7 Gg/yr and found these results to be qualitatively consistent with the peak production of 28,000 ODP tonnes reported by the Russian Federation under Article VII of the Montreal Protocol (or assuming all production was halon-2402 and an ODP of 6, a peak production of approximately 4.650 Gg/yr). Measurements at Mace Head indicate that the levels of halon-2402 are very slowly falling (-0.11 ppt/yr) in the atmosphere and that there is no discernible seasonal cycle. The baseline level in December 2013 was estimated to be 0.44 ppt, however the error bars associated with the measurement are significant. This magnitude of reduction is consistent with declines in global surface mixing ratios reported in the 2010 WMO Ozone Assessment.

6.25 Ethane (C_2H_6)

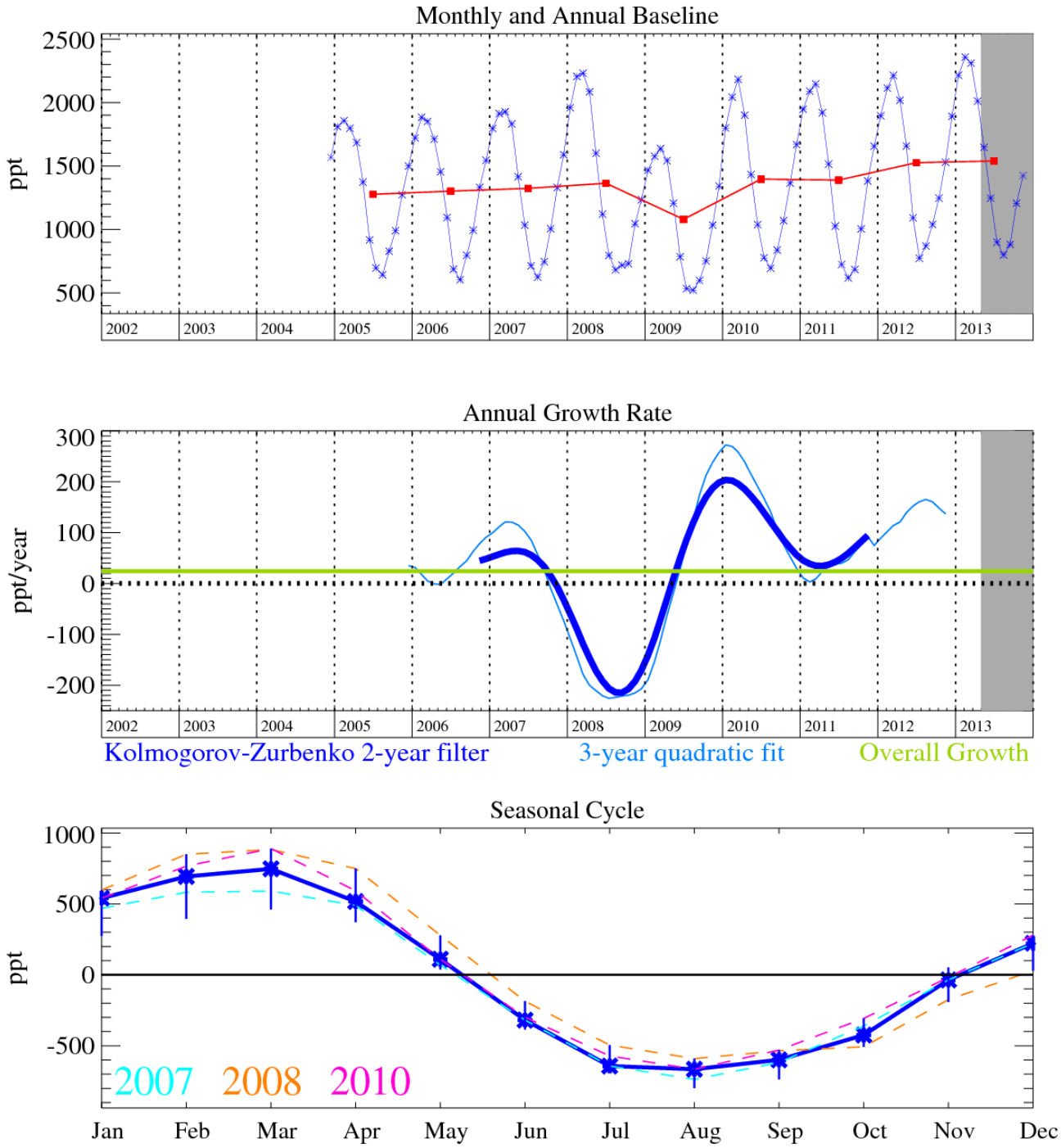

Figure 129: Ethane (C_2H_6): Monthly (blue) and annual (red) baseline (top plot). Annual (blue) and overall average growth rate (green) (middle plot). Seasonal cycle (de-trended) with year-to-year variability (lower plot). Grey area covers un-ratified and therefore provisional data.

Ethane (C_2H_6) has a very pronounced seasonal cycle with an amplitude of over 1.3 ppb. The overall growth rate since 2006 is positive although there have been large swings from negative (2008) to positive (2010) growth. Ethane emissions are strongly linked to anthropogenic emissions of carbon dioxide and can be used in a similar way to carbon monoxide to estimate carbon dioxide emissions through the ratio method. The UK emissions of ethane have remained somewhat static at around 60 kt/yr although the uncertainties are large.

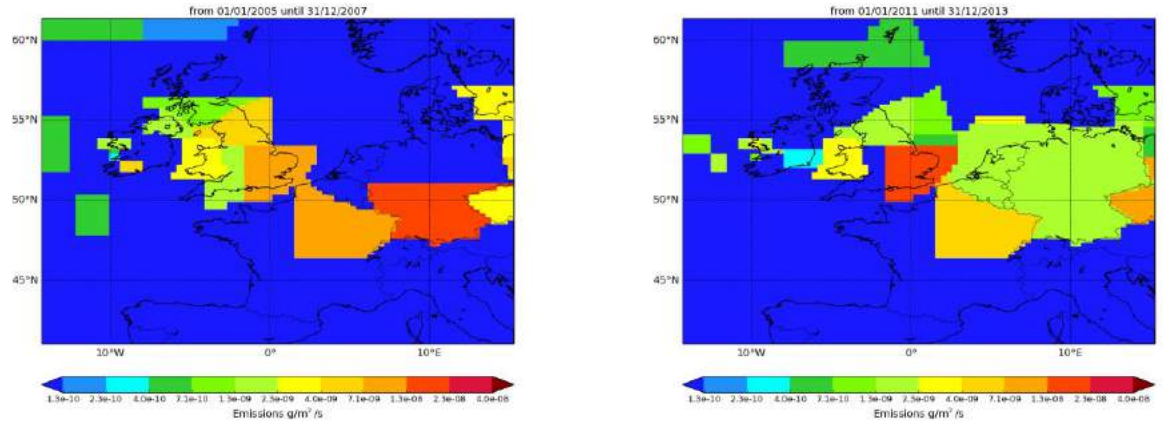

Figure 130: NAME-inversion emission estimates for 1999-2001 (left) and 2011-2013 (right).

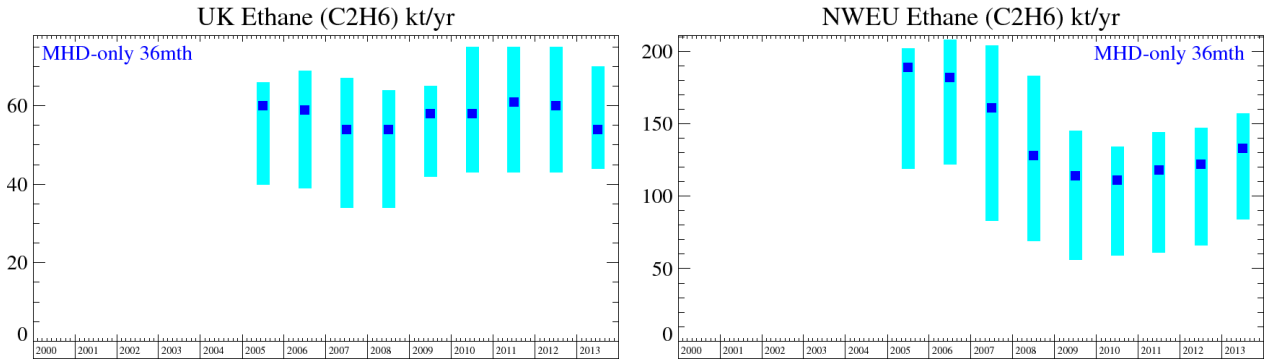

Figure 131: Emission estimates for UK and NWEU (MHD-only). The uncertainty bars represent the 5th and 95th percentiles.

Unit	Year	UK	(5th-95th)	NWEU	(5th-95th)
kt/y	2005	60	(40.- 66.)	189	(119. -202.)
kt/y	2006	59	(39.- 69.)	182	(122. -208.)
kt/y	2007	54	(34.- 67.)	161	(83. -204.)
kt/y	2008	54	(34.- 64.)	128	(69. -183.)
kt/y	2009	58	(42.- 65.)	114	(56. -145.)
kt/y	2010	58	(43.- 75.)	111	(59. -134.)
kt/y	2011	61	(43.- 75.)	118	(61. -144.)
kt/y	2012	60	(43.- 75.)	122	(66. -147.)
kt/y	2013	54	(44.- 70.)	133	(84. -157.)

Table 58: Emission estimates for UK and NWEU with uncertainty (5th – 95th %ile).

6.26 Carbon monoxide (CO)

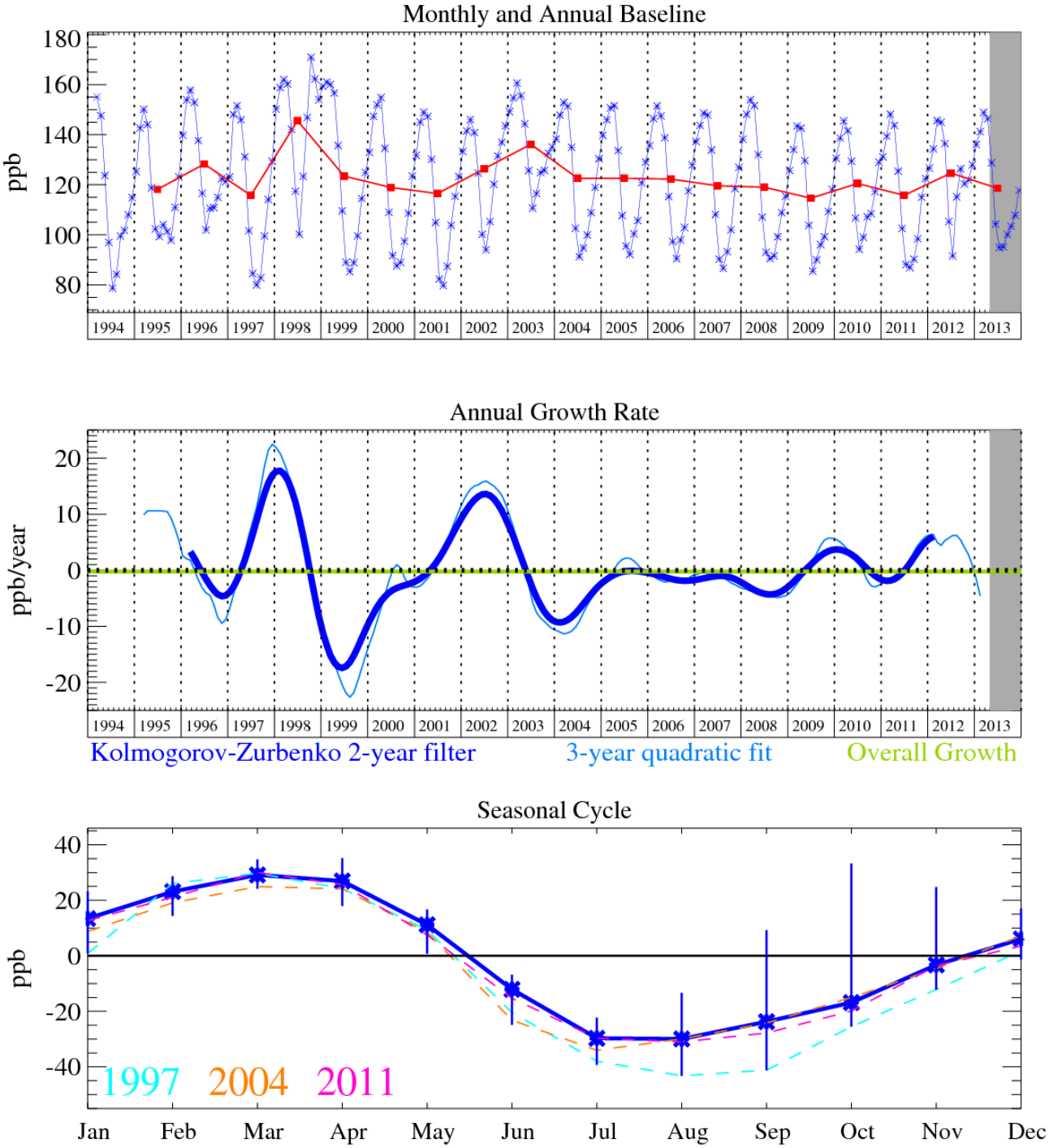

Figure 132: CO: Monthly (blue) and annual (red) baseline mole fractions (top plot). Annual (blue) and overall average growth rate (green) (middle plot). Seasonal cycle (de-trended) with year-to-year variability (lower plot). Grey area covers un-ratified and therefore provisional data.

Annual mean baseline CO levels have remained largely unchanged since 2004, around 120 ppb. Levels in 2010 showed a small step up relative to those in 2009 and 2011, which is attributed to the forest fires in the Russian Federation (WDCGG, 2012). The average baseline mole fraction in 2013 was 119 ppb, which is significantly lower than its peak annual values of 146 ppb in 1998 and 136 ppb in 2003.

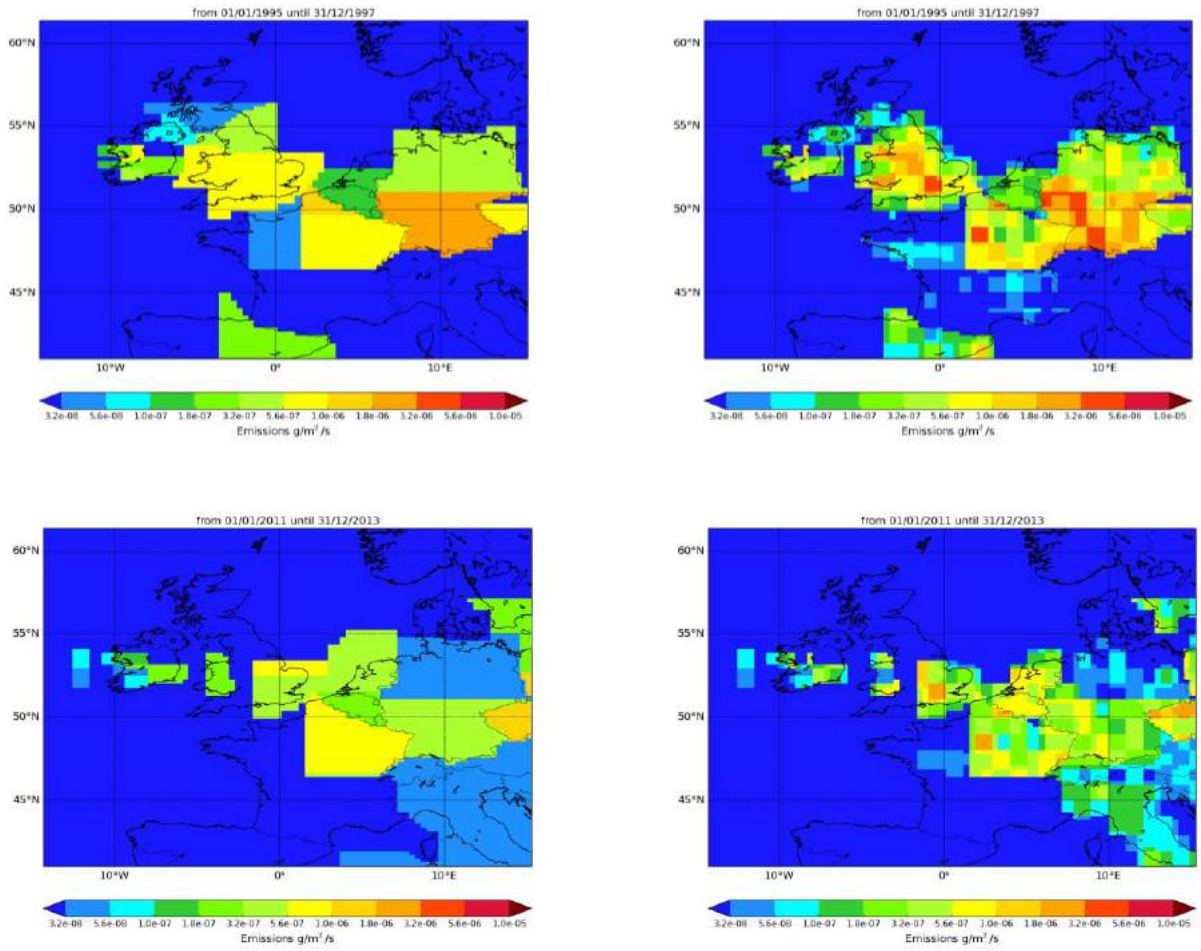

Figure 133: NAME-inversion emission estimates for 1995-1997 (upper) and 2011-2013 (lower). On the right hand side the emissions per grid box have been re-distributed based on population.

The estimated emissions of CO in the UK have declined steadily in both the inventory and the InTEM emission estimates. The latter are, before 2007, approximately 30% smaller than the reported inventory. The magnitude of the pollution events seen at Mace Head have significantly declined since 1995 and the statistical match between the model time-series and observations is good.

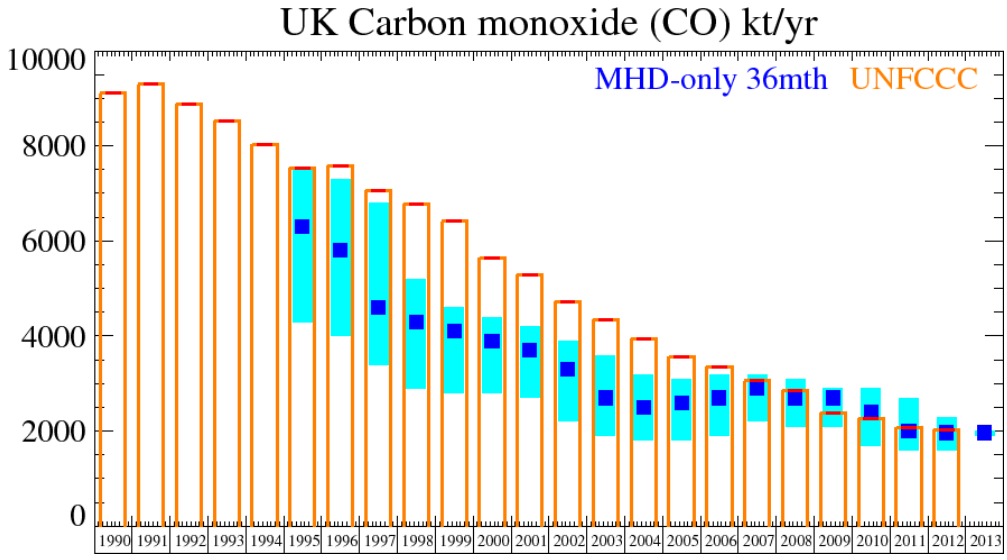

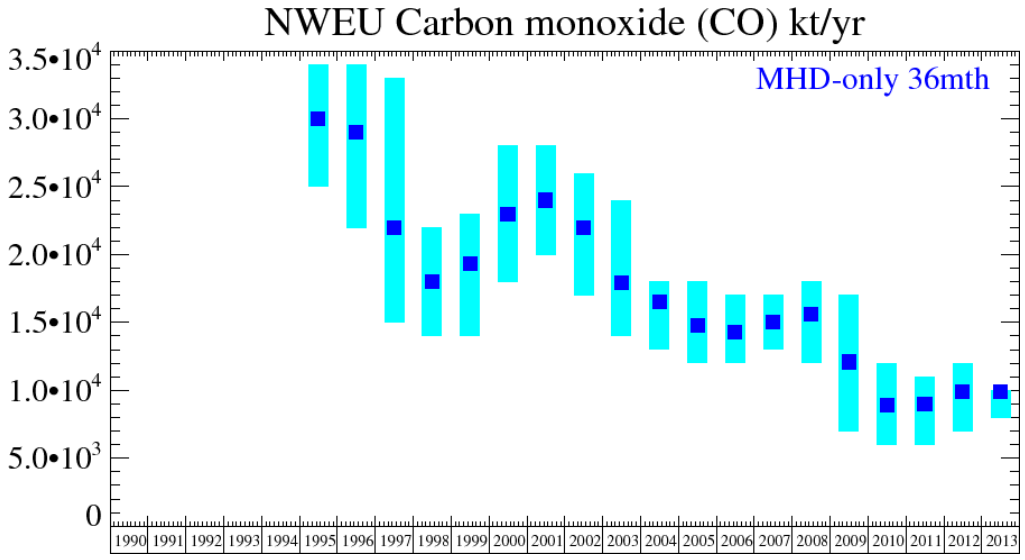

Figure 134: Emission estimates for UK and NWEU (MHD-only). The uncertainty bars represent the 5th and 95th percentiles.

Unit	Year	UK	(5th-95th)	NWEU	(5th-95th)
Mt/y	1995	6.3	(4.3- 7.5)	30	(25. -34.)
Mt/y	1996	5.8	(4.0- 7.3)	29	(22. -34.)
Mt/y	1997	4.6	(3.4- 6.8)	22	(15. -33.)
Mt/y	1998	4.3	(2.9- 5.2)	18	(14. -22.)
Mt/y	1999	4.1	(2.8- 4.6)	19.3	(14. -23.)
Mt/y	2000	3.9	(2.8- 4.4)	23	(18. -28.)
Mt/y	2001	3.7	(2.7- 4.2)	24	(20. -28.)
Mt/y	2002	3.3	(2.2- 3.9)	22	(17. -26.)
Mt/y	2003	2.7	(1.9- 3.6)	17.9	(14. -24.)
Mt/y	2004	2.5	(1.8- 3.2)	16.5	(13. -18.)
Mt/y	2005	2.6	(1.8- 3.1)	14.8	(12. -18.)
Mt/y	2006	2.7	(1.9- 3.2)	14.3	(12. -17.)
Mt/y	2007	2.9	(2.2- 3.2)	15	(13. -17.)
Mt/y	2008	2.7	(2.1- 3.1)	15.6	(12. -18.)
Mt/y	2009	2.7	(2.1- 2.9)	12.1	(7. -17.)
Mt/y	2010	2.4	(1.7- 2.9)	8.9	(6. -12.)
Mt/y	2011	2	(1.6- 2.7)	9	(6. -11.)
Mt/y	2012	1.97	(1.6- 2.3)	9.9	(7. -12.)
Mt/y	2013	1.97	(1.9- 2.0)	9.9	(8. -10.)

Table 59: Emission estimates for UK and NWEU with uncertainty (5th – 95th %ile).

6.27 Ozone (O_3)

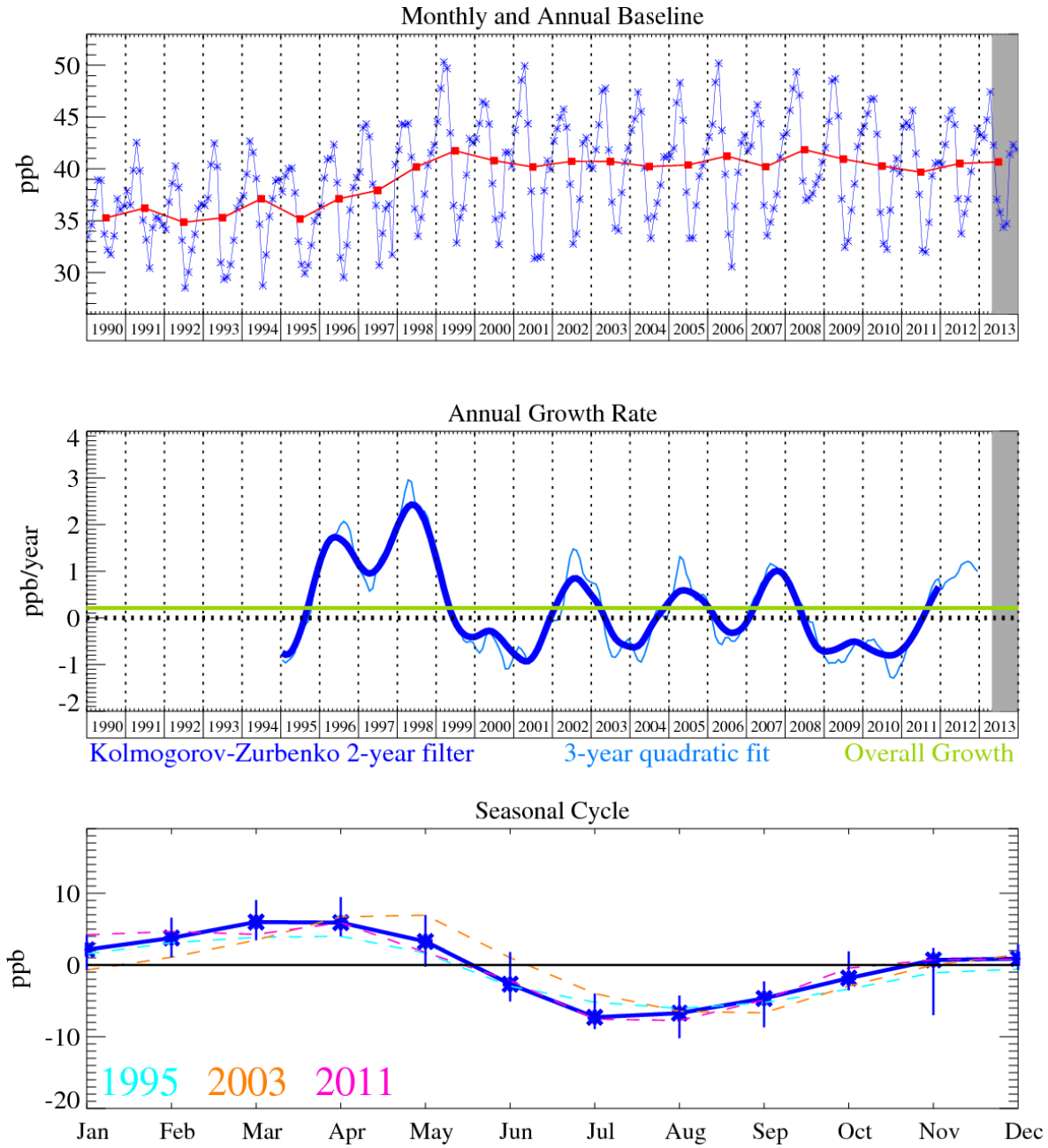

Figure 135: Ozone (O_3): Monthly (blue) and annual (red) baseline mole fractions (top plot). Annual (blue) and overall average growth rate (green) (middle plot). Seasonal cycle (de-trended) with year-to-year variability (lower plot). Grey area covers un-ratified and therefore provisional data.

Tropospheric O_3 measurements first started at Mace Head in 1987 and the trends derived from the baseline-selected monthly means, the growth rate and seasonal cycles are shown in Figure 135. The Mace Head O_3 measurements exhibited a positive trend in some years (1996-1998, 2002, 2005, 2007 and 2012) and a negative in others (1995, 2000-2001, 2003-2004, 2006, 2008-2010). The most recent growth rate is estimated to be 1 ppb/yr. Its average mole fraction in 2013 at Mace Head was 40.7 ppb. Assessment of the long-term trends in tropospheric ozone is difficult due to the scarcity of representative observing sites with long records. The records that do exist vary both in terms of sign and magnitude (Forster *et al.,* 2007). However, the behaviour seen at Mace Head, Ireland is entirely consistent with that reported at two other European baseline stations: Arkona-Zingst and Jungfraujoch (Parrish *et al.*, 2012).

6.28 Hydrogen

Hydrogen (Figure 136) is an oxidation product of methane and isoprene whose main sink is surface uptake mainly in the northern hemisphere. Annual mean baseline levels have remained roughly constant (within measurement uncertainty) for much of the Mace Head record. It shows an average mole fraction in 2013 of 519 ppb. There is evidence of anomalous growth in 2010-2011 through the influence of the forest fires in the Russian Federation.

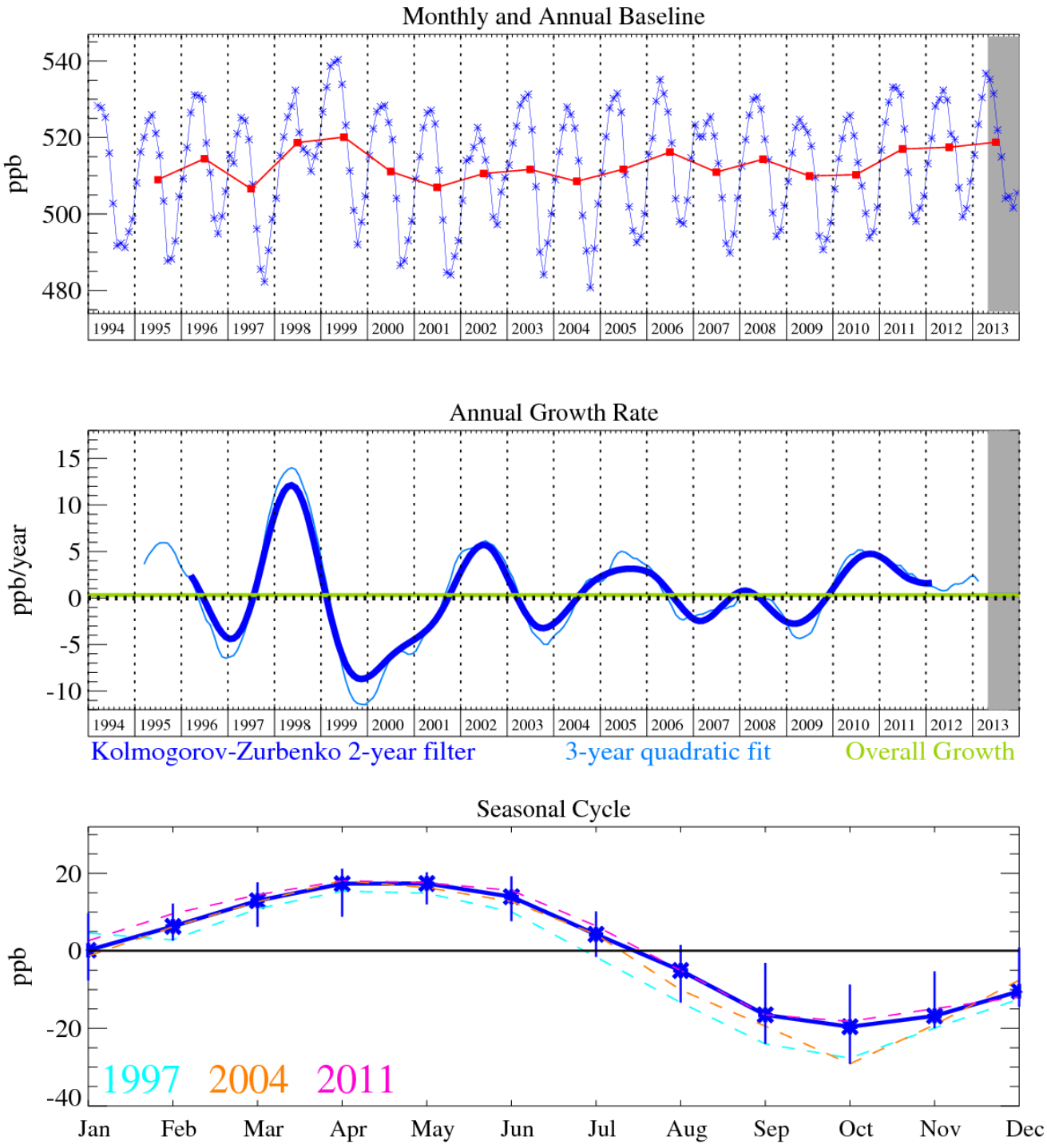

Figure 136: Hydrogen (H_2): Monthly (blue) and annual (red) baseline (top plot). Annual (blue) and overall average growth rate (green) (middle plot). Seasonal cycle (de-trended) with year-to-year variability (lower plot). Grey area covers un-ratified and therefore provisional data.

7 HFC emissions: Comparison of interspecies correlation method with InTEM

Using inversion modelling techniques InTEM provides emission estimates for many trace gases from various source regions [Manning et al., 2003]. Several publications also report emission estimates using an interspecies correlation method which relies on the assumption that the relative pollution enhancements of two tracers reflects the ratio of their emission strengths from co-located emission sources. [Yokouchi et al.,2006; Kim et al.,2010; Li et al.,2011]. In addition it assumes that neither gas is produced or destroyed in the air mass during transport.

Pollution enhancements at Mace Head, Ireland are identified routinely using InTEM by subtracting the time varying baseline observations from the raw data. We can therefore use these "pollution events" to test for consistency between the interspecies correlation method of estimating emissions and those determined by InTEM. As will become apparent, the interspecies correlation method, relying on the ratio of two tracers, is particularly vulnerable to an individual emission of either tracer from a nearby source, thus perturbing the ratio and altering the emissions from a more distant source region.

Here we examine observations of HFC-125, HFC-32, HFC-143a and HFC-134a, which are the principal refrigerants used in both mobile and stationary refrigeration systems, in air masses which have a recent history over North West Europe (NWEU). InTEM defines NWEU as including the following 8 countries (Belgium, Denmark, France, Germany, Luxembourg, the Netherlands, UK, and Ireland). By only selecting pollution events arriving at Mace Head which are predominately associated with transport from the UK and Ireland we can obtain interspecies correlation ratios for each of the four HFCs and compare these with comparable ratios reported by the UNFCCC and those determined using InTEM.

To be confident that we are using only substantial pollution events we first determine the pollution enhancement by subtracting the baseline derived by InTEM from each raw data observation. If this value is greater than the upper limit of the baseline estimate (baseline + 1 standard deviation of the baseline uncertainty) then it is selected as a substantial pollution event. The NAME model has been used to define the relative strength that each source region contributes to the air arriving at Mace Head. Therefore we can further refine each pollution event to a specific source region where it is the major contributor to the arriving air mass.

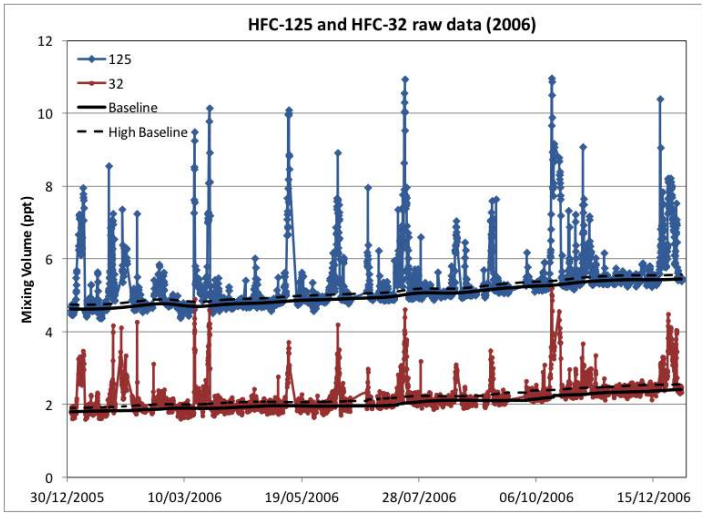

Figure 137: Time-series of mole fractions of HFC-125 (blue) and HFC-32 (red) at Mace Head during 2006. The solid black line is the InTEM baseline. The dashed line is the estimated upper limit of the InTEM baseline.

Figure 137 illustrates the raw observations for HFC-125 and HFC-32 during 2006. Most noticeable is the high degree of temporal correlation between the two tracers during the clearly defined

pollution events. The solid black lines are the InTEM baselines and the dashed black lines represent the upper limit of the baseline.

The comparison of the magnitude of the pollution enhancements of the two HFCs extracted from the raw data is shown in Figure 138. The smaller figure is an XY-scatterplot with a Pearson correlation coefficient r^2 of 0.85, which suggests that the two HFCs are likely to have a common or collocated source.

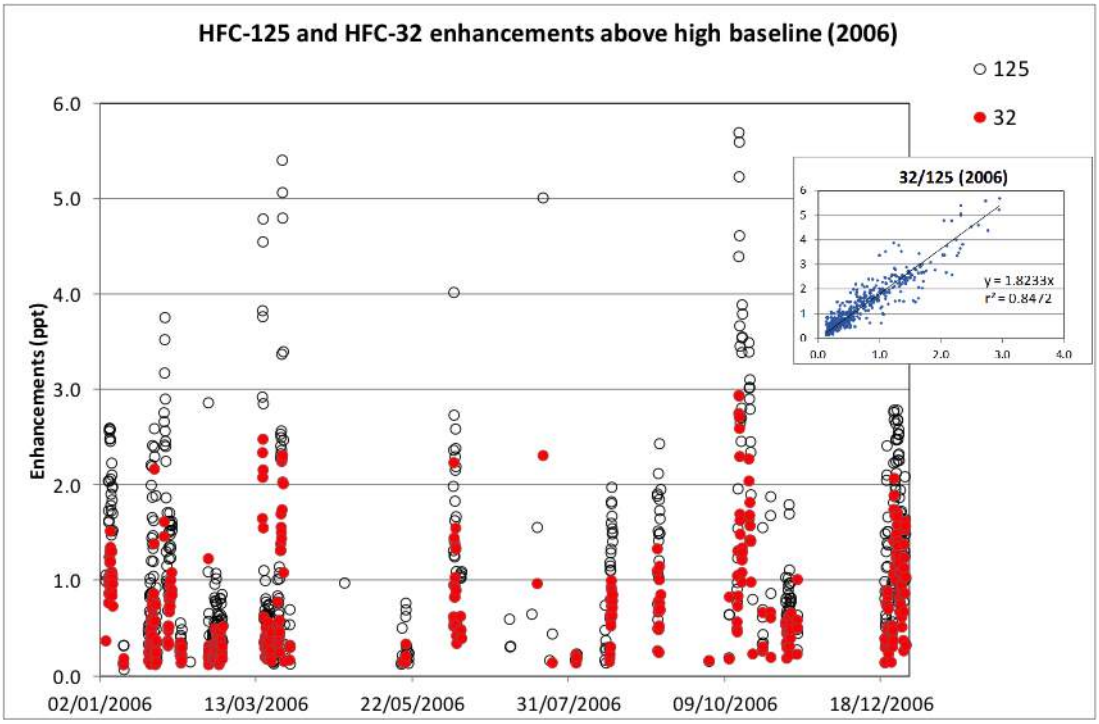

Figure 138: Comparison of the pollution events of HFC-125 and HFC-32 at Mace Head in 2006.

There are five main refrigerant blends in common use, see Table 60, of these, 404A, 407C and 410A include both HFC-125 and HFC-32 in the blend.

REFRIGERANT	125%	32%	134a%	143a%	Ratio 32/125	Ratio 134a/125	Ratio 143a/125	Ratio 134a/32
410A	50	50			1			
407C	25	23	52		0.92	2.08		2.26
407A	40	20	40		0.5			2.0
404A	44		4	52			1.18	
507A	50			50			1	

Table 60: Main refrigerants and their composition. Note HFC-134a is also used as a single refrigerant in both mobile and stationary refrigerant systems.

Figure 139 plots the ratio of HFC-32:HFC-125 enhancements above baseline (open circles) for each significant pollution event identified by the NAME model in 2006. There is considerable variability in the magnitude of these ratios with values ranging from about 0.2 to > 1. Uncertainties in these ratios are reported later as 1σ standard deviations (see Tables 61 & 62). The green line is the median value (0.53) of all of the open circles, while the red line with a ratio of 0.55 is calculated from the XY-scatterplot shown in Figure 138. Note, at this stage these are simply pollution enhancement ratios that have not been converted to emissions. The solid purple line indicates the HFC-32:HFC-125 emission estimates ratio of 0.50 (converted to ppt) determined from InTEM for the 8 countries that are collectively defined as NWEU.

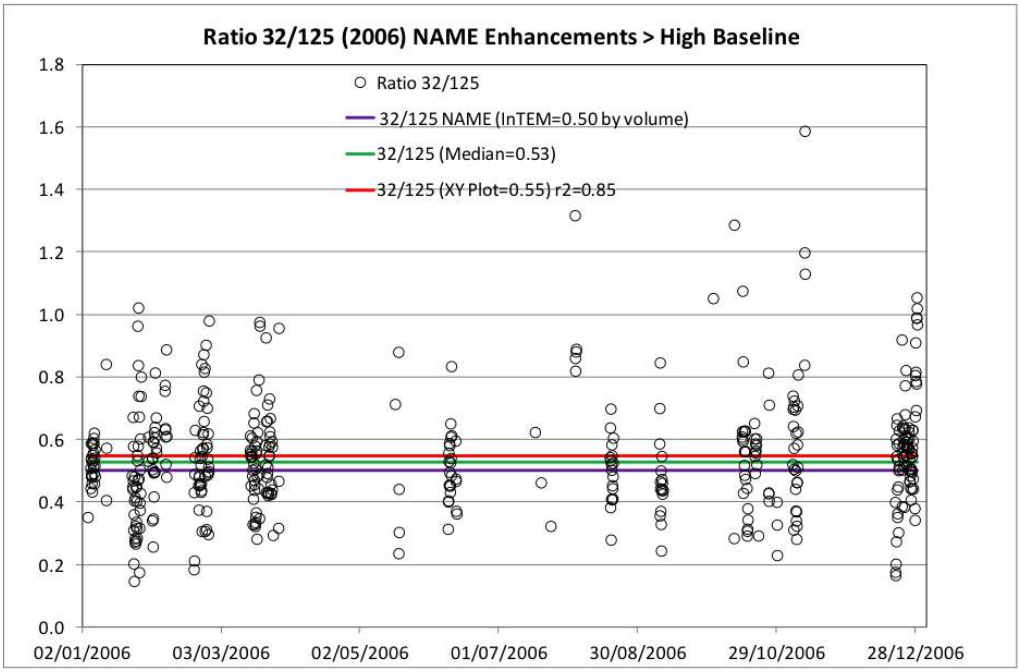

Figure 139: Ratio of HFC-32 to HFC-125 enhancements above baseline at Mace Head in 2006.

In Figures 140-142 we show the same pollution enhancement ratios of HFC-32:HFC-125 for 2005, 2010 and 2011, respectively.

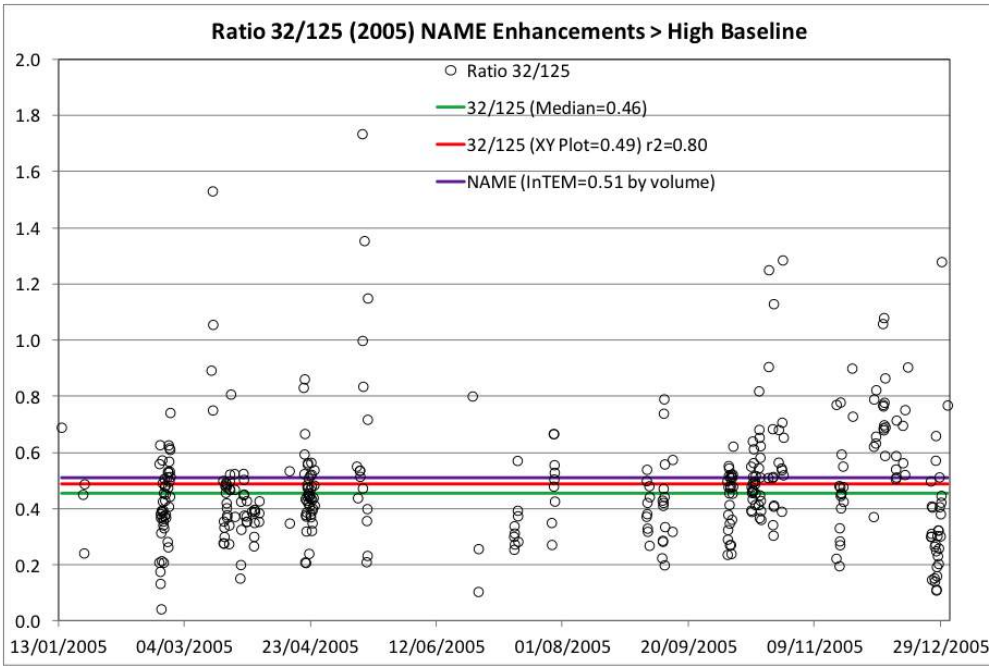

Figure 140: Ratio of HFC-32 to HFC-125 enhancements above baseline at Mace Head in 2005.

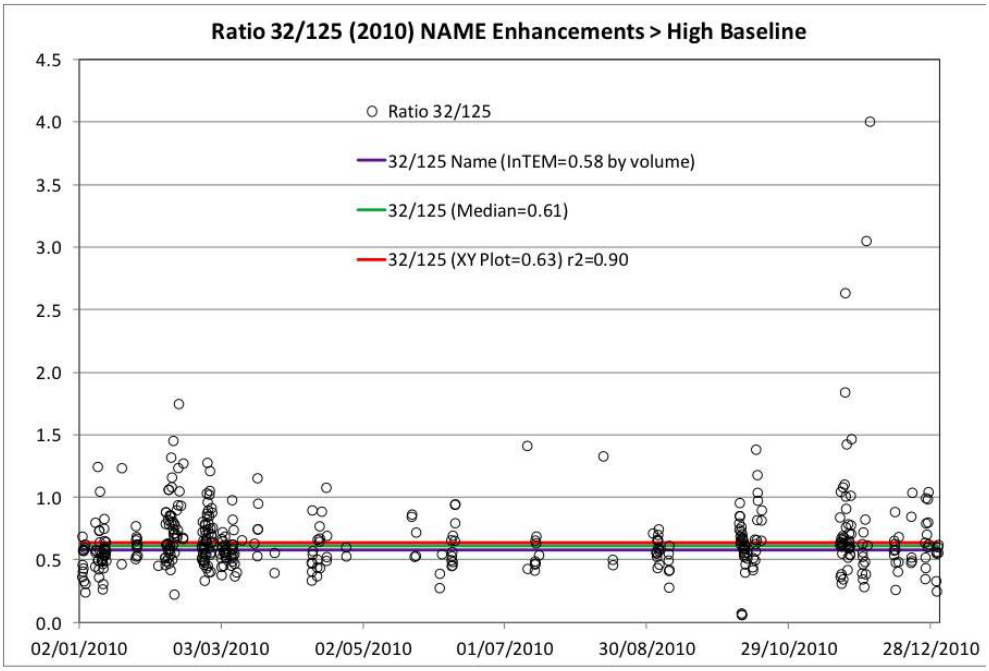

Figure 141: Ratio of HFC-32 to HFC-125 enhancements above baseline at Mace Head in 2010

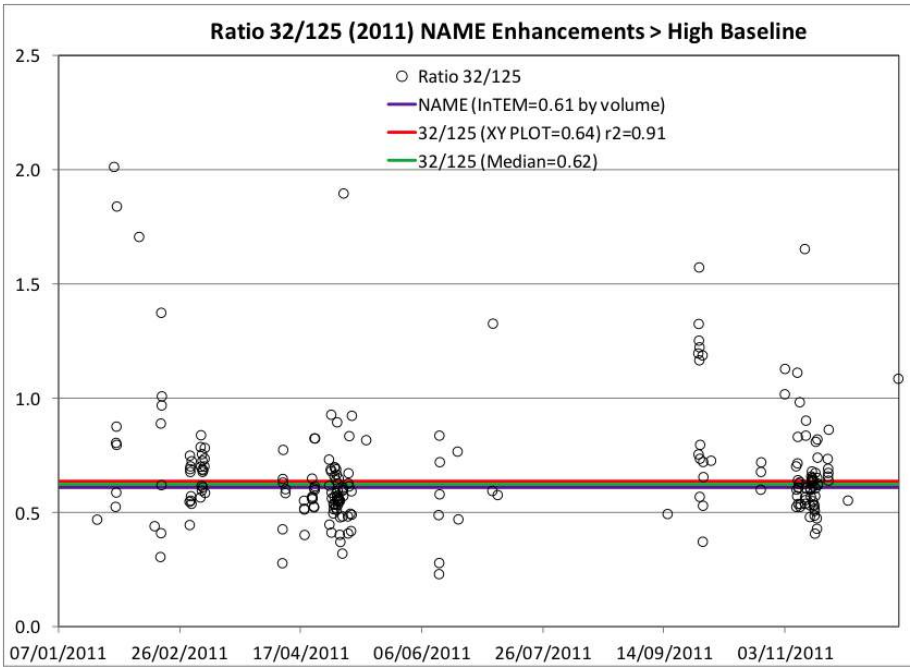

Figure 142: Ratio of HFC-32 to HFC-125 enhancements above baseline at Mace Head in 2011.

For comparison with Figure 139, the pollution enhancement ratios of HFC-143a:HFC-125 (Figure 143), and HFC-134a:HFC-125 at Mace Head for 2006 are also plotted (Figure 144), since HFC-143a and HFC-134a are the other predominant refrigerants currently in use (see Table 60).

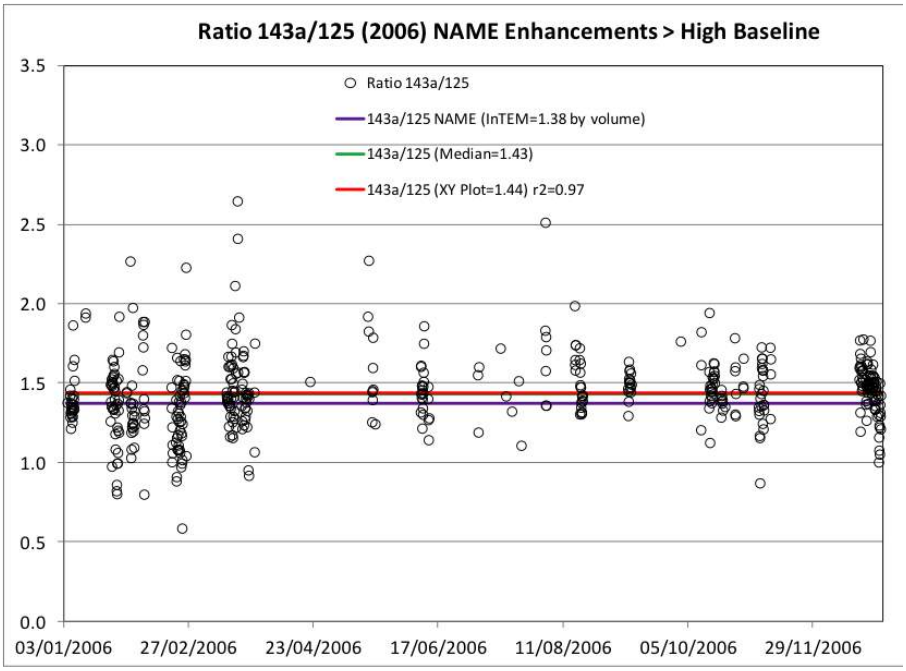

Figure 143: Ratio of HFC-143a to HFC-125 enhancements above baseline at Mace Head in 2006

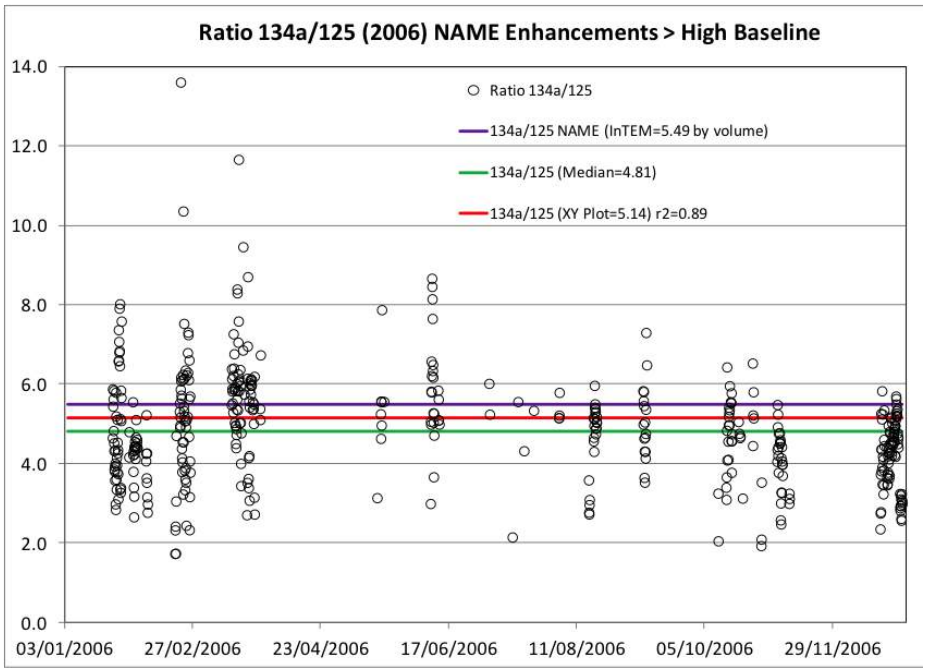

Figure 144: Ratio of HFC-134a to HFC-125 enhancements above baseline at Mace Head in 2006

Figures 143-144, show the InTEM tracer ratio (purple line), the median value of the pollution enhancements (green line) and the tracer ratios determined from the XY-scatter plots (red line) including Pearson correlation coefficients (r^2). There is a particularly strong correlation for HFC-143a to HFC-125 of r^2=0.97 which again infers a co-location of sources or a common source. In the case of HFC-134a to HFC-125 there is more scatter in the ratio determined by the different methods. Notice in Table 60 that refrigerant blends 404A and 507A contain approximately a 50:50 mixture of HFC-143a and HFC-125 giving a ratio of between 1 and 1.2. This ratio is in close agreement with the ratio determined by the XY-plot of 1.4 and the InTEM ratio of 1.38.

By focussing on pollution events specific to the UK and Ireland it is expected that insights into the HFC-32:HFC-125 pollution enhancements ratio can be ascertained. As noted previously InTEM provides a measure of the relative strength that each specific region contributes to the air mass (e.g. UK+Ireland, NWEU, Southern Europe, Eastern Europe, Scandinavia and USA). In the following analysis we isolate those pollution events where the UK+Ireland is the dominant region contributing to the air mass arriving at Mace Head and where all other source regions contribute less than 5% to

the air mass. In Figure 145 we plot a single pollution event during Jan 25-27th, 2006 when the air mass shifts from a combination of NWEU+UK+Ireland to predominantly UK+Ireland and on to Scandavia+UK+Ireland.

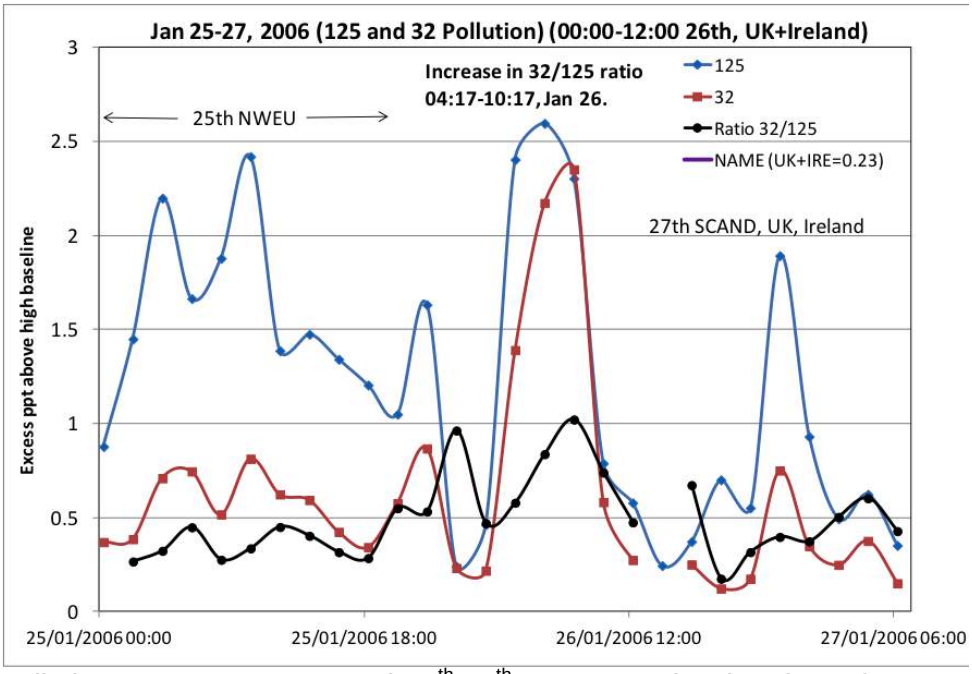

Figure 145: Pollution event at Mace Head 25th-27th Jan 2006 showing the enhancements in HFC-125, HFC-32, the enhancement ratio HFC-32:HFC-125 and the InTEM ratio of emissions from the two gases for UK+Ireland.

The three trajectory plots shown below (available from NILU) illustrate the recent history of the air masses at different times (midnight 25th Jan 2006, 6am 26th Jan 2006 and midnight 27th Jan 2006). We use the NILU trajectories for simplicity, but also shown is 9am-noon January 26th air history plot produced by the NAME model, which is considerably more detailed compared with the NILU trajectory plot, showing possible minor emissions from NWEU (yellow dots) during this time.

There is a significant increase in the HFC-32:HFC-125 ratio to approximately 1 during the period when the air mass arriving at Mace Head passes over the UK+Ireland compared with an air mass which includes NWEU or Scandinavia (Norway+Sweden) when the ratio is between 0.2 and 0.5. This suggests that an air mass passing over the UK and Ireland accumulates greater emissions of HFC-32 relative to HFC-125 compared with other source regions. What is surprising is that the trajectories on Jan 26th and 27th over the UK and Ireland are very similar. The emissions of HFC-32 and HFC-125 reported to UNFCCC by the Scadinavian countries in 2006 give a HFC-32:HFC-125 ratio of 0.15 (0.35 by volume) due to a greater use of HFC-125, which may explain the lower observed ratio when Scadinavian air makes a significant contribution to the air mass. Similarly, the HFC-32:HFC-125 emissions ratio reported for NWEU by UNFCCC is 0.18 (0.42 by volume) and by InTEM is 0.22 (0.5 by volume), which also implies larger emissions of HFC-125 relative to HFC-32. It should be kept in mind that the baseline air masses which arrive at Mace Head will already contain these HFCs in some defined ratio, although it is assumed that they are well mixed during transport across the North Atlantic with fresh emissions added from more local sources as they approach Mace Head.

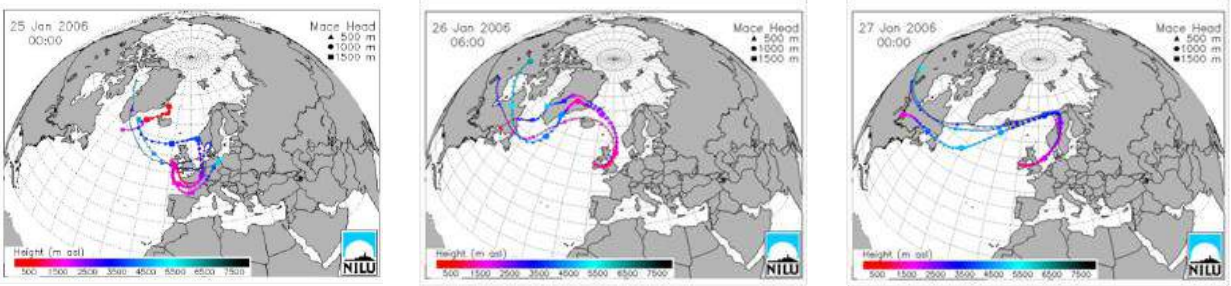

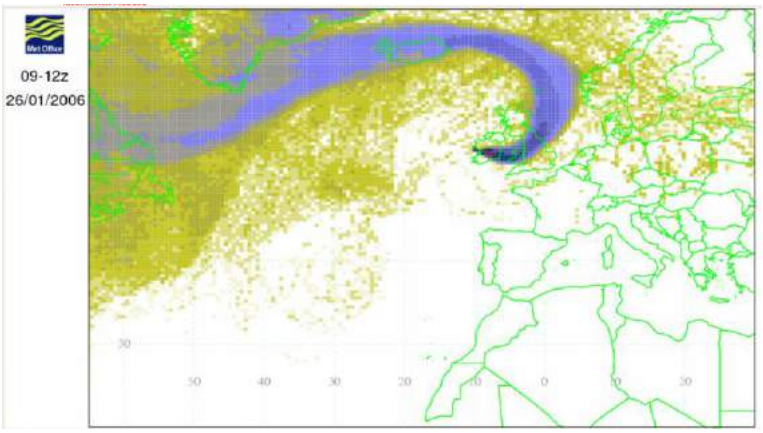

Figure 146: NILU trajectory plots for midnight 25th Jan 2006, 6am 26th Jan 2006 and midnight 27th Jan 2006 and the Met Office NAME air history map for 9am-noon 26th Jan 2006.

The ratios of the other principal refrigerants during this particular pollution event have also been examined. Figure 147 shows the ratio of HFC-143a:HFC-125, Figure 148 the ratio of HFC-134a:HFC-125 and Figure 149 the ratio of HFC-134a:HFC-32.

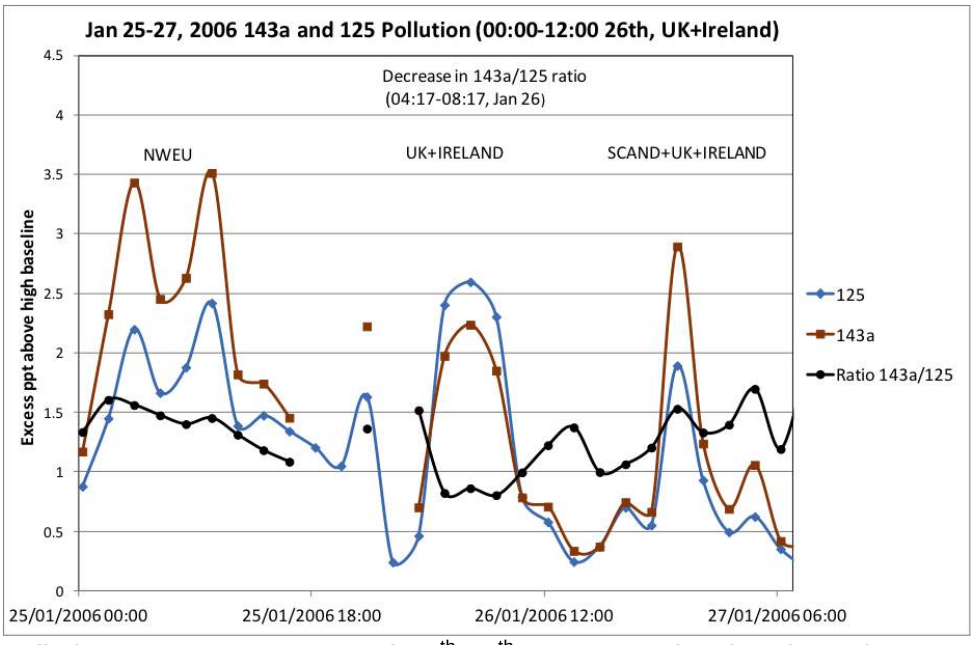

Figure 147: Pollution event at Mace Head 25th-27th Jan 2006 showing the enhancements in HFC-125, HFC-143a, the enhancement ratio HFC-143a/HFC-125 and the InTEM ratio of emissions from the two gases for UK+Ireland.

In Figure 147, the ratio of HFC-143a:HFC-125 drops below 1 during passage over the UK+Ireland but is greater than 1 when the air mass in influenced by NWEU or Scandinavia. This may imply larger emissions of HFC-143a relative to HFC-125 in Continental Europe and the inverse relationship when the air mass is confined to the UK+Ireland source region. Furthermore, this would argue for a proportionally larger use of refrigerant blends in Europe that contain HFC-143a such as 404A and 507A. Conversely, the UK +Ireland would also require significant use of refrigerant blends with a high proportion of HFC-125, such as 410A and 407C with 50% HFC-125 and interestingly also 50% HFC-32. We can speculate that this might help to explain the rise in HFC-32 shown in Figure 145, although it does not rule out a local emission of just HFC-32.

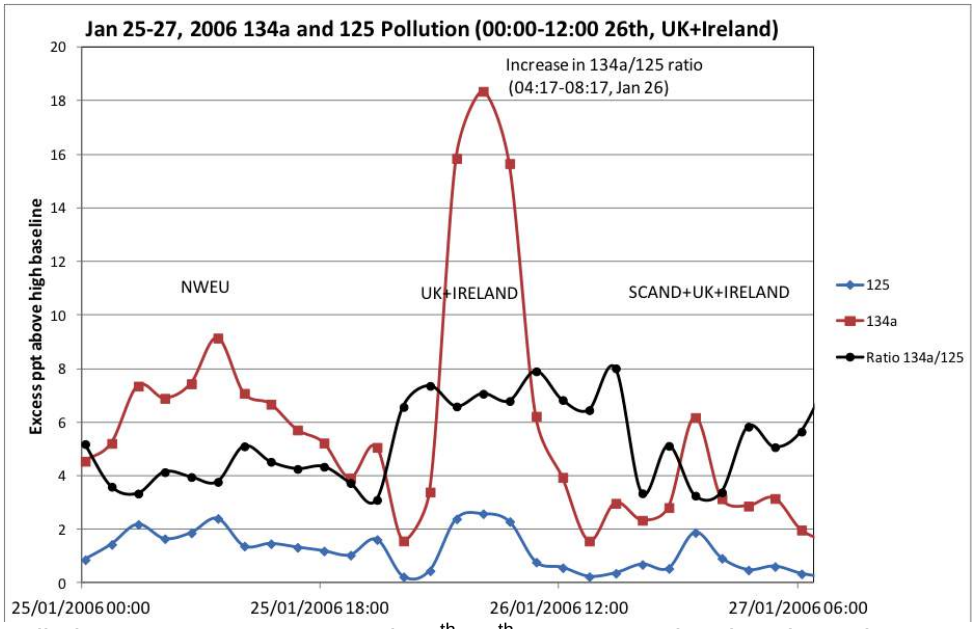

Figure 148: Pollution event at Mace Head 25th-27th Jan 2006 showing the enhancements in HFC-125, HFC-134a, the enhancement ratio HFC-134a/HFC-125 and the InTEM ratio of emissions from the two gases for UK+Ireland.

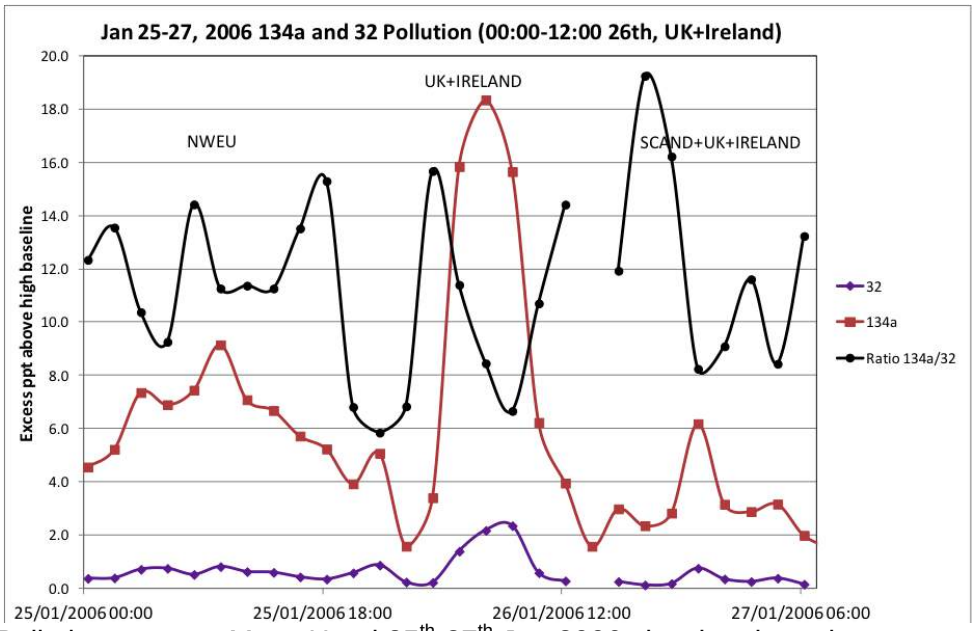

Figure 149: Pollution event at Mace Head 25th-27th Jan 2006 showing the enhancements in HFC-32, HFC-134a, the enhancement ratio HFC-134a/HFC-32 and the InTEM ratio of emissions from the two gases for UK+Ireland.

In Figures 148 and 149 there is clearly a much larger emission source of HFC-134a relative to HFC-125 and HFC-32. In Figure 148 the 134a:125 ratio virtually doubles when the air mass is confined to the UK+Ireland. In Figure 149 the 134a:32 ratio drops to about 6 from an average ratio over NWEU and Scandinavia of about 12. This is expected if we account for the local additional emission of HFC-32 shown in Figure 145 that would in effect reduce the HFC-134a:HFC-32 ratio. It should also be appreciated that 134a will have both mobile and stationary sources and therefore may be less co-located with HFC-32, as would be the case for a refrigerant blend of the two HFCs such as 407A or 407C (see Table 60).

To support the observation in Figure 145 of a HFC-32:HFC-125 pollution enhancement ratio of about 1 in air masses attributed to the UK+Ireland, we show in Figures 150-14 further examples of specific pollution events in 2006 and 2011, where the HFC-32:HFC-125 ratio approaches or exceeds 1.

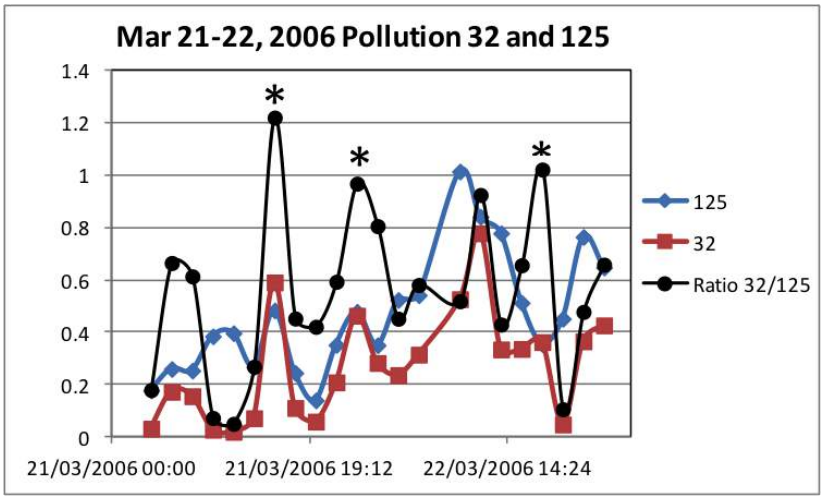

Figure 150: Enhancements above baseline for HFC-125 and HFC-32 and their ratio at Mace Head 21st-22nd Mar 2006.

The asterisks indicate times when the HFC-32:HFC-125 ratio is 1 or larger and are aligned with the relevant trajectories (Figure 151). Figure 152 shows two pollution events in April and November 2011.

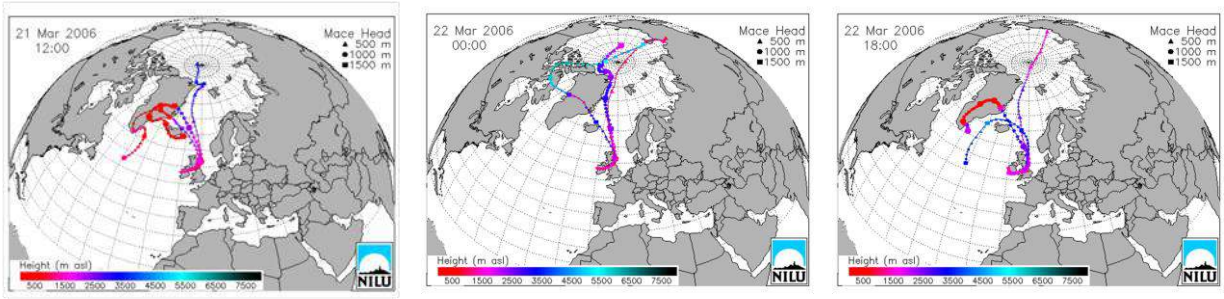

Figure 151: NILU trajectories for noon 21st Mar 2006, 6pm 22nd Mar 2006 and midnight 22nd Mar 2006.

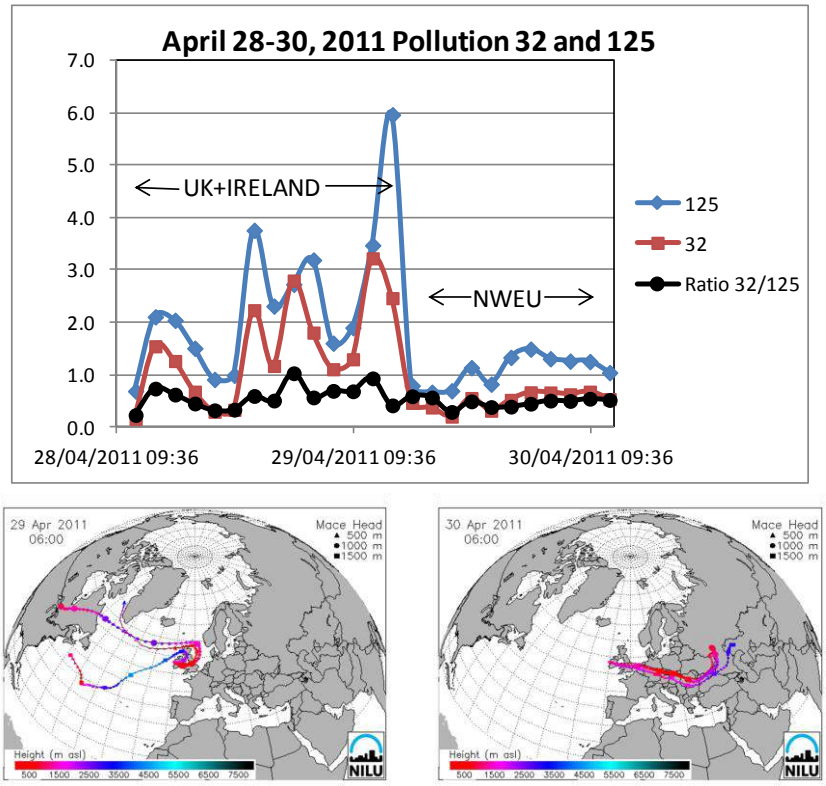

(a)

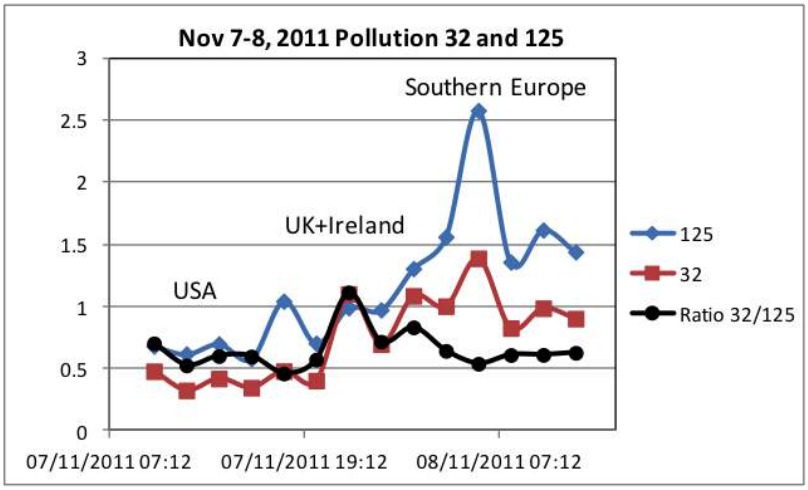

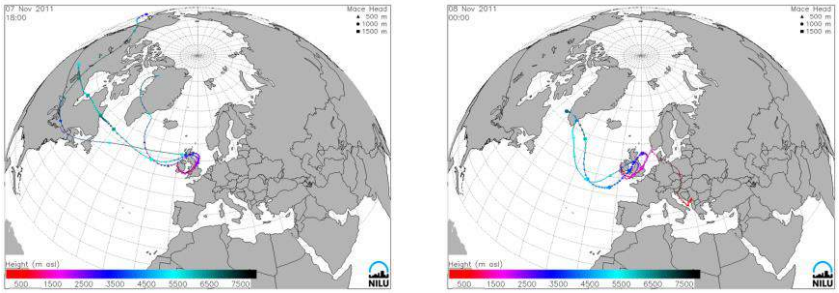

(b)

Figure 152: (a) Enhancements above baseline for HFC-125 and HFC-32 and their ratio at Mace Head 28th-30th Apr 2011 and associated NILU trajectories and (b) Enhancements above baseline for HFC-125 and HFC-32 and their ratio at Mace Head 7th-8th Nov 2011 and associated NILU trajectories.

The two events in 2011 are of special interest as the air mass switches from the UK+Ireland to NWEU or Southern Europe as indicated by the accompanying trajectories. Significantly the HFC-32:HFC-125 ratio increases to ~1 when the air mass is primarily associated with the UK+Ireland but averages ~0.5 when the air mass originates from Europe.

These examples support the contention that air masses which have received emissions primarily from the UK+Ireland will in general have a larger HFC-32:HFC-125 ratio than other major source regions particularly NWEU and consequently HFC-32:HFC-125 ratios in air of European origin will be modified during passage over the UK+Ireland on route to Mace Head. Importantly the European HFC-32:HFC-125 ratio itself will also vary depending on the relative emission of each tracer in each country.

7.1 Calculation of emission estimates using the interspecies correlation method.

The pollution enhancement ratios are now converted to emission estimates using another important feature of the interspecies correlation method, which states if the emission of one species (Er, t/y) from an area is known, then the emission rates of all other compounds (Ex, t/y) in the same dataset can be calculated from the pollution enhancement (ΔC) by using the following equation, (Yokouchi et al, 2006).

$$Ex = Er \times \Delta Cx/\Delta Cr \times Mx/Mr \quad \text{.....(1)}$$

Where Mx and Mr are the molecular weights of species x and reference compound r, respectively and ΔCx and ΔCr are expressed in ppt.

HFC-125 can be used as a reference compound, since it is believed to have the most accurate emission estimates and there is good agreement between InTEM derived HFC-125 emissions and

the UNFCCC estimates. Using the pollution enhancement ratios, we have identified in 2005, 2006, 2010, and 2011 we use the above equation and the annual emission of HFC-125 determined by the NAME model as the reference compound in Table 2 to calculate emissions for the other HFCs in NWEU air masses. The emission estimates from both methods are in good agreement even before the large uncertainties are included. Notably between the two 5-year periods 2005/06 and 2010/11 there is consistently good agreement between the methods of estimated emissions, even though these emission estimates must be related to the actual usage of the various HFCs as blends in refrigerant systems that will have changed over time.

2005 Species (Ratio used)	Ratio calculated from XY-scatterplot	Pearson correlation coefficient (r2)	**Estimated mission (t/y)from the XY-plot ratio	*InTEM Estimated Emission (t/y)
HFC-32 (Ratio 32/125)	0.49	0.78	467 (257-663)	490 (392-585)
HFC-143a (Ratio 143a/125)	1.48	0.98	2281 (1842-2765)	2400 (2092-2678)
134a (Ratio 134a/125)	5.13	0.81	9594 (5787-12435)	11200 (9000-13000)
2006 Species (Ratio used)				
32 (Ratio 32/125)	0.55	0.85	641 (425-854)	580 (405-855)
143a (Ratio 143a/125)	1.44	0.97	2722 (2286-3165)	2600 (2210-3169)
134a (Ratio 134a/125)	5.14	0.89	11798 (7937-14327)	12600 (11000-14000)
2010 Species (Ratio used)				
32 (Ratio 32/125)	0.63	0.90	901 (496-1410)	830 (636-1087)
143a (Ratio 143a/125)	1.21	0.94	2803 (2322-3644)	2700 (2346-3283)
134a (Ratio 134a/125)	4.07	0.86	11412 (6789-14391)	11000 (8000-14000)
2011 Species (Ratio used)				
32 (Ratio 32/125)	0.64	0.91	1101 (723-1633)	1060 (671-1312)
143a (Ratio 143a/125)	1.17	0.97	3271 (2574-3994)	3100 (2413-3803)
134a (Ratio 134a/125)	3.37	0.92	11459 (7998-16655)	11800 (8000-15000)

Table 61: Emissions of HFC-32, HFC-143a and HFC-134a assuming HFC-125 emissions are known using the interspecies correlation method. Notes: column 4 emission estimates by the interspecies correlation method with emission estimates determined from InTEM (last column). (Estimated emissions are for species in bold type; *values in parentheses are the 5th-95th percentiles; **values in parentheses are 1σ standard deviations).

If we now focus on several pollution events which have primarily a UK+Ireland origin we can calculate emission estimates again using the InTEM HFC-125 emission as a reference compound as shown in Table 62. Comparing columns 4 and 5 we see that, in general, the agreement is less robust between the two methods of estimating emissions with closer agreement in 2011 than in 2006 presumably due to changing emissions. Contributions to the air masses from emissions in the UK+Ireland are clearly perturbing the ratios calculated by the interspecies correlation method. However, the timing of these events is still rather subjective and only a few events have been analysed in detail. Nevertheless this does highlight a potential vulnerability of the interspecies correlation method.

Species (Ratio used)	Ratio calculated	Pearson correlation	**Estimated emission (t/y) from the	*InTEM Estimated Emission (t/y)

	from XY-scatterplot	coefficient (r2)	XY-plot ratio	
HFC-32 (32/125). 2006 (Jan 26, 00:00-12:00)	0.84	0.86	272 (163-309)	174 (124-222)
HFC-32 (32/125). 2006 (Mar 21-22, 06:00-18:00)	0.79	0.41	256 (79-328)	174 (124-222)
HFC-32 (32/125). 2011 (Apr 28-29, 13:30-07:30)	0.69	0.53	288 (156-329)	260 (210-341)
HFC-32 (32/125). 2011 (Nov 7, 06:00-18:00)	0.54	0.73	225 (205-254)	260 (210-341)
HFC-143a (Ratio 143a/125) 2006(Jan 26, 00:00-12:00)	0.86	0.95	453 (402-586)	810 (681-889)
HFC-134a (Ratio 134a/125) 2006(Jan 26, 00:00-12:00)	6.89	0.99	4393 (4176-4782)	2900 (2500-3400)

Table 62: Emissions of HFC-32, HFC-143a and HFC-134a assuming HFC-125 emissions are known using the interspecies correlation method. Notes: column 4 emission estimates by the interspecies correlation method with emission estimates determined from InTEM (last column). (Estimated emissions are for species in bold type; *values in parentheses are the 5th-95th percentiles; **values in parentheses are 1σ standard deviations).

We have also obtained estimates of actual sales volumes of refrigerants from the British Refrigeration Association (BRA) for 2011 and 2012, listed in Table 63 as bold black type. Earlier data are unfortunately not available. Also in Table 63 we calculate the fraction (red type) of each HFC from the total volume in each refrigerant blend using the information in Table 60.

For additional information we include in Table 63 the bottom-up UNFCC emission ratios of several HFC pairs for the same 8 countries used by InTEM to characterize NWEU, InTEM results and similar ratios for the UK+Ireland.

Sales by Fillers & Packers	2011 Vol	HFC-125	HFC-32	HFC-134a	HFC-143a
R134a *	1667			1667	
R404A & R507A	1650	807.5		34.4	876.2
R407C	534	133.5	122.8	277.7	
R407A & R407F	91	31.9	22.8	36.4	
R410A	526	331.5	331.5		
Other HFC blends	297	?	?	?	?
Other fluorocarbon blends	13	?	?	?	?
Total HFCs in most used blends		1304.4	477.1	3695.5	876.2

*R134a is only a subset as it does not include imports and cars imported into the UK containing R134a.

Sales by Fillers & Packers	2012 Vol
R134a	1626
R404A & R507A	1441
R407C	587
R407A & R407F	136
R410A	626
Other HFC blends	253
Other fluorocarbon blends	513
Total	4720

Table 63: Sales volumes of the different refrigerants for 2011 and 2012

YEAR (NWEU)	InTEM 32/125	UNFCCC 32/125	InTEM 143a/125	UNFCCC 143a/125	InTEM 134a/125	UNFCCC 134a/125	InTEM 134a/32	UNFCCC 134a/32
2004	0.26	0.28	1.36	1.16	5.92	10.97	22.73	39.69
2005	0.22	0.28	1.09	1.06	5.09	9.52	22.86	34.59
2006	0.21	0.30	0.96	1.01	4.67	8.70	21.72	29.18
2007	0.26	0.32	0.97	0.96	4.50	8.17	17.53	25.68
2008	0.25	0.32	0.93	0.89	4.27	7.44	17.07	23.48
2009	0.25	0.33	0.90	0.89	3.93	7.19	15.73	21.65
2010	0.25	0.35	0.82	0.88	3.33	6.83	13.25	19.27
2011	0.27	0.37	0.78	0.83	2.95	6.39	11.13	17.45

YEAR (UK+IRE)	InTEM 32/125	UNFCCC 32/125	InTEM 143a/125	UNFCCC 143a/125	InTEM 134a/125	UNFCCC 134a/125	InTEM 134a/32	UNFCCC 134a/32
2004	0.25	0.28	1.38	0.82	5.00	10.20	20.28	36.09
2005	0.23	0.30	1.18	0.80	4.12	9.93	17.83	33.03
2006	0.23	0.29	1.08	0.72	3.87	8.32	16.67	28.71
2007	0.25	0.32	1.05	0.74	3.83	8.07	15.50	25.46
2008	0.24	0.33	1.00	0.72	3.64	7.93	15.24	23.94
2009	0.24	0.35	0.90	0.70	3.57	7.53	14.58	21.49
2010	0.24	0.35	0.85	0.63	3.57	6.38	14.58	18.34
2011	0.27	0.37	0.82	0.60	3.33	5.97	12.31	16.19

Table 64: InTEM and UNFCCC emission ratios for different combination of gases.

Finally using the information in Tables 63 and 63 we can calculate emission ratios for each pair of HFCs in the refrigerant blends (410A+404A+507A) that are reported to be most used in UK+Ireland. Table 6 summarises these results and compares them with the same ratios calculated by the NAME inversion method and UNFCCC. It is significant that there is quite close agreement between the NAME inversion determined ratios and the apparent usage of the specific refrigerant blends. We cannot use the BRA data for HFC-134a since it is only a subset of the actual usage as noted in Table 4 and therefore underestimates actual emissions.

Emission ratio	Ratios from BRA 2011 (see Table 63)	Ratios from InTEM 2011	Ratios from UNFCCC 2011
HFC-32/125	0.29	0.27	0.37
HFC-143a/125	0.77	0.82	0.60
HFC-134a/125	X	3.33	5.97
HFC-134a/32	X	12.31	16.19

Table 6: Emission ratios from BRA 2011, InTEM 2011 and UNFCCC 2011.

8 Identification of gases of potential policy interest

8.1 Introduction

In the 1970s, it was recognised that the chlorofluorocarbons (CFCs) were strong greenhouse gases that could have a substantial impact on the radiative forcing of climate change as well as being ozone-depleting substances. Subsequently, a large number of novel substances have been proposed and synthesised as potential replacements for the CFCs and these have included hydrochlorofluorocarbons (HCFCs), hydrofluorocarbons (HFCs), and perfluorocarbons (PFCs). There are therefore a large number of halocarbons and other substances, perhaps numbering over 200, which may be of potential policy interest for their contributions to the radiative forcing of climate change. It would be inconceivable to add over 200 or so novel halocarbons and other substances to the ALE/GAGE/AGAGE observation program so some preliminary assessment is in order to identify the most important substances of potential policy interest.

8.2 Concepts and definitions

8.2.1 Radiative efficiency (RE)

When a trace gas is released into the atmosphere, it may induce changes in the earth's radiation budget and this is known as radiative forcing (RF). In general terms, radiative forcing is measured in W m^{-2} and refers to the effect of a specified change in the trace gas mixing ratio, often over some specified time interval which is usually since the pre-industrial era. The radiative forcing per unit change in trace gas mixing ratio is referred to as the radiative efficiency (RE) and has W m^{-2} ppb^{-1} as its units. The concept of RE assumes that the RF is linear in trace gas mixing ratio. This is usually a good assumption for small perturbations in mixing ratios about current levels and for trace gases with low background levels as is largely the case in this study.

REs are calculated using radiative transfer models from the experimentally measured infrared absorption coefficients for each trace gas. The assumption is often made that the trace gas is well-mixed within the atmosphere. However, this is not a good assumption for short-lived trace gases for which there are no unique RE values.

REs for 235 selected halocarbons have been reviewed by Hodnerbrog *et al.*, (2013). These estimates update those provided by the IPCC (2007) in their 4th Assessment Report and also adds over a 100 additional novel halocarbons and other substances.

8.2.2 Atmospheric lifetimes

The global atmospheric lifetime of a trace gas in years is defined by the IPCC (2001) in their 3rd Assessment Report as the global atmospheric burden of the trace gas in Tg divided by the mean global sink strength of the trace gas in Tg yr^{-1}, when in steady state. Under these conditions, the global source strength (E, Tg yr^{-1}) equals the global sink strength such that:

Atmospheric lifetime (year) = burden (Tg) / source strength (Tg yr^{-1})

In this study, we have assumed an illustrative 1 Tg yr^{-1} emission source strength for all trace gases, hence in steady state:

Burden arising from 1 Tg yr^{-1} emission (Tg) = atmospheric lifetime x 1 Tg yr^{-1}

An atmospheric burden in Tg can be converted into trace gas mixing ratios in a well-mixed atmosphere using the mass of the atmosphere (5.136×10^{21} g; Trenberth and Guillemot, 1994) and the molecular mass of the trace gas and the atmosphere (28.9644 g mol^{-1}; US Standard Atmosphere, 1976). Atmospheric lifetimes are only well-defined quantities for well-mixed trace gases. There are no unique atmospheric lifetimes for short-lived trace gases because they vary with point of release to the atmosphere, with time-of-day and season and whether they are released simultaneously with other trace gases.

Halocarbons are removed from the atmosphere by two main mechanisms: reactions with hydroxyl (OH) radicals and by photolysis. Calvert *et al.,* (2008) have reviewed the mechanisms of OH-reactions and photolysis for a wide range of halocarbons. Atmospheric lifetimes have been extensively reviewed by WMO (2011) and IPCC (2007) and these reviews have been used in this study.

8.2.3 Radiative forcings per 1 Tg yr^{-1} release to the atmosphere

Hodnebrog *et al.,* (2013) provide a comprehensive and self-consistent set of calculations of radiative efficiencies REs for a large number of halocarbons. These when combined with estimates of atmospheric lifetimes from WMO (2011), allow the calculation of the instantaneous radiative forcing per 1 Tg yr^{-1} atmospheric emission for each halocarbon. These instantaneous radiative forcings per 1 Tg yr^{-1} emission were ranked in order and provide the main output of this study.

At this stage, no recognition has been given of any actual, likely or potential atmospheric emission rates for any of the substances considered. The adopted figure of 1 Tg yr^{-1} is merely illustrative and

has no policy significance. It has been chosen so that the large number of halocarbons and other substances could be ranked on a common radiative forcing basis.

The RF per 1 Tg yr^{-1} release to the atmosphere for a given trace gas was calculated using:

RF per 1 Tg yr^{-1} = burden (ppb per 1 Tg yr^{-1}) x atmospheric lifetime (yr) x RE (W m^{-2} ppb^{-1})

So for CFC-11, we estimate the steady state burden for 1 Tg yr^{-1} release as 41.05 ppt, the atmospheric lifetime is 45 years, the RE is 0.26 W m^{-2} ppb^{-1}, giving a RF per 1 Tg yr^{-1} release as 0.48 W m^{-2}. This is an instantaneous radiative forcing since pre-industrial time in steady state.

In this study, the concept of radiative forcing per 1 Tg yr^{-1} atmospheric emission has been used instead of the more commonly used policy concept of Global Warming Potential (GWP). The calculation of the GWP of a compound utilises the same input data as the radiative efficiency per 1 Tg yr^{-1} atmospheric emission in terms of molecular mass, RE and atmospheric lifetime. However, the GWP has distinct disadvantages in that this index involves integrating over a time horizon and expressing the results relative to carbon dioxide. In contrast, the radiative efficiency per 1 Tg yr^{-1} is an instantaneous property of the halocarbon that is independent of our understanding of the atmospheric physics and biogeochemistry of carbon dioxide and obviates policy discussions of time horizons.

8.3 Estimated radiative forcings of halocarbons per 1 Tg yr^{-1} atmospheric emission

The instantaneous radiative forcings per 1 Tg yr^{-1} atmospheric emission were estimated for 223 selected substances as described above in section 2.3. These estimates were then ranked in order from the highest to the lowest, as shown in Table 1.

Carbon tetrafluoride (PFC-14, CF_4) is the highest ranked halocarbon in Table 1, by a large margin. Its radiative efficiency is relatively small and so it appears in this position solely by virtue of its exceedingly long atmospheric lifetime. The second highest ranked halocarbon in Table 1 is PFC-116, C_2F_6, the next member in the homologous series of perfluorocarbons after CF_4. PFC-116 shows a RF per 1 Tg yr^{-1} emission that is close to a factor of three lower than PFC-14. Although the RE of PFC-116 is much higher than that of PFC-14, its atmospheric lifetime is estimated to be much shorter, hence it appears in second place.

The third ranked substance in Table 1 is sulphur hexafluoride, SF_6, which appears with this ranking because of its long atmospheric lifetime and its high RE. SF_6 is not classed as a halocarbon but is a fully fluorinated substance. Other substances in this class include trifluoromethyl sulphur pentafluoride, SF_5CF_3, which is ranked in 12th position, nitrogen trifluoride NF_3 which appears in 17th position and sulphuryl fluoride in 40th position.

Of the top-10 ranked substances, all but one are perfluorocarbons. Of these, seven: PFC-14, PFC-116, PFC-41-12, PFC-51-14, PFC-61-16 and PFC-71-18 are all perfluorinated alkanes and two: PFC-31-10 and PFC-216 are perfluorinated cycloalkanes. They are all ranked highly because of their long atmospheric lifetimes and strong REs. Ranked in 11th, 13th and 14th positions are various perfluorodecalin species which also exhibit long atmospheric lifetimes and strong REs. In summary, there are 12 perfluorocarbons in the list of 223 halocarbons and other substances and they all fall within the top-15 of the rankings.

After the perfluorocarbons and other perfluorinated substances, the next most important class of substances in the rankings are the chlorofluorocarbons: CFC-13 (ranked 16th) and CFC-115 (ranked 18th). These species are highly ranked because of their long atmospheric lifetimes (over 500 years) and their modest REs. Other chlorofluorcarbons appear further down the rankings, see for example: CFC-114 (ranked 22nd), CFC-12 (ranked 23rd), CFC-113 (ranked 24th) and CFC-11 (ranked 35th). This latter group appear lower down the rankings because their atmospheric lifetimes fall in the range of up to 200 years and below.

The fourth most important class of halocarbons and other substances are the hydrofluoroethers HFEs. Perfluoro poly methyl isopropyl ether (PFPMIE) appears at 15th in the rankings because of its long atmospheric lifetime and strong RE. HFE-125 appears at 21st in the rankings because its atmospheric lifetime is over 100 years and it also has a strong RE. Other HFEs appear at ranking 28th (HFE-329mcc2), 29th (HFE-227ea), 30th (HG-20), 31st (HFE-134), 33rd (HFE-236ca12), 34th (1,1'-oxybis[2-fluoromethoxy)-1,1,2,2-tetrafluoroethane), 36th (HFE-338mmzl, 38th (HFE-329me3) because their atmospheric lifetimes are only up to 50 years or so.

The next most important class of halocarbons and other substances are the hydrofluorocarbons HFCs. HFC-23 appears at 19th in the rankings, followed by HFC-236fa (ranked 20th). These substances have lifetimes in excess of 200 years and modest REs. Other HFCs appear at rank 32nd (HFC-143a), rank 37th (HFC-245cb), rank 44th (HFC-227ea), rank 50th (HFC-227ca). These substances have atmospheric lifetimes less than 50 years and, again, modest REs.

8.4 Consequences for the AGAGE program

Out of the 223 halocarbons in this study, 38 are monitored by the AGAGE program, ~17%. These are highlighted in Table 153. However, out of the top 10 most radiatively-active halocarbons in Table 153, one half are monitored by AGAGE. So there is a focus on the most radiatively-active trace gases already within the AGAGE program. Looking at Table 1, a few halocarbons, particularly perfluorocarbons, would make suitable candidates for inclusion in the AGAGE program at some future date. The candidate compounds include: PFC-41-12, PFC-51-14, PFC-61-16, PFC-71-18 and perfluorodecalin.

Table 153: Chemical formulae and radiative efficiencies in W m^{-2} per 1 Tg yr^{-1} atmospheric emission of 223 selected halocarbons and other substances. Halocarbons monitored by the AGAGE program are highlighted.

	Substance	Formulae	Radiative Efficiency W m^{-2} / Tg yr^{-1}
79	PFC-14	CF_4	288.37
80	PFC-116	C_2F_6	102.16
76	sulphur hexafluoride	SF_6	70.43
85	PFC-41-12	n-C_5F_{12}	32.91
83	PFC-31-10	c-C_4F_8	28.87
81	PFC-216	c-C_3F_6	25.94
86	PFC-51-14	n-C_6F_{14}	22.76
82	PFC-218	C_3F_8	21.84
87	PFC-61-16	n-C_7F_{16}	21.80
88	PFC-71-18	n-C_8F_{18}	21.24
90	perfluorodecalin (cis)	cis $C_{10}F_{18}$	13.67
77	trifluoromethyl sulphur pentafluoride	SF_5CF_3	13.58
89	perfluorodecalin (mixed)	$C_{10}F_{18}$	13.42
91	perfluorodecalin (trans)	trans $C_{10}F_{18}$	11.72
170	perfluoro poly methyl isopropyl ether PFPMIE	$CF_3OCF(CF_3)OCF_2OCF_3$	8.73
3	CFC-13	$CClF_3$	8.64
75	nitrogen trifluoride	NF_3	7.94
6	CFC-115	$CClF_2CF_3$	7.45
20	HFC-23	CHF_3	3.22
35	HFC-236fa	$CF_3CH_2CF_3$	2.15
97	HFE-125	CHF_2OCF_3	2.02
2	CFC-12	CCl_2F_2	1.49
4	CFC-113	CCl_2FCClF_2	0.77
210	1,1,1,2,2,3,3-heptafluoro-3-(1,2,2,2-tetrafluoroethoxy)propane	$CF_3CF_2CF_2OCHFCF_3$	0.77
70	halon-1301	$CBrF_3$	0.74
148	HG-30	$HF_2C(OCF_2)_3OCF_2H$	0.74
114	HFE-329mcc2	$CHF_2CF_2OCF_2CF_3$	0.73
100	HFE-227ea	$CF_3CHFOCF_3$	0.69
146	HG-20	$HF_2C(OCF_2)_2OCF_2H$	0.52
98	HFE-134 HG-00	CHF_2OCHF_2	0.51
27	HFC-143a	CH_3CF_3	0.51
141	HFE-236ca12 HG-10	$CHF_2OCF_2OCHF_2$	0.50
221	1,1'-oxybis[2-(fluoromethoxy)-1,1,2,2-tetrafluoroethane	$HF_2CO(CF_2CF_2O)_2CF_2H$	0.48
1	CFC-11	CCl_3F	0.48
115	HFE-338mmz1	$(CF_3)_2CHOCHF_2$	0.48
37	HFC-245cb	$CF_3CF_2CH_3$	0.48
164	HFE-329me3	$CF_3CFHCF_2OCF_3$	0.46
222	1,1,3,3,4,4,6,6,7,7,9,9,10,10,12,12-hexadecafluoro-2,5,8,11-tetraoxadodecane	$HCF_2O(CF_2CF_2O)_3CF_2H$	0.45
78	sulphuryl fluoride	SO_2F_2	0.40
103	HFE-236ca	$CHF_2OCF_2CHF_2$	0.39
223	1,1,3,3,4,4,6,6,7,7,9,9,10,10,12,12,13,13,15,15-	$HCF_2O(CF_2CF_2O)_4CF_2H$	0.37

	eicosafluoro-2,5,8,11,14-pentaoxapentadecane		
147	HG-21	$HF_2COCF_2CF_2OCF_2OCF_2OCF_2H$	0.36
32	HFC-227ea	CF_3CHFCF_3	0.34
23	HFC-125	CHF_2CF_3	0.30
144	HG-02	$HF_2C(OCF_2CF_2)_2OCF_2H$	0.29
134	HFE-43-10pccc (H-Galden 1040x, HG-11)	$CHF_2OCF_2OC_2F_4OCHF_2$	0.27
142	HFE-338pcc13 HG-01	$CHF_2OCF_2CF_2OCHF_2$	0.27
145	HG-03	$HF_2C(OCF_2CF_2)_3OCF_2H$	0.27
31	HFC-227ca	$CF_3CF_2CHF_2$	0.25
43	HFC-329p	$CHF_2CF_2CF_2CF_3$	0.23
45	HFC-43-10mee	$CF_3CHFCHFCF_2CF_3$	0.19
16	HCFC-142b	CH_3CClF_2	0.18
116	HFE-338mcf2	$CF_3CH_2OCF_2CF_3$	0.17
104	HFE-236ea2 desfluorane	$CHF_2OCHFCF_3$	0.16
8	HCFC-22	$CHClF_2$	0.16
60	carbon tetrachloride	CCl_4	0.16
69	halon-1211	$CBrClF_2$	0.16
74	halon-2402	$CBrF_2CBrF_2$	0.13
34	HFC-236ea	CHF_2CHFCF_3	0.12
25	HFC-134a	CH_2FCF_3	0.12
208	1,1,2-trifluoro-2-(trifluoromethoxy)-ethane	$CHF_2CHFOCF_3$	0.12
33	HFC-236cb	$CH_2FCF_2CF_3$	0.11
24	HFC-134	CHF_2CHF_2	0.10
105	HFE-236fa	$CF_3CH_2OCF_3$	0.0906
124	HFE-356pcf2	$CHF_2CH_2OCF_2CHF_2$	0.0814
120	HFE-347pcf2	$CHF_2CF_2OCH_2CF_3$	0.0812
151	1,1,2,2-tetrafluoro-1-(fluoromethoxy)ethane	$CH_2FOCF_2CF_2H$	0.0792
119	HFE-347mcf2	$CHF_2CH_2OCF_2CF_3$	0.0781
40	HFC-245fa	$CHF_2CH_2CF_3$	0.0777
118	HFE-347mcc3 HFE-7000	$CH_3OCF_2CF_2CF_3$	0.0770
107	HFE-245fa1	$CHF_2CH_2OCF_3$	0.0769
108	HFE-245fa2	$CHF_2OCH_2CF_3$	0.0744
44	HFC-336mfc	$CH_3CF_2CH_2CF_3$	0.0729
15	HCFC-141b	CH_3CCl_2F	0.0710
157	trifluoro(fluoromethoxy)methane	CH_2FOCF_3	0.0694
36	HFC-245ca	$CH_2FCF_2CHF_2$	0.0656
21	HFC-32	CH_2F_2	0.0620
106	HFE-245cb2	$CF_3CF_2OCH_3$	0.0608
156	difluoro(fluoromethoxy)methane	CH_2FOCHF_2	0.0558
101	HCFE-235ca2 enflurane	CHF_2OCF_2CHFCl	0.0539
173	trifluoromethyl formate	$HCOOCF_3$	0.0537
174	perfluoroethyl formate	$HCOOCF_2CF_3$	0.0529
13	HCFC-124	$CHClFCF_3$	0.0488
99	HFE-143a	CH_3OCF_3	0.0487
18	HCFC-225cb	$CHClFCF_2CClF_2$	0.0475
130	HFE-374pc2	$CHF_2CF_2OCH_2CH_3$	0.0465
102	HCFE-235da2 isofluorane	$CHF_2OCHClCF_3$	0.0449
136	n-HFE-7100	$n\text{-}C_4F_9OCH_3$	0.0445
125	HFE-356pcf3	$CHF_2OCH_2CF_2CHF_2$	0.0412

135	HFE-449sl (HFE-7100)	$C_4F_9OCH_3$	0.0382
126	HFE-356pcc3	$CH_3OCF_2CF_2CHF_2$	0.0377
137	i-HFE-7100	i-$C_4F_9OCH_3$	0.0371
176	perfluorobutyl formate	$HCOO(CF_2)_3CF_3$	0.0359
122	HFE-356mec3	$CH_3OCF_2CHFCF_3$	0.0353
179	1,2,2,2-tetrafluoroethyl formate	$HCOOCHFCF_3$	0.0343
175	perfluoropropyl formate	$HCOOCF_2CF_2CF_3$	0.0343
12	HCFC-123a	$CHClFCF_2Cl$	0.0339
67	halon-1201	$CHBrF_2$	0.0336
121	HFE-347mmy1	$(CF_3)_2CFOCH_3$	0.0334
117	HFE-347mmz1 sevofluorane	$(CF_3)_2CHOCH_2F$	0.0310
14	HCFC-132c	CH_2FCFCl_2	0.0306
26	HFC-143	CH_2FCHF_2	0.0305
180	1,1,1,3,3,3-hexafluoropropan-2-yl formate	$HCOOCH(CF_3)_2$	0.0304
110	HFE-254cb1	CH_3OCF_2CHF2	0.0278
39	HFC-245eb	$CH_2FCHFCF_3$	0.0261
10	HCFC-122a	$CHFClCFCl_2$	0.0238
159	HG'-02	$CH_3O(CF_2CF_2O)_2CH_3$	0.0227
160	HG'-03	$CH_3O(CF_2CF_2O)_3CH_3$	0.0218
38	HFC-245ea	$CHF_2CHFCHF_2$	0.0215
68	halon-1202	CBr_2F_2	0.0210
73	halon-2401	$CHFBrCF_3$	0.0172
143	1,1,1,3,3,3-hexafluoropropan-2-ol	$(CF_3)_2CHOH$	0.0166
71	halon-2301	CH_2BrCF_3	0.0165
158	HG'-01	$CH_3OCF_2CF_2OCF_3$	0.0151
59	methyl chloroform	CH_3CCl_3	0.0148
7	HCFC-21	$CHCl_2F$	0.0140
154	difluoromethoxymethane	CH_3OCHF_2	0.0129
42	HFC-272ca	$CH_3CF_2CH_3$	0.0128
155	fluoro(fluoromethoxy)methane	CH_2FOCH_2F	0.0118
17	HCFC-225ca	$CHCl_2CF_2CF_3$	0.0116
169	2-chloro-1,1,2-trifluoro-1-methoxyethane	CH_3OCF_2CHFCl	0.0112
29	HFC-152a	CH_3CF_3	0.0101
22	HFC-41	CH_3F	0.0093
185	methyl carbonofluoridate	$FCOOCH_3$	0.0091
11	HCFC-123	$CHCl_2CF_3$	0.0072
41	HFC-263fb	$CH_3CH_2CF_3$	0.0069
9	HCFC-122	$CHCl_2CF_2Cl$	0.0063
139	n-HFE-7200	n-$C_4F_9OC_2H_5$	0.0060
149	1-ethoxy-1,1,2,2,3,3,3-heptafluoropropane	$CF_3CF_2CF_2OCH_2CH_3$	0.0059
129	HFE-365mcf2	$CF_3CF_2OCH_2CH_3$	0.0054
138	HFE-569sf2 HFE-7200	$C_4F_9OC_2H_5$	0.0051
152	2-ethoxy-3,3,4,4,5-pentafluorotetrahydro-2,5-bis(1,2,2,2-tetrafluoro-1-trifluoromethyl)ethyl)-furan	$C_{12}H_5F_{19}O_2$	0.0051
201	methyl-2,2,2-trifluoroacetate	CF_3COOCH_3	0.0048
140	i-HFE-7200	i-$C_4F_9OC_2H_5$	0.0043
72	halon-2311	$CHBrClCF_3$	0.0037
207	2,2,3,3,4,4,4-heptafluorobutan-1-ol	$CF_3(CF_2)_2CH_2OH$	0.0034
177	2,2,2-trifluoroethyl formate	$HCOOCH_2CF_3$	0.0028
195	1,1-difluoroethyl-2,2,2-trifluoroacetate	$CF_3COOCF_2CH_3$	0.0028

112	HFE-263ml	$CF_3OCH_2CH_3$	0.0026
206	difluoromethyl-2,2,2-trifluoroacetate	$CF_3COOCHF_2$	0.0025
191	1,1-difluoroethyl carbonofluoridate	$FCOOCF_2CH_3$	0.0022
209	1-ethoxy-1,1,2,3,3,3-hexafluoropropane	$CF_3CHFCF_2OCH_2CH_3$	0.0022
123	HFE-356mff2	$CF_3CH_2OCH_2CF_3$	0.0019
220	2,2,2-trifluorethanol	CF_3CH_2OH	0.0017
109	2,2,3,3,3-pentafluoropropan-1-ol	$CF_3CF_2CH_2OH$	0.0016
178	3,3,3-trifluoropropyl formate	$HCOO(CH_2)_2CF_3$	0.0015
212	2,2,3,4,4,4-hexafluoro-1-butanol	$CF_3CHFCF_2CH_2OH$	0.0015
63	chloroform	$CHCl_3$	0.0015
28	HFC-152	CH_2FCH_2F	0.0014
213	2,2,3,3,4,4,4-heptafluorobutan-1-ol	$CF_3CF_2CF_2CH_2OH$	0.0014
127	HFE-356mmz1	$(CF_3)_2CHOCH_3$	0.0012
153	fluoromethoxymethane	CH_3OCH_2F	0.0012
133	2,2,3,3,4,4,5,5-octafluoro cyclopentanol HFE-43-10pccc HG-11 H-Galden1040x HFE-449sl HFE 7100	$-(CF_2)_4CH(OH)-$	0.0012
211	2,2,3,3-tetrafluoro-1-propanol	$CHF_2CF_2CH_2OH$	0.0012
61	methyl chloride	CH_3Cl	0.0011
62	methylene dichloride	CH_2Cl_2	0.000797
199	2,2,2-trifluoroethyl-2,2,2-trifluoroacetate	$CF_3COOCH_2CF_3$	0.000648
219	2,2-difluoroethanol	CHF_2CH_2OH	0.000301
205	methyl-2,2-difluoroacetate	HCF_2COOCH_3	0.000281
183	perfluoroethyl acetate	$CH_3COOCF_2CF_3$	0.000190
184	trifluoromethyl acetate	CH_3COOC_{F3}	0.000185
84	perfluoro cyclopentene	$c\text{-}C_5F_8$	0.000181
30	HFC-161	CH_3CH_2F	0.000170
96	perfluorobut-2-ene	$CF_3CF=CFCF_3$	0.000168
182	perfluoropropyl acetate	$CH_3COO(CF_2)_2CF_3$	0.000163
181	perfluorobutyl acetate	$CH_3COO(CF_2)_3CF_3$	0.000146
53	(Z)-HFC-1336	(Z) $CF_3CH=CHCF_3$	0.000145
111	HFE-263fb2	$CF_3CH_2OCH_3$	0.000125
19	(E)-1-chloro-3,3,3-trifluoroprop-1-ene	trans-$CF_3CH=CHCl$	0.000123
198	ethyl-2,2,2-trifluoroacetate	$CF_3COOCH_2CH_3$	0.000119
64	1,2-dichloroethane	CH_2ClCH_2Cl	0.000101
218	2-fluoroethanol	CH_2FCH_2OH	0.000098
66	methylene dibromide	CH_2Br_2	0.000097
128	HFE-365mcf3	$CF_3CF_2CH_2OCH_3$	0.000091
52	Z-HFC-1234ze	(Z) $CF_3CH=CHF$	0.000089
166	3,3,4,4,5,5,6,6,7,7,7-undecafluoroheptan-1-ol	$CF_3(CF_2)_4CH_2CH_2OH$	0.000059
167	3,3,4,4,5,5,6,6,7,7,8,8,9,9,9-pentadecafluorononan-1-ol	$CF_3(CF_2)_6CH_2CH_2OH$	0.000052
214	1,1,2,2-tetrafluoro-3-methoxypropane	$CHF_2CF_2CH_2OCH_3$	0.000045
113	3,3,3-trifluoropropan-1-ol	$CF_3CH_2CH_2OH$	0.000033
168	3,3,4,4,5,5,6,6,7,7,8,8,9,9,10,10,11,11,11-nonadecafluoroundecan-1-ol	$CF_3(CF_2)_8CH_2CH_2OH$	0.000030
51	HFC-1234yf	$CF_3CF=CH_2$	0.000028
50	(Z)-HFC-1234ze	(Z) $CF_3CH=CHF$	0.000027
48	(Z)-HFC-1225ye	(Z) $CF_3CF=CHF$	0.000020
171	HFE-216	$CF_3OCF=CF_2$	0.000016
56	3,3,4,4,5,5,6,6,6-nonafluorohex-1-ene	$C_4F_9CH=CH_2$	0.000014

55	HFC-1345zfc	$CF_3CH=CH_2$	0.000012
54	HFC-1243zf	$CF_3CH=CH_2$	0.000011
215	perfluoro-2-methyl-3-pentanone	$CF_3CF_2C=OCF(CF_3)_2$	0.000010
57	3,3,4,4,5,5,6,6,7,7,8,8,8-tridecafluorooct-1-ene	$C_6F_{13}CH=CH_2$	0.000010
95	perfluorobut-1-ene	$CF_3CF_2CF=CF_2$	0.00000927
58	3,3,4,4,5,5,6,6,7,7,8,8,9,9,10,10,10-heptafluorodec-1-ene	$C_8F_{17}CH=CH_2$	0.00000790
49	€-HFC-1225ye	(E) $CF_3CF=CHF$	0.00000573
93	PFC-1216	$CF_3CF=CF_2$	0.00000505
131	4,4,4-trifluorobutan-1-ol	$CF_3CH_2CH_2CH_2OH$	0.00000482
150	fluoroxene	$CF_3CH_2OCH=CH_2$	0.00000434
46	HFC-1132a	$CH_2=CF_2$	0.00000000
47	HFC-1141	$CH_2=CHF$	0.00000000
65	methyl bromide	CH_3Br	0.00000000
92	PFC-1114	$CF_2=CF_2$	0.00000000
94	perfluorobuta-1,3-diene	$CF_2=CFCF=CF_2$	0.00000000
132	1,1,1,3,3,3-hexafluoro-2-(trifluoromethyl)-2-propanol	$(CF_3)_3COH$	0.00000000
161	HG'-10	$CH_3OCF_2OCH_3$	0.00000000
162	HG'-20	$CH_3O(CF_2O)_2CH_3$	0.00000000
163	HG'-30	$CH_3O(CF_2O)_3CH_3$	0.00000000
165	HFE-338mec3	$CF_3CFHCF_2OCF_3$	0.00000000
172	trifluoro(trifluoromethoxy)methane	CF_3OCF_3	0.00000000
186	fluoromethyl carbonofluoridate	$FCOOCH_2F$	0.00000000
187	difluoromethyl carbonofluoridate	$FCOOCHF_2$	0.00000000
188	trifluoromethyl carbonofluoridate	$FCOOCF_3$	0.00000000
189	perfluoroethyl carbonofluoridate	$FCOOCF_2CF_3$	0.00000000
190	2,2,2-trifluoroethyl carbonofluoridate	$FCOOCH_2CF_3$	0.00000000
192	perfluoropropyl carbonofluoridate	$FCOO(CF_2)_2CF_3$	0.00000000
193	trifluoromethyl-2,2,2-trifluoroacetate	CF_3COOCF_3	0.00000000
194	perfluoroethyl-2,2,2-trifluoroacetate	$CF_3COOCF_2CF_3$	0.00000000
196	1,1,1,3,3,3-hexafluoropropan-2-yl 2,2,2-trifluoroacetate	$CF_3COOCH(CF_3)_2$	0.00000000
197	vinyl-2,2,2-trifluoroacetate	$CF_3COOCH=CH_2$	0.00000000
200	allyl-2,2,2-trifluoroacetate	$CF_3COOCH_2CH=CH_2$	0.00000000
202	phenyl-2,2,2-trifluoroacetate	$CF_3COOC_6H_5$	0.00000000
203	methyl-2-fluoroacetate	$H_2CFCOOCH_3$	0.00000000
204	difluoromethyl-2,2-difluoroacetate	$HCF_2COOCHF_2$	0.00000000
216	3,3,3-trifluoropropanal	CF_3CH_2CHO	0.00000000
217	4,4,4-trifluorobutanal	$CF_3(CH_2)_2CHO$	0.00000000

9 References

Arnold, T., C.M. Harth, J. Mühle, A.J. Manning, P.K. Salameh, J. Kim, D.J. Ivy, L.P. Steele, V.V. Petrenko, J.P. Severinghaus, D. Baggenstos, and R.F. Weiss, Nitrogen trifluoride global emissions estimated from updated atmospheric measurements, PNAS 2013 110 (6) 2029-2034, 2013, doi:10.1073/pnas.1212346110

Bergamaschi, P., M. Krol, F. Dentener, A. Vermeulen, F. Meinhardt, R. Graul, M. Ramonet, W. Peters, and E. J. Dlugokencky (2005), Inverse modeling of national and European CH4 emissions using the atmospheric zoom model TM5, Atmos. Chem. Phys., 5, 2431-2460.

Bloom, A.A, P.I. Palmer, A. Fraser, D.S. Reay, and C. Frankenberg, Large-scale controls of methanogenesis inferred from methane and gravity spaceborne data, Science, 327 (5963), 322-325, doi: 10.1126/science.1175176, 2010

Calvert, J.G., Derwent, R.G., Orlando, J.J., Tyndall, G.S., Wallington, T.J., 2008. Mechanisms of atmospheric oxidation of the alkanes. Oxford University Press, New York, USA.

Cox, M. L., G. A. Sturrock, P. J. Fraser, S. T. Siems, P. B. Krummel and S. O'Doherty, Regional sources of methyl chloride, chloroform and dichloromethane identified from AGAGE observations at Cape Grim, Tasmania, 1998-2000, J. Atmos. Chem., 45 (1): 79-99, 2003

Daniel, J.S., and G.J.M Velders (Lead Authors), A.R. Douglass, P.M.D. Forster, D.A. Hauglustaine, I.S.A. Isaksen, L.J.M. Kuijpers, A. McCulloch, and T.J. Wallington, Halocarbon scenarios, ozone depletion potentials, and global warming potentials, Chapter 8 in Scientific Assessment of Ozone Depletion: 2006, Global Ozone Research and Monitoring, Project—Report No. 50, 572 pp., World Meteorological Organization, Geneva, Switzerland, 2007.

Dlugokencky, E. J., R. C. Myers, P. M. Lang, K. A. Masarie, A. M. Crotwell, K. W. Thoning, B. D. Hall, J. W. Elkins, and L. P. Steele, Conversion of NOAA atmospheric dry air CH4 mole fractions to a gravimetrically prepared standard scale, Journal of Geophysical Research: Atmospheres, 110(D18), doi:10.1029/2005JD006035.

Forster, P., P. Ramaswamy, T. Artaxo, R. Berntsen, D. Betts, J. Fahey, J. Haywood, D. Lean, G. Lowe, J. Myhre, R. Nganga, R. Prinn, M. Raga R. Schulz & R. van Dorland (lead authors), Changes in Atmospheric Constituents and in Radiative Forcing, Chapter 2 in Climate Change 2007: the Physical Science Basis, contribution of Working Group I to the Fourth Assessment Report of the Intergovernmental Panel on Climate Change, Cambridge University Press, 129-234, 2007.

Fraser, P.J., D.E. Oram, C.E. Reeves, S.A. Penkett, and A. McCulloch, Southern Hemispheric halon trends (1978-1998) and global halon emissions, J. Geophys. Res., 104 (D13), 1598515999, 1999.

Hammer, S., D. W. T. Griffith, G. Konrad, S. Vardag, C. Caldow, and I. Levin, Assessment of a multi-species in-situ FTIR for precise atmospheric greenhouse gas observations, Atmos. Meas. Tech. Discuss., 5, 3645-3692, 2012 www.atmos-meas-tech-discuss.net/5/3645/2012/ doi:10.5194/amtd-5-3645-2012

Hodnebrog, O., Etminan, M., Fuglestvedt, J.S., Marston, G., Myhre, G., Nielsen, C.J., Shine, K.P., Wallington, T.J., 2013. Global warming potentials and radiative efficiencies of halocarbons and related compounds: A comprehensive review. Reviews of Geophysics 51, 1-79.

IPCC, 2001. Climate Change 2001: The scientific basis. Cambridge University Press, Cambridge, UK.

IPCC, 2007. Climate Change 2007: The physical science basis. Cambridge University Press, Cambridge, UK.

Ivy, D. J., T. Arnold, C. M. Harth, L. P. Steele, J. Mühle, M. Rigby, P. K. Salameh, M. Leist, P. B. Krummel, P. J. Fraser, R. F. Weiss, and R. G. Prinn, Atmospheric histories and growth trends of C_4F_{10}, C_5F_{12}, C_6F_{14}, C_7F_{16} and C_8F_{18}, Atmos. Chem. Phys., 12(9), 4313–4325, doi:10.5194/acp-12-4313-2012, 2012a.

Ivy, D. J., M. Rigby, M. Baasandorj, J. B. Burkholder, and R. G. Prinn, Global emission estimates and radiative impact of C_4F_{10}, C_5F_{12}, C_6F_{14}, C_7F_{16} and C_8F_{18}, Atmos. Chem. Phys., 12(16), 7635–7645, doi:10.5194/acp-12-7635-2012, 2012b.

Keene, W.C., M.A.K. Khalil, D.J. Erickson, A. McCulloch, T.E. Graedel, J.M. Lobert, M.L. Aucott, S.L. Gong, D.B. Harper, G. Kleiman, P. Midgley, R.M. Moore, C. Seuzaret, W.T. Sturges, C.M. Benkovitz, V. Koropalov, L.A. Barrie, and Y.F. Li, Composite global emissions of reactive chlorine from anthropogenic and natural sources: Reactive Chlorine Emissions Inventory, J. Geophys. Res., 104 (D7), 8429-8440, doi: 10.1029/1998JD100084, 1999.

Kim, J, et al., Geophys. Res. Lett., 37. doi:101029/2010GL043263,2010.

Ko, M., P. Newman, S. Reimann, S. Strahan (Eds.), SPARC Report on the Lifetimes of Stratospheric Ozone-Depleting Substances, Their Replacements, and Related Species, SPARC Report No. 6, WCRP-15/2013.

Lehman, S.J., Miller, J.B., Tans, P.P, Monzka, S.A., Sweeney, C., Andrews, A., Turnbull, J.C., and J. Southon (2012) $14CO_2$ Processing and Measurement Activities at CU-INSTAAR and NOAA/ESRL 16th WMO/IAEA Meeting on Carbon Dioxide, Other Greenhouse Gases, and Related Measurement Techniques (GGMT-2011), (Wellington, NZ, 25-28 Oct. 2011), World Meteorological Organization Global Atmosphere Watch Report No. 206, Geneva CH., p. 139-144.

Li, S, et al., Environ Sci & Technol.,45, 5668-5675, 2012.

Logan, J.A., Staehelin, J., Megretskaia, I.A., Cammas, J.-P, Thouret, V., Claude, H., De Backer, H., Steinbacher, M., Scheel, H.-E., Stubi, R.,Frohlich, M., and Derwent, R. Changes in ozone over Europe: Analysis ofozone measurements from sondes, regular aircraft (MOZAIC) and alpine surfacesites. Journal of Geophys.Res., 117,D09301,doi:10.1029/2011JD016952.

Manning, A. J et al., J. Geophys. Res., 108, 4405, doi:101029/2002JD002312,2003.

Miller, J.B.*, Lehman, S.J.*, Montzka, S.A., Sweeney,C., Miller, B.R., Karion, A., Wolak, C., Miller, L., Dlugokencky, E.J., Southon, J., Turnbull, J.C. and P. P. Tans (2012). Linking emissions of fossil fuel CO_2 and other anthropogenic trace gases using atmospheric $^{14}CO_2$. Journal of Geophysical Research 117,D08302, 23 pp., doi:10.1029/2011JD017048.

Montzka, S. A. and Reimann, S.: Ozone-depleting substances (ODSs) and related chemicals, in: Scientific Assessment of Ozone Depletion: 2010, Global Ozone Research and Monitoring Project, Rep. 52, World Meteorol. Org., Geneva, Switzerland, 1–108, 2011.

NASA (1994), Report on Concentrations, Lifetimes, and Trends of CFCs, Halons, and Related Species, J. A. Kaye, S. A. Penkett, F. M. Ormond (Eds.), NASA RP 1339.

O'Doherty, S., D. M. Cunnold, B. R. Miller, J. Mühle, A. McCulloch, P. G. Simmonds, A. J. Manning, S. Reimann, M. K. Vollmer, B. R. Greally, R. G. Prinn, P. J. Fraser, L. P. Steele, P. B. Krummel, B. L. Dunse, L. W. Porter, C. R. Lunder, N. Schmidbauer, O. Hermansen, P. K. Salameh, C. M. Harth, R. H. J. Wang, and R. F. Weiss, Global and regional emissions of HFC-125 (CHF2CF3) from in situ and air archive atmospheric observations at AGAGE and SOGE observatories, J. Geophys. Res., 114, D23304, doi:10.1029/2009 D012184, 2009.

Oram, D. E., Mani, F. S., Laube, J. C., Newland, M. J., Reeves, C. E., Sturges, W. T., Penkett, S. A., Brenninkmeijer, C. A. M., Rockmann, T., and Fraser, P. J.: Long-term tropospheric trend of

octafluorocyclobutane (c-C_4F_8 or PFC-318), Atmos. Chem. Phys., 12, 261–269, doi:10.5194/acp-12-261-2012

Parrish, D.D., Law, K.S., Staehelin, J., Derwent, R., Cooper, O.R.,Tanimotot, H., Volz-Thomas, A., Gilge, S., Scheel, H.-E., Steinbacher, M.,and Chan, E. Long-term changes in lower tropospheric baseline ozone concentrations at northern mid-latitudes. Atmos. Chem. Phys., 12, 11485-11504, 2012.

Parrish, D.D., Law, K.S., Staehelin, J., Derwent, R., Cooper, O.R.,Tanimotot, H., Volz-Thomas, A., Gilge, S., Scheel, H.-E., Steinbacher, M.,and Chan, E. Lower tropospheric ozone at northern mid-latitudes: Changing seasonal cycle. Geophys. Res. Letters, 40, 1-6, 2013, DOI: 10.1002/grl.50303, 2013.

Prather, M.J, and J. Hsu, NF_3, the greenhouse gas missing from Kyoto, J. Geophys. Res. Letters, 35, L12810, doi:10.1029/2008GL034542, 2008.

Press, W. H., S. A. Teukolsky, W. T. Vetterling, and B. P. Flannery, Numerical Recipes in Fortran: The art of scientific computing, 2nd edition, Publ. Cambridge University Press, UK, 1992.

Prinn, R. G., and R. Zander (Lead Authors), D. M. Cunnold, J. W. Elkins, A. Engel, P. J. Fraser, M. R. Gunson, M. K. W. Ko, E. Mahieu, P. M. Midgley, J. M. Russell III, C. M. Volk, and R. F.Weiss, Long- lived ozone- related compounds, Chapter 1 in Scientific Assessment of Ozone Depletion: 1998, Global Ozone Research and Monitoring Project–Report No. 44, WorldMeteorological Organization, Geneva, Switzerland, 1999.
http://www.esrl.noaa.gov/csd/assessments/ozone/1998/

Prinn, R.G., R.F. Weiss, P.J. Fraser, P.G. Simmonds, D.M. Cunnold, F.N. Alyea, S. O'Doherty, P. Salameh, B.R. Miller, J. Huang, R.H.J. Wang, D.E. Hartley, C. Harth, L.P. Steele, G. Sturrock, P.M. Midgley, and A. McCulloch, A history of chemically and radiatively important gases in air deduced from ALE/GAGE/AGAGE, J. Geophys. Res., 115, 17751-17792, 2000.

Rigby, M., R. G. Prinn, S. O'Doherty, S. A. Montzka, A. McCulloch, C. M. Harth, J. Mühle, P. K. Salameh, R. F. Weiss, D. Young, P. G. Simmonds, B. D. Hall, G. S. Dutton, D. Nance, D. J. Mondeel, J. W. Elkins, P. B. Krummel, L. P. Steele, and P. J. Fraser, Re-evaluation of the lifetimes of the major CFCs and CH3CCl3 using atmospheric trends, Atmos. Chem. Phys., 13(5), 2691–2702, doi:10.5194/acp-13-2691-2013, 2013.

Rigby, M., A. J. Manning, and R. G. Prinn, The value of high-frequency, high-precision methane isotopologue measurements for source and sink estimation, Journal of Geophysical Research, 117(D12), D12312, doi:10.1029/2011JD017384, 2012.

Trenberth, K.E., Guillemot, C.J., 1994. Total mass of the atmosphere. Journal of Geophysical Research 99, 23079-23088.

Turnbull, J.C., Lehman, S.J., Miller, J.B., Tans, P., Sparks, R.J., and J. Southon. (2007). A new high-precision $^{14}CO_2$ time series for North American continental air. Journal of Geophysical Research doi:10.1029/2006JD008184, 10 pp.

Turnbull, J.C., Lehman, S.J., Morgan, S. and C. Wolak (2010). A new automated extraction system of ^{14}C measurement in atmospheric CO_2. Radiocarbon 52, 1261-9.

UNEP (United Nations Environment Program), 2002 Report of the Solvents, Coatings and Adhesives Technical Options Committee - 2002 Assessment (STOC 2002), edited by B. Ellis, UNEP Ozone Secretariat, Nairobi, Kenya. 2003.

US Standard Atmosphere, 1976. United States Government Printing Office, Washington DC, USA.
WMO, 2011. Scientific assessment of ozone depletion: 2010. Global Ozone Research and Monitoring Project-Report No.50, World Meteorological Organization, Geneva, Switzerland.

Vaughn, B.H., Ferretti, D., Miller, J., James W. C. White, 2004: Stable isotope measurements of atmospheric CO_2 and CH_4. Handbook of Stable Isotope Analytical Techniques, volume 1, ch.14. Elsiever, 272-304

Velders, G. J. M., Fahey, D. M., Daniel, J. S., McFarland, M., Andersen, S. O.: The large contribution of projected HFC emissions to future climate forcing, PNAS, 106, 10949–10954, doi:10.1073/pnas.0902817106, 2009.

Weiss, R.F, Muhle, J, Salameh, P.K, Harth, C.M., Nitrogen trifluoride in the global atmosphere Geophys. Res. Lett., 35, (20), 2008, DOI: 10.1029/2008GL035913

Weissflog, L., C. A. Lange, et al. (2005). "Sediments of salt lakes as a new source of volatilehighly chlorinated C1/C2 hydrocarbons." *Geophysical Research Letters* 32(1) 32 (1): Art. No. L01401, Jan 4, 2005

Yokouchi, Y., K. Osada, M. Wada, F. Hasebe, M. Agama, R. Murakami, H. Mukai, Y. Nojiri, Y. Inuzuka, D. Toom-Sauntry, and P. Fraser, Global distribution and seasonal concentration change of methyl iodide in the atmosphere, J. Geophys. Res., 113, D18311, doi: 10.1029/2008JD009861, 2008.

Yokouchi, Y, et al., Geophys. Res. Lett., 33. L12801, doi:101029/2006GL026403,2006.